PG CH S1- 01 (DSC)

TWO YEAR MASTER'S DEGREE COURSE

(CBCS in Accordance with NEP 2020)

SEMESTER - I

INORGANIC CHEMISTRY - I

CHEMISTRY

Hiranya Chandra Bhuyan School of Science and Technology

KRISHNA KANTA HANDIQUI STATE OPEN UNIVERSITY

Subject Experts

Prof. Jyotirekha G. Handique	KKHSOU
Prof. Manjit Kumar Bhattacharya	Cotton University
Prof. Pranjal Saikia	Gauhati University
Prof. Debajyoti Mahanta	Gauhati University

Programme Coordinator: Prof. Jyotirekha G. Handique, KKHSOU

Course Coordinator: Dr. Bedika Phukan, KKHSOU

SLM Preparation Team

UNITS	CONTRIBUTORS
1, 2	Dr. Saitanya Kumar Bharadwaj, Madhabdev University
	Dr. Bedika Phukan, KKHSOU
3,4,7,11,14	Dr. Bedika Phukan, KKHSOU
5,6,8	Dr. Kalyanjyoti Deori, Dibrugarh University
	Dr. Bedika Phukan, KKHSOU
9,10	Dr. Prashurya Pritam Mudoi, Dibrugarh University
12	Dr. Rupinder Singh, Cotton University
	Dr. Bedika Phukan, KKHSOU
13	Dr. Rupinder Singh, Cotton University

Editorial Team

Content Editing : Prof. Sonit Kumar Gogoi, Gauhati University
Dr. Bhabatosh Banik, Cotton University

Structure & Format Editing: Dr. Bedika Phukan, KKHSOU

August, 2026

This Self Learning Material (SLM) is available under the Creative Commons Attribution-Non-Commercial-Share Alike 4.0 License (International)
http://creativecommons.org/licenses/by-nc-sa/4.0/

ISBN: 978-93-7839-007-4

Printed and published by the Registrar on behalf of Krishna Kanta Handiqui State Open University

Head Office: Patgaon, Rani Gate, Guwahati- 781017
City Campus: Resham Nagar, Khanapara, Guwahati- 781022, Website: www.kkhsou.ac.in

Contents

Unit		Page No.
Unit 1:	**Valence Shell Electron Pair Repulsion (VSEPR) Theory** Structure of molecules containing bond pairs of electrons, bond pairs and lone pair(s) of electrons, structure and hybridization, Bent's rule, Bent bond, Non-bonded repulsion and structure.	**9 - 18**
Unit 2:	**Bonding in Covalent Compounds** LCAO-MO methods in homo and heteronuclear diatomic molecules (O_2, N_2, CO, NO, HCl, HF), qualitative MO description of tri- and tetra-atomic molecules (CO_2, NO_2, NO_2^+, CO_3^{2-}).	**19 - 33**
Unit 3:	**Bonding in Coordination Compounds** Types of ligands: monodentate, bidentate, ambidentate, polydentate, and macrocyclic ligand; Werner's theory, Valence Bond Theory (VBT) of coordination compounds.	**34 - 45**
Unit 4:	**Crystal Field Theory** d-orbital splitting in octahedral, square planar, square pyramidal, trigonal bipyramidal and tetrahedral complexes; Crystal Field Stabilisation Energy (CFSE), CFSE for d^1 to d^{10} systems, pairing energy, low-spin and high-spin complexes, Spectrochemical and Nephelauxetic series, Ligand field theory of metal complexes, Jahn-Teller distortion	**46 - 64**
Unit 5:	**Molecular Orbital Theory of Transition Metal complexes** Molecular orbital (MO) theory of octahedral ML_6 (O_h), tetrahedral ML_4 (T_d) and Square planar ML_4 (D_{4h}) complexes and other geometries, transition metal complexes with *σ* and *π bonding ligands.*	**65 - 78**
Unit 6:	**Electronic Spectra of Transition Metal Complexes** Absorption of light, Beer-Lambert Law, Electronic states and terms for transition metals (atomic and molecular term symbols). Selection rules, Orgel diagram and Tanabe Sugano diagrams: Applications in transition metal electronic spectroscopy. *d-d* and charge transfer transitions, calculation of *D*q, *B* and *C* parameters, nephelauxetic ratio.	**79 - 110**
Unit 7:	**Magnetic Properties of Transition Metal Complexes** Types of magnetic bodies (*e.g.*, Diamagnetic, Paramagnetic,	**111 - 123**

ferromagnetic and antiferromagnetic), antiferromagnetic coupling, Magnetic properties based on crystal field theory: spin only magnetic moments, quenching of orbital magnetic moment by CF, orbital contribution, effect of temperature on magnetic behaviour.

Unit 8: Acid-Base and Redox Chemistry **124 - 138**

Hard and soft acid-base (HSAB) concept and its applications. Standard electrode potentials, pH dependence of electrode potentials. Redox stability of metal ions in water, oxidation by atmospheric oxygen. Applications of Latimer and Frost diagrams.

Unit 9: Lanthanides and Actinides **139 - 148**

Electronic configuration, lanthanide contraction, separation of lanthanides.

Unit 10: Properties and Applications of Lanthanides and Actinides **149 - 159**

Magnetic and spectral properties; stability of lanthanide and actinide complexes; lanthanide shift reagents; MRI contrast agents.

Unit 11: Stability and Reactivity of Coordination Compounds **160 – 175**

Lability and inertness, stability constant- formation constant of complexes, chelate effect, Thermodynamic and Kinetic stability; Factor affecting stability, Correlation of stability constant with thermodynamic factors $-\Delta G$, ΔH and ΔS. Determination of stability constant – Jobs and Bjerrum's methods.

Unit 12: Ligand Substitution Reactions in Coordination Compounds **176 - 189**

Substitution reactions in octahedral [Cr(III), Co(III)] and square planar [Rh(I), Pt(II) and Pd(II)] complexes, Rate of water replacement reaction

Unit 13: Solvolysis, Hydrolysis and Trans Effect **190 - 197**

Acid hydrolysis and base hydrolysis reaction, Trans effect and its importance, Theories of trans effect.

Unit 14: Electron Transfer Reactions **198 - 210**

Inner sphere and outer sphere reactions in coordination compounds

COURSE INTRODUCTION

This course provides a systematic understanding of the structure, bonding, properties, and reactivity of inorganic and coordination compounds at the postgraduate level. It introduces fundamental theories such as VSEPR, hybridisation, and Molecular Orbital (MO) theory to explain molecular geometry and covalent bonding in both simple and polyatomic molecules.

The course places strong emphasis on coordination chemistry, covering ligand types, Werner's theory, Valence Bond Theory (VBT), Crystal Field Theory (CFT), and Ligand Field Theory (LFT). Concepts such as d-orbital splitting, Crystal Field Stabilisation Energy (CFSE), spin states, and metal–ligand bonding are discussed to interpret the stability, colour, and magnetic behaviour of transition metal complexes.

Further, the course explores electronic spectra, magnetic properties, and redox behaviour of transition metal ions, along with the chemistry of lanthanides and actinides and their applications. The final units focus on the stability, kinetics, and mechanisms of coordination compounds, including substitution reactions and electron transfer processes.

Overall, this course helps learners develop a strong theoretical foundation in inorganic structure, bonding, spectroscopy, and reaction mechanisms. It also equips learners with the conceptual tools required to understand advanced topics in inorganic chemistry and prepares them for research, teaching, and professional careers in chemical sciences.

UNIT-WISE DESCRIPTION

Unit 1: Valence Shell Electron Pair Repulsion (VSEPR) Theory

This unit introduces the Valence Shell Electron Pair Repulsion (VSEPR) theory, which explains the shapes of molecules based on the repulsion between electron pairs in the valence shell of the central atom. The unit discusses molecular structures containing bond pairs of electrons as well as molecules containing both bond pairs and lone pairs. It also explains the relationship between molecular structure and hybridization of atomic orbitals. Important concepts such as Bent's rule, Bent bonds, and the influence of non-bonded electron pair repulsions on molecular geometry are discussed to understand deviations from ideal geometries.

Unit 2: Bonding in Covalent Compounds

This unit discusses bonding in covalent molecules using the Linear Combination of Atomic Orbitals–Molecular Orbital (LCAO-MO) method. Molecular orbital descriptions of homonuclear and heteronuclear diatomic molecules such as O_2, N_2, CO, NO, HCl, and HF are presented. The unit also provides a qualitative molecular orbital description of triatomic and tetra-atomic molecules such as CO_2, NO_2, NO_2^+, and CO_3^{2-}, highlighting the role of bonding, antibonding, and non-bonding molecular orbitals in determining molecular stability and properties.

Unit 3: Bonding in Coordination Compounds

This unit introduces the basic concepts of coordination chemistry. It begins with the classification of ligands based on their donor properties, including monodentate, bidentate, ambidentate, polydentate, and macrocyclic ligands. The unit then discusses Werner's coordination theory, which laid the foundation for modern coordination chemistry. The Valence Bond Theory (VBT) of coordination compounds is also explained to describe the bonding and geometry of metal complexes.

Unit 4: Crystal Field Theory

This unit presents Crystal Field Theory (CFT), which explains the electronic structure of transition metal complexes based on electrostatic interactions between metal ions and ligands. The splitting of d-orbitals in different geometries such as octahedral, tetrahedral, square planar, square pyramidal, and trigonal bipyramidal complexes is discussed. The concept of Crystal Field Stabilisation Energy (CFSE) and its calculation for d^1–d^{10} configurations are introduced. Other important concepts such as pairing energy, high-spin and low-spin complexes, spectrochemical and nephelauxetic series, ligand field theory, and Jahn–Teller distortion are also explained.

Unit 5: Molecular Orbital Theory of Transition Metal Complexes

This unit explains the bonding in transition metal complexes using Molecular Orbital (MO) theory. Molecular orbital diagrams for octahedral ML_6 (O_h), tetrahedral ML_4 (T_d), and square planar ML_4 (D_{4h}) complexes are discussed. The role of σ-bonding and π-bonding ligands in determining the electronic structure and stability of metal complexes is also explained.

Unit 6: Electronic Spectra of Transition Metal Complexes

This unit discusses the origin of electronic spectra in transition metal complexes. It begins with the absorption of light and the Beer–Lambert law. The unit explains electronic states and term symbols for transition metal ions and introduces the selection rules governing electronic transitions. Orgel diagrams and Tanabe–Sugano diagrams are discussed and applied to interpret electronic spectra. The unit also examines *d*–*d* transitions, charge transfer transitions, and the calculation of parameters such as *D*q, Racah parameters (*B* and *C*), and the nephelauxetic ratio.

Unit 7: Magnetic Properties of Transition Metal Complexes

This unit discusses the magnetic behaviour of inorganic compounds. Different types of magnetic substances such as diamagnetic, paramagnetic, ferromagnetic, and antiferromagnetic materials are introduced. The concept of antiferromagnetic coupling is explained. The unit also discusses magnetic properties based on crystal field theory, including spin-only magnetic moments, quenching of orbital angular momentum, orbital contributions, and the effect of temperature on magnetic behaviour.

Unit 8: Acid–Base and Redox Chemistry

This unit introduces the Hard and Soft Acid–Base (HSAB) concept and its applications in predicting stability and reactivity of chemical species. The unit also discusses electrochemical concepts such as standard electrode potentials and the dependence of electrode potentials on pH. The redox stability of metal ions in aqueous solutions and oxidation by atmospheric oxygen are examined. Applications of Latimer and Frost diagrams in understanding redox behaviour are also discussed.

Unit 9: Lanthanides and Actinides

This unit focuses on the chemistry of lanthanides and actinides. It discusses their electronic configurations, characteristic properties, and the phenomenon of lanthanide contraction. Methods used for the separation of lanthanides are also explained.

Unit 10: Properties and Applications of Lanthanides and Actinides

This unit examines the important properties and applications of lanthanide and actinide elements. Magnetic and spectral properties of these elements are discussed along with the stability of their complexes. Applications such as lanthanide shift reagents and MRI contrast agents are also introduced.

Unit 11: Stability and Reactivity of Coordination Compounds

This unit introduces the concepts of stability and reactivity of coordination compounds. The ideas of lability and inertness are discussed along with stability constants and formation constants of complexes. The chelate effect and factors affecting the stability of complexes are explained. The unit also discusses thermodynamic parameters such as ΔG, ΔH, and ΔS and their relationship with stability constants. Methods for determining stability constants, including Job's method and Bjerrum's method, are also presented.

Unit 12: Ligand Substitution Reactions in Coordination Compounds

This unit discusses substitution reactions in coordination complexes. The mechanisms of ligand substitution in octahedral complexes such as Cr(III) and Co(III), and in square planar complexes such as Rh(I), Pt(II), and Pd(II), are examined. The kinetics of water replacement reactions and factors influencing substitution rates are also discussed.

Unit 13: Solvolysis, Hydrolysis, and Trans Effect

This unit explains the mechanisms of solvolysis and hydrolysis reactions in coordination compounds. Acid hydrolysis and base hydrolysis mechanisms are discussed. The unit also introduces the trans effect, which influences substitution reactions in square planar complexes. Theories explaining the trans effect and its importance in coordination chemistry are also described.

Unit 14: Electron Transfer Reactions

This unit discusses electron transfer reactions in coordination compounds. It explains the mechanisms of inner-sphere and outer-sphere electron transfer reactions, highlighting the role of bridging ligands and electron transfer pathways. These reactions are important in many chemical and biological redox processes.

UNIT 1: VALENCE SHELL ELECTRON PAIR REPULSION (VSEPR) THEORY

UNIT STRUCTURE

1.1 Learning Objectives
1.2 Introduction
1.3 Structure of molecules containing bond pairs of electrons
1.4 Structure of molecules containing bond pairs and lone pair(s) of electrons
1.5 Limitations of VSEPR theory
1.6 Structure and hybridization
1.7 Bent's rule, Bent bond
1.8 Let Us Sum Up
1.9 Answers to Check Your Progress
1.10 Further Reading
1.11 Model Questions

1.1 LEARNING OBJECTIVES

After studying this unit, the learners will be able to:

- Understand the basic principles of the Valence Shell Electron Pair Repulsion (VSEPR) theory for predicting molecular geometry.
- Distinguish between molecules containing only bond pairs and those containing both bond pairs and lone pairs**.**
- Predict the molecular geometry using steric number
- Understand the relationship between molecular geometry and hybridization
- Understand the Bent's rule and its significance

1.2 INTRODUCTION

The geometry or shape of a molecule is essential to know as it determines many of the chemical and physical properties of the molecule. In a simple covalent molecule, the central atom forms covalent bonds with other atoms. The shape of the molecule depends on the number of covalent bonds present on the molecule. The shape of the covalent molecules can be explained by employing the concept of hybridization from valence bond theory (VBT). VBT stems out of the concept of electron pairing as was proposed by Lewis and others. Drawing Lewis structures for molecules follows two simple rules; (1) two electrons with opposite spins pair up to form one bond between two participating atoms and (2) usually atoms try to attain a maximum of eight electrons in their valence shell. Depending on whether a valence shell electron pair in a molecule is shared pair or remains as an unshared pair, they are termed as bond pair (*bp*) or lone pair (*lp*) of electrons respectively.

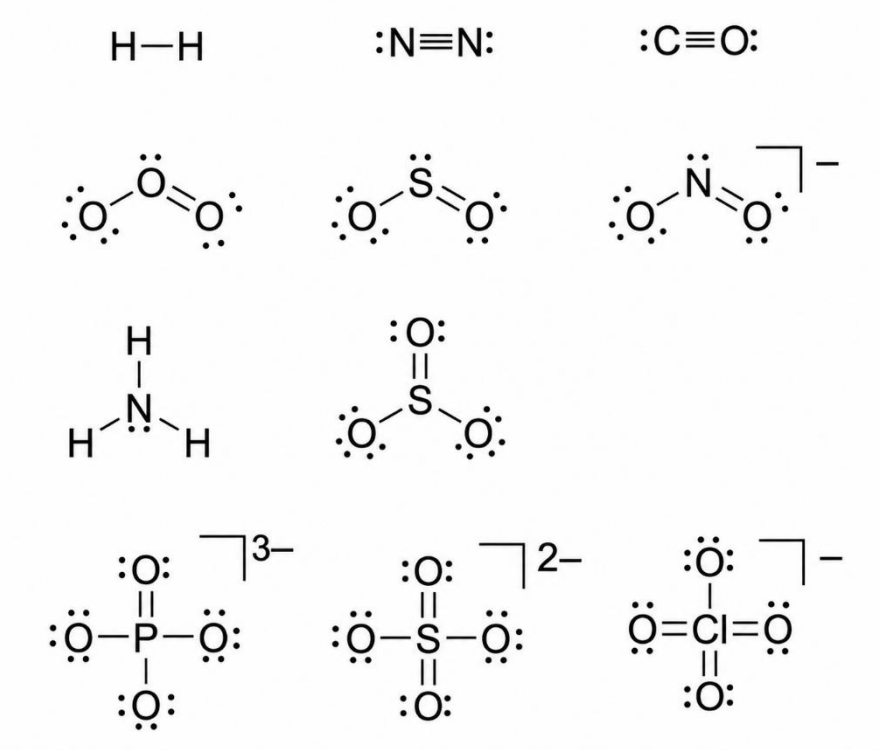


Fig. 1.1: Lewis structures of some simple molecules (*Ref*. Shriver & Atkins Inorg Chem Book, Fifth Edition)

Despite being a greatly successful theory, many molecules remain unexplained in terms of shape by simple hybridization and valence bond theory. In order to solve these limitations, Gillespie and Nyholm modified the previous ideas of Sidgwick and Powell for determining the shape of the molecule and developed valence shell electron pair repulsion (VSEPR) theory.

According to this theory "The shape or the geometry of a polyatomic molecule or ion of non-transition (mostly non-metallic) element depends upon the number and nature of the electron pairs contained in the valence shell of the central atom."

The theory is primarily based upon the fact that in a polyatomic molecule the direction of bonds around the central atom depends upon the total number of electron pairs in its valence shell. These electron pairs place themselves as far apart as possible in space so as to have minimum repulsive interactions between them, which results in maximum stability.

The main points of the VSEPR theory are

a) The geometry and the shape of the molecule depend upon the number of electron pairs in the valence shell of the central atom
b) The surrounding electron pairs repel each other and occupy a space such that minimum repulsion occurs between them.
c) The central atom can have two kinds of electron pairs *viz.* bond pairs (*bp*) and lone pairs (*lp*). The repulsive force between various electron pairs is different and the trend follows *lp*-*lp* > *lp*-*bp* > *bp*-*bp* order.

The orbital of the bonded electron pair (bp) is under the influence of two nuclei and most of the electron cloud is oriented between the nuclei of the two atoms. On the other hand, the lone pair electron is under the influence of only one nucleus or the central atom. Therefore, the electron cloud of the lone pair is closer to the central atom and occupies more space near the central atom. This causes relatively greater repulsive interactions between the lone pairs compared to the bond pairs.

The effect of the variation in the repulsive forces causes deviation from the regular geometry. This results in a contraction in the bond angle. More the number of *lp* (s), on the central atom, greater is the contraction caused in the bond angle. This statement is supported by the bond angles observed in CH_4, NH_3 and H_2O as shown in **Table 1.1**.

Table 1.1: Contraction of angle between bond pairs in presence of lone pairs

Molecules	CH_4	NH_3	H_2O
Number of lone pairs	0	1	2
Bond angle	109.5^0	107.3^0	104.5^0

d) A molecule possesses regular geometry if the central atom is surrounded by all bond pairs. The presence of lone pairs makes the molecular shape distorted or irregular.
e) In the VSEPR theory the multiple bonds are treated as a single electron pair.

1.3 STRUCTURE OF MOLECULES CONTAINING BOND PAIRS OF ELECTRONS

A molecule can be described by the generic formula AX_mE_n where A is the central atom and X is any atom or group surrounding the central atom and E is the lone pairs of electrons present in the valence shell of the central atom. 'm' and 'n' are two integers and represent the number of X and E present around the central atom. The summation of 'm' and 'n' gives a number known as Steric Number (SN). The steric number is the number of positions occupied by the atom or lone pairs around the central atom. The SN determines the shape of the molecule. In case of the molecule where the central atoms contain only bond pairs of electrons, the shape of the molecule will be regular as given in **Table 1.2**.

Table 1.2: Geometry or shape of the molecules containing only bond pairs.

SN number	Geometry	Example	Calculated bond angle (°)
2	Linear	CO_2	180
3	Trigonal planar	SO_3	120
4	Tetrahedral	CH_4	109.5
5	Trigonal bipyramidal	PCl_5	120, 90
6	Octahedral	SF_6	90
7	Pentagonal bipyramidal	IF_7	72, 90
8	Square antiprismatic	TaF_8^{3-}	70.5, 99.6, 109.5

1.4 STRUCTURE OF MOLECULES CONTAINING BOND PAIRS AND LONE PAIR(S) OF ELECTRONS

The shape of the molecule in which the central atom contains both lone pairs and bond pairs will be distorted and irregular. Some examples are given in **Table 1.3**.

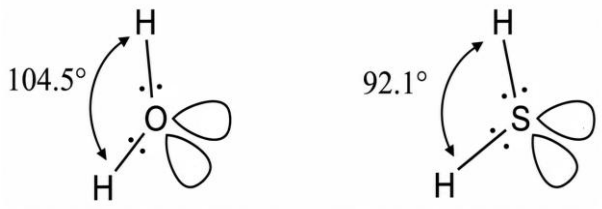
Table1.3: Geometry or shape of the molecules containing both bond pairs and lone pairs.

SN number	Bond pairs	Lone Pairs	Geometry	Example
3	2	1	Bent	SO_2
4	3	1	Pyramidal	NH_3
4	2	2	V-shaped	H_2O
5	4	1	Seesaw	SF_4
5	3	2	T-shaped	ClF_3
5	2	3	linear	XeF_2
6	5	1	Distorted square pyramidal	BrF_5
6	4	2	Square planar	XeF_4

Example 1.1: Explain why the bond angle in H_2O is 104.5°, whereas the same angle in H_2S is only 92.1°.

Solution: Both molecules have a similar overall arrangement of electrons and atoms. Each molecule has tetrahedral geometry around the central atom; however, presence of two lone pairs makes the molecular shape bent. Lone pairs occupy more space than bonding pairs, so they push the bonded atoms closer together. As a result, the bond angle becomes smaller than the ideal 109.5° expected for a perfect tetrahedral geometry.

However, the bond angles in the two molecules are not the same. This difference can be explained by considering the electronegativity of the central atoms oxygen and sulphur. Since sulphur is less electronegative, the bond pairs of electrons around sulphur are located farther away from the sulfur atom compared with the bonding electrons in H_2O. This allows the bond angle in H_2S to decrease more before the bonding pairs begin to repel each other significantly. Consequently, H_2S has a smaller bond angle than H_2O. Additionally, sulphur is a larger atom than oxygen. The H–S bond is therefore longer than the O–H bond, which places the bonding electron pairs even farther from the central atom. This greater distance further reduces the repulsion between bonding pairs and allows the bond angle in H_2S to become even smaller compared with that in H_2O.



1.5 LIMITATION OF VSEPR THEORY

The following are some of the shortcomings of the VSEPR Theory

- The geometries of highly polar molecules with an inactive pair of electrons cannot be explained by this theory.
- This theory does not explain the geometries of molecules with extensive delocalized π electron systems.
- Some transition metal complexes are not covered by this theory.

The actual shape or geometry of some molecules cannot be predicted by Valence Shell Electron Pair Repulsion (VSEPR) model. Examples include $[SeCl_6]^{2-}$, $[TeCl_6]^{2-}$, and $[BrF_6]^-$. According to the VSEPR model, these species should have seven electron pairs around the central atom (six bonding pairs and one lone pair), which would normally lead to a distorted structure rather than a perfectly symmetrical one. However, structural analyses reveal that they actually possess regular octahedral geometries in the solid state. This apparent contradiction can be explained by assuming that the lone pair on the central atom is stereochemically inactive. In other words, although the lone pair exists, it does not significantly influence the shape of the molecule. Such stereochemically inactive lone pairs are most commonly found in heavier elements of a periodic group. The tendency of the valence shell s-electrons to remain non-bonding and not participate in determining molecular geometry is known as the stereochemically inert pair effect. A similar situation is observed for $[SbCl_6]^-$ and $[SbCl_6]^{3-}$, both of which also adopt regular octahedral structures, again suggesting that the lone pair does not affect the geometry.

Important Note: If the presence of a lone pair of electrons influences the shape of a molecule or ion, the lone pair is stereochemically active. If it has no effect, the lone pair is stereochemically inactive. The tendency for the pair of valence s electrons to adopt a non-bonding role in a molecule or ion is termed the stereochemical inert pair effect

1.6 STRUCTURE AND HYBRIDIZATION

Hybridization is the extension of valence bond theory and it is observed that almost all types of molecules can be explained with this concept. The combination of VSEPR theory and the concept of hybridization explain the shapes or geometry of the molecules in a lucid manner. While the VSEPR theory determines the shape or geometry of the molecules by considering the repulsion between electron pairs (bond pairs and lone pairs) present in the valence shell of the central atom, the concept of hybridization, on the other hand, explains the mixing of atomic orbitals of the central atom to form equivalent hybrid orbitals that are oriented in specific spatial directions, thereby determining the geometry of the molecule. Shapes of some molecules are explained below.

a) **Structure of ClF_3**: The structure of Chlorine trifluoride (ClF_3) can be explained using both the VSEPR theory and the concept of Hybridization. The chlorine atom

undergoes sp^3d hybridization**,** producing five hybrid orbitals arranged in a trigonal bipyramidal orientation. Three of these hybrid orbitals overlap with the *p*-orbitals of fluorine atoms to form *σ*-bonds, while the remaining two hybrid orbitals contain lone pairs. According to VSEPR theory, five electron pairs arrange themselves in a trigonal bipyramidal geometry to minimize repulsion. In this geometry, the two lone pairs occupy the equatorial positions because this arrangement reduces electron–pair repulsion. The three fluorine atoms then occupy two axial positions and one equatorial position, resulting in a *T*-shaped molecular geometry with bond angles slightly less than 90° due to the stronger repulsion of lone pairs. Therefore, both VSEPR theory and hybridization explain that ClF_3 has a trigonal bipyramidal electron-pair arrangement and a T-shaped molecular structure as shown in **Fig. 1.2**.

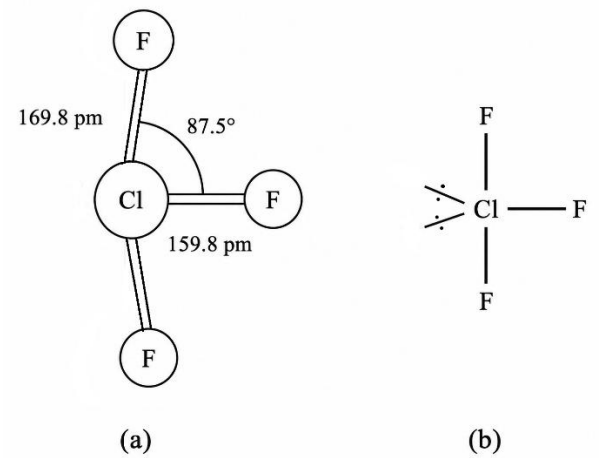


Fig. 1.2: (a) The experimentally determined structure of ClF_3 and (b) the rationalization of this structure using the VSEPR.

b) **Structure of Xenon difluoride (XeF_2):** In XeF_2, xenon undergoes sp^3d hybridization, which corresponds to a trigonal bipyramidal electron-pair arrangement. The central xenon atom contains five electron pairs around it—two bonding pairs formed with fluorine atoms and three lone pairs. According to VSEPR theory, the three lone pairs occupy the equatorial positions because this arrangement minimizes repulsion among electron pairs. As a result, the two fluorine atoms occupy the two axial positions opposite each other. Therefore, although the electron pair geometry is trigonal bipyramidal, the molecular geometry becomes linear with a bond angle of 180°.

c) **Structure of Xenon tetrafluoride (XeF_4):** In XeF_4, xenon undergoes sp^3d^2 hybridization, giving an octahedral arrangement of electron pairs. Out of six electron pairs—four are bonding pairs with fluorine atoms and two are lone pairs. To minimize repulsion, the two lone pairs occupy positions opposite to each other along the axial direction of the octahedron. The four fluorine atoms therefore lie in the same plane forming a square around the xenon atom. Consequently, the molecule exhibits a square planar geometry with bond angles of **90°** between adjacent Xe–F bonds.

d) **Structure of Xenon oxytetrafluoride ($XeOF_4$)**: In $XeOF_4$, xenon undergoes sp^3d^2 hybridization and an octahedral electron-pair environment. In this molecule, xenon forms five σ bonds—four with fluorine atoms and one with oxygen, and another pi bond with the oxygen atom. This also possesses one lone pair electron. One position is occupied by a lone pair while the oxygen atom usually occupies an axial position due to the strong multiple bonding. The four fluorine atoms lie in a square plane around xenon. Because one position of the octahedron is occupied by the lone pair, the molecular geometry becomes square pyramidal.

e) **Structure of Xenon hexafluoride (XeF_6):** In XeF_6, xenon forms six bonds with fluorine atoms and retains one lone pair, giving a total of seven electron domains around the central atom. This requires sp^3d^3 hybridization, corresponding to a pentagonal bipyramidal electron-pair arrangement. However, the presence of one lone pair causes distortion of the ideal geometry. The six fluorine atoms arrange themselves around xenon while the lone pair occupies one position, resulting in a distorted octahedral or pentagonal pyramidal molecular shape. The distortion arises because the lone pair exerts stronger repulsive forces on the bonding pairs, slightly altering the bond angles.

1.7 BENT'S RULE, BENT BOND

In general, the hybridization results in new set of equivalent orbitals called hybrid orbitals. These hybrid orbitals possess identical shapes and energies and are oriented in specific directions in space to minimize electron repulsion and facilitate effective bond formation.

In the case of sp^3 hybridization, the four hybrid orbitals have similar energies as the mixing of *s* and *p* orbitals is similar in all four cases. When a central atom is bonded to atoms of different electronegativities, the hybrid orbitals adjust their s and p character accordingly. Since the energy of an s orbital is lower than that of a p orbital, an increase in *s*-character lowers the energy of the hybrid orbital and influences the stability and geometry of the molecule. This observation was proposed by Henry A. Bent, and later it is known as Bent's rule.

Bent's rule states that "atomic *s*-character concentrates in hybrid orbitals directed toward electropositive substituents." In other words, orbitals directed toward less electronegative (more electropositive) substituents contain greater *s*-character, whereas those directed toward more electronegative substituents possess greater p-character. This redistribution helps stabilize the molecule because the lower-energy *s* character is placed in bonds where electron density is closer to the central atom.

A useful illustration is fluoromethane (CH_3F). In this molecule, carbon forms bonds with three hydrogen atoms and one fluorine atom. Hydrogen is less electronegative than carbon, while fluorine is significantly more electronegative. As a result, electron density in the C–F bond shifts toward fluorine, whereas in the C–H bonds it is drawn slightly toward carbon. According to Bent's rule, the hybrid orbitals of carbon directed toward hydrogen contain relatively more *s*-character, stabilizing the bond by keeping electron density closer to carbon. Conversely, the hybrid orbital directed toward fluorine

contains more *p*-character, because electron density is already drawn toward the highly electronegative fluorine atom.

Thus, Bent's rule provides a qualitative explanation of how hybrid orbitals are distributed in molecules containing substituents of different electronegativities. Although fluoromethane is a simple example, the principle applies broadly to many molecular systems where a central atom is bonded to two or more different substituents, helping explain variations in bond angles, bond strengths, and molecular geometry.

Apart from the above example, Bent's rule can be applied to PCl_2F_3 or other same type of molecules and predict the position of fluoride atom in molecules. According to VSEPR theory, a molecule with five bonding pairs around the central atom adopts trigonal bipyramidal geometry. In this arrangement, three positions lie in the equatorial plane and two positions are axial. Because the equatorial positions provide slightly more space and experience less repulsion, larger substituents tend to occupy these sites. Therefore, the two chlorine atoms are expected to occupy the equatorial positions, while the three fluorine atoms occupy one equatorial and two axial sites.

The maximum overlapping occurs when the orbitals approach each other directly along the line joining the two nuclei, i.e. "head-on." This arrangement allows the maximum electron density to lie between the nuclei, producing a strong bond. However, in small ring systems the atoms are forced into tight angles, which leads to poor orbital overlap and results in what is known as ring strain. As the size of the ring becomes smaller, the orbitals undergo rehybridization to adapt to these constraints. In this process, the bonds within the ring gain more *p* character, while the bonds extending outside the ring acquire more *s* character.

Even with this adjustment, the smallest possible angle between *s* and *p* orbitals is about **90°**, which corresponds to pure *p* orbitals. In very small rings such as three-membered rings, the orbitals cannot align properly along the internuclear axis. As a result, the σ bonds formed are not symmetrical around the bonding axis but instead become bent bonds. Experimental observations show that these bent bonds lead to a concentration of electron density outside the ring. The 3-[(p-nitrophenoxy)methyl]-3-chlorodiazirine (**Fig. 1.3**) molecule is one of the examples where bent bond is observed.

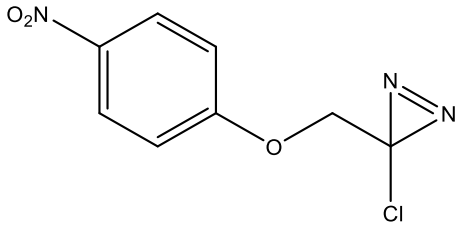


Fig. 1.3: Structure of 3-[(p-nitrophenoxy)methyl]-3-chlorodiazirine

W CHECK YOUR PROGRESS

Q1. What is the basic principle of the Valence Shell Electron Pair Repulsion (VSEPR) theory?

Q2. Define bond pair and lone pair of electrons.

Q3. Write the order of repulsion among different electron pairs.
Q4. What is meant by steric number?
Q5. Write the general formula used in VSEPR notation to represent molecules.
Q6. Predict the geometry of a molecule with steric number 4.
Q7. State Bent's rule.
Q8. How does Bent's rule explain the distribution of *s*- and *p*-character in hybrid orbitals?
Q9. In which direction does the hybrid orbital with more *s*-character tend to point?

2 1.8 LET US SUM UP

This unit can be summarised as follows-

- Valence Shell Electron Pair Repulsion (VSEPR) theory states that the shape of a molecule is determined by the number of electron pairs present in the valence shell of the central atom and arrange themselves in space to reduce the repulsive forces.
- Electron pairs around the central atom may be bond pairs or lone pairs. Since lone pairs occupy more space than bond pairs, the repulsive interactions follow the order:

lp–lp > lp–bp > bp–bp

- The presence of lone pairs therefore leads to distortion of the ideal geometry and reduction of bond angles.
- The shapes of molecules can be described using the AX_mE_n notation, where A represents the central atom, X the surrounding atoms, and E the lone pairs. The steric number (m + n) determines the basic electron-pair geometry.
- Shape and geometry of the molecules containing delocalized π-systems, transition metals, or stereochemically inactive lone pairs cannot be explained by VSEPR theory.
- **Bent's rule** states that *atomic s-character concentrates in hybrid orbitals directed toward electropositive substituents*.

K 1.9 ANSWERS TO CHECK YOUR PROGRESS

Answer to Q1: The VSEPR theory states that electron pairs present in the valence shell of the central atom repel each other and arrange themselves as far apart as possible to minimize repulsion, thereby determining the molecular geometry.
Answer to Q2: a) Bond pair (*bp*): A pair of electrons shared between two atoms in a covalent bond.
Lone pair (lp): A pair of electrons localized on the central atom that does not participate in bonding.
Answer to Q3: The order of repulsion is: *lp–lp* > *lp–bp* > *bp–bp*
Answer to Q4: The steric number is the total number of electron pairs (bond pairs + lone pairs) surrounding the central atom.
Answer to Q5: The general notation used in VSEPR theory is AX_mE_n,
where A = central atom, X = bonded atoms, E = lone pairs on the central atom.

Answer to Q6: A molecule with steric number 4 generally has tetrahedral electron pair geometry.

Answer to Q7: Bent's rule states that atomic s-character concentrates in hybrid orbitals directed toward electropositive substituents, while p-character concentrates toward electronegative substituents.

Answer to Q8: According to Bent's rule, hybrid orbitals adjust their s and p composition depending on the electronegativity of the substituents bonded to the central atom.

Answer to Q9: Hybrid orbitals with greater s-character are directed toward electropositive atoms, while those with greater p-character point toward electronegative atoms.

O 1.10 FURTHER READING

- Cotton, F. A.; Wilkinson, G.; Murillo, C. A.; Bochmann, M. *Advanced Inorganic Chemistry*; Wiley.
- Housecroft, C. E.; Sharpe, A. G. *Inorganic Chemistry*, 4th ed.; Pearson Education: Harlow, 2012.
- Huheey, J. E.; Keiter, E. A.; Keiter, R. L. *Inorganic Chemistry: Principles of Structure and Reactivity*, 4th ed.; Pearson.
- Miessler, G. L.; Fischer, P. J.; Tarr, D. A. *Inorganic Chemistry*, 5th ed.; Pearson: Boston, 2014.
- Shriver, D. F.; Atkins, P. W.; Langford, C. H. *Inorganic Chemistry*; Oxford University Press.

M 1.11 MODEL QUESTIONS

Q1. State the basic postulates of VSEPR theory.
Q2. What is meant by steric number?
Q3. Distinguish between bond pair and lone pair electrons.
Q4. Why do lone pairs cause distortion in molecular geometry?
Q5. State Bent's rule.
Q6. Explain the shapes of molecules containing only bond pairs according to VSEPR theory.
Q7. Discuss the geometry of molecules containing both bond pairs and lone pairs with suitable examples.
Q8. Explain the structure and hybridization of XeF_2 and XeF_4.
Q9. Discuss the limitations of the VSEPR theory.
Q10. Explain the VSEPR theory in detail and discuss how it predicts molecular geometry.
Q11. Describe the structures of ClF_3, $XeOF_4$, and XeF_6 using VSEPR theory and hybridization concepts.
Q12. Show that the VSEPR model is consistent with a trigonal planar structure for SO_3.
Q13. Using the VSEPR model, rationalize why a CO_2 molecule is linear whereas an $[NO_2]^-$ ion is bent.

UNIT 2: BONDING IN COVALENT COMPOUNDS

UNIT STRUCTURE

2.1 Learning Objectives
2.2 Introduction
2.3 LCAO-MO methods in homonuclear diatomic molecules (O_2, N_2)
2.4 LCAO-MO methods in heteronuclear diatomic molecules (CO, NO, HCl, HF)
2.5 Qualitative MO description of tri-atomic molecules (CO_2, NO_2, NO_2^+)
2.6 Qualitative MO description of tetra-atomic molecules (CO_3^{2-})
2.7 Let Us Sum Up
2.8 Answers to Check Your Progress
2.9 Further Reading
2.10 Model Questions

2.1 LEARNING OBJECTIVES

After studying this unit, the learners will be able to:

- Understand the LCAO–MO approach in describing chemical bonding, homonuclear and heteronuclear diatomic molecules**.**
- Interpret the qualitative molecular orbital description of triatomic (CO_2, NO_2, NO_2^+) and tetra-atomic molecules such as CO_3^{2-}.
- The student will also be able to explain other molecules with LCAO-MO approach apart from the examples given in this unit.

2.2 INTRODUCTION

The chemical bonding theories explain how atoms combine to form a molecule. Valence Bond Theory (VBT) is one of the mostly used theory in which the atomic identity retains in a molecule, the only valence electrons are taking part in the bonding phenomenon. Later the concept of hybridization was introduced to explain the directionality and strength of bonds, where atomic orbitals of the central atom undergo hybridization to form a new set of orbitals and combine with other atoms. Although valence bond theory successfully explains many molecular structures and bond angles, it does not always provide a satisfactory explanation for several important properties such as magnetic behavior, electronic spectra, and the relative stability of molecules.

To overcome these limitations, a more comprehensive description of bonding was developed in the early twentieth century known as Molecular Orbital (MO) Theory. This theory was first proposed by scientists such as Friedrich Hund and Robert S. Mulliken in the 1930s and was later refined by John Lennard-Jones and Charles Coulson. In contrast to valence bond theory, MO theory assumes that electrons in a molecule are not confined to individual atoms or localized bonds. Instead, they occupy molecular orbitals that extend over the entire molecule. These orbitals are influenced simultaneously by all the nuclei present making them polycentric.

The molecular orbital theory is a quantum mechanical treatment where the wave nature of electrons is considered and is described by a wave function (Ψ), which is obtained as a solution of the Schrödinger equation. The wave function assigned for the molecular orbital or electron provides the description of the probability of finding electrons in the molecular space.

There are two main procedures by which molecular orbitals may be obtained. One method is the united atom method, which treats the molecule as if it were a single atom with a combined nuclear charge. The second and more widely used method is the Linear Combination of Atomic Orbitals (LCAO) approach.

LCAO approximation explains the formation of molecular orbitals by linear combination of the atomic orbitals. Linear combination of such wave function is the simple mathematical addition and subtraction of wave functions.

Considering Ψ_A and Ψ_B the two wave functions of two atoms A and B, the molecular orbital wave function for the system can then be expressed as a linear combination of the atomic orbital wave functions:

$$\Psi_{MO}=N(c_1\Psi_A \pm c_2\Psi_B)$$

where **N** is a normalization constant ensuring that the total probability of finding the electron in space is unity. When the function is normalised then the value of N is one. The constants $\mathbf{c_1}$ and $\mathbf{c_2}$ are coefficients that determine the relative contribution of the atomic orbitals to the molecular orbital. If the two atoms are identical, these coefficients are equal or one; if the atoms are different, their values depend on the relative energies and contributions of the atomic orbitals involved. The MO wave functions generated by addition is called bonding MO and subtraction is known as antibonding orbitals. The probability of finding an electron in a given region of space is proportional to the square of the wave function. When the above expression is squared, three terms appear: two terms correspond to the electron densities associated with the individual atomic orbitals, while the third term represents the overlap between the two orbitals. This overlap term is extremely important because it reflects the interaction between the electron clouds of the atoms. As the overlap increases, the interaction becomes stronger, leading to a stronger chemical bond.

$$\Psi_b^2=(\Psi_A+\Psi_B)^2=\Psi_A^2+\Psi_B^2+2\,\Psi_A\,\Psi_B$$

$$\Psi_a^2=(\Psi_A-\Psi_B)^2=\Psi_A^2+\Psi_B^2-2\,\Psi_A\,\Psi_B$$

Where Ψ_b and Ψ_a are wave functions of bonding and antibonding orbitals respectively. It is clear from the above that

$$\Psi_b^2 > \Psi_A^2+\Psi_B^2 \text{ and } \Psi_a^2 < \Psi_A^2+\Psi_B^2$$

From the above mathematical statements, it can be observed that in case of bonding orbitals, the electron density between the nuclei increases whereas in the case of antibonding orbitals, the electron density decreases between the nuclei.

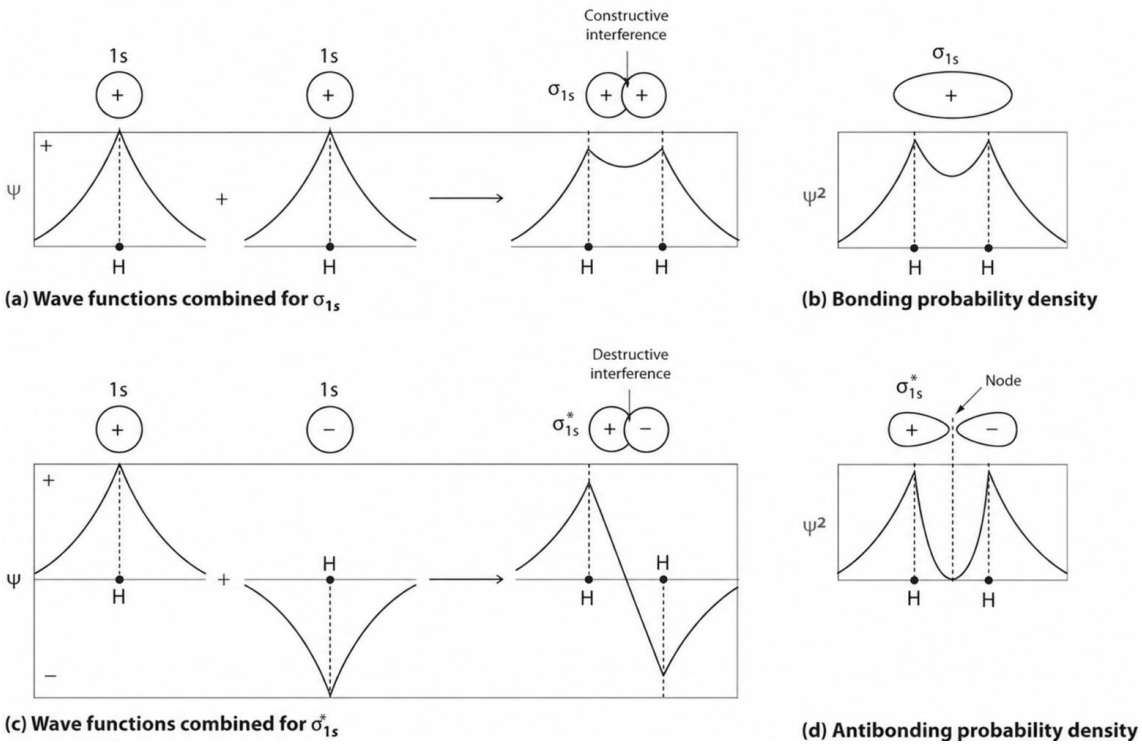


Fig. 2.1. (a) Constructive interference, (b) probability density of bonding MO, (c) Destructive interference and (d) probability density of antibonding MO of wave function of 1s orbital

In the LCAO approach, atomic orbitals may combine in two different ways- **constructive** and **destructive**. Constructive interference gives a bonding molecular orbital. This orbital has lower energy and greater stability than the original atomic orbitals. On the other hand, when the combination results in destructive interference, the electron density between the nuclei decreases and an antibonding molecular orbital is formed, which has higher energy and lower stability. Bonding orbitals are commonly denoted by symbols such as σ, π, or δ depending on the type of overlap, while antibonding orbitals are represented by σ^*, π^*, or δ^*.

In the bonding MO, the nuclei are shielded from each other and the attraction of both nuclei for the electrons is enhanced. This results in a lowering of energy of the molecule. However, in case of antibonding MO, the electrons tend to be in those regions of space in which mutual attraction by both nuclei is severely reduced.

One of the main postulates of molecular orbital theory is that the number of molecular orbitals formed is equal to the number of atomic orbitals combined. These molecular orbitals are arranged in order of increasing energy, and electrons occupy them according to the same principles that govern the filling of atomic orbitals, namely the Aufbau principle, the Pauli exclusion principle, and Hund's rule.

The LCAO–MO approach can be applied to both homonuclear diatomic molecules (for example H_2 and O_2), and heteronuclear diatomic molecules (such as CO, NO, HCl and HF), and even tri & polyatomic molecules (for example CO_2, NO_2, NO_2^+ CO_3^{2-}). In both cases, the theory provides a powerful framework for understanding bond formation, bond order, magnetic properties, and electronic structure.

Thus, molecular orbital theory, particularly through the LCAO approximation, offers a unified and quantitative description of chemical bonding. It not only explains how atoms combine to form molecules but also provides insight into many physical and chemical properties that cannot be adequately described by earlier bonding models.

2.3 LCAO-MO METHODS IN HOMONUCLEAR DIATOMIC MOLECULES

In a homonuclear diatomic molecule, the two atoms are identical and therefore possess atomic orbitals of the same energy. As a result, the atomic orbitals contribute equally to the formation of molecular orbitals. The simplest example is hydrogen molecule. In this unit, we will discuss the MO theory of N_2 and O_2. Because of the identical nature of the atoms, the coefficients (c_1 and c_2) in the LCAO expression for the molecular orbital wave function are equal, and the electron density is symmetrically distributed between the two nuclei.

When two atoms approach each other, their atomic orbitals interact or we can say wave function electron of the two atoms undergo constructive and destructive interference. The resultant molecular orbitals are generally classified according to the type of overlap between atomic orbitals. When the overlap occurs along the internuclear axis, a σ (sigma) orbital is formed, whereas sidewise overlap produces a π (pi) orbital. The corresponding antibonding orbitals are denoted by σ^* and π^*. The pictorial representation is given in **Fig. 2.2**. Electrons occupy molecular orbitals in order of increasing energy following the principles of quantum mechanics, namely the Aufbau principle, the Pauli Exclusion Principle, and Hund's rule.

a) Lithium and Beryllium (Li_2 and Be_2)

Each of the Lithium atoms has three electrons, hence a total of six electrons will be distributed in the molecular orbitals, first four electrons fill the σ_{1s} and σ^*_{1s} orbitals. The last two electrons enter in the σ_{2s} orbital, giving a net bond order of one in the Li_2 molecule. Eight electrons from two beryllium atoms fill the four lowest energy levels, σ_{1s}, σ^*_{1s}, σ_{2s}, σ^*_{2s} yielding a net bond order of zero, as in He_2. Therefore, Be_2 is not expected to exist. This MO explanation is in line with the experimental results, that is lithium is diatomic in the gas phase but beryllium is monatomic.

b) Oxygen, Fluorine, and Neon (O_2, F_2 and Ne)

The oxygen molecule was one of the first applications of molecular orbital theory in which it is proved to be more successful than valence bond theory. The molecule contains sixteen electrons. Four of these electrons occupy the σ_{1s} and σ^*_{1s} orbitals, which are generally not shown in the MO diagram. The next four electrons occupy σ_{2s} and σ_{2s^*} orbitals and also cancel out. The remaining eight electrons occupy the σ_{2pz}, π_{2px}, π_{2py}, π^*_{2px}, π^*_{2py} orbitals. Thus, the configuration of O_2 is KK σ_{2s}^2 $\sigma^*_{2s}{}^2$ σ_{2pz}^2 π_{2px}^2 π_{2py}^2 $\pi^*_{2px}{}^1$ $\pi^*_{2py}{}^1$. This electronic arrangement explains that the oxygen molecule is paramagnetic with bond order 2. Similarly, in case of F_2 and Ne_2, filling the electrons in MO, it is observed that F_2 is hold by single bond where no bond forms between two neon atoms.

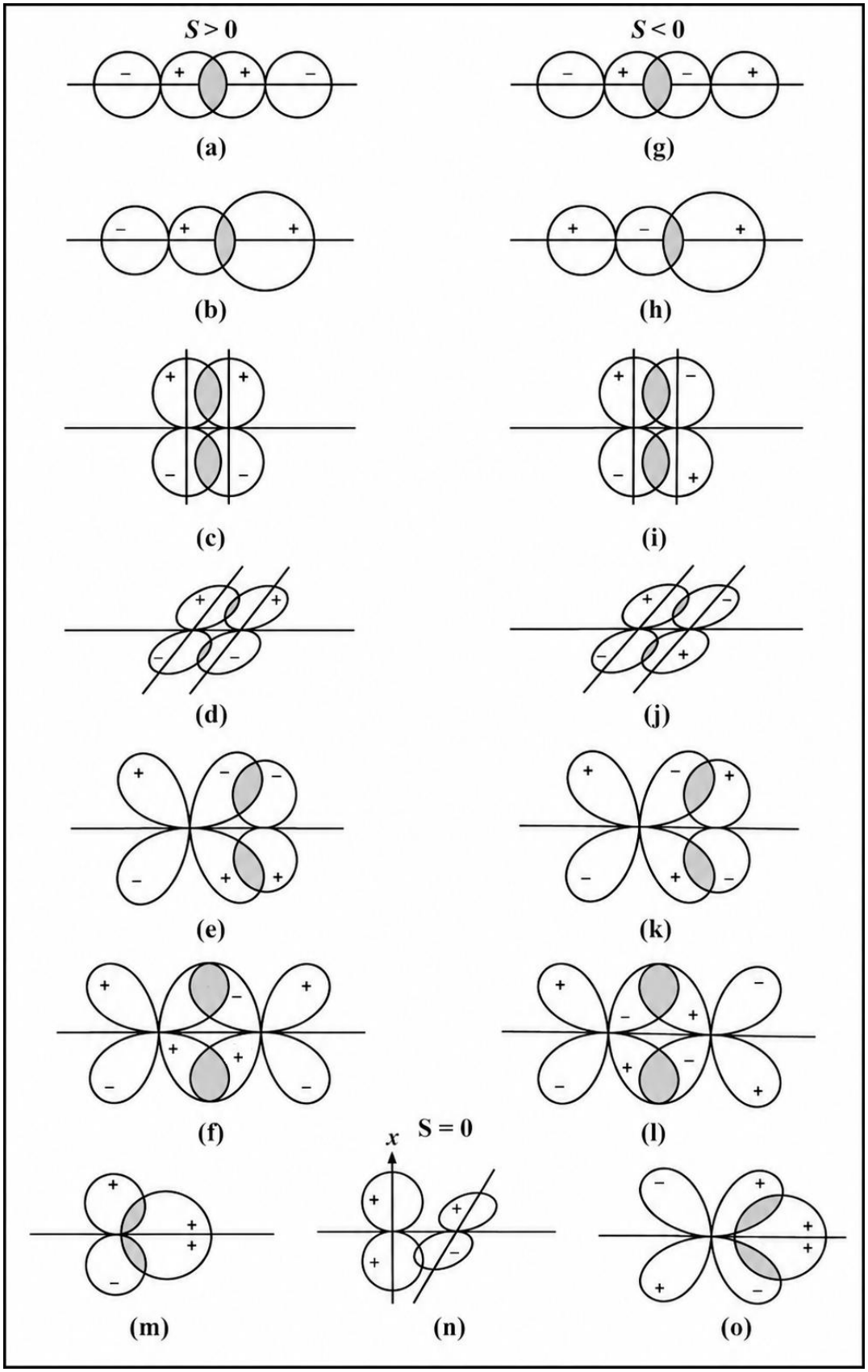


Fig. 2.2. Pictorial representation of orbital with positive overlap (a-f), negative overlap (g-j) and zero overlap (m-o). (This picture is adopted from Inorganic Chemistry, Huheey, Keiter, and Keiter 4th edition, Pearson, p 158.)

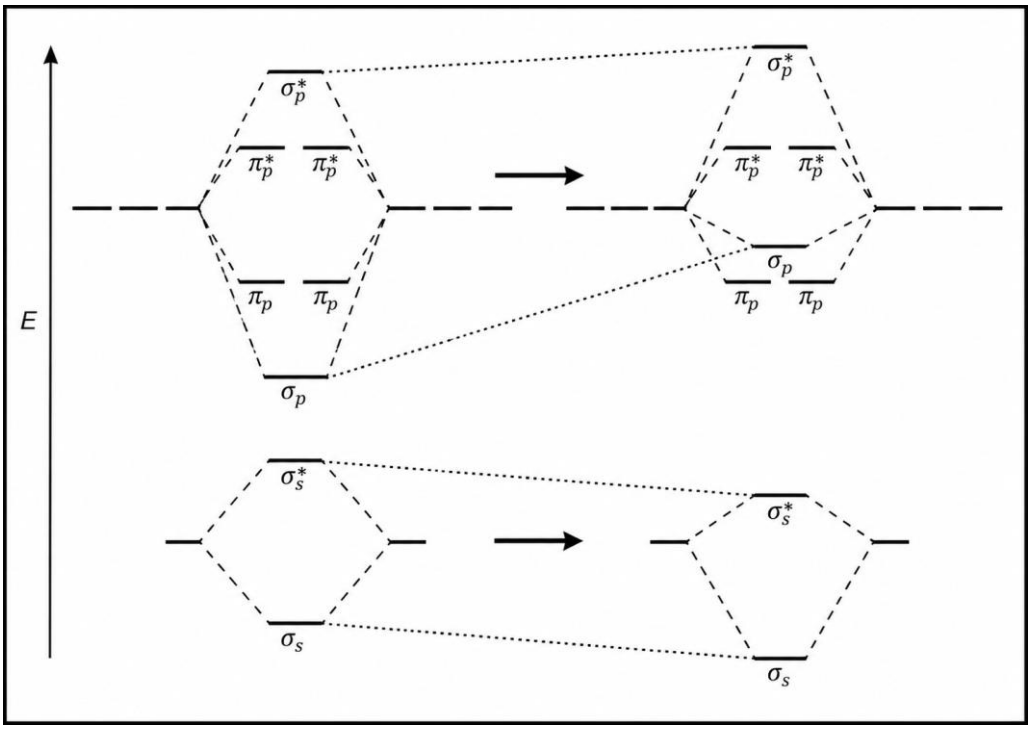


Fig. 2.3. Representative MO diagrams of homonuclear diatomic molecule with atomic number 5 to 7 (right) and atomic number 8 to 9 (left)

c) Boron, Carbon, and Nitrogen (B_2, C_2 and N_2)

According to the standard ordering of orbitals, the B_2 molecule would be diamagnetic. However, experimentally B_2 is found to be paramagnetic having two unpaired electrons. Similarly, the experimental evidence indicates that the ground state of C_2 is diamagnetic. Therefore, the energy consideration for these molecular orbitals is considered and calculated. It is found that the energy difference between the 2*s* and 2*p* orbitals is small for the lighter elements (B, C, N). Therefore, these orbitals undergo mixing of their characters between themselves, known as *s*–*p* mixing, which alters the ordering of molecular orbitals as shown in the **Fig. 2.3 (right)**. As a result, π_{2px} and π_{2py} orbitals become lower in energy than σ_{2pz} orbitals. Now filling the electrons in this order of molecular orbitals provide the magnetic behaviour in line with experimental results.

2.4 LCAO-MO METHODS IN HETERONUCLEAR DIATOMIC MOLECULES

Construction of MO for heteronuclear diatomic molecules requires same conditions, like same symmetry, comparable energy and appreciable overlap as in homonuclear diatomic molecules. However, the molecular orbitals of heteronuclear diatomic molecules differ from that of homonuclear diatomic molecules as the participation of atomic orbitals varies.

In case of heteronuclear diatomic molecules, due to different electronegativity and hence differ in their orbital energy and the atomic orbitals will not contribute equally.

$$\Psi_b = c\Psi_A + d\Psi_B$$

'c' and 'd' are contributing factor and d>c if atom B is more electronegative than A. Conversely, in case of antibonding orbital the more electronegative atom has less contribution

$$\Psi_a = d\Psi_A - c\Psi_B$$

As the electronegativity differences increases, the covalency of a molecule decreases. The trend in MO diagram with increase in electronegativity differences can be drawn as follows:

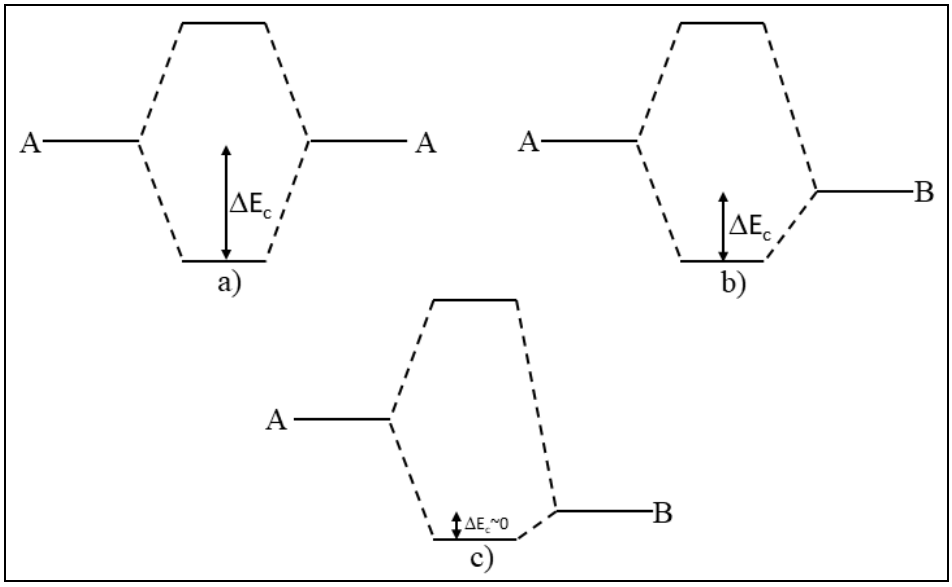


Fig. 2.4. The covalent of energy of (a) Homonuclear diatomic molecule, b) heteronuclear diatomic molecule with small electronegativity difference, c) heteronuclear diatomic molecule with large electronegativity difference

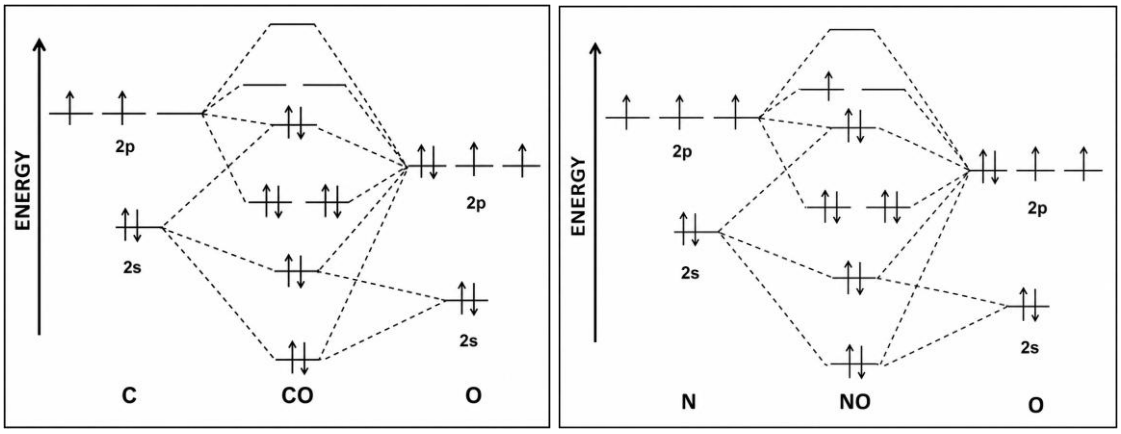
The energy difference (ΔE_C) between the isolated atomic orbital and molecular orbital can determine the extent of covalency. As ΔE_C increases covalency increases.

Examples

CO molecule: In the carbon monoxide molecule, the O atom is more electronegative than C atom. Therefore, O will contribute more to the bonding molecular orbital and C-atom will contribute more to the antibonding molecular orbitals. The MO diagram with the arrangement and filling the electrons in different orbitals is shown in the **Fig. 2.5 (a**).

NO molecule: The LCAO–MO theory successfully explains the electronic structure, bond order, and magnetic behaviour of nitric oxide. In nitric oxide molecule, nitrogen contributes five valence electrons ($2s^2 2p^3$) while oxygen contributes six valence electrons ($2s^2 2p^4$), giving a total of eleven valence electrons. Since oxygen is more electronegative than nitrogen, its atomic orbitals are lower in energy than those of nitrogen. The atomic orbitals from N and O combine to form bonding and antibonding molecular orbitals and their order in energy increases as $\sigma_{2s} < \sigma^*_{2s} < \pi_{2px} = \pi_{2py} < \sigma_{2pz} < \pi^*2_{px} = \pi^*2_{py} < \sigma^*_{2pz}$. Electrons occupy their positions giving one unpaired electron in

antibonding π^*, as a result this molecule become paramagnetic with bond order of 2.5. The MO diagram of NO is given in **Fig. 2.5 (b).**

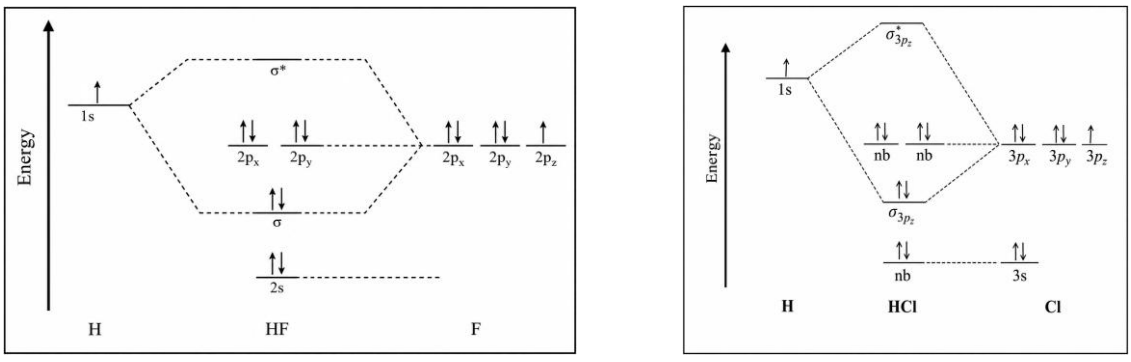


a) b)

Fig. 2.5. Energy level diagram for the molecular orbitals of (a) Carbon monoxide (CO), (b) Nitric oxide (NO).

HF Molecule: In hydrogen fluoride (HF) molecule, the molecular orbitals can be understood using a method similar to that applied for carbon monoxide. The 2*s* orbital of the fluorine atom lies much lower in energy than the 1*s* orbital of hydrogen. Therefore, these two orbitals interact only very weakly and do not contribute significantly to bonding.

However, the fluorine $2p_z$ orbital (−18.65 eV) and the hydrogen 1*s* orbital (−13.61 eV) have energies that are closer to each other. This similarity in energy allows them to combine effectively, forming a bonding σ molecular orbital and a corresponding antibonding σ^* molecular orbital. In contrast, the fluorine $2p_x$ and $2p_y$ orbitals do not participate in bonding and remain as non-bonding orbitals. As a result, the HF molecule contains one bonding pair of electrons and three lone pairs on the fluorine atom. Unlike the simple picture given by the Lewis dot structure, these lone pairs are not completely equivalent because they originate from different orbitals. The molecular orbital also explains the polarity of the HF bond. The occupied molecular orbitals are concentrated more toward the fluorine atom. Consequently, the electron density in HF is greater around fluorine than hydrogen, making fluorine the negative end of the molecule and hydrogen the positive end.



a) b)

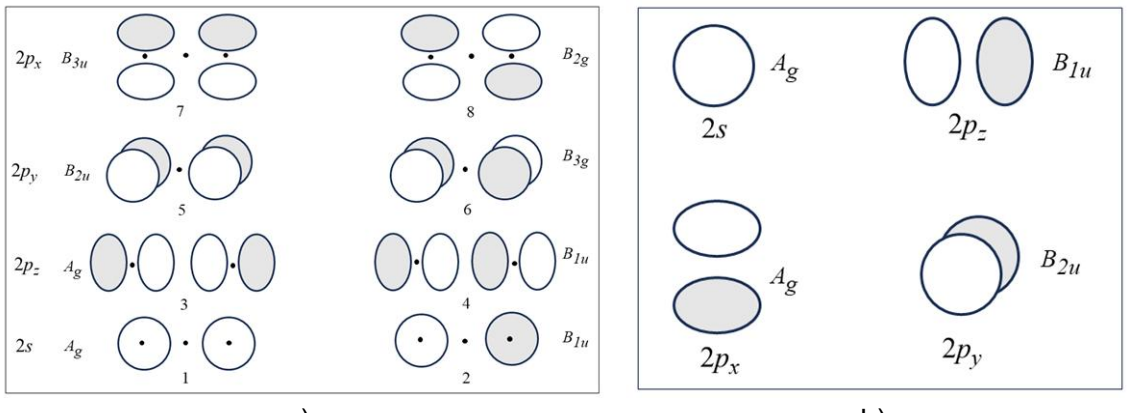
Fig. 2.6. Energy level diagram for the molecular orbitals of a) Hydrogen Fluoride (HF), b) Hydrogen Chloride (HCl).

HCl Molecule: In hydrogen chloride molecule (HCl), Cl-atom is more electronegative, hence attraction for electron is greater than that of H-atom. The energies of the 3*s* and 3*p* orbitals of Cl-atom is less than that of 1*s* orbitals. There is one sigma bond holding the atoms together. The remaining electrons occupy the non-bonding orbitals which are almost unchanged atomic orbitals of Cl-atom. These non-bonding electrons correspond to the lone pairs of electrons of valence bond theory. They are orthogonal to the 1s orbital of H-atom and have zero overlap. It is believed that the effective overlap occurs between $1s^1$ of H-atom and $3p_z^1$ of Cl-atom and the remaining orbitals 3*s*, $3p_x$, $3p_y$ retain almost AO character and regarded as non-bonding orbitals. The MOs can be drawn as in **Fig. 2.6 b)**.

2.5 QUALITATIVE MO DESCRIPTION OF TRI-ATOMIC MOLECULES

MO descriptions for triatomic molecules are similar to that of diatomic molecules. However, this approach becomes more complicated as group of atoms bind with the central atoms. Also, the triatomic molecules vary from linear to bent or V-shaped. The group of atomic orbitals first undergoes linear combination with respect to their similarity in symmetry, popularly known as Symmetry Adapted Linear Combination (SALC).

The methods described in the previous sections for diatomic molecules can be extended for constructing MO diagrams for tri-atomic molecules, but that approach would be complex to deal with. Construction of group orbitals (GOs) by combination of matching orbitals on the outer atoms provide a rather convenient approach to tackle this problem. The outer atoms are identified leaving the central atom and matching orbitals on the outer atoms are combined to generate a set of GOs equal in number to that of the combining atomic orbitals. The GOs are then combined with the matching atomic orbitals on the central atom to obtain the final MO diagram. The following two examples provide a suitable introduction to the concept of group orbital approach.

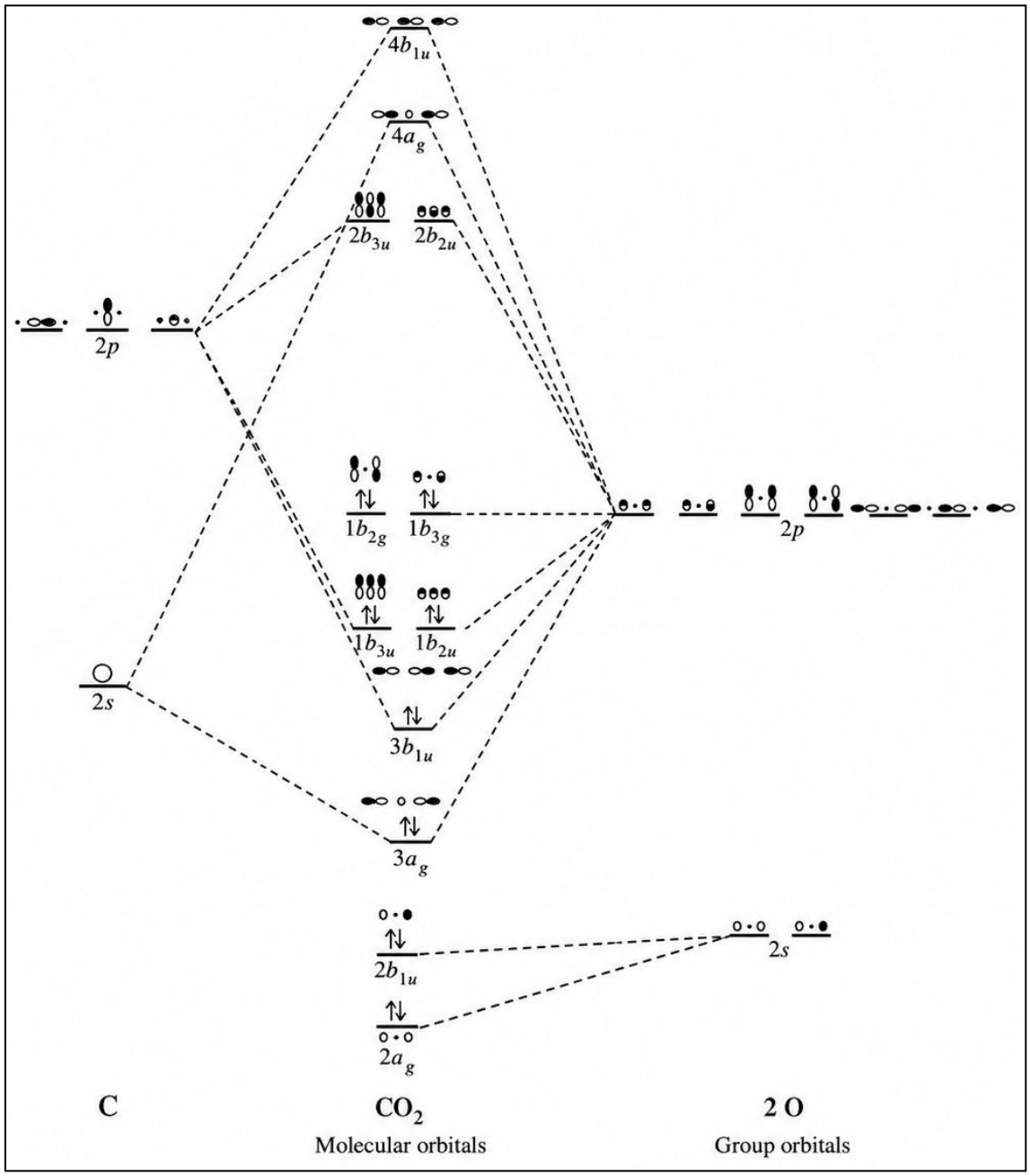


a) b)

Fig. 2.7. a) Oxygen group orbitals with symmetry in CO_2, and b) Orbitals of carbon atom with symmetry.

CO_2 Molecule: In carbon dioxide, the orbitals from two oxygen atoms undergo linear combination of all valence orbitals, resulting in new set of group orbitals as shown in

Fig. 2.7 (a). In **Fig. 2.7 (b),** the orbital symmetry of carbon-atom is shown. The oxygen group orbitals can interact with the orbitals with same symmetry of carbon atom and form molecular orbitals as shown in **Fig. 2.7 (c)**. The 16 valence electrons occupy, from the bottom, two essentially nonbonding s orbitals, two bonding *s* orbitals, two bonding *p* orbitals, and two nonbonding *p* orbitals. In other words, two of the bonding electron



pairs are in *s* orbitals, two are in *p* orbitals, and there are four bonds in the molecule.

Fig. 2.7(c). Molecular orbitals in CO_2

NO_2 Molecule: Like carbon dioxide molecule, in NO_2 molecule the oxygen orbitals of two oxygen atom undergo linear combination to form group orbitals. These group orbitals form MO with the orbitals of nitrogen with same symmetry. The MO diagram can be drawn as shown in **Fig. 2.8**.

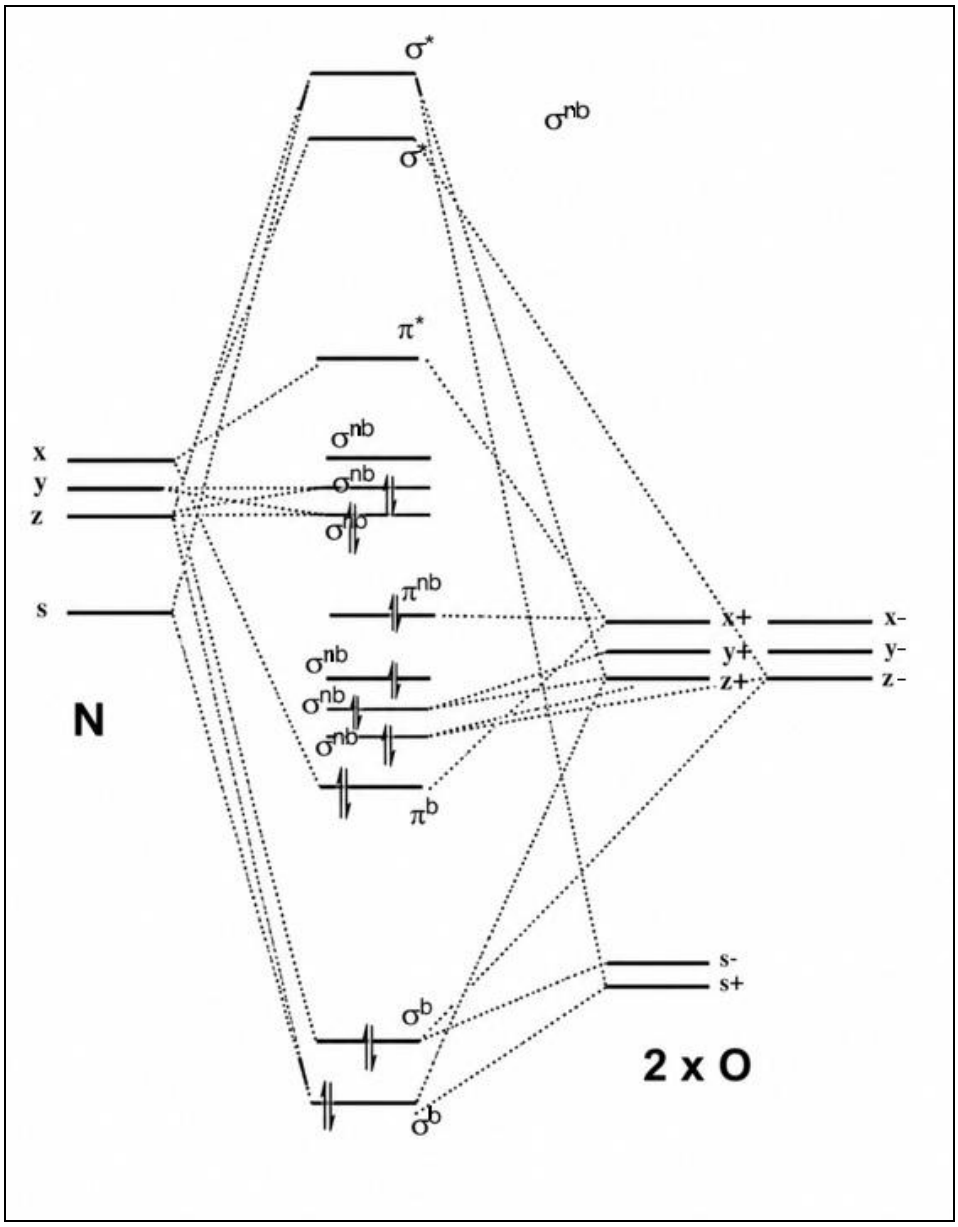


Fig. 2.8. MO diagram of NO_2

2.6 QUALITATIVE MO DESCRIPTION OF TETRA-ATOMIC MOLECULES (CO_3^{2-})

The molecular orbital (MO) description of the carbonate ion (CO_3^{2-}) can be explained qualitatively using LCAO-MO approach. The tetra-atomic carbonate ion consists of one carbon atom bonded to three oxygen atoms and carries a –2 charge. Structurally, CO_3^{2-} is trigonal planar with D_{3h} symmetry, where the carbon atom lies at the centre and the three oxygen atoms occupy the corners of an equilateral triangle.

In the MO treatment, the valence atomic orbitals of three oxygen atoms (2*s*, $2p_x$, $2p_y$, $2p_z$) undergo symmetry-adapted linear combinations (SALCs) and interact with suitable atomic orbitals of the central carbon atom. The σ bonding framework is primarily formed by the overlap of carbon sp^2 hybrid orbitals with the oxygen orbitals producing three equivalent C–O σ bonds.

The unhybridized $2p_z$ orbital of carbon (perpendicular to the molecular plane) and three $2p_z$ orbitals of the three oxygen atoms form four molecular orbitals and hence form π MOs of CO_3^{2-}. These generate one bonding π molecular orbital and two degenerate non-bonding π orbital and one antibonding π^* orbitals. The electrons occupying the π bonding orbital are delocalized over all three C–O bonds, which explains why all C–O bonds in CO_3^{2-} have equal bond lengths and intermediate bond order between single and double bonds.

Fig. 2.9 shows the sigma and pi interaction of orbitals of carbon and oxygen atoms in carbonate ion.

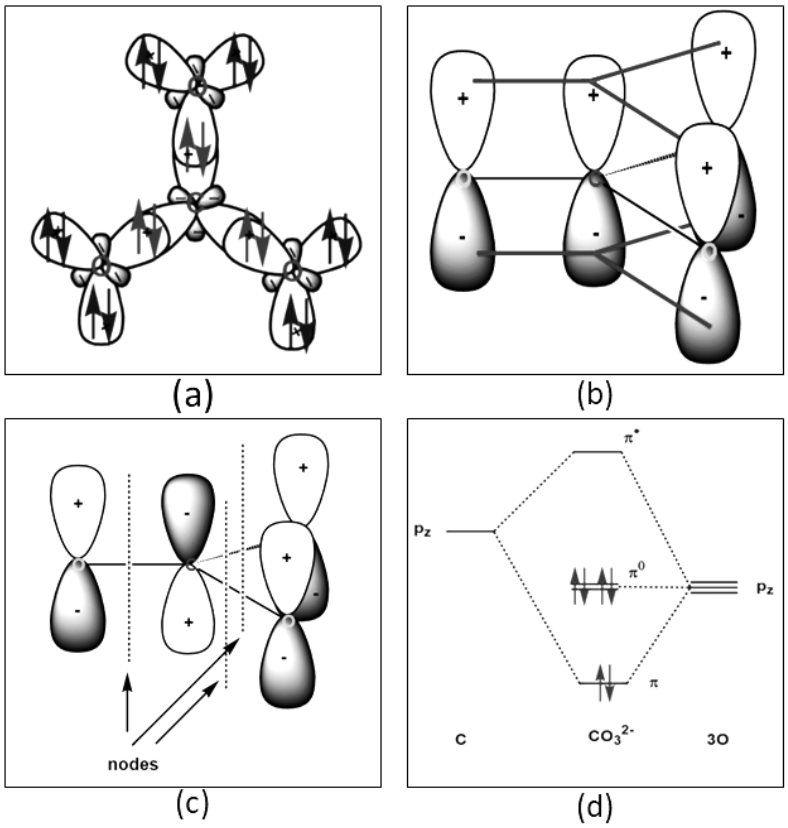


Fig. 2.9. Different MOs of carbonate ion. (a) orbitals with σ bond, (b) interaction of π bonding orbitals, (c) interaction of π^* antibonding bonding orbitals, (d) MO diagram of π system of carbonate ion.

W CHECK YOUR PROGRESS

Q1. What are molecular orbitals? How do they differ from atomic orbitals?
Q2. What is meant by the Linear Combination of Atomic Orbitals (LCAO) approach?
Q3. What do you mean by constructive interference and destructive interference of wave function?
Q4. What is the significance of the normalization constant (N) in the LCAO wave function?
Q5. Why is O_2 paramagnetic according to MO theory?
Q6. Why does Be_2 not exist based on molecular orbital considerations?
Q7. What is meant by bond order, and how is it related to stability?

Q8. Why do heteronuclear molecules have **unequal contribution** from atomic orbitals?
Q9. Why are bonding molecular orbitals lower in energy than atomic orbitals?
Q10. Why are antibonding orbitals higher in energy and less stable?

2 2.7 LET US SUM UP

- Molecular Orbital (MO) theory with the LCAO approach explains the formation of molecular orbitals through constructive and destructive combinations of atomic orbitals, producing bonding and antibonding orbitals.
- The MO theory successfully explains the bonding, bond order, and magnetic behaviour of both homonuclear and heteronuclear diatomic molecules.
- The theory also extends to polyatomic molecules, where symmetry and group orbital approaches help in understanding bonding.
- Qualitative MO descriptions for triatomic molecules like CO_2 and NO_2, and tetra-atomic molecules such as the carbonate ion (CO_3^{2-}), illustrate how electron delocalization leads to molecular stability and equivalent bond lengths.

K 2.8 ANSWERS TO CHECK YOUR PROGRESS

Answer to Q1: Molecular orbitals (MOs) are orbitals that extend over the entire molecule and describe the probability distribution of electrons influenced by all nuclei of the molecule. In contrast, atomic orbitals (AOs) belong to a single atom and are influenced by only one nucleus.

Answer to Q2: The Linear Combination of Atomic Orbitals (LCAO) approach is a method used to construct molecular orbitals by mathematically combining the atomic orbitals of the participating atoms.

Answer to Q3: Constructive interference occurs when two atomic orbitals with the same phase overlap, resulting in increased electron density between the nuclei and formation of a bonding molecular orbital. Destructive interference occurs when two atomic orbitals with opposite phases overlap, resulting in a decrease in electron density between the nuclei and formation of an antibonding molecular orbital.

Answer to Q4: The normalization constant (N) ensures that the total probability of finding the electron in all space is equal to unity.

Answer to Q5: According to Molecular Orbital (MO) theory, O_2 has two unpaired electrons in the degenerate antibonding π^* (2p) orbitals.
The electronic configuration is:

$$KK\ \sigma_{2s^2}\ \sigma^*_{2s^2}\ \sigma_{2pz^2}\ \pi_{2px^2}\ \pi_{2py^2}\ \pi_{2px^1}\ \pi^*_{2py^1}$$

Since there are unpaired electrons, O_2 exhibits **paramagnetism** (it is attracted to a magnetic field).

Answer to Q6: In **Be_2**, each Be atom has 4 electrons → total 8 electrons.
According to MO theory, filling order:

$\sigma_{1s^2}, \sigma^*_{1s^2}, \sigma_{2s^2}, \sigma^*_{2s^2}$

Bond order = ½ ($N_b - N_a$)
= ½ (4 − 4)
= 0

Answer to Q7: Bond order (B.O.) is defined as:

$$\text{Bond Order} = 1/2(N_b - N_a)$$

where:
N_b = number of electrons in bonding orbitals
N_a = number of electrons in antibonding orbitals

Answer to Q8: In heteronuclear molecules, the combining atoms have different electronegativities and ionisation energies, which means their atomic orbitals possess different energies. According to molecular orbital (MO) theory, effective combination of atomic orbitals requires comparable energies and proper symmetry. Since the atomic orbitals of the more electronegative atom are lower in energy, they contribute more significantly to the bonding molecular orbital. Conversely, the less electronegative atom, having higher-energy orbitals, contributes more to the antibonding molecular orbital. As a result, the electron density in the bonding molecular orbital is not equally shared but is skewed toward the more electronegative atom, leading to polar character in the bond. Thus, unequal orbital energies directly cause unequal contributions from atomic orbitals in heteronuclear molecules.

Answer to Q9: Bonding molecular orbitals are formed by the constructive (in-phase) overlap of atomic orbitals. This overlap leads to an increase in electron density in the region between the two nuclei, which enhances the attractive electrostatic interaction between the negatively charged electrons and both positively charged nuclei. This increased electron density between the nuclei effectively reduces the potential energy of the system, making the bonding molecular orbital more stable and lower in energy compared to the original atomic orbitals.
Therefore, the stabilization arises from increased electron–nucleus attraction and reduced repulsion between the nuclei due to electron shielding.

Answer to Q10: Antibonding molecular orbitals are formed by destructive (out-of-phase) overlap of atomic orbitals. This results in a node (a region of zero electron density) between the two nuclei. Because electron density is depleted in the internuclear region, there is less electron–nucleus attraction to hold the nuclei together. At the same time, the positively charged nuclei experience greater repulsion due to insufficient shielding by electrons. This leads to an increase in the potential energy of the system, making antibonding orbitals higher in energy and less stable than both bonding molecular orbitals and the original atomic orbitals.

2.9 FURTHER READING

- Huheey, J. E.; Keiter, E. A.; Keiter, R. L. Inorganic Chemistry: *Principles of Structure and Reactivity*, 4th ed.; Pearson.
- Miessler, G. L.; Tarr, D. A. *Inorganic Chemistry*, 5th ed.; Pearson.

- Housecroft, C. E.; Sharpe, A. G. *Inorganic Chemistry*, 3rd ed.; Pearson.
- Lee, J. D. *Concise Inorganic Chemistry*, 4th ed.; Chapman and Hall.

M 2.10 MODEL QUESTIONS

Q1. Describe the LCAO–MO method for homonuclear diatomic molecules with suitable examples.
Q2. Discuss the MO diagram of nitric oxide (NO) and explain its magnetic behaviour.
Q3. Explain the MO description of hydrogen fluoride (HF).
Q4. Discuss the concept of s–p mixing in diatomic molecules.
Q5. Construct the molecular orbital diagram of N_2 and explain its bond order and magnetic properties.
Q6. Discuss the MO description of heteronuclear diatomic molecules with suitable examples.
Q7. Explain the qualitative molecular orbital description of CO_2.
Q8. Describe the MO diagram of NO_2 and explain its electronic structure.
Q9. Discuss the qualitative MO description of the carbonate ion (CO_3^{2-}) and explain the delocalization of π electrons.

UNIT 3: BONDING IN COORDINATION COMPOUNDS

UNIT STRUCTURE

3.1 Learning Objectives
3.2 Introduction
3.3 Types of Ligands
  3.3.1 Monodentate Ligands
  3.3.2 Bidentate Ligands
  3.3.3 Ambidentate Ligands
  3.3.4 Polydentate Ligands
  3.3.5 Macrocyclic Ligands
3.4 Werner's Coordination Theory
3.5 Valence Bond Theory (VBT) of Coordination Compounds
3.6 Limitations of Werner's Theory and VBT
3.7 Let Us Sum Up
3.8 Answers to Check Your Progress
3.9 Further Reading
3.10 Model Questions

3.1 LEARNING OBJECTIVES

After studying this unit, you should be able to:

- classify ligands based on their mode of coordination
- explain the concepts of primary and secondary valency in coordination compounds
- describe Werner's coordination theory with suitable examples
- explain the bonding and geometry of coordination compounds using Valence Bond Theory
- identify the limitations of early bonding theories in coordination chemistry.

3.2 INTRODUCTION

Coordination chemistry is a fascinating and important branch of inorganic chemistry. It deals with the compounds in which a central metal atom or metal ion is surrounded by a number of ions or neutral molecules called ligands. Such compounds are known as coordination compounds and they constitute a significant area of modern inorganic research.

In coordination compounds, the metal ion and the ligands are held together by coordinate covalent bonds, where the ligand donates one or more pairs of electrons to the metal ion and they behave as Lewis bases. The metal ion, which acts as a Lewis

acid accepts these electron pairs to form the bonding interaction between the ligand and the metal ion.

To understand coordination compounds in a systematic manner, it is essential to study the types of ligands and the theories proposed to explain metal–ligand bonding. Over time, several theories have been developed to explain how ligands bond with metal ions and how the structures of coordination compounds are formed.

In this unit, you will first learn about the classification of ligands based on their mode of attachment to the metal ion. This will be followed by a discussion of two theories of coordination chemistry, namely Werner's Theory and the Valence Bond Theory (VBT). These theories laid the foundation for our present understanding of bonding in coordination compounds and continue to be of great educational importance.

3.3 TYPES OF LIGANDS

In coordination compounds, the metal ion is surrounded by ions or neutral molecules called **ligands**. The word "ligand" originates from the Latin verb "ligare," which means "to connect" or "to bind," well related to its role in binding to the metal ion. They form coordination covalent bonds by donating lone pair of electrons (Lewis base) to empty orbitals of the metal ion (Lewis acid). Simple ligands include small ions such as F^-, Cl^-, CN^-, small neutral molecules such as H_2O, NH_3, CO etc. Larger molecules such as $H_2NCH_2CH_2NH_2$ or $N(CH_2CH_2NH_2)_3$ or even macromolecules, such as porphyrin, crown ether etc also act as ligands in coordination chemistry.

On the basis of their charge, ligands are classified as anionic (negatively charged, e.g. Cl^-, Br^-, F^-, OH^-, etc), cationic (positively charged, e.g. NO^+, $N_2H_5^+$), or neutral ligands (ligands having no charge, e.g. NH_3, H_2O, CO, etc).

Based on the number of donor atoms through which they connect to the central metal ion, ligands can be further classified as monodentate ligands, bidentate ligands, polydentate ligands, ambidentate ligands, macrocyclic ligands etc.

3.3.1 Monodentate Ligands

Monodentate ligands are ligands that bind to the central metal ion through only one donor atom. These types of ligands donate a single pair of electrons to the metal ion and form one coordinate bond. Since they attach through a single point, they are also known as unidentate ligands.

Common examples of monodentate ligands include anions such as Cl^-, Br^-, F^-, OH^- and CN^-, and neutral molecules such as H_2O, NH_3 and CO etc. In all these cases, the ligand uses one atom to donate a lone pair of electrons to the metal ion. Common examples include $[Co(NH_3)_6]^{3+}$ (ammine), $[Fe(H_2O)_6]^{3+}$(aqua), $[Cu(Cl)_4]^{2-}$ (chlorido), and $[Ni(CO)_4]$ (carbonyl) etc.

3.3.2 Bidentate Ligands

When the ligands possess two donor sites and can simultaneously coordinate to the same metal ion through both the donor sites, they are called bidentate ligands. A bidentate ligand forms two coordinate covalent bonds with the metal ion.
The most common example of a bidentate ligand is ethylenediamine (en), $H_2NCH_2CH_2NH_2$, which coordinates through its two nitrogen atoms. Another important bidentate ligand is the oxalate ion ($C_2O_4^{2-}$), which binds through its two oxygen atoms.

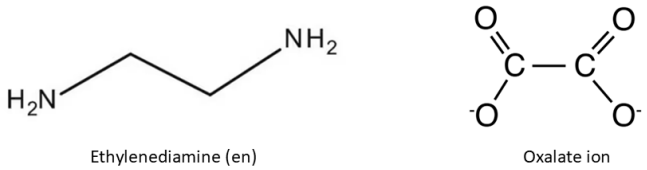


Fig 3.1: Examples of bidentate ligands (a) ethylenediamine (en) and (b) oxalate ion ($C_2O_4^{2-}$)

3.3.3 Polydentate Ligands

Polydentate ligands are ligands that possess more than two donor atoms and can attach themselves to the same metal ion through several coordination sites simultaneously. Depending on the number of donor atoms involved, polydentate ligands may be tridentate, tetradentate, pentadentate or hexadentate.

Example of polydentate ligand includes diethylenetriamine (dien), which is a tridentate ligand and you can see from the figure how it coordinates through three nitrogen atoms (Fig 3.2).

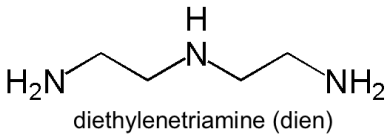


Fig 3.2: A tridentate ligand diethylenetriamine (dien)

A well-known hexadentate ligand is ethylenediaminetetraacetate ion ($EDTA^{4-}$), which can bind to a metal ion through six donor atoms (two nitrogen and four oxygen atoms, see Fig 3.3).

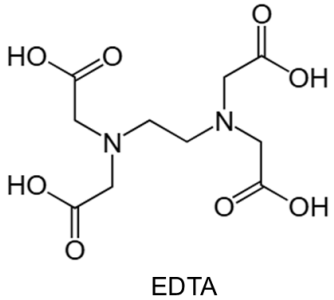


Fig 3.3: Hexadentate ligand ethylenediaminetetraacetate ion ($EDTA^{4-}$)

When these polydentate ligands coordinate to a metal ion, the resulting complexes are generally highly stable. This increased stability is explained by the chelate effect, which is an important concept in coordination chemistry and finds wide applications in analytical chemistry, medicine and industry. The enhanced stability of chelate complexes is primarily attributed to thermodynamic factors, particularly the favourable entropy change associated with the replacement of several monodentate ligands by a single polydentate ligand. This phenomenon is conceptually significant in advanced coordination chemistry.

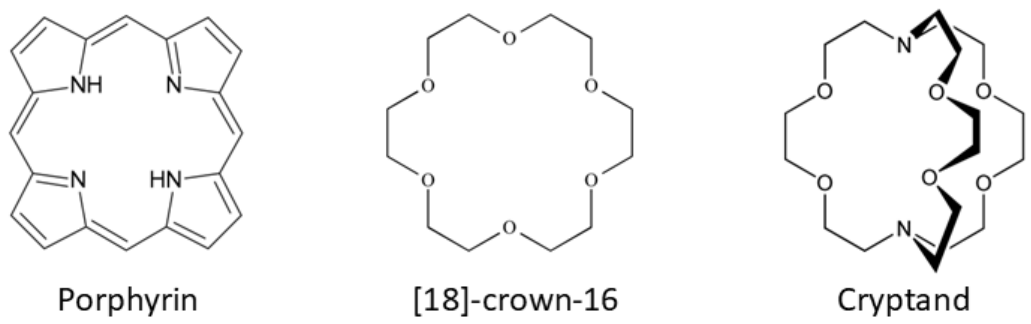
3.3.4 Ambidentate Ligands

Some ligands contain more than one donor atom, but unlike bidentate ligands, they can coordinate to the metal ion through only one donor atom at a time. Such ligands are known as ambidentate ligands.

Common examples of ambidentate ligands include cyanide ion (CN^-), which can coordinate through either the carbon atom or the nitrogen atom, and nitrite ion (NO_2^-), which can bind through nitrogen or oxygen. However, at any given time, an ambidentate ligand attaches to the metal ion through only one of its possible donor atoms.
Thus, by examining the number and nature of donor atoms present in a ligand, we can understand how ligands bind to metal ions and how they influence the structure and properties of coordination compounds

3.3.5 Macrocyclic Ligands

These are special class of polydentate ligands. They contain large ring structures with donor atoms arranged in such a way that they can effectively surround a metal ion and form a complex. Examples of macrocyclic ligands include porphyrins, crown ethers, cryptands, etc (Fig 3.4). In these ligands, the donor atoms are held in a rigid cyclic framework, which allows the metal ion to fit into the cavity formed by the ligand. This leads to the formation of very stable complexes, often showing high selectivity for particular metal ions.



Porphyrin [18]-crown-16 Cryptand

Fig 3.4: Examples of macrocyclic ligands.

Macrocyclic ligands play a crucial role in biological systems. For instance, the porphyrin ligand is present in haemoglobin, myoglobin and chlorophyll, where it binds to iron and magnesium ions. Due to their high stability and selectivity, macrocyclic ligands are also widely used in catalysis, ion transport and molecular recognition.

3.4 WERNER'S COORDINATION THEORY

Alfred Werner's coordination theory, proposed in 1893 was the first systematic theory to explain the bonding in coordination compounds. This theory provided a simple and systematic explanation and laid the foundation of modern coordination chemistry. According to Werner's theory, a metal ion in a coordination compound exhibits two different types of valencies: ***primary valency*** and ***secondary valency***.

Primary valency corresponds to the oxidation state of the metal. In compounds, these valencies are satisfied by the negative ions surrounding the metal ion. Primary valency is applicable to simple salts in the same manner as it is to coordination compounds. For example, in cobalt(III) chloride, $CoCl_3$, the primary valency of cobalt is three. In $[Co(NH_3)_6]Cl_3$, cobalt also has a primary valency of three, and this valency is satisfied by three chloride ions present outside the coordination sphere. These chloride ions are ionisable in solution.

The secondary valency corresponds to the number of ligands coordinated to the metal ion. This is also called coordination number. Ligands are generally neutral molecules or negative ions such as Cl^-, NH_3 etc. Less commonly, the ligands are positive ions. Thus, in $[Co(NH_3)_6]Cl_3$, the secondary valency is 6, satisfied by six NH_3 ligands whereas its primary valency is satisfied by three chloride ions.

The secondary valencies are non-ionisable and have a fixed spatial arrangement, giving rise to a definite geometry of the coordination compound. Werner further proposed that ligands satisfying the secondary valency are directly attached to the metal ion and are written inside square brackets, whereas ions satisfying the primary valency are written outside the square brackets.

To support his theory, Werner studied a series of cobalt(III) ammine complexes, such as $CoCl_3 \cdot 6NH_3$, $CoCl_3 \cdot 5NH_3$ and $CoCl_3 \cdot 4NH_3$. On the basis of conductivity measurements and precipitation reactions, he showed that these compounds differ in the number of chloride ions present outside the coordination sphere. For example, in the compound $[Co(NH_3)_6]Cl_3$, all three chloride ions are ionisable and lie outside the coordination sphere, whereas in $[Co(NH_3)_4Cl_2]Cl$, only one chloride ion is ionisable.

Werner also explained the geometry of coordination compounds by assuming fixed arrangements of secondary valencies. He proposed octahedral geometry for coordination number six and tetrahedral or square planar geometry for coordination number four. His theory successfully explained the existence of isomerism in coordination compounds, particularly geometrical and optical isomerism.

Although Werner's theory successfully explained composition and geometry, it did not provide an electronic explanation of bonding. This limitation became significant with the development of quantum theory and necessitated the formulation of more advanced

bonding models. However, it remains historically significant and forms the basis for more advanced theories such as the Valence Bond Theory and Crystal Field Theory.

3.5 VALENCE BOND THEORY OF COORDINATION COMPOUNDS

Till now, you have learned how Werner's theory successfully explained the composition and geometry of coordination compounds. However, this theory could not explain the nature of bonding interaction between the metal ion and ligands. To overcome this limitation, much work has been done to describe the bonding in coordination compounds and to rationalise and predict their properties. The first success among these was the Valence Bond Theory (VBT) which applies the principles of atomic orbital overlap to explain bonding in coordination compounds.

According to Valence Bond Theory, the formation of a complex involves the reaction between ligands (which acts as a Lewis base) and metal ions (acts as Lewis acid). The metal ions having empty orbitals accept the electron pairs donated by the ligands and form coordinate covalent bond (or dative bond) between them. Before bonding takes place, the metal ion undergoes hybridisation of its atomic orbitals (*s*, *p* and *d* orbitals) to form equivalent hybrid orbitals. It is important to note that d orbitals possess specific directional properties. Some d orbitals are oriented along the axes, while others lie between the axes. Since ligands approach the metal ion along definite directions, effective bonding requires suitable orientation and overlap between ligand orbitals and metal orbitals. This directional nature of d orbitals therefore plays an important role in determining the geometry of coordination compounds. These hybrid orbitals are directed towards specific positions in space, thereby determining the geometry and magnetic properties of the complex.

Let us consider the case of Pd(II) and Pt(II) complexes. You will observe that these metal ions usually form four-coordinate square planar complexes and are diamagnetic. A similar structural arrangement is often encountered in certain Ni(II) complexes as well.

Now, let us pause and think carefully.

The free metal ion in each of these cases has a d^8 electronic configuration, and in its ground state it corresponds to the term symbol ^3F. This indicates that the free ion possesses unpaired electrons and is therefore paramagnetic. However, the experimentally observed complexes are diamagnetic. This means that, during complex formation, the unpaired electrons undergo pairing.

Therefore, any acceptable bonding description must account for two important features: electron pairing within the d orbitals, and a geometry in which the ligand–metal–ligand bond angles are approximately 90°, characteristic of a square planar arrangement. Pauling suggested that this type of bonding arises through hybridisation involving one (n–1)*d* orbital, one *ns* orbital, and two *np* orbitals of the metal ion. These orbitals combine to form four equivalent dsp^2 hybrid orbitals, which are oriented towards the corners of a square, thereby giving rise to a square planar geometry.

Let us consider the complex $[PtCl_4]^{2-}$. In this case, the $5d_{x^2-y^2}$ orbital combines with the 6s orbital and the 6px and 6py orbitals and undergo hybridisation to form four equivalent dsp^2 hybrid orbitals. Each of these hybrid orbitals overlaps with a ligand orbital to form a σ (sigma) bond, with the electron pairs being donated by the ligands. The eight 5d electrons of the free Pt(II) ion are accommodated as paired electrons in the four hybridised metal d orbitals, resulting in a diamagnetic complex.

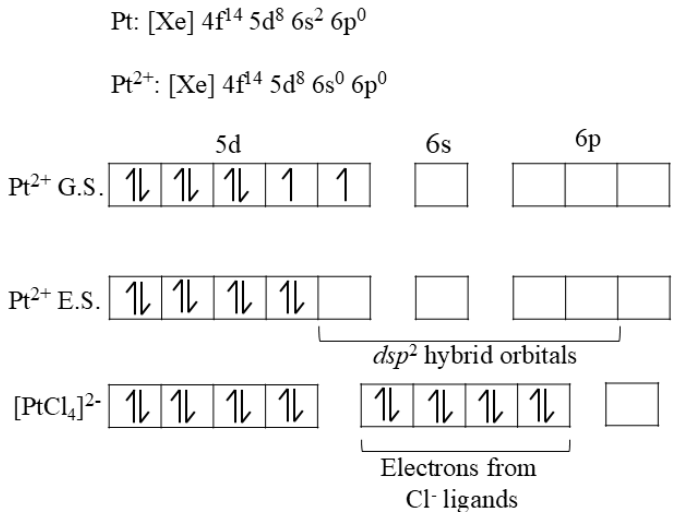


Fig. 3.5: Formation of the square planar $[PtCl_4]^{2-}$ complex through pairing of 5d electrons and dsp^2 hybridization in Pt(II).

When certain ligands, such as chloride ions (Cl^-), are coordinated to Ni(II), the metal ion forms four-coordinate complexes that are tetrahedral and paramagnetic. In such cases, Valence Bond Theory assumes that the d-orbital occupancy of the complex remains the same as that of the free metal ion. As a result, the valence-level d orbitals are not available for accepting electron pairs from the ligands.

To account for bonding in these complexes, hybridisation involves either:

- sp^3 or sd^3 orbitals (involving 4*p* (p_x, p_y, p_z) or 4*d* (d_{xz}, d_{yz}, d_{xy})) orbitals or
- using combinations of sp^3 or sd^3 orbitals

These hybrid orbitals provide the appropriate symmetry for σ bonding, while still allowing the presence of two unpaired electrons, thereby explaining the paramagnetic nature of such complexes.

From these examples, a useful generalisation emerges. This principle was originally referred to as the “magnetic criterion of bond type.” According to this, if the magnetic behaviour of a four-coordinate d^8 complex is known, its geometry can often be predicted:

- Diamagnetic complexes are generally square planar, and
- Paramagnetic d^8 complexes are generally tetrahedral.

Let us now extend the valence bond approach to six-coordinate octahedral complexes. In such complexes, bonding is explained using d^2sp^3 hybridisation of the metal ion. The specific d orbitals that satisfy the symmetry requirements for metal–ligand σ bonding

are the d_z^2 and $d_{x^2-y^2}$ orbitals. However, as in the case of four-coordinate d^8 complexes, the presence of unpaired electrons in some octahedral complexes makes the (n–1)*d* orbitals unavailable for bonding. For example, in the paramagnetic complex $[CoF_6]^{3-}$, the valence bond model proposes the participation of 4*s*, 4*p*, and 4*d* orbitals in hybridisation, leading to an **outer orbital octahedral complex**. In contrast, for the diamagnetic complex $[Co(NH_3)_6]^{3+}$, the $3d_z^2$ and $3d_{x^2-y^2}$ orbitals are vacant and participate in hybridisation along with the 4s and 4p orbitals, giving rise to an **inner orbital octahedral complex**.

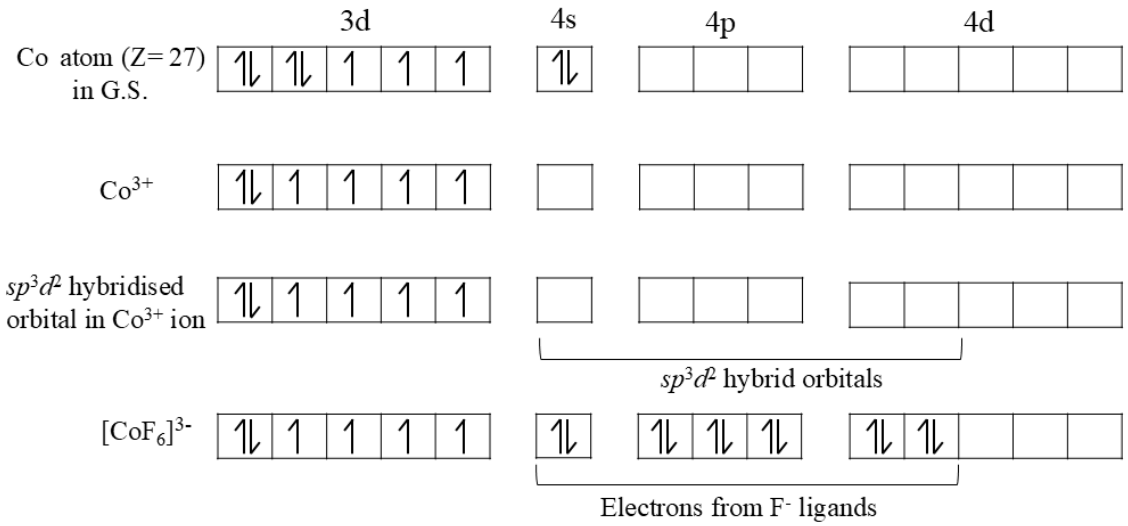


Fig. 3.6: Formation of the octahedral $[CoF_6]^{3-}$ complex through sp^3d^2 hybridization

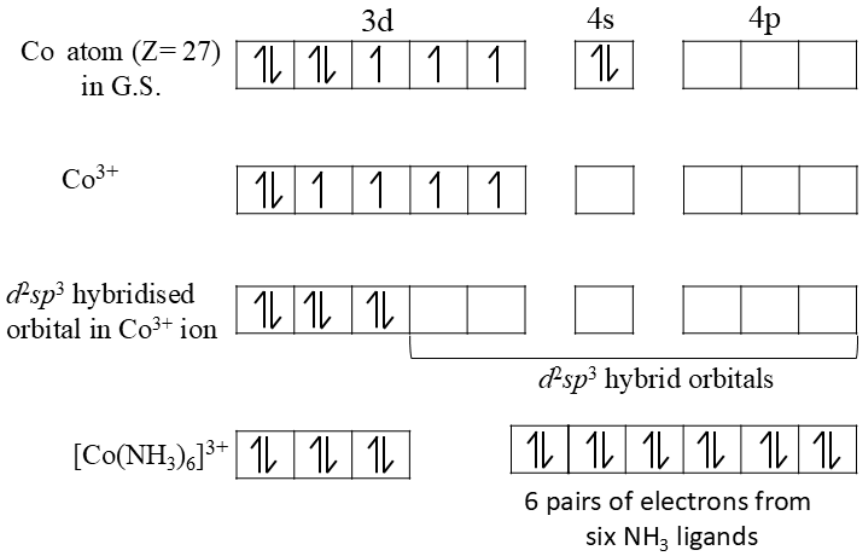


Fig. 3.7: Formation of the octahedral $[Co(NH_3)_6]^{3+}$ complex through d^2sp^3 hybridization in Co(III).

The distinction between inner-orbital and outer-orbital complex depends primarily on whether the metal ion is able to pair its *d*-electrons during complex formation. If electron pairing occurs, two of the inner $(n–1)d$ orbitals become vacant and are available for hybridisation along with the ns and np orbitals. Such complexes are described as inner-orbital complexes. On the other hand, if electron pairing does not occur, the inner $(n–1)d$ orbitals remain fully occupied and cannot participate in bonding. In this situation, the metal ion utilises the outer nd orbitals along with the ns and np orbitals to form hybrid orbitals, giving rise to outer-orbital complexes. This difference in orbital participation also explains the observed magnetic behaviour: inner-orbital complexes generally contain fewer or no unpaired electrons and are therefore diamagnetic or weakly paramagnetic, whereas outer-orbital complexes usually contain a greater number of unpaired electrons and are paramagnetic.

3.6 LIMITATIONS OF WERNER'S THEORY AND VALENCE BOND THEORY

Although Werner's theory and Valence Bond Theory significantly improved our understanding of coordination compounds, neither theory provides a complete description of bonding and properties. Werner's theory was a major milestone in the development of coordination chemistry, but it could not explain the nature of the metal–ligand bond in terms of atomic orbitals or electronic structure. It is essentially a structural theory and therefore cannot account for properties such as colour, magnetic behaviour or bond strength.

Valence Bond Theory, while improving upon Werner's ideas by introducing orbital overlap and hybridisation, also suffers from several limitations. It does not consider the splitting of d-orbitals in the presence of ligands and hence fails to explain the colour and electronic spectra of coordination compounds. Further, VBT does not provide any explanation for the spectrochemical series and cannot predict why certain ligands cause electron pairing while others do not.

The theory offers only a qualitative explanation of magnetic behaviour and does not allow quantitative prediction of pairing energy or magnetic moments. In addition, the distinction between inner-orbital and outer-orbital complexes, though useful for understanding magnetic properties, is not always supported by rigorous experimental evidence. Because of these limitations, Werner's theory and Valence Bond Theory were eventually supplemented by more advanced approaches such as Crystal Field Theory and Ligand Field Theory. Nevertheless, these theories remain important as they introduced key structural and bonding concepts in coordination chemistry.

W CHECK YOUR PROGRESS

Q1. What is meant by a ligand in coordination chemistry?

Q2. Why are ligands considered Lewis bases and metal ions considered Lewis acids?

Q3. How do ambidentate ligands differ from bidentate ligands? Give examples.

Q4. What is meant by the chelate effect?

Q5. What are macrocyclic ligands? Mention one biological example.

Q6. What are the two types of valencies proposed by Werner?

Q7. What does the primary valency of a metal ion represent?

Q8. What is meant by secondary valency?

Q9. Where are ligands and ionisable ions written in the formula of a coordination compound?

Q10. State True or False

a) Werner's theory explains the electronic structure of metal–ligand bonding.
b) Valence Bond Theory can satisfactorily explain the colour of coordination compounds.
c) VBT provides a quantitative explanation of magnetic moments.
d) The inner-orbital and outer-orbital distinction is always strongly supported by experimental evidence.
e) Crystal Field Theory was developed to overcome some limitations of VBT.

2 3.7 LET US SUM UP

In this unit, you have studied the following key concepts:

- Coordination compounds consist of a central metal ion bonded to ligands through coordinate covalent bonds.
- Ligands act as Lewis bases and donate lone pairs of electrons to metal ions, which behave as Lewis acids.
- Ligands can be classified:
  - On the basis of charge: anionic, cationic and neutral ligands.
  - On the basis of denticity: monodentate, bidentate, polydentate, ambidentate and macrocyclic ligands.
- Polydentate ligands form chelates, and the enhanced stability of such complexes is explained by the chelate effect.
- Macrocyclic ligands possess pre-organised cyclic frameworks and often form highly stable and selective complexes, especially in biological systems.
- Werner's Coordination Theory:
  - Introduced the concepts of primary and secondary valencies.
  - Explained ionisable and non-ionisable groups in coordination compounds.
  - Established coordination number and fixed spatial arrangement of ligands.
  - Accounted for geometrical and optical isomerism.
  - Did not explain bonding in terms of electronic structure.
- Valence Bond Theory (VBT):
  - Explains bonding using hybridisation of *s*, *p* and *d* orbitals.
  - Predicts geometry based on type of hybridisation (sp^3, dsp^2, d^2sp^3, etc.).
  - Explains magnetic behaviour qualitatively through presence or absence of unpaired electrons.
  - Introduces the concepts of inner-orbital and outer-orbital complexes.

- Applies the magnetic criterion of bond type, particularly for d^8 systems.

- Limitations of Werner's Theory and VBT:
  - Werner's theory does not describe orbital interactions.
  - VBT does not explain colour, electronic spectra or the spectrochemical series.
  - Magnetic predictions are qualitative, not quantitative.
  - These limitations led to the development of Crystal Field Theory and Ligand Field Theory.

K 3.8 ANSWERS TO CHECK YOUR PROGRESS

Answer to Q1: A ligand is an ion or neutral molecule that binds to a central metal atom or metal ion by donating one or more pairs of electrons to form a coordinate covalent bonds.

Answer to Q2: Ligands donate lone pairs of electrons and therefore act as Lewis bases, while metal ions accept these electron pairs into their vacant orbitals and hence act as Lewis acids.

Answer to Q3: Ambidentate ligands have more than one donor atom but can coordinate through only one donor atom at a time, whereas bidentate ligands coordinate through two donor atoms simultaneously.

Answer to Q4: The chelate effect refers to the increased stability of complexes formed by polydentate ligands compared to similar complexes formed by monodentate ligands

Answer to Q5: Macrocyclic ligands are large cyclic ligands with donor atoms arranged in a ring that can surround a metal ion. Porphyrin, present in haemoglobin, is a biological example.

Answer to Q6: The two types of valencies are primary valency and secondary valency.

Answer to Q7: Primary valency represents the oxidation state of the metal ion and is satisfied by negative ions. It is ionisable in solution.

Answer to Q8: Secondary valency represents the coordination number of the metal ion and is satisfied by ligands. It is non-ionisable and has a fixed spatial arrangement.

Answer to Q9: Ligands satisfying secondary valency are written inside square brackets, while ions satisfying primary valency are written outside the brackets.

Answer to Q10: a) **False** (Werner's theory is structural and does not describe bonding in terms of orbitals or electronic structure)

b) **False** (VBT does not account for d-orbital splitting and electronic transitions responsible for colour)

c) **False** (It gives only a qualitative explanation based on unpaired electrons)

d) **False** (This distinction is not always experimentally verified in all cases)

e) **True** (CFT explains colour, spectra, and d-orbital splitting more effectively)

O 3.9 FURTHER READING

- Huheey, J. E.; Keiter, E. A.; Keiter, R. L. *Inorganic Chemistry: Principles of Structure and Reactivity*, 4th ed.; Pearson.
- Lee, J. D. *Concise Inorganic Chemistry*, 5th ed.; Wiley-Blackwell: Oxford, 1996.
- Miessler, G. L.; Fischer, P. J.; Tarr, D. A. *Inorganic Chemistry*, 5th ed.; Pearson: Boston, 2014.
- Cotton, F. A.; Wilkinson, G.; Murillo, C. A.; Bochmann, M. *Advanced Inorganic Chemistry*; Wiley.
- Prakash, S.; Tuli, G. D.; Basu, S. K.; Madan, R. D. *Advanced Inorganic Chemistry*; S. Chand & Company.

M 3.10 MODEL QUESTIONS

Q1.Classify ligands on the basis of denticity with suitable examples.

Q2.Explain Werner's coordination theory and its significance.

Q3.Describe Valence Bond Theory as applied to coordination compounds.

Q4.Discuss the limitations of VBT.

Q5.Mention limitations of Werner's coordination theory.

Q6.Differentiate between inner-orbital and outer-orbital complexes.

UNIT 4: CRYSTAL FIELD THEORY

UNIT STRUCTURE

4.1 Learning Objectives
4.2 Introduction
4.3 Crystal Field Theory (CFT)
4.4 *d*-Orbital Splitting in Different Geometries
4.4.1 Octahedral Complexes
4.4.2 Tetrahedral Complexes
4.4.3 Square Planar Complexes
4.4.4 Square Pyramidal Complexes
4.4.5 Trigonal Bipyramidal Complexes
4.5 Crystal Field Stabilisation Energy (CFSE), Pairing Energy, High-Spin and Low-Spin Complexes
4.6 Jahn–Teller Distortion
4.7 Spectrochemical Series
4.8 Nephelauxetic Effect and Nephelauxetic Series
4.9 Ligand Field Theory (LFT): An Overview
4.10 Let Us Sum Up
4.11 Answers to Check Your Progress
4.12 Further Reading
4.13 Model Questions

4.1 LEARNING OBJECTIVES

After studying this unit, you should be able to:

- explain the basic principles of Crystal Field Theory (CFT).
- describe d-orbital splitting in different geometries like octahedral, tetrahedral, square planar, square pyramidal, and trigonal bipyramidal complexes.
- calculate Crystal Field Stabilisation Energy (CFSE) and relate it to pairing energy and spin states (high-spin and low-spin).
- discuss Jahn–Teller distortion and its consequences.
- interpret the spectrochemical series and the nephelauxetic effect.
- outline the limitations of CFT and the basic concept of Ligand Field Theory (LFT).

4.2 INTRODUCTION

In the previous units, you have already studied Werner's Theory and Valence Bond Theory of coordination compounds, which helped you to understand the basic concepts of bonding in coordination compounds. However, as we have seen, these theories

have certain limitations, particularly in explaining properties such as colour, magnetic behaviour and stability of complexes; Crystal Field Theory (CFT) provides answers to many of these questions. In this unit, we shall study Crystal Field Theory in a step-by-step and discussion-oriented manner. This theory explains the interaction between a central metal ion and surrounding ligands in terms of electrostatic forces. A key outcome of this interaction is the splitting of the five degenerate *d*-orbitals of the metal ion into sets of different energies, depending on the geometry of the complex. Understanding *d*-orbital splitting patterns in common geometries such as octahedral, tetrahedral, square planar, square pyramidal, and trigonal bipyramidal forms the basis for interpreting the electronic configuration and properties of coordination compounds.

Building on this foundation, the unit introduces the concept of Crystal Field Stabilisation Energy (CFSE), which provides a quantitative measure of the stability of a complex arising from d-orbital splitting. The roles of pairing energy and the distinction between high-spin and low-spin complexes are also discussed to help learners analyse the factors governing electron distribution in metal complexes.

The unit further explores structural distortions through the Jahn–Teller effect, which accounts for deviations from ideal geometry in certain electronically degenerate systems. The spectrochemical series is presented to classify ligands according to their field strength, thereby enabling prediction of splitting magnitude and spin states. Additionally, the nephelauxetic effect is discussed to highlight the limitations of purely ionic models and to introduce the concept of covalency in metal–ligand bonding.

4.3 CRYSTAL FIELD THEORY

In 1929, Hans Bethe proposed the Crystal Field Theory, which provided an alternative approach to the Valence Bond Theory and offered improved explanations for several properties of coordination compounds.

In Crystal Field Theory, the bonding between the metal ion and surrounding ligands is treated as an electrostatic interaction, with no explicit consideration of covalent effects. This means that ligands behave either as point charges (in the case of anions like Cl^- or CN^-) or as point dipoles (in the case of neutral ligands like NH_3 or H_2O). Although the basic assumption of this theory is somewhat unrealistic, it is highly successful in explaining many important properties of coordination complexes. This electrostatic model provides a useful starting point for understanding modern theories of coordination chemistry.

In order to study the crystal field theory, let us first recall the *d*-orbitals, which are degenerate for an isolated, gaseous metal ion. The most convenient representation of the d-orbitals is shown in **Fig. 4.1**.

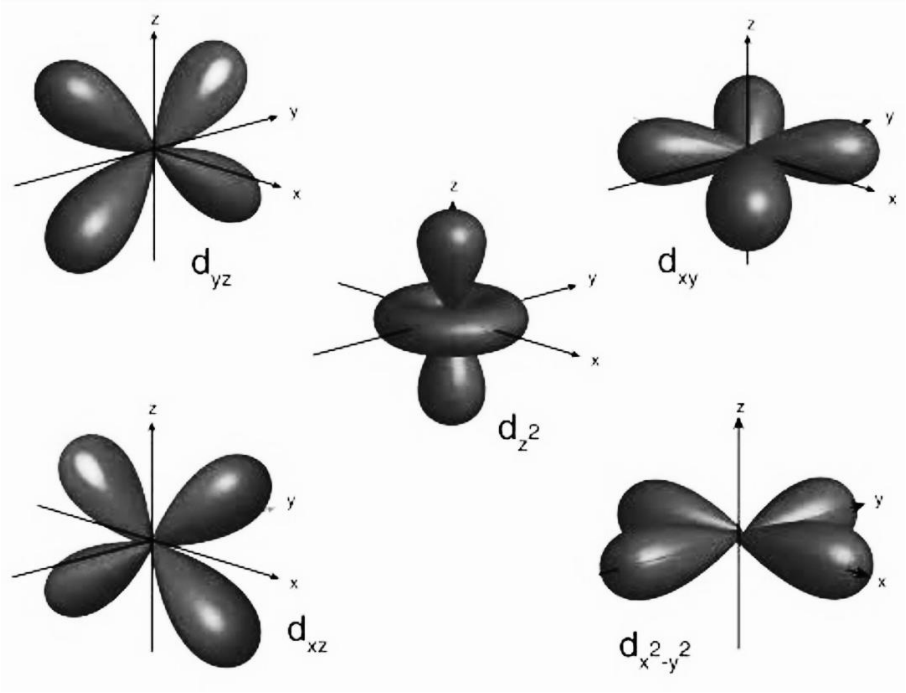


Fig. 4.1. Shapes and orientations of five *d*-orbitals.

4.4 *d*-ORBITAL SPLITTING IN DIFFERENT GEOMETRIES

If a spherically symmetrical field of negative charge is placed around a metal ion, all the five d-orbitals remain degenerate. However, due to electrostatic repulsion between the negative charge of the field and the electrons present in the d-orbitals, the energy of all the orbitals will be raised equally.

When this field arises due to the influence of real ligands, such as anionic ligands or the negative ends of dipolar ligands like NH_3 or H_2O, the field is no longer spherically symmetrical. As a result, the degeneracy of the *d*-orbitals is removed and the orbitals split into groups of different energies. This splitting of the *d*-orbitals and its consequences is the heart of Crystal Field Theory. The extent and pattern of splitting depend on geometry and type of ligands. You should remember that CFT does not explicitly consider covalent bonding. This limitation will be addressed later through Ligand Field Theory.

4.4.1 Octahedral Complexes

The most common geometry observed in coordination compounds is the octahedral geometry. In an octahedral arrangement, six ligands approach the metal ion along the three Cartesian axes (*x*, *y* and *z*). For simplicity, we first consider that the ligands are symmetrically positioned along the axes and the metal ion is at the centre. When ligands approach the metal ion, electrostatic repulsion occurs between the electron pairs of the ligands and the d-electrons of the metal ion. As a result, the energy of the metal d-orbitals increases relative to that of the free metal ion. To understand the splitting pattern, it is necessary to examine the shapes of the five *d*-orbitals (**Fig. 4.1**). The lobes of the $d_{x^2-y^2}$ and d_z^2 orbitals are oriented directly along the Cartesian axes,

whereas the lobes of the d_{yz}, d_{zx} and d_{xy} orbitals lie in between the axes. The orbitals lying along the axes experience stronger repulsion than those with lobes between the axes. The five *d*-orbitals will now split into two sets:

- The $d_{x^2-y^2}$ and d_z^2 orbitals form higher energy e_g set, and
- The d_{yz}, d_{zx} and d_{xy} orbitals form lower energy t_{2g} set

The energy separation in between these two sets of orbitals in an octahedral complex is denoted by Δ_o or 10 *Dq* (*o* in Δ_o is for octahedral; older references use 10 *Dq* instead of Δ_o). The three orbitals of the t_{2g} set lie 0.4 Δ_o below the barycentre (average energy level), whereas the other two orbitals $d_{x^2-y^2}$ and d_z^2 of e_g set are 0.6 Δ_o above the barycentre, as shown in **Fig. 4.2**.

For the three orbitals in the t_{2g} set, their total stabilization energy is given by:

$$-0.4\ \Delta_o \times 3 = -1.2\ \Delta_o$$

Similarly, the two orbitals in the e_g set together possess a total destabilization energy of:

$$+0.6\ \Delta_o \times 2 = +1.2\ \Delta_o$$

Thus, the total energy of the five *d* orbitals remains unchanged relative to the barycentre, although individual orbitals differ in their energy.

The magnitude of Δ_o depends on the nature of the metal ion, its oxidation state, and the type of ligands present.

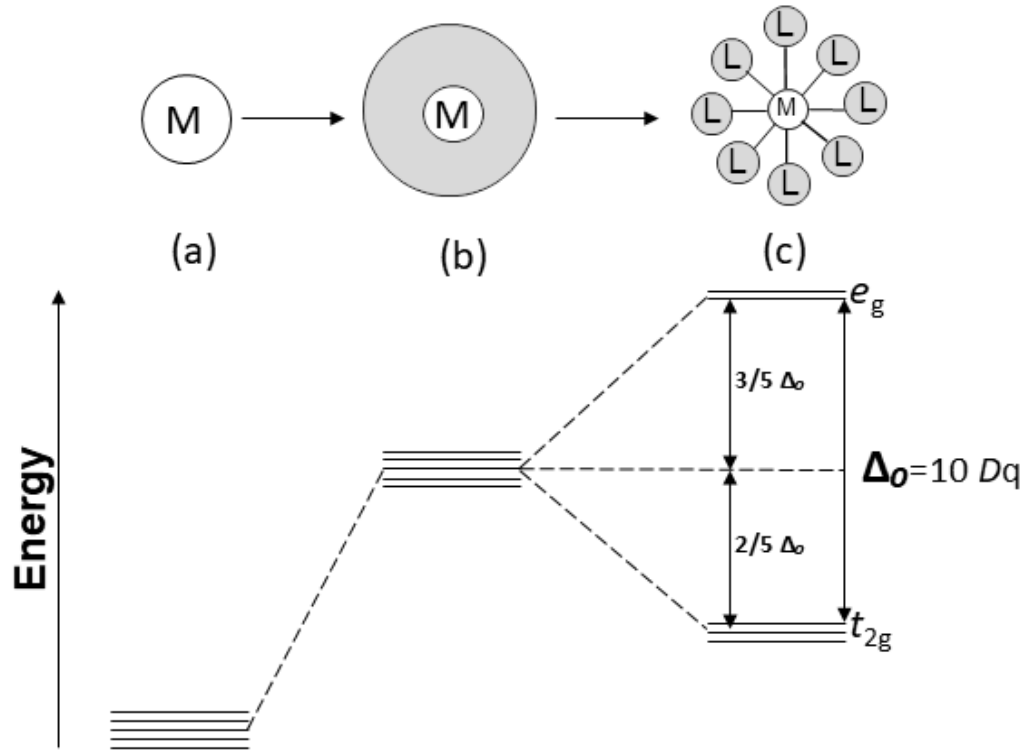


Fig. 4.2. *d*-orbital splitting in an octahedral environment: (a) all the five metal ion *d*-orbitals are degenerate and low in energy, (b) metal *d*-orbitals in presence of a spherical ligand field, (c) splitting of *d*-orbitals in octahedral environment.

4.4.2 Tetrahedral Complexes

Having discussed octahedral complexes, we now consider the tetrahedral complexes. When the metal ion is surrounded by four ligands, the two most common geometries observed for such coordination compounds are tetrahedral and square planar complexes. In this section, we will discuss how splitting of *d*-orbitals occurs in case of tetrahedral complexes. Here, unlike octahedral complexes, the four ligands do not directly approach the metal ion *d*-orbitals, instead they come closer to the orbitals that are directed to the edges of the cube. Hence, the orbitals d_{yz}, d_{zx} and d_{xy} (t_2 orbitals) whose lobes lie between the axes, experience greater repulsion and are raised in energy while the other two orbitals ($d_{x^2-y^2}$ and d_z^2, *e* orbitals) are stabilised relative to the barycentre and lowered in energy. Here, in a tetrahedral environment, the two sets of degenerate orbitals are represented as t_2 and *e* sets of orbitals (no *g*- subscripts) as tetrahedron geometry lacks centre of inversion.

Since the centre of gravity (barycentre) rule is obeyed, the upper set of orbitals (t_2 orbitals) is raised in energy by 0.4Δ, while the lower set of orbitals (*e* set) is stabilised by 0.6Δ with respect to the barycentre. As a result, the energy level diagram obtained is exactly the reverse of that observed for an octahedral field. The splitting of d-orbitals in a tetrahedral environment is shown in **Fig 4.3**. It is important to note that the extent of crystal field splitting in tetrahedral complexes is always smaller than that in corresponding octahedral complexes. This is because a tetrahedral complex contains only four ligands, which is two-thirds of the number present in an octahedral complex, and these ligands approach the metal ion in directions that interact less directly with the *d*-orbitals. On the basis of the point charge model, when the metal ion, ligands, and metal–ligand distances are the same, the crystal field splitting in a tetrahedral complex (Δ_t) is equal to 4/9 of the octahedral splitting (Δ_o). Because of this smaller splitting, the energy separation between the orbitals in tetrahedral complexes is generally insufficient to cause pairing of electrons. Consequently, tetrahedral complexes are usually high-spin, and low-spin configurations are rarely observed.

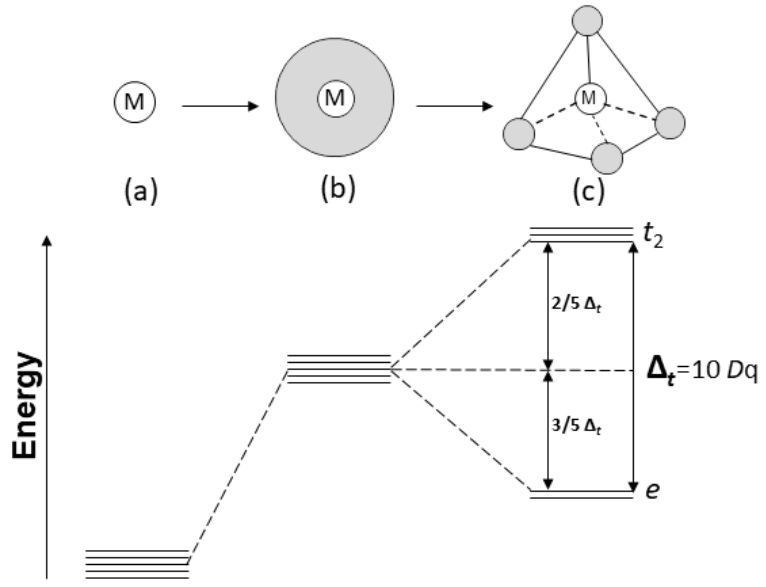


Fig. 4.3. *d*-orbital splitting in a tetrahedral environment: (a) all the five metal ion *d*-orbitals are degenerate and low in energy, (b) metal *d*-orbitals in presence of a spherical ligand field, (c) splitting of *d*-orbitals in tetrahedral environment.

4.4.3 Square Planar Complexes

To understand the *d*-orbital splitting in square planar complexes, let us first imagine an octahedral complex ML_6. If two ligands situated trans to each other (say, those lying along the *z*-axis) are moved either towards or away from the metal ion, the octahedral geometry undergoes a tetragonal distortion. When the two ligands along the *z*-axis are moved away from the metal ion (*z*-axis elongation), the metal–ligand interactions along the *z*-direction decrease. With increasing elongation, the repulsion between the metal ion and the axial ligands becomes progressively smaller. In the limiting case, when the two axial ligands are completely removed, the coordination number reduces from six to four, giving rise to a square planar complex, ML_4.

In a square planar field, the four ligands lie in the *xy*-plane. Consequently, the $d_{x^2-y^2}$ orbital, which points directly towards the ligands, experiences the maximum repulsion and attains the highest energy. The d_{xy} orbital also lies in the *xy*-plane and is raised in energy, but to a lesser extent. The d_{z^2} orbital, having its electron density mainly along the *z*-axis, is comparatively less affected and lies at a lower energy. The d_{xz} and d_{yz} orbitals, which do not point directly towards the ligands, experience the least repulsion and are the most stabilised (see **Fig 4.4**). Thus, the typical energy ordering in a square planar field is:

$$d_{x^2-y^2} > d_{xy} > d_{z^2} > d_{xz} \approx d_{yz}$$

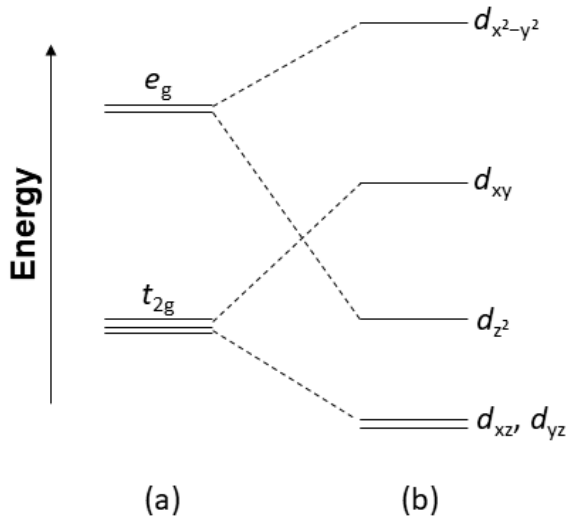


Fig. 4.4. *d*-orbital splitting in: (a) octahedral complex, (b) square planar complex.

Many d^8 metal ions, particularly those of Ni(II), Pd(II) and Pt(II), preferentially form square planar complexes in the presence of strong field ligands. Under these conditions, low-spin complexes are formed, in which the eight *d* electrons occupy the lower-energy d_{xz}, d_{yz}, d_{z^2}, and d_{xy} orbitals, while the highest-energy $d_{x^2-y^2}$ orbital remains unoccupied.

As the ligand field strength increases, the energy of the $d_{x^2-y^2}$ orbital is raised further. However, as long as this orbital remains vacant, the complex becomes increasingly stabilised, since the occupied lower-energy orbitals are correspondingly lowered in

energy. This redistribution of orbital energies results in an overall stabilisation of square planar complexes. Common examples of low-spin square planar d^8 complexes include $[Ni(CN)_4]^{2-}$, $[PdCl_4]^{2-}$, $[Pt(NH_3)_4]^{2+}$, $[PtCl_4]^{2-}$ and $[AuCl_4]^-$.

4.4.4 Square Pyramidal Complexes

The *d*-orbital splitting pattern in a square pyramidal complex is derived from an octahedral field by removing one ligand along the *z*-axis. This geometry consists of four ligands in the *xy*-plane and one ligand on the *z*-axis and can be considered as an intermediate between octahedral and square planar geometries. The orbital $d_{x^2-y^2}$ will be highest in energy as the lobes in this orbital point directly at the four ligands in the basal plane, causing the greatest electrostatic repulsion. Since there is only one ligand on the *z*- axis (compared to two in an octahedral field), the repulsion experienced by the d_{z^2} orbital is lower than that for $d_{x^2-y^2}$. Nevertheless, the repulsion is still appreciable because the axial ligand points directly towards this orbital (**Fig. 4.5**).

Although the d_{xy} orbital lies in the basal plane, its lobes are directed between the ligands and therefore experience less repulsion than the $d_{x^2-y^2}$ orbital. Hence, this orbital has an intermediate energy. The d_{xz} and d_{yz} orbitals point between the axes and have only partial interaction with the axial ligand. With a minimal interaction with the ligands, they possess lowest energy and are doubly degenerate (both are equal in energy). Thus, the typical energy ordering in a square pyramidal field is:

$$d_{x^2-y^2} > d_{z^2} > d_{xy} > d_{xz} \approx d_{yz}$$

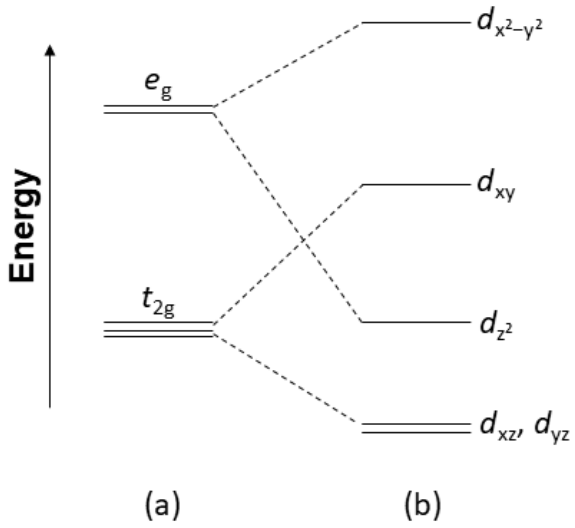


Fig. 4.5. *d*-orbital splitting in: (a) octahedral complex, (b) square pyramidal complex.

4.4.5 Trigonal Bipyramidal Complexes

In a trigonal bipyramidal geometry, the metal ion is surrounded by five ligands. Three ligands occupy the equatorial positions in the *xy*-plane at 120° to each other, while two ligands occupy the axial positions along the *z*-axis.

Because the ligands approach the metal ion in different directions, the five d-orbitals experience unequal repulsions and are split into three energy levels. These unequal ligand–metal interactions lead to a characteristic splitting pattern distinct from octahedral and tetrahedral fields. The d_{z^2} orbital is directed along the *z*-axis and points directly towards the two axial ligands. Hence, it experiences the maximum repulsion and is raised to the highest energy level. The $d_{x^2-y^2}$ and d_{xy} orbitals lie in the *xy*-plane and interact strongly with the three equatorial ligands. These two orbitals are therefore raised in energy but to a lesser extent than the d_{z^2} orbital. They form a degenerate set of intermediate energy. The d_{xz} and d_{yz} orbitals are oriented between the ligand directions and interact least with both axial and equatorial ligands. As a result, they experience the least repulsion and lie at the lowest energy level.

Trigonal bipyramidal splitting is generally smaller than octahedral splitting, and both high-spin and low-spin configurations may be observed depending on the metal ion and ligand field strength.

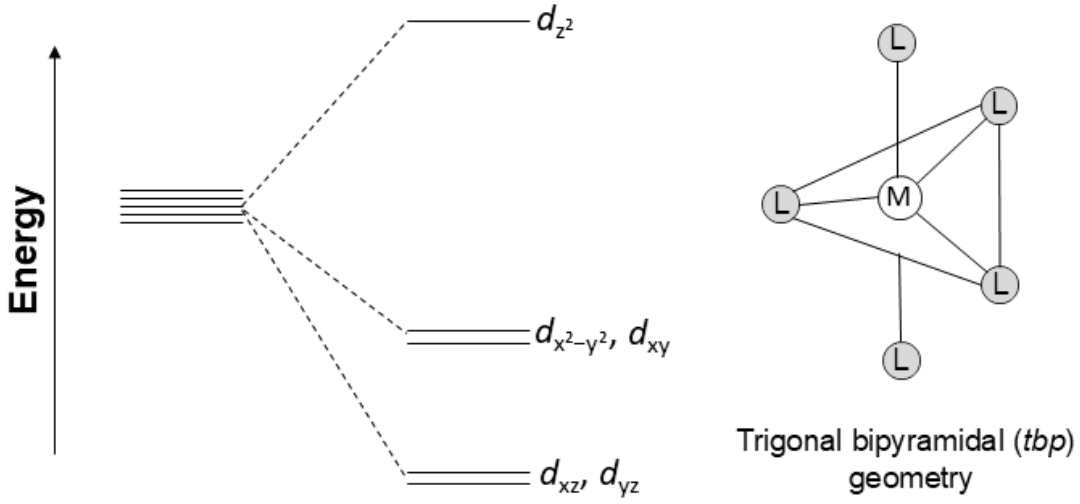


Fig. 4.6. *d*-orbital splitting in trigonal bipyramidal (*tbp*) complex

4.5 CRYSTAL FIELD STABILISATION ENERGY (CFSE), PAIRING ENERGY (P), HIGH-SPIN AND LOW-SPIN COMPLEXES

Till now we have learned how the degeneracy of the five d orbitals is removed due to electrostatic interactions between the ligands and the metal ion when ligands approach a metal ion. The *d*-orbitals split into sets of different energies depending on the geometry of the complex. The crystal field stabilisation energy (CFSE) is defined as the net difference in energy of the d electrons in a crystal field compared to their energy in a hypothetical spherical (uniform) field, in which all five *d*-orbitals are degenerate.

Let us first consider an octahedral complex where the five *d*-orbitals split into a lower-energy t_{2g} set and a higher-energy e_g set. Each electron occupying a t_{2g} orbital contributes −0.4 Δ_o to the CFSE, while each electron in an e_g orbital contributes +0.6 Δ_o. Therefore, CFSE for an octahedral complex is calculated using the expression:

CFSE = (number of t_{2g} electrons x −0.4 Δ_o) + (number of e_g electrons x +0.6 Δ_o)

In a tetrahedral field, as we have found that the splitting pattern is reversed and smaller in magnitude, each electron in the lower-energy orbitals contributes −0.6 Δ_t, while each electron in the higher-energy orbitals contributes +0.4 Δ_t.

Consider a metal ion having a d^1 electronic configuration placed in an octahedral ligand field. Since there is only one d-electron, it will occupy one of the three degenerate t_{2g} orbitals which lie at lower energy compared to the e_g orbitals. This electron will have an energy of –0.4 Δ_o with respect to the barycentre of the *d*-orbitals. Therefore, for a d^1 octahedral complex, the total crystal field stabilisation energy (CFSE) is –0.4 Δ_o and the complex is stabilised by 0.4 Δ_o relative to the hypothetical situation where no crystal field splitting occurs (*i.e.*, a spherical field).

For a d^2 metal ion in an octahedral ligand field, both electrons occupy the lower-energy t_{2g} orbitals. According to Hund's rule, the electrons enter separate t_{2g} orbitals with parallel spins. Each electron in a t_{2g} orbital contributes –0.4 Δ_o to the stabilisation energy. Therefore, the total CFSE for a d^2 octahedral complex is:

$$\text{CFSE} = 2 \times (-0.4\,\Delta_o) = -0.8\,\Delta_o$$

Thus, the complex is stabilised by 0.8 Δ_o relative to the spherical field.

Similarly, in a d^3 octahedral complex, all three electrons occupy the t_{2g} orbitals, one in each orbital and the total stabilisation energy becomes:

$$\text{CFSE} = 3 \times (-0.4\,\Delta_o) = -1.2\,\Delta_o$$

Hence, a d^3 octahedral complex shows a stabilisation of 1.2 Δ_o, which is the maximum CFSE for high-spin octahedral complexes without electron pairing.

When one more electron is added to the system, *i.e.* in the d^4 system, two possibilities are there: either the electron may enter the high energy e_g level (high spin) or it can pair with another electron in one of the t_{2g} orbitals (low spin). (**Fig 4.7**)

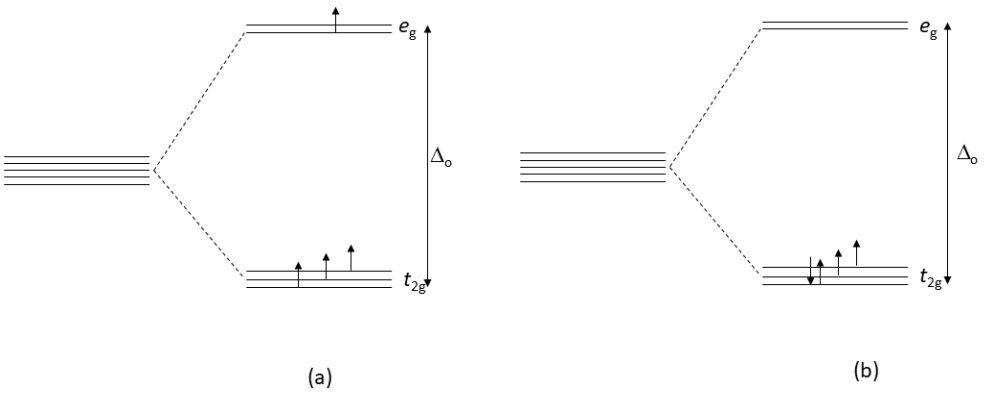


Fig. 4.7. Electronic configuration of d^4 system in (a) high-spin state, (b) low-spin state.

For the first case (**Fig 4.7a**), where three electrons occupy the t_{2g} orbitals and one electron enters one of the higher-energy e_g orbitals, CFSE will be:

$$\text{CFSE} = 3 \times (-0.4\,\Delta_o) + 1 \times (0.6\,\Delta_o) = -1.2\,\Delta_o + 0.6\,\Delta_o = -0.6\,\Delta_o$$

Thus, the net stabilisation is $0.6\,\Delta_o$.

In the second case (Fig 4.7b), the configuration will be t_{2g}^4 and the net stabilisation energy will be:

$$4 \times (-0.4\,\Delta_o) = -1.6\,\Delta_o + P$$

where P is called the **pairing energy**, which is the energy necessary to cause electron pairing in a single orbital.

The electronic arrangement actually adopted by a complex is the one that has the minimum overall energy and will be determined by the relative values of the octahedral crystal field splitting energy (Δ_o) and the pairing energy (P). If Δ_o is smaller than P, electrons prefer to remain unpaired and occupy higher-energy orbitals. Such complexes are known as high-spin complexes. If Δ_o is greater than P, electrons pair up in the lower-energy orbitals. Such complexes are known as low-spin complexes. Generally, strong-field ligands form low-spin complexes, whereas weak-field ligands form high-spin complexes.

In case of weak field ligands, d^5 metal ions will form high spin complexes having the configuration $t_{2g}^3 e_g^2$ and CFSE will be zero. The stabilisation due to t_{2g} level is exactly balanced by the two electrons in the e_g level. However, with strong-field ligands, electrons pairing will occur in t_{2g} orbitals and two electron pairs will be formed. The CFSE becomes $5 \times (-0.4\,\Delta_o) + 2P = -2.0\,\Delta_o$, but the cost of pairing must be included.

When the splitting of the d-orbitals (Δ_o) is sufficiently large compared to the pairing energy (P), it becomes energetically more favourable for electrons to pair within the lower-energy t_{2g} orbitals rather than occupying the strongly unfavourable e_g level. In these strong field or low spin complexes, for metal ions with d^1 to d^6 configurations, all electrons are accommodated in the t_{2g} level and the e_g orbitals remain unoccupied. Because electrons are confined to the lower-energy orbitals, complexes containing four to seven d electrons exhibit greater crystal field stabilisation in strong-field environments compared to weak-field environments.

For example, consider the case of d^4, as we have discussed earlier, CFSE for a low spin configuration is $1.6\,\Delta_o$ compared to $0.6\,\Delta_o$ for high spin arrangement. A summary of the electronic configurations, crystal field stabilisation energies (CFSE), and the number of unpaired electrons for d^1 to d^{10} configurations, under both weak-field (high-spin) and strong-field (low-spin) conditions, is presented in the following table (**Table 4.1**)

Important Observations for Students

- High-spin = weak-field ligands (Δ_o < P)
- Low-spin = strong-field ligands (Δ_o > P)
- Spin-state difference occurs only for: d^4, d^5, d^6, d^7
- d^1–d^3 and d^8–d^{10} show **no spin-state difference** in octahedral complexes.
- Maximum CFSE (most stabilized low-spin case): d^6 low-spin.

Table 4.1. Crystal field effects for weak and strong field octahedral complexes

d^n	High-spin complex			Low-spin complex		
	Configuration	Unpaired Electrons	CFSE	Configuration	Unpaired Electrons	CFSE
d^1	$t_{2g}^1 e_g^0$	1	$-0.4\Delta_o$	$t_{2g}^1 e_g^0$	1	$-0.4\Delta_o$
d^2	$t_{2g}^2 e_g^0$	2	$-0.8\Delta_o$	$t_{2g}^2 e_g^0$	2	$-0.8\Delta_o$
d^3	$t_{2g}^3 e_g^0$	3	$-1.2\Delta_o$	$t_{2g}^3 e_g^0$	3	$-1.2\Delta_o$
d^4	$t_{2g}^3 e_g^1$	4	$-0.6\Delta_o$	$t_{2g}^4 e_g^0$	2	$-1.6\Delta_o$
d^5	$t_{2g}^3 e_g^2$	5	$0.0\Delta_o$	$t_{2g}^5 e_g^0$	1	$-2.0\Delta_o$
d^6	$t_{2g}^4 e_g^2$	4	$-0.4\Delta_o$	$t_{2g}^6 e_g^0$	0	$-2.4\Delta_o$
d^7	$t_{2g}^5 e_g^2$	3	$-0.8\Delta_o$	$t_{2g}^6 e_g^1$	1	$-1.8\Delta_o$
d^8	$t_{2g}^6 e_g^2$	2	$-1.2\Delta_o$	$t_{2g}^6 e_g^2$	2	$-1.2\Delta_o$
d^9	$t_{2g}^6 e_g^3$	1	$-0.6\Delta_o$	$t_{2g}^6 e_g^3$	1	$-0.6\Delta_o$
d^{10}	$t_{2g}^6 e_g^4$	0	$0.0\Delta_o$	$t_{2g}^6 e_g^4$	0	$0.0\Delta_o$

The electron-pairing energy (*P*) consists of two main components. The first component is due to electrostatic (coulombic) repulsion between electrons. When two electrons are forced to occupy the same orbital, this repulsion must be overcome, which requires energy. The magnitude of this repulsion generally decreases down a group in the periodic table, as the d-orbitals become larger and the electrons are more widely separated. The second component comes from the loss of exchange energy. Exchange energy is associated with electrons having parallel spins in different orbitals and contributes to the overall stability of a configuration. When electrons are forced to pair, their spins become antiparallel, leading to a reduction in exchange energy. For a given electronic configuration, the exchange energy is proportional to the number of electron pairs with parallel spins. Within a *d* subshell, the maximum exchange energy is present in the d^5 configuration, where the number of unpaired electrons is highest. Consequently, forcing electron pairing in d^5 systems results in a large loss of exchange energy. For this reason, d^5 complexes such as Mn^{2+} and Fe^{3+} commonly exist as high-spin complexes, even in the presence of moderately strong ligand fields.

4.6 JAHN-TELLER DISTORTION

The Jahn–Teller theorem states that any non-linear molecule or complex ion possessing a degenerate electronic ground state will undergo a distortion that removes the degeneracy and results in a more stable, lower-energy structure. In coordination chemistry, this effect is most commonly observed in octahedral complexes.

In an ideal octahedral complex, the five d orbitals split into two degenerate sets: the lower-energy t_{2g} set and the higher-energy e_g set. If these orbitals are unevenly occupied, particularly the e_g orbitals, the complex becomes electronically unstable. To reduce this instability, the metal–ligand bond lengths change slightly, leading to a distortion from perfect octahedral geometry.

The most common form of Jahn–Teller distortion in octahedral complexes is tetragonal distortion, in which two axial metal–ligand bonds either elongate or shorten relative to the four equatorial bonds. In an axial elongation, the axial bonds become longer and weaker, while the equatorial bonds become shorter and stronger. In an axial compression, the opposite effect is observed, although elongation is more common.

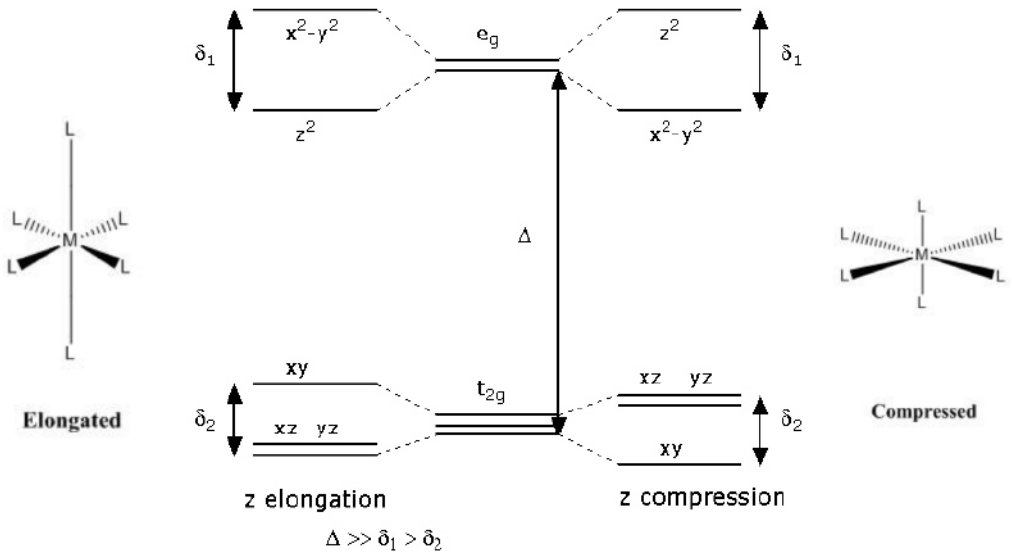


Fig. 4.8. Splitting of the e_g and t_{2g} orbitals in an octahedral crystal field under tetragonal distortion (changes in orbital energies for ***z*-axis elongation** and ***z*-axis compression**).

The Jahn–Teller effect is particularly strong in complexes with d^9 electronic configuration, such as Cu^{2+} complexes. In a d^9 octahedral complex, the e_g level is unevenly occupied, leading to significant destabilisation. Distortion lowers the energy of one e_g orbital relative to the other, thereby stabilising the complex. As a result, most octahedral Cu^{2+} complexes show pronounced tetragonal distortion.

Complexes with d^4 (high-spin) and d^7 (low-spin) configurations may also exhibit Jahn–Teller distortion, although the effect is usually weaker. In an octahedral field, a high-spin d^4 configuration has the electronic arrangement $t_{2g}^3e_g^1$, while a low-spin d^7 configuration corresponds to $t_{2g}^6e_g^1$. In both cases, the e_g level is unevenly occupied.

Since the e_g orbitals (d_{z^2} and $d_{x^2-y^2}$) are directed along the metal–ligand axes, this unequal occupancy produces electronic instability and gives rise to Jahn–Teller distortion. Strong Jahn–Teller distortion occurs when degeneracy involves e_g orbitals, because these orbitals are directed along the metal–ligand axes and therefore experience greater ligand repulsion.

The Jahn–Teller effect has important consequences for the geometry, spectra, and magnetic properties of coordination complexes. It influences electronic absorption spectra, causes splitting of spectral bands, and affects reactivity by altering metal–ligand bond strengths. The Jahn–Teller effect may be static, where a permanent structural distortion is observed and the differences in metal–ligand bond lengths are experimentally measurable. In contrast, in the dynamic Jahn–Teller effect, the complex rapidly interconverts between equivalent distorted geometries.

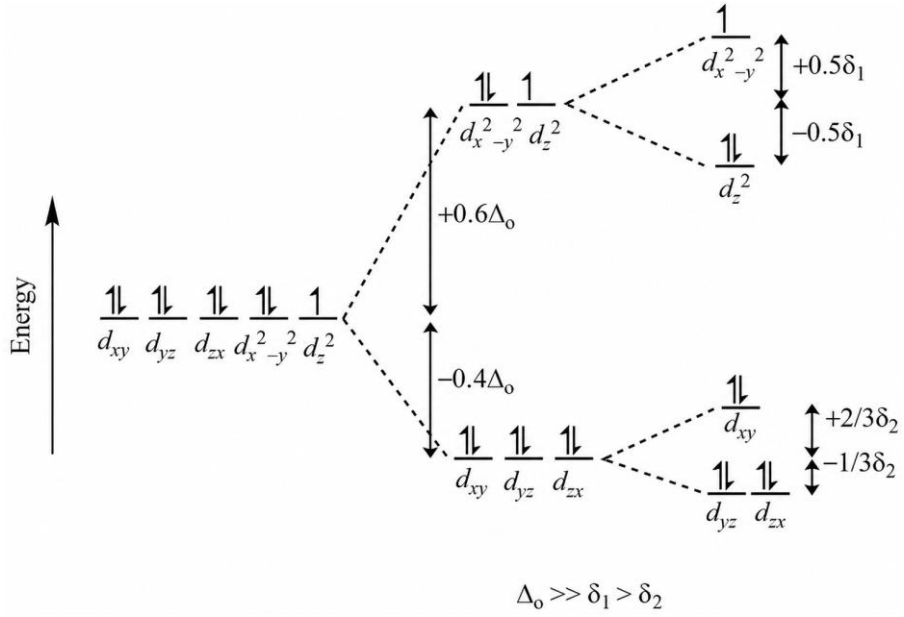


Fig. 4.9. Alteration of octahedral orbital energies (centre) under tetragonal distortion

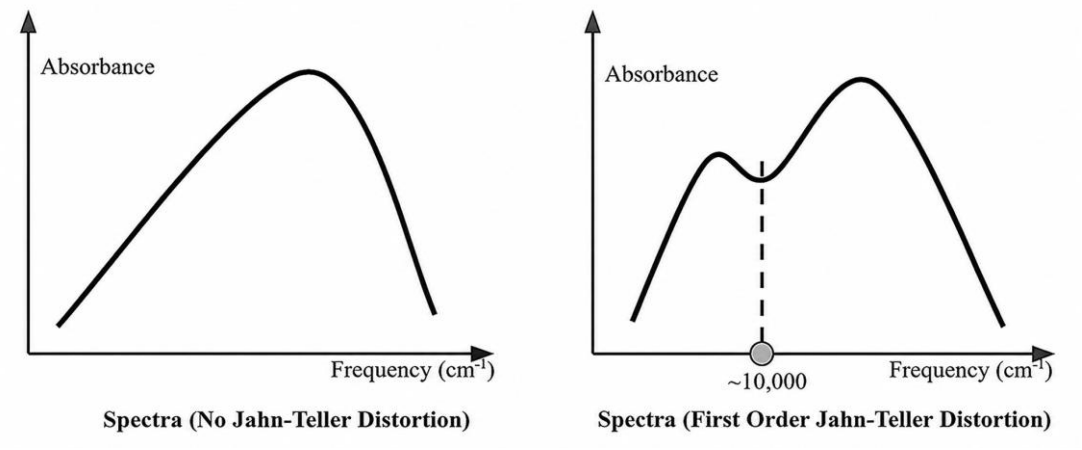


Fig. 4.10. Absorption spectra of a molecule undergoing first order Jahn-Teller distortion

4.7 SPECTROCHEMICAL SERIES

Experimental studies show that different ligands cause different extents of splitting of the metal *d*-orbitals. This difference in splitting is reflected in the colour, magnetic behaviour, and spin state of coordination complexes. On this basis, ligands are arranged in an empirical order known as the **spectrochemical series**, which ranks ligands according to their ability to produce crystal field splitting (Δ). This spectrochemical series is empirical and cannot be fully explained by simple crystal field theory; ligand field theory provides a more complete explanation.

The origin of the spectrochemical series lies in the nature of metal–ligand bonding. Ligands differ in their ability to donate and accept electron density to and from the metal. These interactions may involve σ donation, *π* donation, or *π* back-bonding, and each type of interaction influences the magnitude of Δ in a different way. Some ligands, such as ammonia (NH_3), donate electron density to the metal ion mainly through σ bonding using a lone pair of electrons. These ligands show little or no π interaction with the metal. For such ligands, the extent of d-orbital splitting depends largely on the energy match between the metal and ligand orbitals and the degree of orbital overlap. Among σ-donor ligands, ethylenediamine (en) produces a larger splitting than NH_3 due to stronger metal–ligand interaction and better orbital overlap. This trend generally parallels their relative donor strengths.

A second group of ligands contains filled p orbitals and can act as *π* donors in addition to σ donation. The electron density is transferred into the metal orbitals. This interaction reduces the crystal field splitting energy (Δ) and therefore favours high spin configuration. Common π-donor ligands include halide ions (F^-, Cl^-, Br^-, I^-) as well as H_2O, OH^-, and carboxylate ions (RCO_2^-). These ligands have ligand field strength in the order:

$$H_2O > F^- > RCO_2^- > OH^- > Cl^- > Br^- > I^-$$

In contrast, when some ligands possess vacant π* or d orbitals of suitable energy, they may accept electron density from the metal through π back-bonding. This interaction leads to a larger value of Δ. Ligands such as CO, CN^-, and aromatic nitrogen-donor ligands like phenanthroline (phen) are effective π acceptors. These ligands strongly favour low-spin configurations.

When ligands are arranged together combining their *σ*-donor, *π*-donor, and *π*-acceptor properties, the following spectrochemical series is obtained (from strong-field to weak-field ligands):

CO, CN^- > phen > NO_2^- > en > NH_3 > NCS^- > H_2O > F^- > RCO_2^- > OH^- > Cl^- > Br^- > I^-

Ligands placed higher in the series produce large d-orbital splitting (large Δ) and usually favour low-spin complexes. Ligands placed lower in the series produce small splitting (small Δ) and favour high-spin complexes.

4.8 NEPHELAUXETIC EFFECT AND NEPHELAUXETIC SERIES

The *nephelauxetic* series is the arrangement of ligands on the basis of their "*nephelauxetic* effect", a term frequently encountered in the chemistry of transition metal complexes. The term *nephelauxetic* is derived from a Greek word meaning "cloud-expanding". It refers to the expansion or spreading of the d-electron cloud of the metal ion when it forms a complex. As a result of this expansion, the repulsion between d electrons decreases compared to that in the free metal ion. This decrease in inter-electronic repulsion is reflected in a reduction of the Racah parameter B for the complex relative to that of the free metal ion. The extent of this reduction provides a measure of the covalent character of the metal–ligand bond. A larger decrease in the Racah parameter indicates greater covalency.

Different ligands cause different degrees of electron cloud expansion. On this basis, ligands can be arranged in an order known as the nephelauxetic series, which ranks ligands according to their ability to reduce inter-electronic repulsion in the metal ion. A commonly observed nephelauxetic series is:

$I^- > Br^- > S^{2-} > SCN^- > Cl^- > NO_3^- > F^- > OH^- > H_2O > NH_3 >$ en $> NO_2^- > CN^- > CO$

The nephelauxetic series is closely related to, but distinct from, the spectrochemical series. While the spectrochemical series is concerned with the ability of ligands to produce *d*-orbital splitting (Δ), the nephelauxetic series reflects changes in electron–electron repulsion and bond covalency. In general, ligands that are strong π acceptors tend to show a smaller nephelauxetic effect, whereas soft, polarizable ligands show a larger effect.

Thus, the nephelauxetic effect clearly reveals a limitation of Crystal Field Theory, since it provides evidence that metal–ligand bonding involves appreciable covalent character rather than being purely electrostatic.

4.9 LIGAND FIELD THEORY (LFT): AN OVERVIEW

Although Crystal Field Theory has been successful in explaining several important properties of coordination compounds, such as colour, magnetic behaviour, and crystal field stabilisation energy (CFSE), it has certain limitations. Experimental evidence, including electronic spectra, bond lengths, and spectrochemical trends, clearly indicates that metal–ligand bonding involves significant orbital overlap and electron sharing. The nephelauxetic effect also serves as indirect evidence that electrons are shared between the metal ion and the surrounding ligands. To account for these observations, it becomes necessary to go beyond the purely electrostatic approach of CFT.

Ligand Field Theory (LFT) extends Crystal Field Theory by incorporating molecular orbital concepts into the description of metal–ligand bonding. In LFT, ligands are treated as having orbitals that can overlap with the metal *d*, *s*, and *p* orbitals, leading to bonding and antibonding interactions. This approach provides a more realistic picture of bonding while retaining the useful framework of d-orbital splitting introduced by CFT.

Thus, Ligand Field Theory may be viewed as an extension and refinement of Crystal Field Theory, integrating molecular orbital principles into the description of metal–ligand bonding.

W CHECK YOUR PROGRESS

Q1. What is meant by *d*-orbital splitting in Crystal Field Theory? Why does it occur when ligands approach a metal ion?

Q2. Describe the pattern of *d*-orbital splitting in an octahedral complex. Name the orbitals in each set.

Q3. How does d-orbital splitting in a tetrahedral complex differ from that in an octahedral complex?

Q4. Why are most tetrahedral complexes high spin?

Q5. Fill in the blanks:

(a) In Crystal Field Theory, the metal–ligand interaction is treated as purely _____ in nature.

(b) In an octahedral field, the energy separation between the two sets of d-orbitals is denoted by _____.

(c) In a tetrahedral complex, the crystal field splitting (Δ_t) is equal to _____ of the octahedral splitting (Δ_o) when other factors remain the same.

(d) In a tetrahedral field, the orbitals that experience greater repulsion and are raised in energy belong to the _____ set.

(e) In a square planar complex, the orbital having the highest energy is _____.

(f) In a square pyramidal complex, the two lowest-energy orbitals are _____ and _____.

(g) In a trigonal bipyramidal complex, the orbital that experiences maximum repulsion due to axial ligands is _____.

Q6. What is meant by crystal field stabilisation energy (CFSE)?

Q7. Write the general expression for CFSE in an octahedral complex.

Q8. Calculate CFSE for high-spin and low-spin d^4 octahedral complexes.

Q9. For which *d*-electron configurations does pairing energy become significant in octahedral complexes?

Q10. State true or false**:**

(a) A d^3 octahedral complex has a CFSE of $-1.2\ \Delta_o$.

(b) High-spin complexes are formed when the pairing energy (P) is smaller than Δ_o.

(c) In a weak-field octahedral complex, a d^5 metal ion has a CFSE of $-0.6\ \Delta_o$.

(d) Spin-state differences in octahedral complexes occur only for d^4, d^5, d^6, and d^7 configurations.

(e) Pairing energy (P) includes contributions from both electrostatic repulsion and loss of exchange energy.

Q11. State the Jahn–Teller theorem.

Q12. Which electronic configurations in octahedral complexes commonly show a strong Jahn–Teller effect? Give one example.

Q13. What is the spectrochemical series?

Q14. What is meant by the nephelauxetic effect? What does it indicate about metal–ligand bonding?

Q15. State whether the following statement is true or false and justify your answer: "Ligands showing a strong nephelauxetic effect always produce high-spin complexes."

2 4.10 LET US SUM UP

- In this unit, you have studied the fundamental principles and applications of **Crystal Field Theory (CFT)** and its role in explaining the structure and properties of coordination compounds. CFT treats the metal–ligand interaction as purely electrostatic and explains how the degeneracy of the five d-orbitals of a free metal ion is removed when ligands approach in specific geometrical arrangements.
- You learned that the pattern and magnitude of **d-orbital splitting** depend on the geometry of the complex. In **octahedral complexes**, the *d*-orbitals split into lower-energy t_{2g} and higher-energy e_g sets separated by Δ_o.
- In **tetrahedral complexes**, the splitting pattern is reversed and smaller in magnitude ($\Delta_t = 4/9\ \Delta_o$), leading most tetrahedral complexes to be high spin.
- In **square planar complexes**, strong tetragonal distortion produces a large energy gap, often stabilising low-spin d^8 configurations.
- The splitting patterns in **square pyramidal** and **trigonal bipyramidal** geometries were also discussed, highlighting how unequal ligand interactions influence orbital energies.
- The concept of **Crystal Field Stabilisation Energy (CFSE)** was introduced as a quantitative measure of the stabilisation gained due to *d*-orbital splitting. You examined how CFSE is calculated for different d^n configurations and how it influences stability, magnetic behaviour, and geometry. The importance of **pairing energy (*P*)** in determining whether a complex is high spin or low spin was explained. Spin-state differences occur mainly for d^4 to d^7 configurations in octahedral complexes.
- The **Jahn–Teller effect** was discussed as a consequence of electronic degeneracy in non-linear complexes. Uneven occupancy of degenerate orbitals, particularly e_g orbitals in octahedral complexes (e.g., d^9 systems), leads to structural distortion and lowering of symmetry.
- The **spectrochemical series** was introduced as an empirical arrangement of ligands based on their ability to produce crystal field splitting (Δ). Ligands with strong *π*-acceptor ability generally produce large Δ values and favour low-spin complexes, whereas *π*-donor ligands produce smaller Δ and favour high-spin configurations.
- The **nephelauxetic effect** provided evidence that metal–ligand bonding is not purely ionic. The reduction in the Racah parameter (*B*) upon complex formation indicates expansion of the *d*-electron cloud and partial covalent character. This

limitation of CFT led to the development of **Ligand Field Theory (LFT)**, which incorporates molecular orbital concepts to provide a more complete description of metal–ligand bonding while retaining the useful framework of *d*-orbital splitting.

K 4.11 ANSWERS TO CHECK YOUR PROGRESS

Answer to Q1: In Crystal Field Theory, *d*-orbital splitting refers to the removal of degeneracy of the five *d*-orbitals of a metal ion in the presence of ligands. It occurs due to electrostatic repulsion between the electrons in the metal d orbitals and the ligand electron pairs approaching the metal ion.

Answer to Q2: In an octahedral complex, the five *d* orbitals split into two sets: (i) Lower-energy t_{2g} set (d_{xy}, d_{xz}, d_{yz}), and (ii) higher-energy e_g set ($d_{x^2-y^2}$, d_{z^2})

Answer to Q3: In a tetrahedral complex, the order of splitting is reversed compared to an octahedral complex. The ***e*** set (d_{z^2}, $d_{x^2-y^2}$) lies at lower energy, while the $\boldsymbol{t_2}$ set (d_{xy}, d_{xz}, d_{yz}) lies at higher energy. The magnitude of splitting (Δ_t) is smaller than that in octahedral complexes.

Answer to Q4: The crystal field splitting in tetrahedral complexes (Δ_t) is relatively small. As a result, the energy required for electron pairing is greater than the splitting energy, so electrons prefer to remain unpaired, leading to high-spin configurations.

Answer to Q5: (a) electrostatic (b) Δ_o (or 10 Dq) (c) 4/9

(d) t_2 (e) $d_{x^2-y^2}$ (f) d_{xz} and d_{yz}

(g) d_{z^2}

Answer to Q6: Crystal field stabilisation energy (CFSE) is the net lowering of energy of d electrons in a crystal field compared to their energy in a hypothetical spherical field in which all five *d* orbitals are degenerate.

Answer to Q7: CFSE = (number of t_{2g} electrons × $-0.4\Delta_0$) + (number of e_g electrons × $+0.6\Delta_0$)

Answer to Q8:

High-spin d^4: $t_{2g}^{\ 3}\ eg^1$ CFSE = $(3 \times -0.4\Delta_0) + (1 \times +0.6\Delta_0) = -0.6\Delta_0$

Low-spin d^4: $t_{2g}^{\ 4}$ CFSE = $4 \times (-0.4\Delta_0) = -1.6\Delta_0 + P$

Answer to Q9: Pairing energy becomes significant for d^4 to d^7 configurations, where both high-spin and low-spin arrangements are possible.

Answer to Q10: (a) True (b) False (c) False (d) True (e) True

Answer to Q11: The Jahn–Teller theorem states that any non-linear molecule in a degenerate electronic state will undergo a distortion to remove the degeneracy and attain a lower energy state.

Answer to Q12: Octahedral complexes with uneven occupancy of the e_g orbitals, such as high-spin d^4, low-spin d^7, and d^9 configurations, show a strong Jahn–Teller effect.
Example: $[Cu(H_2O)_6]^{2+}$ (d^9).

Answer to Q13: The spectrochemical series is an empirical arrangement of ligands in order of increasing crystal field splitting energy (Δ), based on their ability to split the d orbitals of a metal ion.

Answer to Q14: The nephelauxetic effect refers to the expansion (diffusion) of the *d*-electron cloud of a metal ion upon complex formation, resulting in reduced inter-electronic repulsion. It indicates that metal–ligand bonding has partial covalent character and is not purely ionic.

Answer to Q15: False. Ligands showing a strong nephelauxetic effect often have significant covalent character and may act as strong-field ligands, which can lead to low-spin complexes depending on the magnitude of Δ_0 relative to pairing energy.

O 4.12 FURTHER READING

- Huheey, J. E.; Keiter, E. A.; Keiter, R. L.; Medhi, O. K. *Inorganic Chemistry: Principles of Structure and Reactivity*, 4th ed.; Pearson.
- Miessler, G. L.; Tarr, D. A. *Inorganic Chemistry*, 5th ed.; Pearson.
- Housecroft, C. E.; Sharpe, A. G. *Inorganic Chemistry*, 4th ed.; Pearson Education: Harlow, 2012.

M 4.13 MODEL QUESTIONS

Q1. Discuss *d*-orbital splitting in octahedral complexes. Draw the splitting diagram for d^7 high-spin octahedral complex.
Q2. Explain the *d*-orbital splitting pattern in a square planar complex.
Q3. Compare the *d*-orbital splitting in square pyramidal and trigonal bipyramidal complexes.
Q4. What is pairing energy (*P*)? Why is it important in determining electronic configuration?
Q5. What is meant by tetragonal distortion in the context of the Jahn–Teller effect?
Q6. How does the position of a ligand in the spectrochemical series influence the spin state of a complex?
Q7. How does Ligand Field Theory differ from Crystal Field Theory in its treatment of metal–ligand bonding?
Q8. How does the nephelauxetic effect support the development of Ligand Field Theory?
Q9. Compare the extent of Jahn–Teller distortion in d^9, high-spin d^4, and low-spin d^7 configurations.
Q10. Explain why tetrahedral complexes are rarely low-spin, even when strong-field ligands are present.

UNIT 5: MOLECULAR ORBITAL THEORY OF TRANSITION METAL COMPLEXES

UNIT STRUCTURE

5.1 Learning Objectives
5.2 Introduction
5.3 Molecular Orbital (MO) Theory of Octahedral Complexes (ML_6, O_h)
5.4 Sigma Bonding in Tetrahedral Complexes (ML_4, T_d)
5.5 Sigma Bonding in Square Planar Complexes (ML_4)
5.6 Let Us Sum Up
5.7 Answers to Check Your Progress
5.8 Further Reading
5.9 Model Questions

5.1 LEARNING OBJECTIVES

After studying this unit, learners will be able to:

- Understand the fundamental concepts of Molecular Orbital (MO) Theory and explain how the linear combination of atomic orbitals leads to the formation of bonding, antibonding, and non-bonding molecular orbitals.
- Explain the molecular orbital description of bonding in transition metal complexes, particularly in octahedral, tetrahedral, and square planar geometries, using symmetry and ligand group orbitals.
- Describe the role of σ and *π* interactions in metal–ligand bonding, including the effect of *π*-donor and *π*-acceptor ligands on the electronic structure of coordination compounds.
- Apply MO theory to interpret the bonding characteristics and electronic structure of transition metal complexes, thereby gaining a deeper understanding of their chemical behaviour and stability.

5.2 INTRODUCTION

Understanding how atoms combine to form molecules is one of the fundamental objectives of chemistry. Several theoretical models have been developed to explain chemical bonding, among which Molecular Orbital Theory (MOT) provides one of the most comprehensive descriptions. This theory considers that when atoms approach each other, their atomic orbitals interact and combine to form molecular orbitals that extend over the entire molecule rather than remaining localized between individual atoms. As a result, electrons in a molecule are treated as being distributed throughout these molecular orbitals, giving a more realistic picture of bonding and electron distribution.

The formation of molecular orbitals occurs through the Linear Combination of Atomic Orbitals (LCAO) approach. According to this concept, atomic orbitals from different atoms combine mathematically to generate new orbitals called molecular orbitals. When two atomic orbitals combine, two molecular orbitals are produced. One of them is a bonding molecular orbital, which results from constructive overlap of orbitals and leads to an increase in electron density between the nuclei, thereby stabilizing the molecule. The other is an antibonding molecular orbital, which arises from destructive overlap and contains a nodal region between the nuclei, making it higher in energy and less stable. The stability of a molecule depends on the relative occupation of these bonding and antibonding orbitals. For effective formation of molecular orbitals, certain important conditions must be satisfied.

(a) The first requirement is that the interacting orbitals must have compatible symmetry with respect to the bonding axis. Orbitals that are oriented in a way that allows proper overlap can interact successfully, whereas orbitals with incompatible symmetry do not combine effectively.
(b) The second requirement is that the energies of the atomic orbitals should be comparable. If the energy difference between two orbitals is very large, their interaction becomes weak and the resulting overlap is negligible.
(c) A third important factor is the extent of overlap between orbitals, because greater spatial overlap leads to stronger bonding interactions and greater stabilization of the system.

These principles govern the formation and energy ordering of molecular orbitals in all chemical systems.

The concepts of Molecular Orbital Theory become particularly important in the study of transition metal complexes, where bonding involves interactions between the orbitals of a metal center and those of surrounding ligands. In such complexes, ligands usually donate lone pairs of electrons from their orbitals to the metal ion, while the metal contributes its available s, p, and d orbitals. The interaction of these orbitals leads to the formation of molecular orbitals that are distributed over both the metal and the ligands. The electrons occupying these orbitals determine many of the physical and chemical properties of the complex, including stability, colour, magnetism, and reactivity.

Earlier theories such as Valence Bond Theory and Crystal Field Theory were useful in explaining certain aspects of coordination compounds, but they provided only a partial description of metal–ligand bonding. Valence Bond Theory focuses mainly on hybridization and localized bonds, whereas Crystal Field Theory treats ligands as point charges and considers the interaction to be purely electrostatic. Experimental observations from various spectroscopic techniques have shown that the bonding in many coordination compounds contains a significant covalent component, which cannot be fully explained by purely ionic models. Evidence from methods such as electron spin resonance, nuclear magnetic resonance, nuclear quadrupole resonance, and the nephelauxetic effect demonstrates that electron density can be shared between the metal and the ligands. Molecular Orbital Theory accounts for these observations by allowing orbital mixing and electron delocalization across the entire complex.

In coordination compounds, two major types of metal–ligand interactions can be understood using this approach. The most common interaction is *σ* bonding, where ligand orbitals containing lone pairs overlap with metal orbitals along the metal–ligand axis. In addition to σ interactions, some ligands are capable of participating in π bonding, which involves sideways overlap of orbitals. Depending on the nature of the ligand, these interactions may involve donation of electron density from filled ligand orbitals to the metal or acceptance of electron density from the metal into empty ligand orbitals, a process often referred to as back bonding. Such interactions significantly influence the electronic structure and stability of transition metal complexes.

When the principles of Molecular Orbital Theory are applied to coordination compounds, the approach is often referred to as Ligand Field Theory, which combines the orbital interaction concepts of MOT with the symmetry considerations used in Crystal Field Theory. This framework provides a more realistic description of metal–ligand bonding by considering both electrostatic and covalent contributions. It also allows the construction of molecular orbital diagrams for different geometries such as octahedral, tetrahedral, and square planar complexes, helping students understand how orbitals interact in these common coordination environments. This theoretical framework therefore forms the foundation for understanding the electronic structure of coordination compounds and serves as the basis for the detailed discussion of molecular orbital diagrams for various geometries of transition metal complexes in the following sections.

5.3 MOLECULAR ORBITAL (MO) THEORY OF OCTAHEDRAL COMPLEXES (ML_6, O_h)

Octahedral complexes are among the most common coordination compounds formed by transition metals. In these complexes, a central metal atom or ion is surrounded by six ligands arranged symmetrically along the Cartesian axes, forming an octahedral geometry. Each ligand approaches the metal along the ±*x*, ±*y*, and ±*z* directions. Because of this highly symmetrical arrangement, the interactions between the orbitals of the metal and the ligands can be analyzed systematically using Molecular Orbital Theory.

In an octahedral complex, bonding arises from the interaction between the orbitals of the metal center and the orbitals of the six ligands. The ligands usually donate electron pairs from orbitals containing lone pairs, which interact with the available orbitals of the metal atom. The resulting molecular orbitals extend over both the metal and the ligands and determine the electronic structure of the complex.

Metal Orbitals Involved in Bonding

A transition metal atom possesses several valence orbitals that can participate in bonding. These include: one *s* orbital, three *p* orbitals (p_x, p_y, p_z), and five *d* orbitals (d_{xy}, d_{yz}, d_{zx}, $d_{x^2-y^2}$, d_{z^2}). Thus, the metal has nine valence orbitals available for interaction with ligand orbitals. The six ligands also contribute orbitals containing lone pairs that can overlap with the metal orbitals. However, not all metal orbitals interact equally with ligand orbitals. The possibility of interaction depends mainly on the symmetry and orientation of the orbitals relative to the approaching ligands. Each ligand donates an orbital containing a lone pair directed toward the metal center. Instead of treating these

six orbitals individually, they are combined into groups known as symmetry-adapted linear combinations (SALCs) or ligand group orbitals (LGOs). These combinations possess specific symmetry properties that match the symmetry of certain metal orbitals. In an octahedral complex, the six ligand orbitals combine to form sets of orbitals with different symmetries. Some of these combinations match the symmetry of the metal *s* and *p* orbitals, while others match the symmetry of certain d orbitals. Only orbitals with the same symmetry can interact and form molecular orbitals.

Sigma Bonding in Octahedral Complexes

The most basic interaction present in an octahedral complex is the σ-bonding between ligand orbitals and metal orbitals. Because the ligands approach the central metal ion directly along the metal–ligand axis, the lone pair orbitals of the ligands can overlap with the metal orbitals that are oriented along the octahedral bonding directions. This overlap results in the formation of σ bonds between the metal and the ligands.

In an octahedral environment, the symmetry of the metal atomic orbitals changes and these orbitals are classified into different symmetry sets. The *s* orbital of the metal corresponds to the a_{1g} symmetry, while the p orbitals transform as t_{1u}. Among the five d orbitals, the d_{xy}, d_{yz}, and d_{zx} orbitals belong to the t_{2g} set, whereas the $d_{x^2-y^2}$ and d_{z^2} orbitals form the e_g set. The a_{1g} orbital, which originates from the metal s orbital, possesses a spherical shape and therefore can overlap with LGOs along all axes. The orbitals belonging to t_{1u} and e_g symmetry are oriented along the coordinate axes, so they are able to participate in σ-bond formation along the octahedral bonding directions through overlap with the corresponding LGOs. In contrast, the t_{2g} orbitals are directed between the coordinate axes rather than along them. Due to this orientation, these orbitals are unable to overlap effectively with LGOs in order to form σ bonds. Consequently, among the nine valence orbitals of the metal, only six orbitals (one a_{1g}, three t_{1u}, and two e_g) take part in the formation of σ bonds. The t_{2g} orbitals therefore remain non-bonding molecular orbitals in octahedral complexes when there is no possibility of *π*-bonding. However, if the ligands possess orbitals with symmetry similar to that of the metal t_{2g} orbitals, then these metal orbitals can participate in π bonding interactions.

At this stage, an important question arises regarding the nature of LGOs and the method by which they are constructed. In an octahedral complex, each of the six equivalent ligand atoms contributes an atomic orbital or a hybrid atomic orbital for the formation of σ bonds with the metal center. These six orbitals are directed toward the metal along the six octahedral axes, namely $+x$, $-x$, $+y$, $-y$, $+z$, and $-z$. The orbitals directed along these axes are represented as σ_x, σ_{-x}, σ_y, σ_{-y}, σ_z, and σ_{-z}, respectively.

Construction of Ligand Group Orbitals (LGOs)

The combinations of these six ligand orbitals give rise to six LGOs, which possess symmetries that correspond to certain metal orbitals. These LGOs are classified according to the symmetry labels of the octahedral point group. One of these combinations has a_{1g} symmetry, which corresponds to the symmetry of the metal s orbital. This LGO can therefore interact with the metal a_{1g} orbital to produce bonding and antibonding molecular orbitals. Another set of ligand combinations possesses t_{1u} symmetry. Since the metal p orbitals (p_x, p_y, p_z) also belong to the t_{1u} symmetry set,

these ligand combinations can overlap with the metal *p* orbitals to form *σ*-bonding interactions.

A further pair of ligand combinations has e_g symmetry, which matches the symmetry of the metal $d_{x^2-y^2}$ and d_{z^2} orbitals. Thus, the six ligand orbitals combine to produce LGOs of a_{1g}, t_{1u}, and e_g symmetry, which are capable of interacting with the corresponding metal orbitals of the same symmetry.

However, none of the LGOs produced from *σ*-type ligand orbitals possess t_{2g} symmetry. As a consequence, the metal orbitals belonging to the t_{2g} set (d_{xy}, d_{yz}, d_{zx}) cannot interact with the ligand *σ* orbitals. Therefore, in a purely *σ*-bonding description, these orbitals remain non-bonding molecular orbitals.

Construction of Molecular Orbitals in Octahedral ML_6 Complexes (*σ*-Bonding)

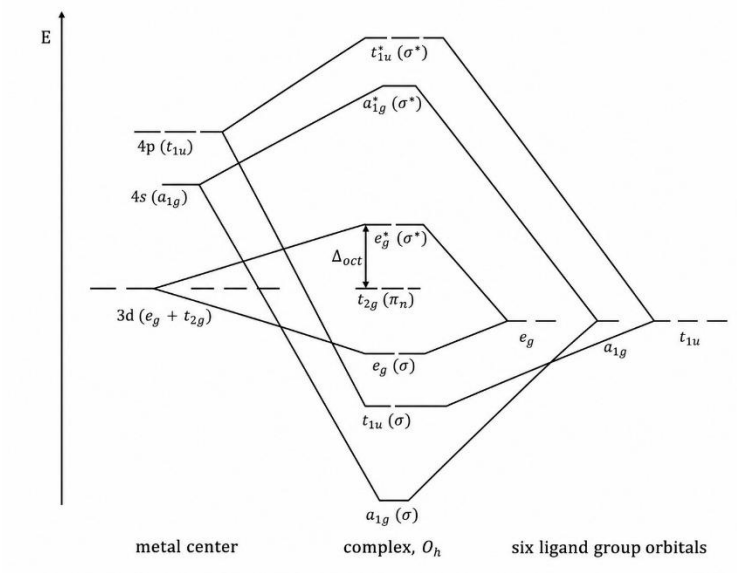


Fig. 5.1. MO diagram for an octahedral complex involving only *σ*-bonding.

After identifying the symmetry of metal orbitals and the ligand group orbitals (LGOs), the next step is the construction of the molecular orbital energy diagram for an octahedral complex.

To construct the molecular orbital diagram, the energy levels of the metal atomic orbitals are placed on the left-hand side, while the energy levels of the ligand group orbitals are placed on the right-hand side. The resulting molecular orbitals formed from their interaction are shown in the middle. In general, the energies of the ligand group orbitals are lower than those of the metal atomic orbitals. This occurs because the donor atoms in ligands (such as N, O, Cl *etc.*) are usually more electronegative than the metal center. As a result, the electrons in ligand orbitals are held more tightly and therefore lie at lower energy. Another important factor is the nature of the orbitals involved in bonding. In most ligands, the bonding orbitals are mainly *s* and *p* orbitals, which are relatively compact and strongly bound to the nucleus. In contrast, the metal orbitals involved in bonding often contain d orbitals, which are generally more diffuse and higher in energy. Because of these reasons, the ligand group orbitals are typically drawn below the metal orbitals in the energy diagram.

Once the relative energies are established, interactions between orbitals of matching symmetry can be considered. The metal a_{1g} orbital, which originates from the metal *s* orbital, interacts with the a_{1g} ligand group orbital. Since both orbitals possess the same symmetry, they can overlap effectively. This interaction produces two molecular orbitals: a bonding molecular orbital (a_{1g}) and an antibonding molecular orbital (a_{1g}^*). Because the metal *s* orbital and the ligand group orbital overlap very effectively, the splitting between a_{1g} and a_{1g}^* is relatively large. The bonding a_{1g} orbital lies at much lower energy, while the antibonding a_{1g}^* orbital lies at much higher energy. Next, the three metal *p* orbitals (t_{1u}), interact with the t_{1u} ligand group orbitals.

Since these orbitals are triply degenerate, their interaction produces: three bonding molecular orbitals (t_{1u}) and three antibonding molecular orbitals (t_{1u}^*). The metal d_{z^2} and $d_{x^2-y^2}$ orbitals belong to the e_g symmetry and interact strongly with the e_g ligand group orbitals, producing: two bonding molecular orbitals (e_g) and two antibonding molecular orbitals (e_g^*) (**Fig. 5.1**). The metal t_{2g} symmetry set is oriented between the coordinate axes rather than along them and hence they cannot overlap effectively with the *σ*-type LGOs. As a result, they do not participate in *σ*-bond formation and remain non-bonding molecular orbitals in a purely σ-bonding description. However, if ligands possess orbitals of appropriate symmetry, these t_{2g} orbitals may participate in *π* interactions. Thus, the molecular orbitals formed in an octahedral σ-bonding framework can be grouped as follows: (i) Bonding molecular orbitals (a_{1g}, t_{1u}, e_g), (ii) Non-bonding molecular orbitals (t_{2g}) and (iii) Antibonding molecular orbitals (e_g^*, t_{1u}^*, a_{1g}^*). The bonding orbitals are mainly ligand-centered, while the antibonding orbitals contain a greater metal character.

Energy Order of Molecular Orbitals:

The relative energies of the molecular orbitals depend on the nature of the ligands and the magnitude of the octahedral splitting parameter. The arrangement of orbitals also depends on whether the complex is low-spin or high-spin. When the ligand field splitting energy is large, the complex is classified as a low-spin complex. Under such conditions, the energies of the molecular orbitals generally follow the order:

$$a_{1g} < t_{1u} < e_g < t_{2g} < e_g^* < a_{1g}^* < t_{1u}^*$$

In this situation, electrons tend to occupy the lower-energy orbitals before entering the higher-energy antibonding orbitals. As an example, the complex $[Co(NH_3)_6]^{3+}$ contains eighteen valence electrons. Of these, twelve electrons are donated by the six ammonia ligands to the six bonding orbitals (a_{1g}, t_{1u}, e_g), while the remaining six electrons belong to the metal ion which occupy the t_{2g} orbital. So Δ_o assignment will be $t_{2g} \rightarrow e_g^*$. Here highest occupied molecular orbital (HOMO) is t_{2g} and LUMO is e_g^*.

In high spin complex like $[Co(F_6)]^{3-}$, the ligand field splitting energy is relatively small, the complex becomes a high-spin complex. In such cases, the energies of certain orbitals become closer, and electrons occupy them according to Hund's rule before pairing occurs. Here highest occupied molecular orbital (HOMO) will be e_g^* and LUMO is a_{1g}^*.

π-Bonding in Octahedral Complexes (ML_6)

The discussion of molecular orbital formation in octahedral complexes based only on σ-bonding provides an incomplete picture of the metal–ligand interaction. Many ligands possess orbitals that are capable of interacting with the metal through *π* bonding in addition to *σ* bonding. These interactions significantly influence the electronic structure, stability, and spectroscopic properties of transition metal complexes. *π* interactions arise when orbitals of suitable symmetry on the ligand overlap sideways with metal orbitals. These interactions may involve filled or empty orbitals on the ligand, depending on the nature of the ligand.

Before constructing the *π*-bonding molecular orbital diagram, it is useful to examine the different types of *π* interactions that can occur between metal and ligand orbitals.

(i) *dπ–pπ* Bonding: In this interaction, a metal *d* orbital of *π* symmetry overlaps with a filled *p* orbital of the ligand. Here the ligand donates electron density toward the metal through sideways overlap. Therefore, this type of interaction is commonly called *π*-donor interaction. Typical ligands showing *dπ–pπ* interaction include: F^-, Cl^-, Br^-, OH^-, OR^- etc. These ligands possess filled *p* orbitals which can donate electron density into the metal *d* orbitals.

(ii) *dπ–dπ* Bonding: In certain complexes, both the metal and ligand possess suitable d orbitals capable of interacting through sideways overlap. This interaction is described as d*π*–d*π* bonding. Here the filled d-orbitals of metal overlap with the empty orbitals of the ligands. Lligands such as R_3P, R_2S, R_3As have empty *d*-orbitals of *π* symmetry.

(iii) *dπ–π Bonding:** In this interaction, a metal *d* orbital overlaps with an empty antibonding *π** orbital of the ligand. This process involves back donation of electron density from the metal to the ligand and is known as *π* back-bonding. Typical ligands capable of accepting electron density through *π** orbitals include: CO, CN^-, NO^+, C_2H_4, N_2, ethylene, *etc*. These ligands are commonly referred to as *π*-acceptor ligands or *π*-acid ligands.

(iv) *dπ–σ Bonding:** In some cases, interaction may occur between a metal *d*-orbital and an antibonding *σ** orbital of the ligand. Although this interaction is generally weaker, it may contribute to bonding in certain complexes where suitable antibonding orbitals are available. The ligands having the empty *σ** orbitals are H_2, R_3P, alkanes, *etc*.

In an octahedral complex ML_6, each ligand possesses orbitals that can interact with the metal through *π* bonding. When the six ligands are considered together, their *π* orbitals combine to form ligand group orbitals (LGOs). For *π* interactions in an octahedral complex, twelve ligand orbitals participate because each ligand provides two orbitals capable of π interaction. These twelve orbitals combine to form LGOs of the following symmetries: t_{1g}, t_{2g}, t_{1u} and t_{2u}. These sets represent the symmetry-adapted combinations of ligand orbitals capable of *π* interaction. For *π* interaction to occur, the metal must possess orbitals having the same symmetry as the ligand group orbitals. In an octahedral complex, the metal orbitals with appropriate symmetry are: t_{1u} and t_{2g}. However, an important consideration must be noted. The t_{1u} orbitals originate from the

metal *p* orbitals, and these orbitals are already involved in *σ* bonding with the ligands. Since they are engaged in *σ* interactions along the metal–ligand axes, they are generally not available for *π* bonding. Therefore, in practice, only the metal t_{2g} orbitals (d_{xy}, d_{xz}, d_{yz}) are available for *π* interactions. Thus, the *π* bonding in octahedral complexes mainly involves interaction between ligand LGOs and the metal t_{2g} orbitals.

<u>*π* Bonding with Weak Field Ligands (*π*-Donor Ligands)</u>

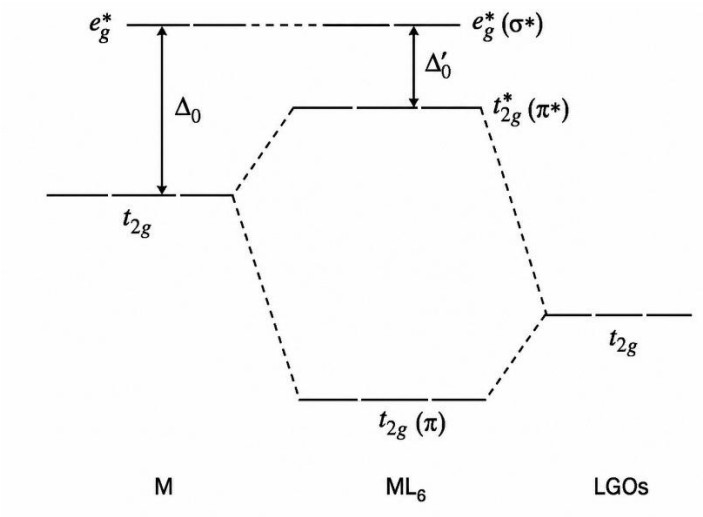


Fig. 5.2. Molecular orbital energy level diagram for octahedral ***π*-donor** complex (ML_6)

When ligands possess filled p orbitals, they can donate electron density into the metal t_{2g} orbitals. These ligands (F^-, Cl^-, Br^-, OH^-, OR^- etc.) behave as *π* donors. In this situation, the filled ligand *π* orbitals interact with the metal t_{2g} orbitals. This interaction produces a bonding molecular orbital of lowered energy mainly contributed by LGOs and an antibonding molecular orbital with increased energy mainly contributed by metal ion.

Because the ligand orbitals are already filled, the interaction tends to raise the energy of the metal t_{2g} orbitals. As a consequence, the t_{2g} level becomes higher in energy and consequently the crystal field splitting (Δ_0) becomes smaller (**Fig. 5.2**). For this reason, *π*-donor ligands are generally weak-field ligands and often produce high-spin complexes.

<u>*π* Bonding with Strong Field Ligands (*π*-Acceptor Ligands)</u>

Some ligands possess empty *π** orbitals that can accept electron density from the metal.

These ligands (CO, CN^-, NO^+, C_2H_4, N_2, ethylene *etc.*) are known as *π*-acceptor ligands.

In this case electron density is transferred from the metal t_{2g} orbitals to the empty ligand *π** orbitals. Because electron density is withdrawn from the metal t_{2g} orbitals, the energy of the t_{2g} level decreases. As a result, the energy gap between t_{2g} and e_g^* increases and therefore, the crystal field splitting (Δ_0) becomes larger (**Fig. 5.3**). Therefore, *π*-acceptor ligands usually produce strong-field complexes, which often exhibit low-spin configurations.

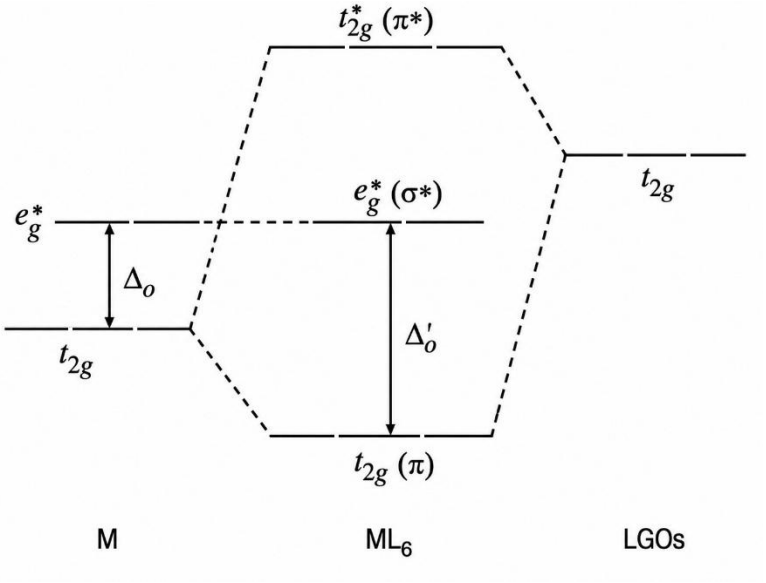


Fig. 5.3. Molecular orbital energy level diagram for octahedral ***π*-acceptor** complex.

5.4 SIGMA BONDING IN TETRAHEDRAL COMPLEXES (ML_4, T_d)

In tetrahedral complexes, the metal ion is surrounded by four ligands located at the corners of a tetrahedron. The ligands approach the metal along the directions that correspond to the tetrahedral axes, and therefore σ bonds are formed by direct overlap between ligand orbitals and suitable metal orbitals. In a tetrahedral environment, the symmetry of the metal orbitals changes due to the influence of the ligand field. The metal orbitals transform into the following symmetry sets under T_d symmetry:

(i) The *s* orbital transforms as a_1

(ii) The *p* orbitals (p_x, p_y, p_z) transform as t_2

(iii) The *d* orbitals split into two sets:

d_{xy}, d_{xz}, $d_{yz} \rightarrow t_2$

$d_{x^2-y^2}$, $d_{z^2} \rightarrow e$

Thus, the metal orbitals available for interaction with ligands belong to the a_1, t_2, and *e* symmetry sets.

Each of the four ligands contributes one orbital for σ bonding. These orbitals are directed toward the metal center along the metal–ligand axes. When these four ligand orbitals combine, they form ligand group orbitals (LGOs). The four ligand orbitals combine to produce LGOs of symmetries a_1 and t_2. Thus, in a tetrahedral complex, the σ-bonding LGOs consist of one a_1 orbital and three t_2 orbitals.

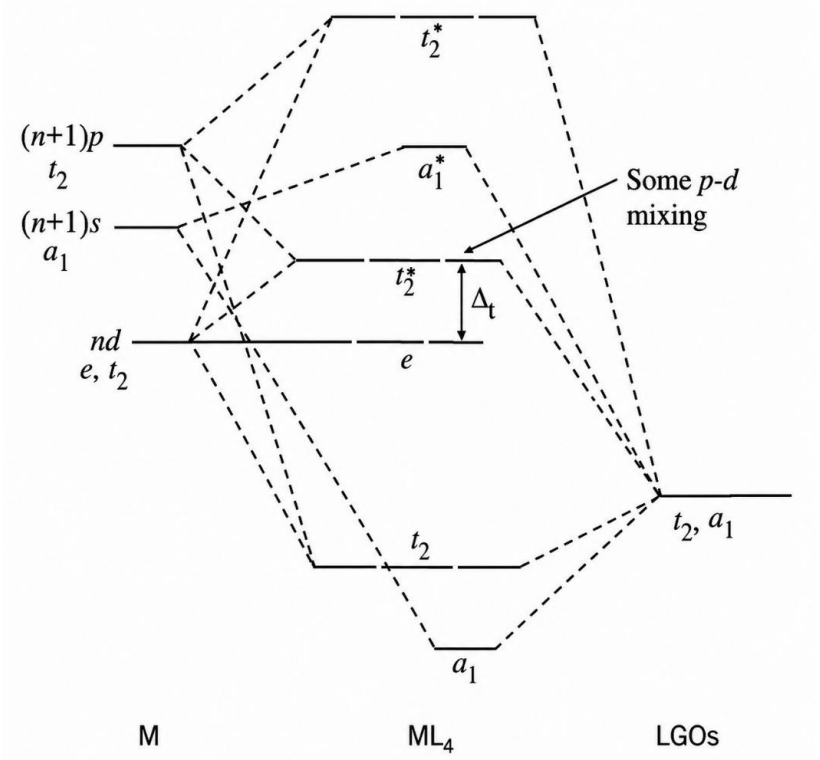


Fig. 5.4. Molecular orbital energy level diagram for tetrahedral complex, ML_4

For bonding to occur, orbitals must possess compatible symmetry and comparable energy. Therefore, only metal orbitals having the same symmetry as the ligand group orbitals can interact with them. The metal *s* orbital, which belongs to the a_1 symmetry, interacts with the a_1 ligand group orbital. This interaction results in the formation of a bonding molecular orbital (a_1) and an antibonding molecular orbital (a_1*). Because the metal *s* orbital overlaps effectively with the ligand orbital combination, the bonding–antibonding splitting between a_1 and a_1* is relatively large. The metal *p* orbitals (p_x, p_y, p_z) and the *d* orbitals (d_{xy}, d_{xz}, d_{yz}) belong to the t_2 symmetry set. These orbitals can interact with the t_2 ligand group orbitals. The interaction between these orbitals produces bonding molecular orbitals (t_2) and antibonding molecular orbitals (t_2*) (**Fig. 5.4**). The metal *e* orbitals ($d_{x^2-y^2}$ and d_{z^2}) do not have corresponding ligand group orbitals of the same symmetry for *σ* interaction. Therefore, these orbitals do not participate in *σ* bonding in a tetrahedral complex. As a result, the *e* orbitals remain essentially non-bonding in the *σ*-bonding molecular orbital scheme.

5.5 SIGMA BONDING IN SQUARE PLANAR COMPLEXES (ML_4)

In a square planar complex, the metal ion is surrounded by four ligands arranged in the same plane, forming a square geometry. The ligands approach the metal along the *x*- and *y*-axes, and therefore the bonding between the metal and ligands primarily occurs through σ interactions along these axes.

The symmetry of square planar complexes is described by the D_{4h} point group. When the metal atom is placed in this ligand field, its atomic orbitals transform into different symmetry sets according to D_{4h} symmetry.

The metal orbitals transform as follows: (i) the *s* orbital transforms as a_{1g}; (ii) the *p* orbitals split into two sets p_x and $p_y \rightarrow e_u$ and $p_z \rightarrow a_{2u}$; (iii) the *d* orbitals split into four symmetry sets: $d_{x^2-y^2} \rightarrow b_{1g}$, $d_{z^2} \rightarrow a_{1g}$, $d_{xy} \rightarrow b_{2g}$ and d_{xz} and $d_{yz} \rightarrow e_g$. These orbitals form the basis for possible interactions with ligand orbitals in a square planar complex.

Each of the four ligands contributes one orbital directed toward the metal center for *σ* bonding. Since the ligands are positioned along the +*x*, −*x*, +*y*, and −*y* directions, their orbitals combine to form symmetry-adapted ligand group orbitals (LGOs). The four ligand orbitals combine to produce LGOs having the symmetries a_{1g}, b_{1g} and e_u. Thus, the *σ*-bonding ligand group orbitals in square planar complexes consist of one a_{1g} orbital, one b_{1g} orbital, and two e_u orbitals (**Fig. 5.5**).

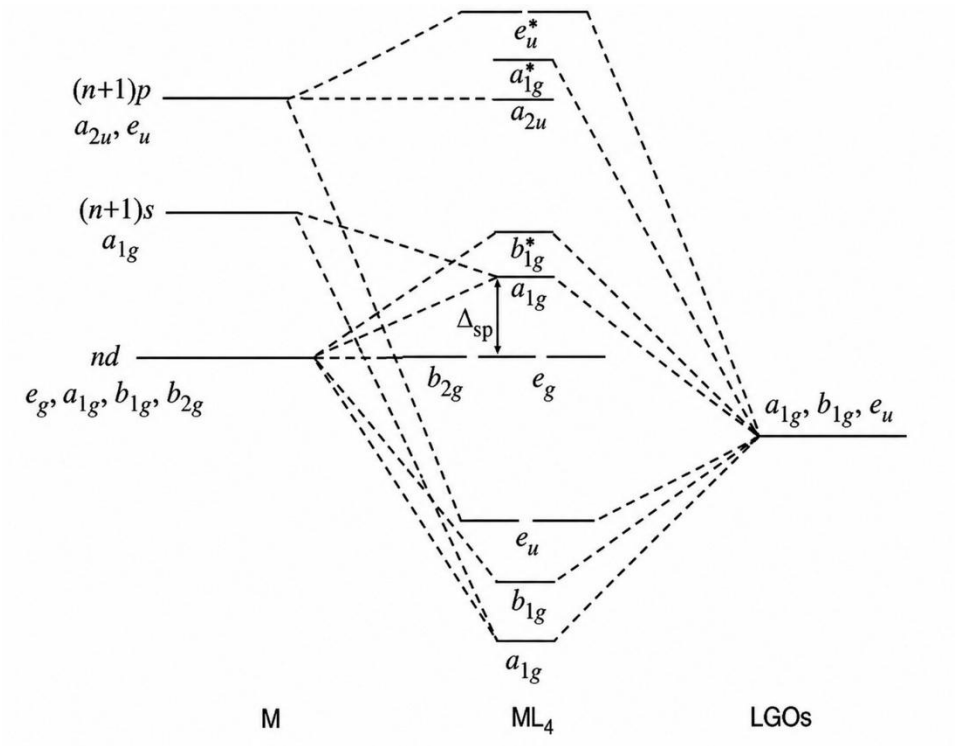


Fig. 5.5. Molecular orbital energy level diagram for square planar complex, ML_4

For effective bonding, the interacting orbitals must possess the same symmetry and comparable energies. Therefore, only those metal orbitals that match the symmetry of the ligand group orbitals will participate in *σ* bonding. The metal *s* orbital (a_{1g}) and the metal d_{z^2} orbital (also a_{1g}) can interact with the a_{1g} ligand group orbital.

These interactions lead to the formation of bonding a_{1g} molecular orbitals and antibonding a_{1g}* molecular orbitals. The degree of splitting depends on the extent of overlap between the metal and ligand orbitals. The metal $d_{x^2-y^2}$ orbital belongs to the b_{1g} symmetry set. This orbital lies directly along the *x* and *y* axes and therefore points directly toward the ligand positions. Because of this orientation, it overlaps very strongly with the b_{1g} ligand group orbital, resulting in a bonding b_{1g} orbital and an antibonding b_{1g}* orbital. Similarly, the metal p_x and p_y orbitals, which transform as e_u, interact with the e_u ligand group orbitals. Since the e_u set consists of two degenerate orbitals, the resulting bonding and antibonding orbitals are also doubly degenerate.

Some metal orbitals do not have corresponding ligand group orbitals with the same symmetry for *σ* interaction. These orbitals remain non-bonding in the *σ*-bonding description.

W CHECK YOUR PROGRESS

Q1. Why is Molecular Orbital (MO) Theory considered more comprehensive than Valence Bond Theory (VBT) and Crystal Field Theory (CFT) in explaining bonding in transition metal complexes?
Q2. State the main conditions required for the combination of atomic orbitals to form molecular orbitals according to the LCAO principle.
Q3. In an octahedral complex (ML_6), which metal orbitals participate in σ-bond formation and which orbitals remain non-bonding in the *σ*-bonding scheme?
Q4. What are ligand group orbitals (LGOs)? Why are they important in the molecular orbital description of coordination complexes?
Q5. What is the difference between *π*-donor ligands and *π*-acceptor ligands? Give one example of each.
Q6. Which metal orbitals are mainly involved in *π*-bonding in octahedral complexes, and why?
Q7. In tetrahedral complexes (ML_4), which symmetry sets of metal orbitals participate in σ-bonding?
Q8. Why is the $d_{x^2-y^2}$ orbital usually the highest energy orbital in square planar complexes?

5.6 LET US SUM UP

- Molecular Orbital (MO) Theory provides a more complete explanation of bonding in transition metal complexes compared to Valence Bond Theory (VBT) and Crystal Field Theory (CFT) because it considers the actual overlap of metal and ligand orbitals and explains the covalent as well as ionic character of metal–ligand bonding.
- The foundation of MO theory is the Linear Combination of Atomic Orbitals (LCAO) approach, according to which atomic orbitals combine to form molecular orbitals when they have comparable energies, suitable orientation, and matching symmetry.
- Molecular orbitals formed through these interactions may be bonding, antibonding, or non-bonding, depending on the nature and extent of overlap between the interacting orbitals.
- In octahedral complexes (ML_6), the metal orbitals transform into symmetry sets such as a_{1g}, t_{1u}, e_g, and t_{2g}, while ligand orbitals combine to form ligand group orbitals (LGOs) that interact with metal orbitals of identical symmetry.
- In *σ*-bonding of octahedral complexes, the a_{1g}, t_{1u}, and e_g metal orbitals participate in bonding with ligand orbitals, whereas the t_{2g} orbitals remain non-bonding in the absence of *π* interactions.
- *π*-Bonding in octahedral complexes involves mainly the t_{2g} metal orbitals and may occur through *π*-donor ligands (which donate electron density to the metal) or *π*-

acceptor ligands (which accept electron density from the metal through back-bonding).

- In tetrahedral complexes (ML_4), the metal orbitals transform into a_1, t_2, and e symmetry sets, and σ bonding mainly occurs through interactions of a_1 and t_2 metal orbitals with the corresponding ligand group orbitals.
- In square planar complexes (ML_4) belonging to D_{4h} symmetry, σ bonding primarily involves interactions of a_{1g}, b_{1g}, and e_u metal orbitals with the corresponding ligand group orbitals, while some orbitals remain non-bonding.
- The molecular orbital approach helps explain the electronic structure, ligand field strength, bonding characteristics, and stability of coordination compounds.
- Thus, MO theory serves as an important tool for understanding the structure and properties of transition metal complexes, including the role of σ and π interactions in metal–ligand bonding.

K 5.7 Answers to Check Your Progress

Answer to Q1: Molecular Orbital Theory is more comprehensive because it considers the actual overlap of metal and ligand orbitals and explains both the covalent and ionic nature of metal–ligand bonding, whereas VBT mainly explains geometry and CFT considers only electrostatic interactions.

Answer to Q2: According to the LCAO principle, atomic orbitals combine to form molecular orbitals when:

(*i*) they have comparable energies,
(*ii*) they possess appropriate orientation, and
(*iii*) they have matching symmetry.

Answer to Q3: In octahedral complexes, the a_{1g}, t_{1u}, and e_g metal orbitals participate in σ bonding with ligand orbitals, while the t_{2g} orbitals remain non-bonding in the absence of π interactions.

Answer to Q4: Ligand Group Orbitals (LGOs) are symmetry-adapted combinations of ligand atomic orbitals that interact with metal orbitals of the same symmetry to form molecular orbitals. They simplify the description of bonding in coordination complexes.

Answer to Q5: π-Donor ligands donate electron density to the metal through filled orbitals (example: Cl^-), whereas π-acceptor ligands accept electron density from the metal through empty antibonding orbitals (example: CO).

Answer to Q6: In octahedral complexes, the t_{2g} metal orbitals (d_{xy}, d_{xz}, d_{yz}) are mainly involved in π bonding because they are oriented between the axes and have the correct symmetry for sideways overlap with ligand π orbitals.

Answer to Q7: In tetrahedral complexes, the a_1 and t_2 metal orbitals participate in σ bonding with ligand group orbitals.

Answer to Q8: In square planar complexes, the $d_{x^2-y^2}$ orbital points directly toward the ligands along the *x* and *y* axes, resulting in strong antibonding interaction, which makes it the highest energy orbital.

O 5.8 Further Reading

- Lee, J. D. *Concise Inorganic Chemistry*, 5th ed.; Wiley-Blackwell: Oxford, 1996.
- Shriver, D. F.; Atkins, P. W. *Inorganic Chemistry*, 5th ed.; Oxford University Press: Oxford, 2010.
- Huheey, J. E.; Keiter, E. A.; Keiter, R. L. *Inorganic Chemistry: Principles of Structure and Reactivity*, 4th *ed*.; Pearson.

M 5.9 Model Questions

Q1. Explain the basic principles of Molecular Orbital (MO) Theory. How does it differ from Valence Bond Theory (VBT) and Crystal Field Theory (CFT) in explaining bonding in transition metal complexes?

Q2. Describe the conditions required for the linear combination of atomic orbitals (LCAO) in the formation of molecular orbitals.

Q3. Explain the *σ*-bonding molecular orbital diagram of octahedral complexes (ML_6). Discuss the role of metal orbitals and ligand group orbitals in the formation of bonding and antibonding molecular orbitals.

Q4. What are ligand group orbitals (LGOs)? Explain their importance in the molecular orbital description of coordination compounds.

Q5. Discuss the *π*-bonding in octahedral complexes. Explain the role of *π*-donor and *π*-acceptor ligands and their effect on ligand field splitting.

Q6. Describe the molecular orbital treatment of σ bonding in tetrahedral complexes (ML_4).

Q7. Explain the *σ*-bonding molecular orbital diagram of square planar complexes (ML_4) and discuss the relative energies of the metal *d* orbitals in such complexes.

Q8. Compare the molecular orbital approach for octahedral, tetrahedral, and square planar complexes.

Q9. Explain the different types of *π* interactions such as *dπ–pπ*, *dπ–dπ*, *dπ–π**, and *dπ–σ** in transition metal complexes with suitable examples.

Q10. Discuss how *π* interactions influence the electronic structure and stability of transition metal complexes.

UNIT 6: ELECTRONIC SPECTRA OF TRANSITION METAL COMPLEXES

UNIT STRUCTURE

6.1 Learning Objectives
6.2 Introduction
6.3 Absorption of light and Beer-Lambert law
6.4 Electronic states and term symbols
6.5 Selection rules
6.6 Orgel diagram
6.7 Tanabe-Sugano diagram
6.8 *d*-*d* and charge transfer transitions
6.9 Calculation of Racah Parameters
6.10 Nephelauxetic effect
6.11 Applications of Electronic Spectroscopy in Transition Metal Complexes
6.12 Let us Sum Up
6.13 Answers to Check Your Progress
6.14 Further Reading
6.15 Model Questions

6.1 LEARNING OBJECTIVES

After studying this unit, learners will be able to:

- Understand the basic principles of electronic spectroscopy, including the interaction of UV–Visible radiation with transition metal complexes and the origin of electronic transitions.
- Explain the different types of electronic transitions such as *d*–*d* transitions and charge transfer transitions, and interpret their significance in determining the electronic structure and properties of coordination compounds.
- Apply spectroscopic concepts and tools such as the Beer–Lambert law, molar absorptivity, term symbols, Orgel diagrams, and Tanabe–Sugano diagrams to analyze and interpret the spectral behaviour of transition metal complexes.

6.2 INTRODUCTION

After having a solid knowledge on the molecular orbital theory of transition metal complexes let's walk through this topic Electronic Spectra of Transition Metal Complexes step by step. Electronic spectroscopy of transition metal complexes deals with the absorption of electromagnetic radiation in the ultraviolet and visible regions that results in transitions of electrons between different energy levels. These transitions arise mainly from *d*–*d* transitions within the metal ion and charge transfer transitions between metal and ligands. By studying these spectra, we can determine important

information about electronic structure, ligand field strength, geometry of complexes, and bonding characteristics.

6.3 ABSORPTION OF LIGHT AND BEER-LAMBERT LAW

Let's go through Absorption of Light and Beer–Lambert Law. These two concepts form the basic foundation of electronic spectroscopy. So, understanding them properly makes the rest of the chapter much easier. When electromagnetic radiation passes through a substance, several things may happen. The radiation may be reflected, transmitted, scattered, or absorbed. In spectroscopy we are mainly concerned with absorption, because absorption of light tells us about the electronic structure of atoms and molecules. Light behaves as packets of energy called photons. Each photon carries a definite amount of energy. The energy of a photon is related to its frequency according to the Planck relation.

$$E = h\nu$$

Here, E represents the energy of the photon, *h* is Planck's constant, and ν (nu) is the frequency of radiation. Since frequency and wavelength are related by the speed of light, the energy of radiation can also be expressed in terms of wavelength.

$$\nu = \frac{c}{\lambda}$$

$$E = \frac{hc}{\lambda}$$

Where, *c* = speed of light, *λ* = wavelength of radiation. This equation shows that energy is inversely proportional to wavelength. Radiation with shorter wavelength therefore carries higher energy.

Interaction of Light with Atoms and Molecules

Atoms and molecules possess discrete energy levels. These energy levels correspond to different electronic, vibrational, or rotational states. Under normal conditions, electrons occupy the lowest possible energy level, known as the ground state. When a photon with the correct energy strikes the atom or molecule, an electron can absorb this energy and move to a higher energy level, known as the excited state. This process is called electronic excitation.

$$\Delta E = E_{excited} - E_{ground}$$

The condition for absorption is that the energy of the photon must exactly match the energy difference between two electronic levels.

Absorption of Light in Transition Metal Complexes

In transition metal complexes, absorption of light generally occurs in the UV-visible region of the electromagnetic spectrum (200–800 nm). The absorption originates mainly from two types of electronic transitions. The first type is *d–d* transitions. Transition metal ions contain partially filled d orbitals. In a ligand field, these orbitals split into groups with different energies. When light of appropriate energy is absorbed,

an electron moves from a lower energy *d* orbital to a higher energy *d* orbital. For example, in an octahedral complex, the five *d* orbitals split into two groups:

- t_{2g} (lower energy)
- e_g (higher energy)

When light of energy equal to the splitting energy is absorbed, an electron is promoted from the t_{2g} level to the e_g level. The second type of absorption is charge transfer transition, where electrons move between metal and ligand orbitals. These transitions are usually much more intense than *d*–*d* transitions.

Beer–Lambert Law

Now that we understand how light is absorbed, the next important question is: how much light is absorbed by a solution? This relationship is explained by the Beer–Lambert law, which is one of the most important laws in spectroscopy. The Beer–Lambert law states that the absorbance of a solution is directly proportional to the concentration of the absorbing species and the path length of the light through the solution.

$$A = \varepsilon c l$$

In this expression *A* represents the absorbance of the solution, *ε* is the molar absorptivity or molar extinction coefficient, c is the concentration of the absorbing species, l is the path length of the solution (usually 1 cm)

Absorbance and Light Intensity

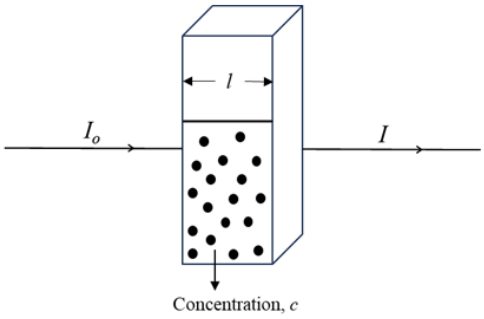


Fig. 6.1. Absorption of light

Absorbance can also be defined in terms of the intensity of light entering and leaving the sample.

$$A = log_{10}(\frac{I_0}{I})$$

Where, I_0 is the intensity of incident light, I is the intensity of transmitted light. If a large amount of light is absorbed, the transmitted intensity becomes small and the absorbance becomes high.

Limitations of Beer–Lambert Law

Although the Beer–Lambert law works well in many situations, it has some limitations. At very high concentrations, molecules interact with each other and the linear

relationship between absorbance and concentration may fail. Deviations may also occur due to:

(i) chemical equilibrium in solution;

(ii) stray light in the instrument;

(iii) polychromatic radiation instead of monochromatic light;

(iv) changes in refractive index of the solution.

For accurate results, measurements are usually performed at low concentrations using monochromatic light.

6.4 ELECTRONIC STATES AND TERM SYMBOLS FOR TRANSITION METALS

To understand electronic spectra, we must first understand electronic states of transition metal ions. An electronic state describes the arrangement of electrons in orbitals along with their spin and orbital angular momentum. These states are represented using term symbols. A general atomic term symbol is written as

$$^{2S+1}L_J$$

where,
S = total spin quantum number
$2S+1$ = spin multiplicity
L = total orbital angular momentum
J = total angular momentum

Values of L are represented by letters:

L value	Symbol
0	S
1	P
2	D
3	F
4	G

For example, ^2D, ^3F, ^4P etc. In transition metal complexes the orbital degeneracy is affected by ligand fields. Therefore, molecular term symbols are used. For example, in octahedral symmetry (O_h) terms are written as:

- A (non-degenerate)
- E (doubly degenerate)
- T (triply degenerate)

and subscripts g and u indicate symmetry:
g = gerade (symmetric with inversion)
u = ungerade (antisymmetric)

Example:
$^3T_{1g}$
$^3T_{2g}$
^1E_g

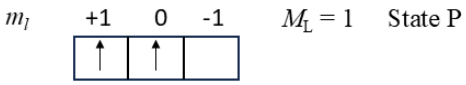
These molecular term symbols describe energy levels of *d*-electron configurations in ligand fields.

Calculations of Ground State Term and Ground State Term Symbol:

Following steps are used for determining the ground state.

1. Write the electronic configuration
2. Determine the spin multiplicity ($2S+1$)
3. Determine the maximum possible value M_L ($=\sum m_l$)
4. Select maximum value of J for more than half filled subshell and minimum J value for less than half filled subshell.

p^2-configuration:



Since both the electrons have parallel spins

$\therefore \quad S = \frac{1}{2} + \frac{1}{2} = 1$

$2S + 1 = 2 \times 1 + 1 = 3$

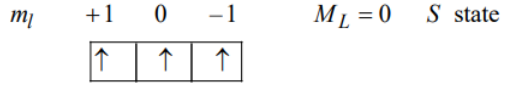
Ground state term= ^3P

For ^3P, L=1, S=1

$J = |L + S| \ldots\ldots\ldots |L - S| = 2,1,0$

$\therefore$ Ground state term symbol=$^3P_0$ (Less than half filled subshell p^2)

p^3-configuration (N-atom⟶ $1s^2.2s^2.2p^3$)



$S = \frac{1}{2} + \frac{1}{2} + \frac{1}{2} = \frac{3}{2}$

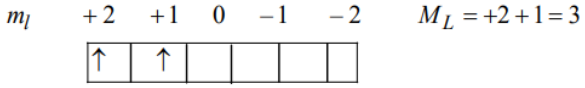
$2S + 1 = 2 \times \frac{3}{2} + 1 = 4$

Term = ^4S

For L=0, S=3/2, J=3/2

Term symbol $^4S_{3/2}$

Ground state term for V^{3+} for (d^2-configuration)



$\therefore$ F state

$S = \frac{1}{2} + \frac{1}{2} = 1$

Spin multiplicity ($2S$+1) = 2×1+1 = 3

J = |L+S|……..|L-S|

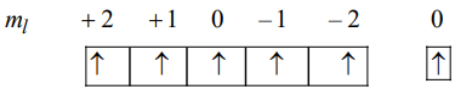
= |3+1|…….3-1

= 4,3,2

Ground state term symbol= $^3F_2$ (for less than half filled subshell d^2)

Ground state term symbols for high spin d^5s^1 and d^5 configuration

High spin d^5s^1



$\therefore$ S state

$$s = \frac{1}{2} + \frac{1}{2} + \frac{1}{2} + \frac{1}{2} + \frac{1}{2} + \frac{1}{2} = 3$$

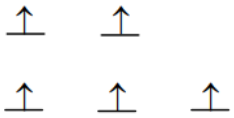
$2S$+1 = 2×3+1 = 7

Ground state term = ^7S

For L= 0 and S = 3, J = 3

Therefore, ground state Term Symbol $^7S_3$

High spin d^5



$$\boldsymbol{S = \frac{1}{2} + \frac{1}{2} + \frac{1}{2} + \frac{1}{2} + \frac{1}{2} = \frac{5}{2}} \qquad \boldsymbol{M_L = 2 + 1 + 0 - 1 + 2 = 0}$$

$\therefore$ S state

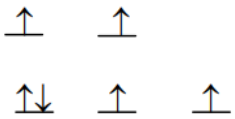
$$\boldsymbol{2S + 1 = 2 \times \frac{5}{2} + 1 = 6S}$$

J value for L=0 and S = 5/2 is 5/2

Ground state term symbol $^6S_{5/2}$

Ground State Terms for High Spin and Low Spin d^6-octahedral Complex:

High spin d^6:



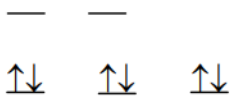
Spin multiplicity= $2S$+1 = 2×2+1= 5

Maximum value of M_L= 2+2+1+0-1-2 = 2

$\therefore L$=2, D state

Therefore, ground state term= ^5D

Low spin d^6:



$$S = \frac{1}{2} - \frac{1}{2} + \frac{1}{2} - \frac{1}{2} + \frac{1}{2} - \frac{1}{2} = 0$$

Spin multiplicity = $2S+1 = 2\times0+1 = 1$

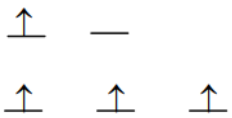
Maximum value of $M_L = 2+2+1+1+0 = 6$

$\therefore L=6$, I state

Ground state term=^1I

Ground State Terms for High Spin and Low Spin d^4 Octahedral Complex

d^4 (High spin):



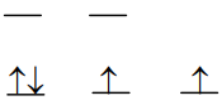
$$S = \frac{1}{2} + \frac{1}{2} + \frac{1}{2} + \frac{1}{2} = 2$$

Spin multiplicity= $2S+1 = 2\times2+1= 5$

Maximum value of $M_L = 2+1+0-1 = 2$

$\therefore$D state and Ground state term = ^5D

d^4 (Low spin):



$$S = \frac{1}{2} - \frac{1}{2} + \frac{1}{2} + \frac{1}{2} = 1$$

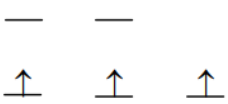
Spin multiplicity = $2S+1 = 2\times1+1= 3$

Maximum value of $M_L = 2+2+1+0 = 5$

$\therefore L= 5$ and H state

Ground state term = ^3H

d^3-configuration in Octahedral Symmetry:



$$S = \frac{1}{2} + \frac{1}{2} + \frac{1}{2} = \frac{3}{2}$$

Spin multiplicity = $2S+1 = 2 \times 3/2 + 1 = 4$

Maximum value of $M_L = 2+1+0=3$

$\therefore L= 3,$ F state

$\therefore$ Ground state term=^4F

Table 6.1: Terms arising for *p* and *d* configurations:

Electronic configuration	Ground state term	Other term
p^1, p^5	^2P	
p^2, p^4	^3P	^1S, ^1D
p^3	^4S	^2P, ^2D
p^6	^1S	
d^1, d^9	^2D	
d^2, d^8	^3F	^3P, ^1G, ^1D, ^1S
d^3, d^7	^4F	^4P, ^2H, ^2G, ^2F,^2D,^2P
d^4, d^6	^5D	^3H, ^3G, ^3F, ^3D, ^3P, ^1I, ^1G, ^1F, ^1D, ^1S
d^5	^6S	^4G, ^4F, ^4D, ^4P, ^2I, ^2H, ^2G, ^2F, ^2D, ^2P, ^2S

6.5 SELECTION RULES

Now, let's dive carefully into Selection Rules in Electronic Spectroscopy of Transition Metal Complexes. This is one of those concepts that really helps to explain why some spectral bands are strong while others are weak. When a transition metal complex absorbs light, an electron moves from a lower energy electronic state to a higher energy electronic state. However, not every possible transition between two states is permitted. Quantum mechanics imposes certain restrictions known as selection rules.
Selection rules determine:

- whether an electronic transition is allowed
- whether it is forbidden
- and therefore, how intense the absorption band will appear in the spectrum.

In transition metal complexes, two major selection rules are important:

1. Spin Selection Rule, and
2. Laporte Selection Rule

These rules explain why *d*–*d* transitions are usually weak in many complexes.

1. Spin Selection Rule

The spin selection rule states that during an electronic transition, the total spin of the electrons must remain unchanged. Mathematically, the rule is written as

$\Delta S = 0$

where, *S* = total spin quantum number.
This means the spin multiplicity must remain the same before and after the transition. The spin multiplicity of a term is given by $2S+1$

Example
Consider two electronic states:
$^3T_{1g}$
$^3T_{2g}$

Both states have multiplicity 3, meaning they have the same spin state. Therefore, the transition $^3T_{1g} \rightarrow {}^3T_{2g}$ is spin allowed.

Now consider another transition:
$^3T_{1g} \rightarrow {}^1E_g$
The first state has multiplicity 3 while the second has multiplicity 1. Since the spin multiplicity changes, the transition violates the spin selection rule. Therefore, this transition is spin forbidden.

Intensity of Spin Allowed vs Spin Forbidden Transitions
Spin-allowed transitions produce relatively strong absorption bands. Spin-forbidden transitions produce very weak absorption bands because the probability of the transition occurring is very small. For example, high-spin Mn^{2+} (d^5) complexes show very weak spectral bands because most transitions are spin forbidden.

2. Laporte Selection Rule

The second important rule is the Laporte selection rule, which applies to molecules or complexes that possess a center of symmetry. This rule states that during an electronic transition there must be a change in parity of the orbital. Parity refers to the symmetry of orbitals with respect to inversion through the center of symmetry. Orbitals are classified as:

- gerade (*g*) → symmetric with respect to inversion
- ungerade (*u*) → antisymmetric with respect to inversion

The Laporte rule states: Transitions of the type $g \rightarrow g$ or $u \rightarrow u$ are forbidden.

Allowed transitions must involve

$g \rightarrow u$ or $u \rightarrow g$.

Application to Transition Metal Complexes

In octahedral complexes, the *d* orbitals are gerade (g) orbitals. A typical *d*–*d* transition involves movement of an electron between two *d* orbitals. Thus, the transition is
$d(g) \rightarrow d(g)$

Since both orbitals have the same parity, the transition violates the Laporte rule. Therefore *d*–*d* transitions in octahedral complexes are Laporte forbidden. This is the main reason why most transition metal complexes show weak absorption bands in the UV–visible spectrum.

Relaxation of the Laporte Rule

Although the Laporte rule predicts that *d*–*d* transitions should be forbidden, in practice these transitions do occur, though with low intensity. This happens because the rule can be partially relaxed by certain effects. In real molecules, atoms are constantly vibrating. These vibrations temporarily distort the molecular symmetry. When symmetry is disturbed, orbitals can mix slightly with *p* orbitals (which are *u* type). This mixing allows the transition to gain some allowed character, making weak absorption possible. If a complex deviates from perfect octahedral symmetry, the center of symmetry may be lost.

For example:

- tetrahedral complexes
- distorted octahedral complexes

In these cases, the Laporte rule does not strictly apply. Tetrahedral complexes do not possess a center of symmetry. Therefore, the Laporte rule does not apply. As a result, *d–d* transitions in tetrahedral complexes are more intense than in octahedral complexes.

This explains why many tetrahedral complexes show stronger colours. The intensity of electronic absorption bands depends on whether the transitions obey or violate the selection rules.

We can summarize the situation like this:

Type of Transition	**Allowed/Forbidden**	**Intensity**
Spin allowed + Laporte allowed	Strong	Very intense
Spin allowed + Laporte forbidden	Weak	Moderate
Spin forbidden	Very weak	Very faint

For example,

Laporte (orbital)	**Spin**	**Type of Spectra**	**ε (L mol^{-1} cm^{-1})**	**Example**
Allowed	Allowed	Charge transfer	1000	$[TiCl_6]^{2-}$
Partly allowed, some *p*-*d* mixing	Allowed	*d*-*d*	500	$[CoBr_4]^2$.$[CoCl_4]^{2-}$
Forbidden	Allowed	*d*-*d*	8-10	$[Ti(H_2O)_6]^{3+}$.$[V(H_2O)_6]^{3+}$
Partly allowed, some *p*-*d* mixing	Forbidden	*d*-*d*	4	$[MnBr_4]^{2-}$
Forbidden	Forbidden	*d*-*d*	0.02	$[Mn(H_2O)_6]^{2+}$

Importance of Selection Rules in Electronic Spectroscopy

Selection rules are extremely important because they help us understand:

- intensity of spectral bands
- nature of electronic transitions
- differences between octahedral and tetrahedral spectra
- why charge transfer transitions are much stronger than *d–d* transitions.

For example, charge transfer transitions involve movement of electrons between orbitals of different symmetry (often $g \rightarrow u$). Therefore, they are both spin allowed and Laporte allowed, producing very intense absorption bands. In short, selection rules act like quantum mechanical guidelines that determine which electronic transitions are probable and which are unlikely. They are essential for interpreting the electronic spectra of transition metal complexes.

6.6 ORGEL DIAGRAMS

The main purpose of Orgel diagrams is to show how the electronic energy levels of a transition metal ion split when ligands approach the metal ion and how these levels give rise to electronic absorption bands in the UV–visible spectrum. Unlike more advanced diagrams such as Tanabe–Sugano diagrams, Orgel diagrams are simplified and qualitative. They do not give exact energy values but help us understand:

- relative energy levels of electronic states
- number of possible electronic transitions
- approximate positions of spectral bands.

To understand Orgel diagrams, we first consider a free transition metal ion. In a free ion, the five *d* orbitals are degenerate, meaning they all have the same energy. When ligands approach the metal ion and form a complex, the electric field created by the ligands interacts with the d orbitals and causes them to split into different energy levels. This phenomenon is described by crystal field theory or ligand field theory.

In an octahedral complex, the five d orbitals split into two groups:

- t_{2g} orbitals (lower energy)
- e_g orbitals (higher energy)

The energy difference between these two sets is the octahedral crystal field splitting energy.

Orgel diagrams show how the electronic terms of a free ion split into several states when the ion is placed in an octahedral or tetrahedral ligand field.

Splitting of Electronic Energy Levels

In the one electron cases s^1 p^1 d^1 f^1, there is a direct correspondence between the splitting of electronic energy levels which occurs in a crystal field and the splitting of spectroscopic states. Thus, in an octahedral field the *S* and *P* states are not split. *D* states are split into two states and *F* states are split into three states (**Fig. 6.2**).

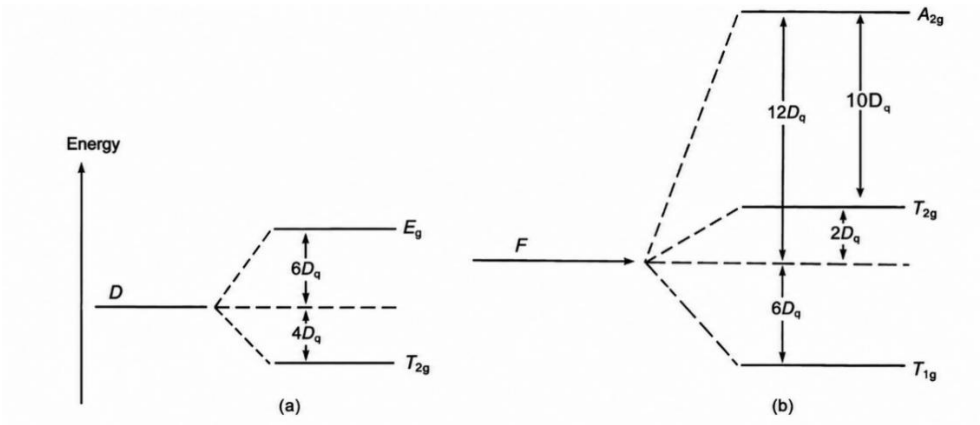


Fig. 6.2. Splitting of *D* and *F* states in octahedral field.

An Orgel diagram is drawn with ***(i)*** Energy on the vertical axis ***(ii)*** ligand field strength on the horizontal axis. At the left side of the diagram, we consider the free ion state, where no ligand field is present. As the ligand field strength increases, the electronic terms split into different states depending on the symmetry of the complex. Separate diagrams are usually drawn for octahedral complexes and tetrahedral complexes.

Table 6.2: Transforming spectroscopic terms into Mulliken symbols

Spectroscopic term	Mulliken Symbols	
	Octahedral field	**Tetrahedral field**
S	A_{1g}	A_1
P	T_{1g}	T_1
D	$E_g + T_{2g}$	$E + T_2$
F	$A_{2g} + T_{1g} + T_{2g}$	$A_2 + T_1 + T_2$
G	$A_{1g} + E_g + T_{1g} + T_{2g}$	$A_1 + E + T_1 + T_2$

In tetrahedral complexes, the ligand field splitting is reversed compared to octahedral complexes. Here the orbitals split into: *e* (lower energy) and t_2 (higher energy)**.** Although the order of energy levels changes, the general pattern of term splitting remains similar. Since tetrahedral complexes do not have a center of symmetry, their *d*–*d* transitions are more intense than those of octahedral complexes.

a) Orgel Diagram for d^1 and d^6 Configurations

d^1 octahedral

Let us first consider a d^1 octahedral configuration. For a free ion with one *d* electron, the ground term is ^2D. When the metal ion is placed in an octahedral ligand field, the *D* term splits into two states: $^2T_{2g}$ (lower energy) and ^2E_g (higher energy). When light is absorbed, the electron can move from the lower energy state to the excited state: $^2T_{2g} \rightarrow {}^2E_g$

This transition produces one absorption band in the electronic spectrum. Because of electron–hole symmetry, a d^6 high-spin complex shows similar behaviour.

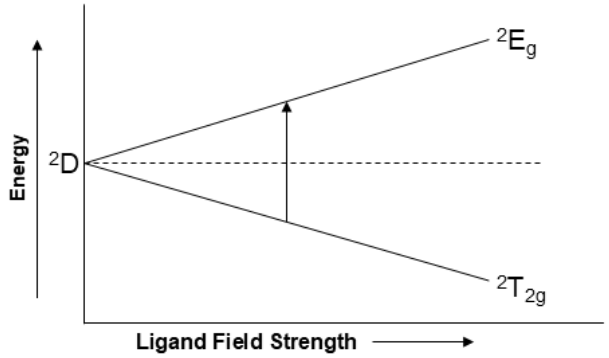
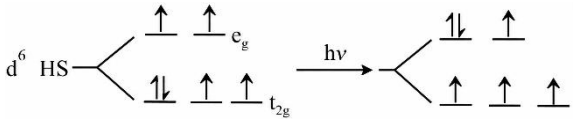


Fig. 6.3. Orgel diagram for d^1 octahedral complexes

d^6 octahedral

Spectra of high spin(HS) d^6 Octahedral Complexes: The ground state term for d^6 is ^5D. The d^6 has configuration $t^4_{2g}\ e^2_g$. According to selection rule, transition of electron which is paired in t_{2g} will take place (spin allowed).



From this it is clear that this transition is similar to d^1. Now ^5D splits into $^5T_{2g}$ and ^5E_g. Thus, there must be only one sharp transition band observed. However, broadening of band takes place.

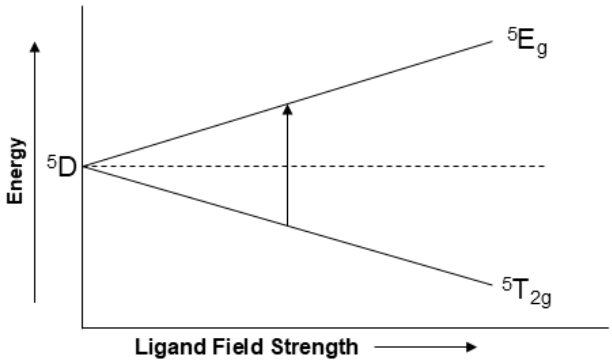


Fig. 6.4. Orgel diagram for d^6 octahedral complexes

d^6 tetrahedral

Electronic Spectra of d^6 tetrahedral complex: Fe(II) forms many tetrahedral complexes of formula $[Fe\ X_4]^{2-}$ where X = Cl^-, Br^-, I^-, NCS^-. The ground state term symbol is ^5D and the d^6 configuration is $t^3_2\ e^3$

Transition of paired electron can only take place (spin selection rule). In $[FeCl_4]^{2-}$ only single absorption band appears at 4000 cm^{-1} (near IR region) which is due to $^5T_2 \leftarrow {}^5E$.

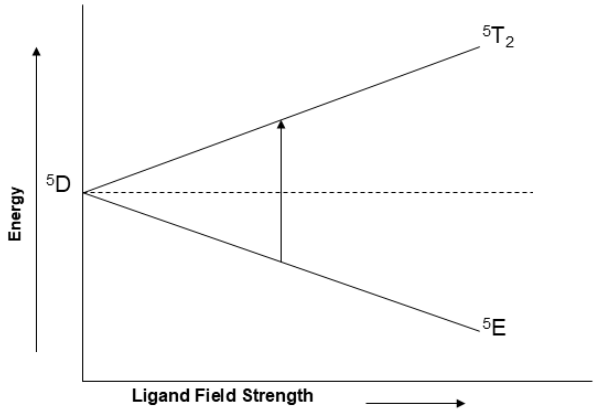


Fig. 6.5. Orgel diagram for d^6 tetrahedral complexes

Some feature of these diagrams may be stated as follows:

(a) For the d^1 configuration note that the energy levels diverge linearly, as they must do since the energy gap is a function of only the one parameter Δ_0.

(b) In the other diagram only some of the levels diverge linearly,

(c) Those levels which do not diverge linearly are the ones involved in configuration interaction.

For example, **Spectrum of $[Ti(H_2O)_6]^{3+}$** : The absorption band in spectra of $[Ti(H_2O)_6]^{3+}$ is broad because of John-Teller Distortion which splits ^2E_g state into $^2A_{1g}$ and $^2B_{1g}$. This splits ground state $^2T_{2g}$ into ^2E_g and $^2B_{2g}$ also in some extent.

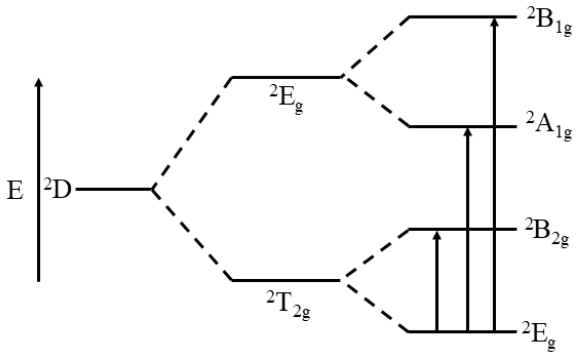


Fig. 6.6. Splitting in $[Ti(H_2O)_6]^{3+}$

In complex ion $[Ti(H_2O)_6]^{3+}$ absorption maximum observed at 20300 cm^{-1} and also the absorption maximum has a shoulder at 17400 cm^{-1} because of John-Teller Distortion. The shoulder is responsible for broad band.

b) Orgel Diagram for d^9 and d^4 Configurations

d^9 octahedral

Spectra of d^9 octahedral Complex: In octahedral d^9 complexes, the term ^2D splits into ^2E_g and $^2T_{2g}$. In d^9 octahedral a hole may be considered in e_g orbital. When transition takes place hole moves from e_g to t_{2g}. This is similar to electron transition *i.e.* $^2T_{2g} \leftarrow {}^2E_g$. However, hole and electron as moves in opposite direction hence the diagram of d^9 will be inverse of d^1.

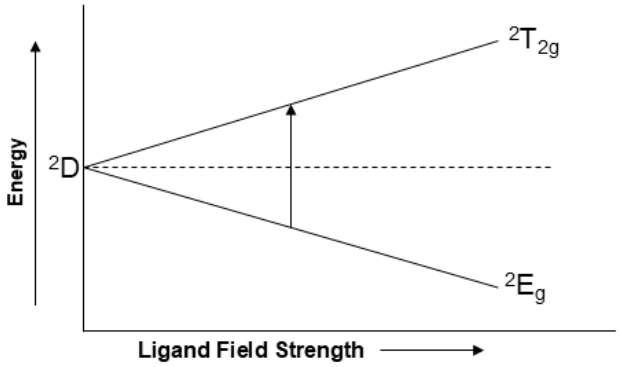


Fig. 6.7: Orgel diagram for d^9 octahedral complexes

d^9 tetrahedral

Spectra of d^9 in Tetrahedral: In tetrahedral complex of d^9, the splitting is reverse of d^9 octahedral. The ground state term is ^2D which splits into lower $^2T_2$ and higher ^2E. Only one transition is possible.

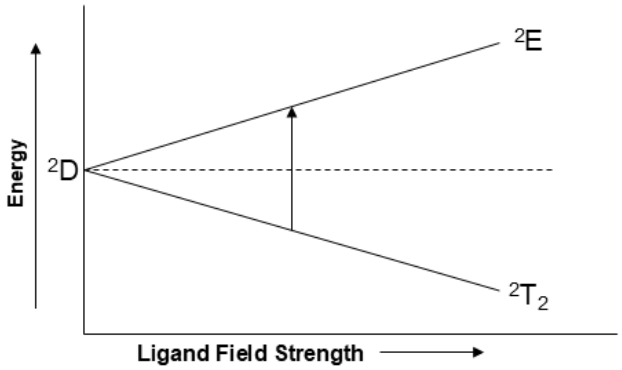


Fig. 6.8. Orgel diagram for d^9 tetrahedral complexes

Spectra of $[Cu(H_2O)_6]^{2+}$: The $[Cu(H_2O)_6]^{2+}$ complex show absorption in visible region at 12000 cm^{-1} and complex is of blue coloured.

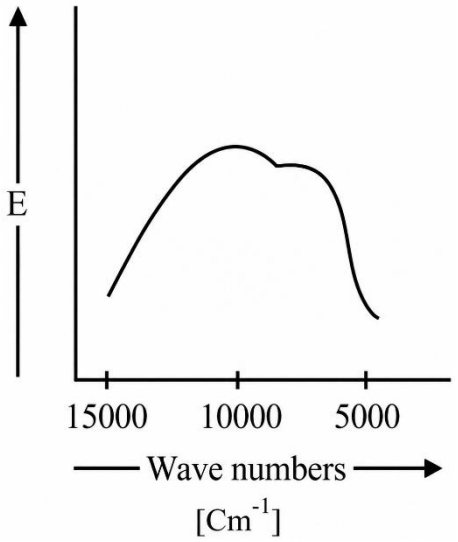


Fig. 6.9. Absorption spectrum of $[Cu(H_2O)_6]^{2+}$ complex

The complex show, intact a broad band, not sharp. This broadening can be explained on the basis that in d^9 system, John-Teller splitting takes place. Due to distortion, ^2E_g states splits into lower energy $^2B_{1g}$ and higher energy $^2A_{1g}$. Same time $^2T_{2g}$ state splits into lower energy $^2B_{2g}$ and higher energy ^2E_g. Hence now three transitions are possible. As the splitting is poor, the three absorption bands overlap together showing broad band.

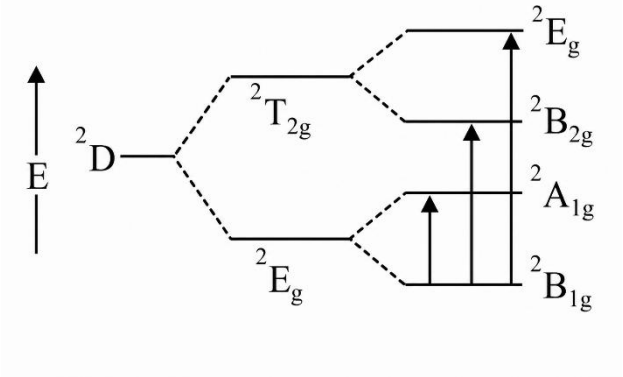


Fig. 6.10. Splitting in d^9 system due to John-Teller distortion.

d^4 octahedral

Spectra of high spin d^4 Octahedral Complex: In a high-spin (HS) d^4 octahedral complex, absorption of light causes a hole transition. This means that the empty orbital (hole) shifts from the e_g level to the t_{2g} level when the complex absorbs energy (hv).

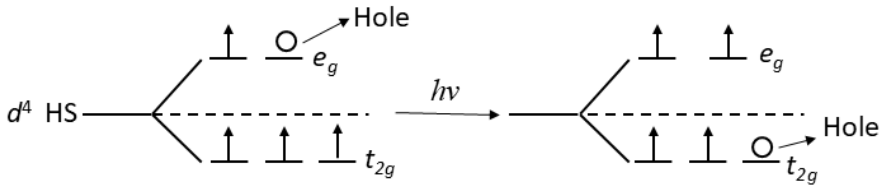


Fig. 6.11. Transition of holes from t_{2g} to e_g in d^4 HS Octahedral Complex.

This is similar to d^9 octahedral.

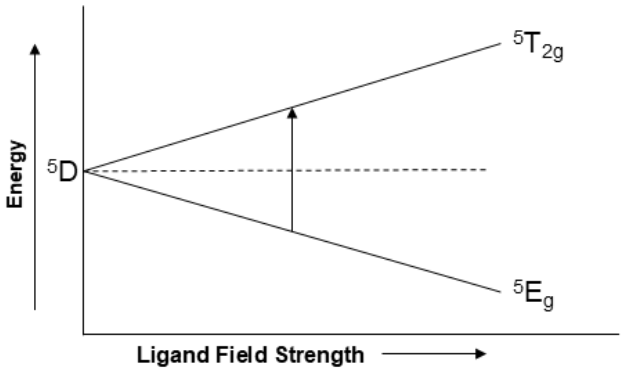


Fig. 6.12: Orgel diagram for d^4 octahedral complexes

d^4 tetrahedral

Spectra of d^4 Tetrahedral Complex: In tetrahedral complexes, d^4 splits into *e* and t_2. However, the splitting is reverse of d^4 high spin octahedral.

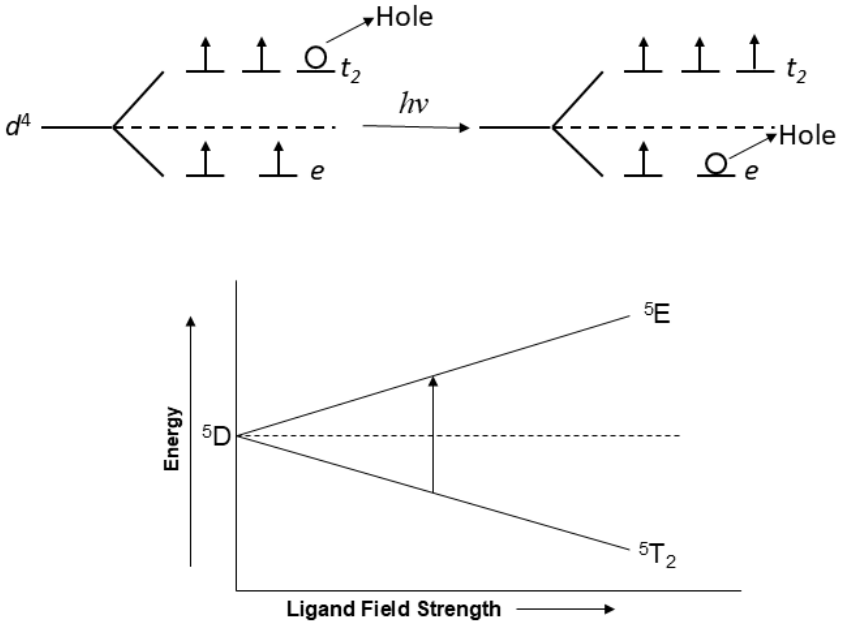


Fig. 6.13. Splitting of d^4 tetrahedral complex.

Above figures can be combined into a single diagram called an Orgel diagram, which describes in a qualitative way the effect of electron configurations with one electron; one electron more than a half-filled level; one electron less than a full shell; and one electron less than a half-filled shell.

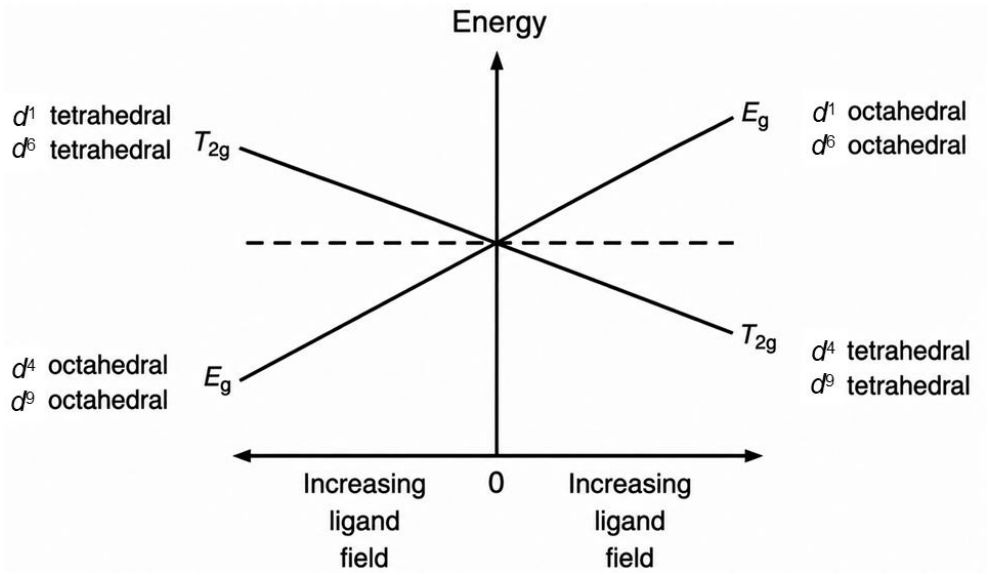


Fig. 6.14. Orgel diagram for d^1, d^4, d^6 and d^9 in tetrahedral and octahedral field.

c) Orgel Diagram for d^2 and d^7 Configurations

d^2 octahedral

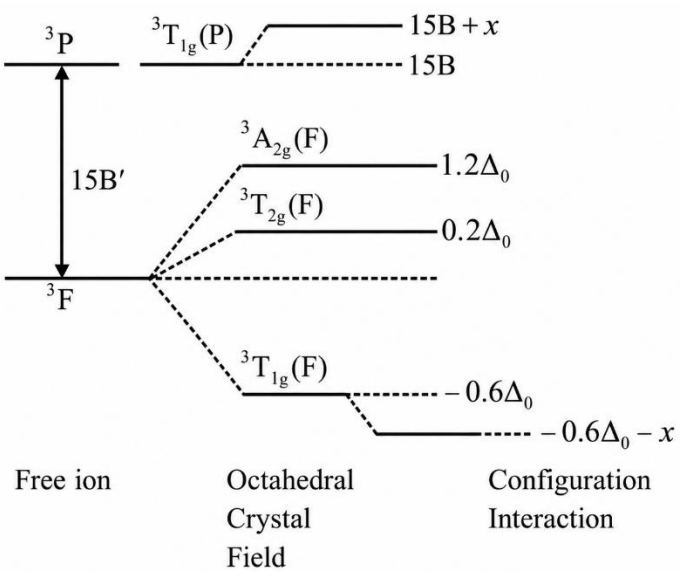


Fig. 6.15. Splitting of ^3P and ^3F in octahedral field.

Now consider the d^2 configuration. The ground term for a free d^2 ion is ^3F. There is also a higher energy term ^3P. When these terms are placed in an octahedral field, they split as follows. The *F* term splits into three levels: $^3T_{1g}$, $^3T_{2g}$, $^3A_{2g}$. The *P* term transforms into: $^3T_{1g}$ (excited state). The lowest level among these becomes the ground state, usually $^3T_{1g}$. Possible transitions include:

$^3T_{1g} \rightarrow {}^3T_{2g}$

$^3T_{1g} \rightarrow {}^3A_{2g}$

$^3T_{1g} \rightarrow {}^3T_{1g}(P)$

These transitions produce three absorption bands in the spectrum. Similarly, d^7 high-spin complexes show comparable splitting patterns.

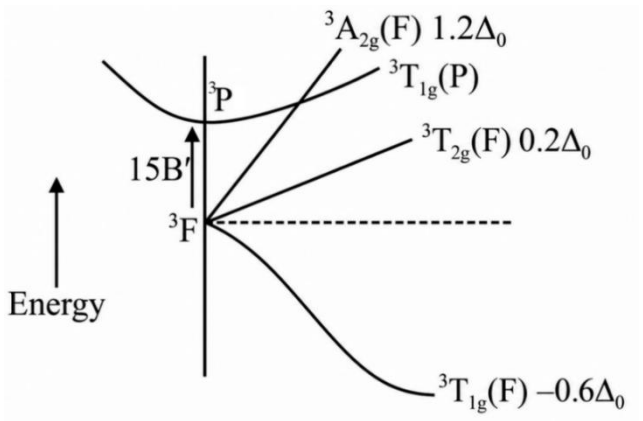


Fig. 6.16. Orgel diagram for d^2 octahedral complexes

d^2 tetrahedral

Electronic spectra of d^2-tetrahedral complexes: In tetrahedral complexes of d^2-metals ions like $[VCl_4]^-$ and $[VBr_4]^-$ the *d*-orbitals split into *e* (lower energy) and t_2 (higher energy) orbitals giving rise to electronic configuration $e^2t^0{}_2$. In ground state there is only one arrangement of two electrons with parallel spins $d^1{}_{x^2-y^2}d^1{}_{z^2}$. Thus, this state is electronically non degenerate and is represented as $^3A_2$. If one of the two electrons is excited to a t_2 orbital, the electronic configuration becomes $e_1\ t_2{}^1$. Corresponding to this electronic configuration, the lower energy state will be that when the two electrons are present in orbitals as far apart as possible. The two electrons can be arranged in either of the three ways- $d^1{}_{z^2}\ d^1{}_{xy}$, $d^1{}_{x^2-y^2}d^1{}_{zx}$ and $d^1{}_{x^2-y^2}\ d^1{}_{yz}$. Therefore, this state is triply degenerate and is represented as $^3T_2$. There is another triplet state corresponding to e^1t^1 configuration in which the two electrons occupy the orbitals which are relatively closer together: $d^1{}_{x^2-y^2}d^1{}_{xy}$, $d^1{}_{z^2}\ d^1{}_{xz}$ and $d^1{}_{z^2}\ d^1{}_{yz}$. This state is of higher energy and is represented as $^3T_1$. If both the electrons are excited to t_2 orbitals, the electronic configuration becomes $e^0t^2{}_2$. Corresponding to this electronic configuration, there are three ways of arrangement of two electrons in any of the three orbitals of t_2 orbitals: $d^1{}_{xy}\ d^1{}_{yz}$ or $d^1{}_{yz}\ d^1{}_{zx}$ or $d^1{}_{xy}\ d^1{}_{zx}$. Therefore, this state, once again is triply degenerate and is represented as $^3T_1(P)$. This state is of highest energy. It has been seen that the order of energies of these states $^3A_2$, $^3T_2$, $^3T_1$ is reverse of the energies of $^3A_{2g}$, $^3T_{2g}$ and $^3T_{1g}$ for d^2- octahedral complexes. The terms having same spin multiplicity arising for d^2-configuration are ^3F and ^3P. ^3F is the ground state term. The *P* state does not split in a complex but ^3F state splits into $^3A_2$, $^3T_2$ and $^3T_1$ states in tetrahedral complex as shown in **Fig. 6.17**.

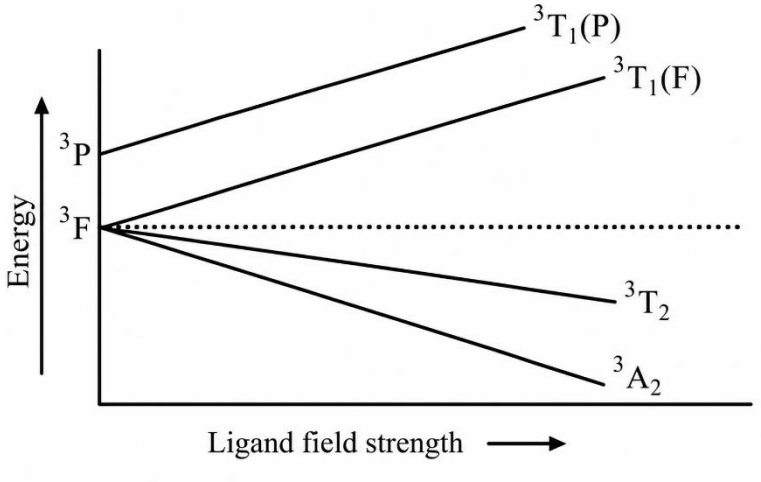


Fig. 6.17. Orgel diagram for d^2 tetrahedral complex

Three possible transitions are: $^3T_2 \leftarrow {}^3A_2$

$^3T_1(F) \leftarrow {}^3A_2$

$^3T_1(P) \leftarrow {}^3A_2$

d^7 Octahedral

Electronic spectra of d^7-High spin octahedral complexes: The Free ion ground state term for Co^{2+} (d^7) is ^4F and its other term with same spin multiplicity of higher energy is ^4P. In high spin octahedral complexes, the splitting of ^4F state is same as for d^2-octahederal complexes. The ^4F term splits into $^4T_{1g}$, $^4T_{2g}$ and $^4A_{2g}$ states as shown in the figure.

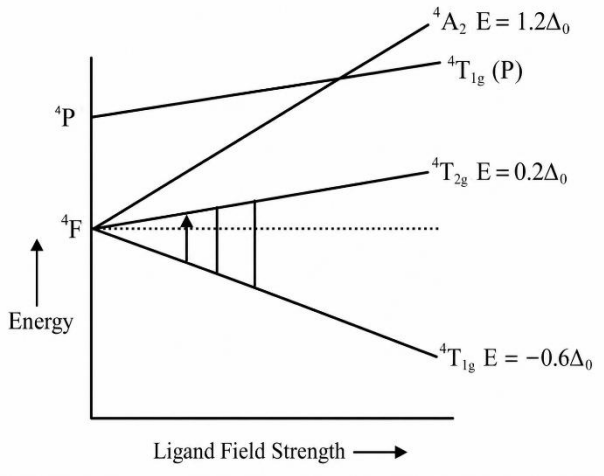


Fig. 6.18. Orgel diagram for d^7-High spin complexes

For crystal of $KCoF_3$ in which Co^{2+} ion is surrounded octahedrally by six F– ligands. There are three absorption bands at 7150 cm^{-1}, 15200 cm^{-1} and 19200 cm^{-1} corresponding to three transitions.

d^7 tetrahedral

Electronic Spectra of d^7 Tetrahedral Complexes:

In a tetrahedral complex ion, say $[CoCl_4]^{2-}$ the splitting of free ion ground term is the reverse of that in octahedral complexes so that for d^7 – ion in tetrahedral complex $^4A_2$ is of lowest energy. There are three possible transitions:

$$^4T_2 \leftarrow {}^4A_2 \quad \nu_1 = 3300 \text{ cm}^{-1} \text{ (IR region)}$$

$$^4T_1(F) \leftarrow {}^4A_2 \quad \nu_2 = 5500 \text{ cm}^{-1} \text{ (IR region)}$$

$$^4T_1(P) \leftarrow {}^4A_2 \quad \nu_3 = 14700 \text{ cm}^{-1} \text{ (Visible region)}$$

Only one band corresponding to $^4T_1(P) \leftarrow {}^4A_2$ appears in visible region at 14700 cm^{-1} (ν_3). Two bands corresponding to and $^4T_2 \leftarrow {}^4A_2$ and $^4T_1(F) \leftarrow {}^4A_2$ appear at 3300 cm^{-1} (ν_1) and 5500 cm^{-1} (ν_2) respectively. These two bands are in infrared region. The electronic transitions are shown in figure.

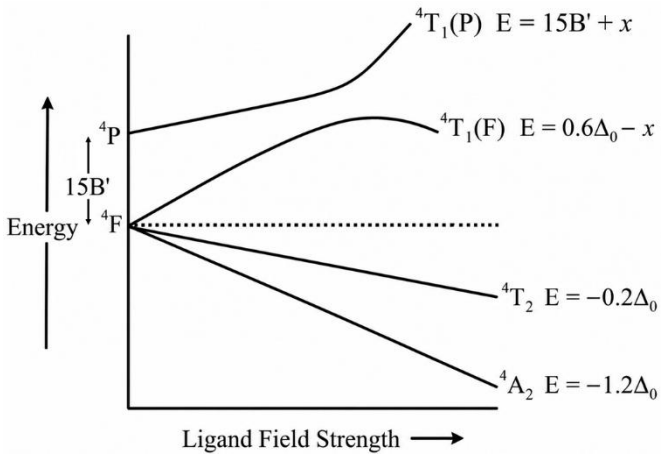


Fig. 6.19. Orgel diagram of d^7 tetrahedral complexes.

d) Orgel Diagram for d^3 and d^8 Configurations

For a d^3 configuration, the ground term of the free ion is again ^4F. There is also a higher energy term ^4P. Electronic transitions occur from the ground state to these excited states. Typical transitions are:

$^4A_{2g} \rightarrow {}^4T_{2g}$

$^4A_{2g} \rightarrow {}^4T_{1g}(F)$

$^4A_{2g} \rightarrow {}^4T_{1g}(P)$

These transitions lead to three absorption bands in the spectrum.

d^8 octahedral

Electronic spectra of d^8 – octahedral complexes: In d^8- octahedral complexes, the *d*-orbitals split into t_{2g} (lower energy) and e_g (higher energy) orbitals. Thus, in ground state the electronic configuration is $t_{2g}^6\ e_g^2$. There is only one electronic arrangement for this electronic configuration *i.e.* $t_{2g}^6 d^1{}_{x^2-y^2} d^1{}_{z^2}$ and the ground state term corresponding to this configuration is represented as $^3A_{2g}$. In a d^8-octahedral complex, two holes may be considered in e_g orbitals as shown in figure (**Fig. 6.20**).

When ligand field strength increases, there will be bending of $^3T_{1g}$ (*F*) and $^3T_{1g}$ (*P*) line because these states are of same symmetry and there is interelectronic repulsion (or mixing of two T_{1g} states). This electronic repulsion lowers the energy of lower state and increases energy of the higher state. Thus, due to inter electronic repulsion the two T_{1g} states do not cross. This is called non crossing rule. Electronic spectra of octahedral Ni(II), d^8 complexes usually consist of three bands according to the following transitions:

$$^3T_{2g} \leftarrow {}^3A_{2g} = \nu_1$$

$$^3T_{1g}(F) \leftarrow {}^3A_{2g} = \nu_2$$

$$^4T_1(P) \leftarrow {}^4A_2 = \nu_3$$

The lowest energy transition *i.e.* $^3T_{2g} \leftarrow {}^3A_{2g}$ gives the value of Δ_0.

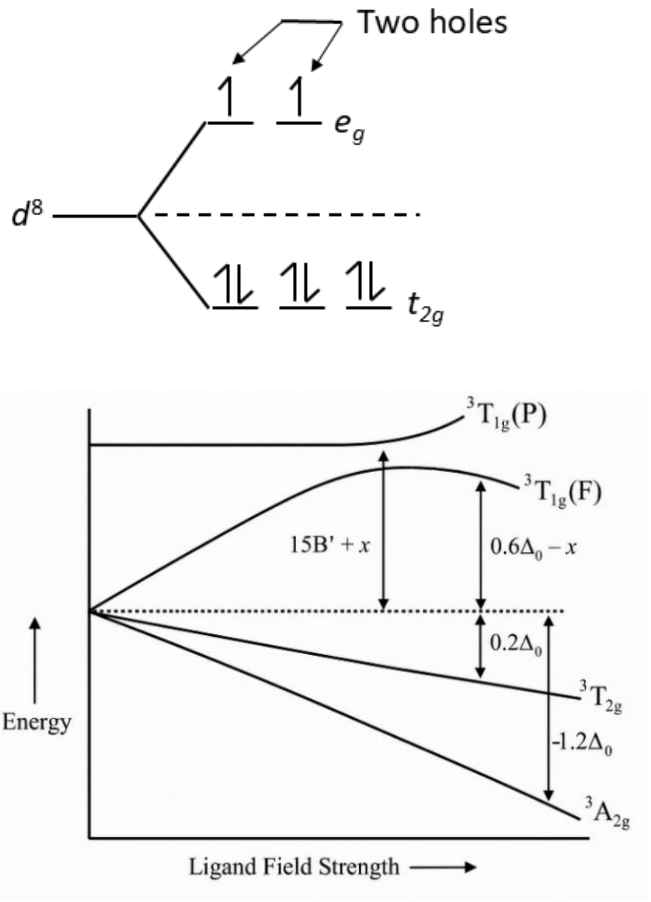


Fig. 6.20. Orgel diagram of d^8 octahedral complex

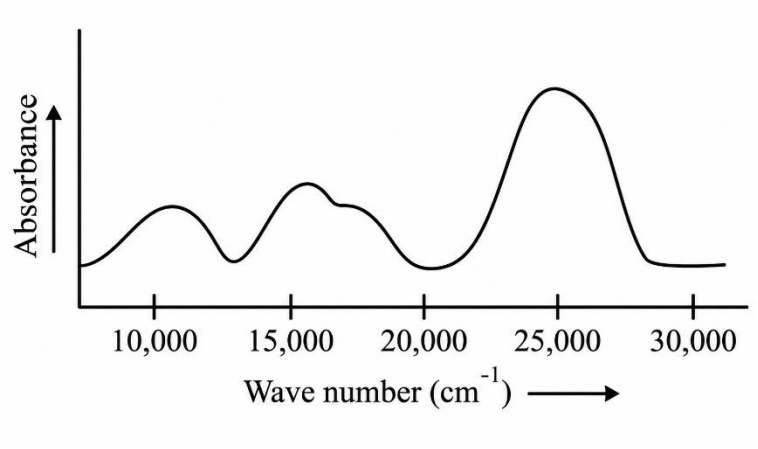


Fig. 6.21. Absorption spectrum of $[Ni(H_2O)_6]^{2+}$

d^8 Tetrahedral

Electronic spectra for d^8 tetrahedral complexes: For d^8-metal ion in tetrahedral fields, the splitting of the free ion ground state term is the inverse of its splitting in octahedral fields as shown in the figure (**Fig. 6.22).**

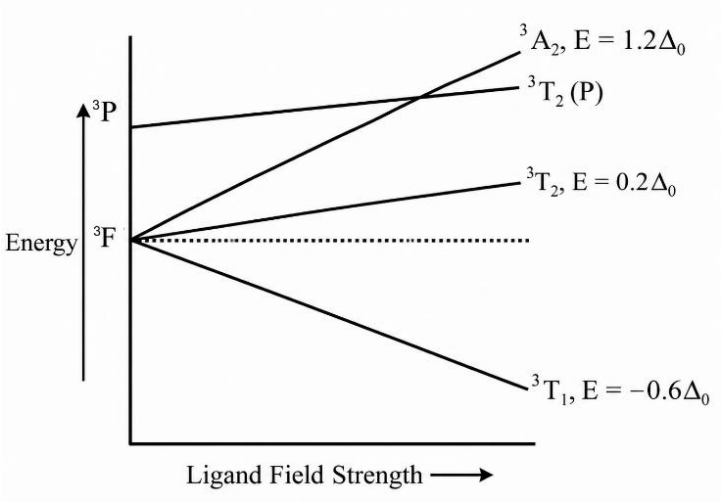


Fig. 6.22. Orgel diagram for d^8 tetrahedral complexes

The following three transition are possible for d^8-tetrahedral complex:

$$^3T_2 \leftarrow {}^3T_1$$

$$^3A_2 \leftarrow {}^3T_1$$

$$^3T_1(P) \leftarrow {}^3T_1$$

Corresponding to these transitions, three relatively intense bands are expected. For $[NiCl_4]^{2-}$, two bands are observed at 7549 cm^{-1}, 14250 – 15240 cm^{-1} as in **Fig. 6.23**. The band appears at 14250 – 15240 cm^{-1} is due to Jahn-Teller distortion.

The $^3T_2 \leftarrow {}^3T_1$ transition shows an absorption band at 3400 cm^{-1} but it is not observed in visible region because it lies in infra-red region.

.

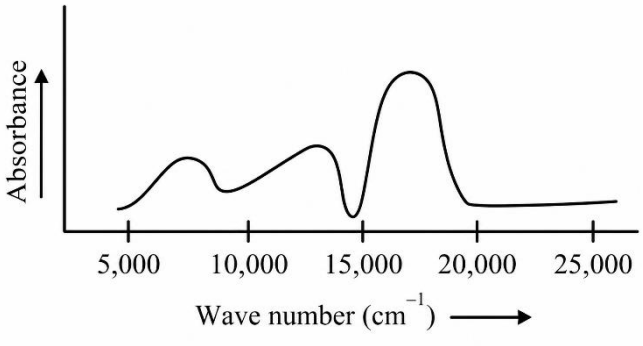


Fig. 6.23. Spectrum of $[NiCl_4]^{2-}$ complex ions

Combined Orgel diagram for d^2 , d^3 , d^7 and d^8 octahedral and tetrahedral complex is shown in figure

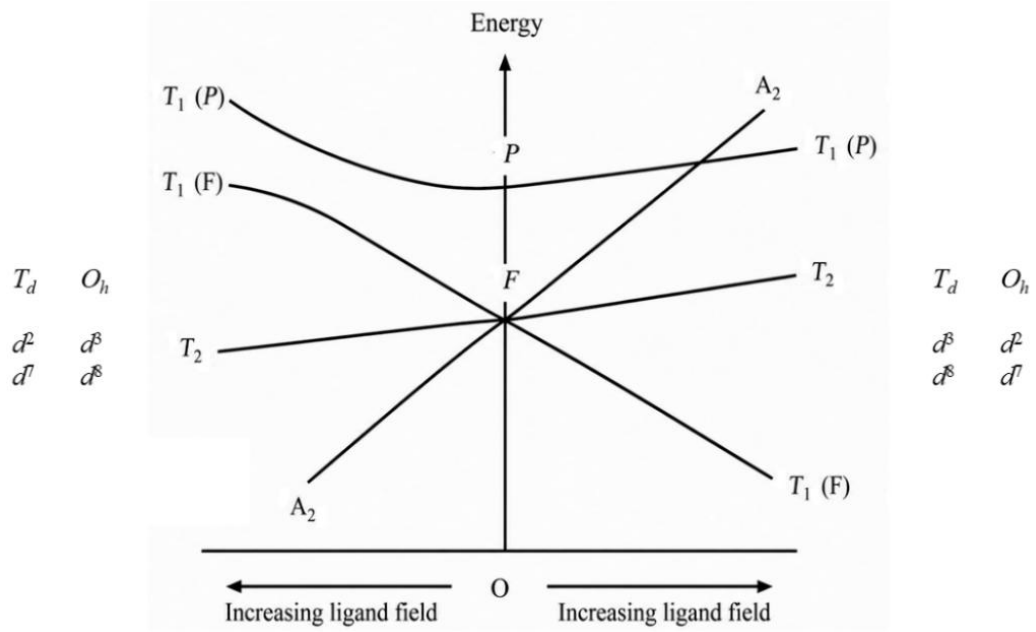


Fig. 6.24. Combined Orgel energy level diagram for two-electron and two-hole configurations.

Interpretation of Electronic Spectra Using Orgel Diagrams

Orgel diagrams help chemists interpret electronic spectra by predicting:

1. The number of absorption bands expected for a given electronic configuration.
2. The relative energies of electronic states.
3. The nature of electronic transitions occurring in the complex.

For example, if a complex with a d^3 configuration shows three absorption bands, we can attribute them to the transitions predicted by the Orgel diagram.

Table 6.3: Combined table for d^n configurations in octahedral and tetrahedral complexes

Configuration	Ground term	Excited terms with the same spin multiplicity as the ground term
d^1 (O_h), d^9 (T_d)	$^2T_{2g}$	$^2E_{2g}$
d^2 (O_h), d^8 (T_d)	$^2T_{1g}(F)$	$^3T_{2g}$, $^3A_{2g}$, $^3T_{1g}(P)$
d^3 (O_h), d^7 (T_d)	$^4A_{2g}$	$^4T_{2g}$, $^4T_{1g}$F, $^4T_{1g}(P)$
d^4 (O_h), d^6 (T_d)	$^5E_{2g}$	$^2T_{2g}$
d^5 (O_h), d^5 (T_d)	$^6A_{1g}$	None
d^6 (O_h), d^4 (T_d)	$^5T_{2g}$	$^5E_{2g}$
d^7 (O_h), d^3 (T_d)	$^4T_{1g}(F)$	$^4T_{2g}$, $^4A_{2g}$, $^4T_{1g}(P)$
d^8 (O_h), d^2 (T_d)	$^3A_{2g}$	$^3T_{2g}$, $^3A_{1g}$F, $^3T_{1g}(P)$
d^9 (O_h), d^1 (T_d)	$^2E_{2g}$	$^2T_{2g}$

Limitations of Orgel Diagrams

Although Orgel diagrams are useful, they have certain limitations. They are qualitative diagrams, meaning they do not provide exact energy values. They only indicate relative positions of energy levels. They are also mainly applicable to high-spin complexes and cannot properly describe low-spin systems. Because of these limitations, more detailed diagrams called Tanabe–Sugano diagrams are often used for quantitative analysis.

6.7 TANABE–SUGANO DIAGRAMS

Tanabe–Sugano diagrams are more advanced and quantitative compared to Orgel diagrams. They plot

$$\frac{E}{B} \; vs \; \frac{Dq}{B}$$

where
E = transition energy
B = Racah parameter
D_q = crystal field splitting parameter
Each diagram corresponds to a particular d^n configuration.

Important features of Tanabe–Sugano diagrams:

i) applicable to both high spin and low spin complexes
ii) allow calculation of ligand field parameters
iii) show how electronic states change with ligand field strength

By locating experimental absorption bands on the diagram, we can determine D_q, Racah parameter B and type of electronic transitions. Thus Tanabe–Sugano diagrams are widely used in transition metal electronic spectroscopy.

6.8 *d-d* AND CHARGE TRANSFER TRANSITIONS

d–d transitions occur when an electron moves between split d orbitals produced by the ligand field. When light of CFSE energy is absorbed, electrons move from $t_{2g} \rightarrow e_g$. This is called a *d–d* transition. These transitions are usually weak and responsible for colour of complexes.
Let's now carefully discuss Charge Transfer Transitions in transition metal complexes. This topic is extremely important in electronic spectroscopy because these transitions are responsible for some of the most intense absorption bands observed in UV–Visible spectra.

Charge Transfer Transitions

In transition metal complexes, electronic absorption usually occurs through two main types of transitions:

1. *d–d* transitions
2. charge transfer transitions

In *d–d* transitions, electrons move between different *d* orbitals of the same metal ion. However, in charge transfer transitions, an electron moves between orbitals centered on different parts of the complex, typically between the metal and the ligand. Thus, charge transfer transitions involve the movement of electronic charge from one atom or group to another within the complex. Because of this large redistribution of electron density, these transitions generally require higher energy and therefore occur mostly in the UV or visible region. Charge transfer transitions are usually very intense, producing strong absorption bands. The molar absorptivity values (ε) are often between 10^3 and 10^5 $Lmol^{-1}cm^{-1}$, which is much higher than the values observed for *d–d* transitions.

Basic Concept of Charge Transfer

To understand charge transfer transitions, we need to consider the molecular orbitals of a metal complex. In coordination compounds, molecular orbitals are formed by interaction of:

- metal atomic orbitals (such as *d* orbitals)
- ligand orbitals (such as *p* orbitals or π orbitals)

If the energy difference between these orbitals is suitable, absorption of light can promote an electron from a ligand orbital to a metal orbital or from a metal orbital to a ligand orbital.

This movement of an electron corresponds to transfer of electronic charge, which gives rise to the name charge transfer transition.

Types of Charge Transfer Transitions

Charge transfer transitions are generally classified into two main types:

1. Ligand-to-Metal Charge Transfer (LMCT)
2. Metal-to-Ligand Charge Transfer (MLCT)

Ligand-to-Metal Charge Transfer (LMCT)

In ligand-to-metal charge transfer, an electron is transferred from a ligand orbital to an empty orbital of the metal ion. In other words, the ligand acts as an electron donor, and the metal acts as an electron acceptor. This type of transition occurs when the metal ion is in a high oxidation state and the ligand has lone pair electrons that can be easily donated.

Examples of such ligands include: halide ions (Cl^-, Br^-, I^-), oxide ions (O^{2-}), sulfide ions (S^{2-}) etc.

Example of LMCT

A well-known example is the complex having Fe^{3+} – O^{2-}. In such a complex, an electron can move from the oxygen ligand orbital to the iron metal orbital. This process can be represented as:

$$\text{Ligand orbital} \rightarrow \text{Metal } d \text{ orbital}$$

The transition corresponds to:

$$O^{2-} \rightarrow Fe^{3+}$$

This transfer of electron density gives rise to intense absorption bands. Many complexes containing Fe^{3+}, Mn^{7+}, Cr^{6+}, and other high oxidation state metals show LMCT transitions.

Metal-to-Ligand Charge Transfer (MLCT)

In metal-to-ligand charge transfer, an electron moves from a metal orbital to an empty ligand orbital. In this case the metal acts as an electron donor and the ligand acts as an electron acceptor. This type of transition occurs mainly when ligands possess *low-lying empty π orbitals** capable of accepting electrons. Typical ligands involved in MLCT include: bipyridine, phenanthroline, carbon monoxide, cyanide ions *etc*. These ligands are often referred to as *π*-acceptor ligands. A common example is the complex $Ru(bipy)_3^{2+}$ where bipy stands for bipyridine. In this complex, an electron from the metal *d* orbital can be transferred to the *π** orbital of the ligand. This transition can be represented as: Metal *d* orbital → Ligand *π** orbital. Thus, the electron moves from Ru^{2+} → bipyridine. This type of transition produces strong absorption bands in the visible region.

Charge transfer transitions are generally much more intense than *d*–*d* transitions. The reason lies in the selection rules. Most *d*–*d* transitions violate the Laporte selection rule, making them weak. However, charge transfer transitions involve orbitals with different symmetry, so they satisfy the selection rules and therefore occur with much higher probability. As a result, their molar absorptivity values are very large. Charge transfer transitions play a crucial role in the interpretation of UV–visible spectra of coordination compounds. They are important because they (i) explain intense colours of many complexes; (ii) provide information about metal–ligand bonding; (iii) help identify oxidation states of metal ions; (iv) assist in studying electron transfer processes. Charge transfer transitions are also very important in photochemistry, catalysis and solar energy conversion systems.

Comparison Between *d–d* and Charge Transfer Transitions

A comparison between these two types of transitions helps clarify their differences:

Property	***d-d* Transition**	**Charge Transfer Transition**
Electron movement	Between *d* orbitals of same metal	Between metal and ligand
Intensity	Weak	Very strong
Molar absorptivity	10-100	10^3-10^5
Selection rule	Usually Laporte forbidden	Usually allowed
Spectral bands	Narrow	Broad and intense

6.9 CALCULATION OF D_q, B AND C PARAMETERS

The parameters D_q, B, and C describe electronic interactions in transition metal complexes. D_q represents the splitting of d orbitals caused by ligands. For octahedral complexes: $\Delta_0 = 10Dq$

The value of D_q can be obtained from the energy of the lowest absorption band in electronic spectra. The Racah parameter B measures electron–electron repulsion within the d orbitals. It can be calculated using the energies of two absorption bands obtained from the spectrum. When a metal forms a complex, the value of B decreases compared to the free ion because of covalent interactions between metal and ligands. Parameter C also represents electron repulsion but is less commonly determined experimentally. Usually, $c \approx 4B$.

6.10 NEPHELAUXETIC EFFECT

When a transition metal ion forms a coordination complex with ligands, the electron distribution around the metal ion changes. In a free metal ion, the *d* electrons are strongly localized on the metal atom, and therefore the electron–electron repulsion between the *d* electrons is relatively large. However, when ligands coordinate to the metal ion, some of the electron density spreads toward the ligand orbitals because of covalent interaction between the metal and the ligands. As a result, the *d* electrons are no longer completely confined to the metal ion. Instead, their electron cloud becomes slightly expanded or delocalized. This expansion of the electron cloud reduces the repulsion between the *d* electrons. The phenomenon is known as the nephelauxetic effect.

Nephelauxetic Ratio

The extent of the nephelauxetic effect is expressed using the nephelauxetic ratio, represented by the symbol *β* (beta). The nephelauxetic ratio is defined as the ratio of the Racah parameter of the complex to the Racah parameter of the free metal ion.

$$\beta = \frac{B_{complex}}{B_{free\ ion}}$$

where,

$B_{complex}$ = Racah parameter for the metal ion in the complex

$B_{free\ ion}$ = Racah parameter for the free metal ion

Interpretation of the Nephelauxetic Ratio

The value of *β* tells us about the nature of bonding between the metal and the ligands. If the value of *β* is close to 1, the electron–electron repulsion in the complex is almost the same as in the free ion. This means the metal–ligand bond is largely ionic, and there is little delocalization of electron density. If *β* is less than 1, the Racah parameter has decreased, indicating that electron density has expanded toward the ligands. This means that the metal–ligand bond has covalent character. The smaller the value of *β*, the greater the covalent character of the metal–ligand bond. Thus, the nephelauxetic ratio provides an important method for estimating the degree of covalency in coordination compounds.

Different ligands influence the nephelauxetic effect to different extents. Ligands that are highly polarizable or capable of strong orbital overlap with the metal ion tend to produce a greater nephelauxetic effect. The magnitude of the nephelauxetic effect generally follows a sequence known as the nephelauxetic series. A typical order is

$$I^- > Br^- > Cl^- > F^- > OH^- > H_2O > NH_3$$

Ligands toward the left side of this series produce a greater decrease in the Racah parameter, leading to smaller β values. This indicates that these ligands form more covalent metal–ligand bonds. Ligands toward the right side produce smaller nephelauxetic effects and therefore more ionic bonding character.

Several factors influence the magnitude of the nephelauxetic effect. One important factor is the nature of the ligand. Large, highly polarizable ligands tend to allow greater overlap with metal orbitals, which increases covalency and enhances the nephelauxetic effect. Another factor is the oxidation state of the metal ion. Higher oxidation states often increase metal–ligand interaction, affecting the distribution of electron density. The size and electronic configuration of the metal ion also play a role, because they influence the ability of the metal orbitals to overlap with ligand orbitals.

The nephelauxetic effect provides important insights into the nature of bonding in coordination compounds. It helps chemists understand how electron density is distributed between the metal and ligands. It also helps in comparing different ligands in terms of their ability to form covalent bonds with metal ions. In addition, the nephelauxetic ratio is often used together with other ligand field parameters, such as crystal field splitting energy and Racah parameters, to analyze the electronic spectra of transition metal complexes. Thus, the concept of the nephelauxetic ratio is extremely useful for studying metal–ligand covalency, electronic structure, and bonding characteristics in coordination chemistry.

6.11 APPLICATIONS OF ELECTRONIC SPECTROSCOPY IN TRANSITION METAL COMPLEXES

Electronic spectroscopy is extremely useful for studying transition metal complexes. From spectral data we can determine:

i) oxidation state of metal ions
ii) geometry of complexes (octahedral, tetrahedral, square planar)
iii) ligand field strength
iv) nature of electronic transitions
v) metal–ligand bonding characteristics
vi) covalency of complexes through nephelauxetic ratio

Thus, electronic spectroscopy provides deep insight into the electronic structure and bonding of coordination compounds.

W CHECK YOUR PROGRESS

Q1. What is meant by electronic spectroscopy in transition metal complexes?

Q2. In which region of the electromagnetic spectrum do most electronic transitions of coordination compounds occur?
Q3. What condition must be satisfied for the absorption of light by a substance?
Q4. State the Beer–Lambert law and explain its significance.
Q5. How does absorbance vary with concentration of the absorbing species?
Q6. What is molar absorptivity (*ε*)? How does it differ for *d–d* transitions and charge transfer transitions?
Q7. What are atomic term symbols? Explain the meaning of the terms in the expression $^{2S+1}L_J$.
Q8. What is the difference between Orgel diagrams and Tanabe–Sugano diagrams?
Q9. Distinguish between *d–d* transitions and charge transfer transitions.
Q10. What is the nephelauxetic effect and what causes it in coordination complexes?

2 6.12 LET US SUM UP

- Electronic spectroscopy studies the absorption of UV–Visible light by transition metal complexes.
- Absorption occurs when electrons move from lower energy orbitals to higher energy orbitals.
- Most electronic transitions occur in the UV–Visible region (200–800 nm).
- These transitions provide information about electronic structure, ligand field strength, geometry, and bonding in coordination compounds.
- Light consists of photons, each carrying energy.
- The energy of radiation depends on frequency and wavelength.
- Absorption occurs when the energy of a photon equals the energy difference between two electronic states.
- The Beer–Lambert law relates absorbance to concentration and path length.
- Absorbance increases with increasing concentration of the absorbing species.
- The relationship allows quantitative determination of concentration using spectrophotometry.
- The molar absorptivity (*ε*) indicates how strongly a substance absorbs light.
- *d–d* transitions usually have small ε values, while charge transfer transitions have large ε values.
- Electronic states describe the energy and arrangement of electrons in atoms or ions.
- Atomic term symbols are written as: $^{2S+1}L_J$, *S* represents total spin, *L* represents orbital angular momentum.
- In complexes, molecular term symbols are used, which depend on symmetry. For octahedral complexes, symbols such as *A*, *E*, and *T* represent degeneracy of orbitals. Subscripts *g* and *u* indicate symmetry with respect to inversion.
- Orgel diagrams are qualitative diagrams showing splitting of electronic terms in ligand fields.
- Tanabe–Sugano diagrams provide a quantitative description of electronic states.
- *d–d* transitions occur when electrons move between split d orbitals of the same metal ion. Charge transfer transitions involve movement of electrons between

metal and ligand orbitals. These transitions are much more intense than *d–d* transitions.

- When a metal forms a complex, the electron cloud expands toward ligands. This reduces electron–electron repulsion. The phenomenon is called the nephelauxetic effect.

K 6.13 ANSWERS TO CHECK YOUR PROGRESS

Answer to Q1: Electronic spectroscopy is the study of the absorption of UV–Visible light by transition metal complexes, which leads to electronic transitions.
Answer to Q2: Most electronic transitions occur in the UV–Visible region (200–800 nm).
Answer to Q3: Absorption occurs when the energy of the incident photon matches the energy difference between two electronic states.
Answer to Q4: The Beer–Lambert law states that absorbance is directly proportional to the concentration of the absorbing species and the path length of the solution. It is important for quantitative analysis using spectrophotometry.

Answer to Q5: Absorbance increases with increasing concentration of the absorbing species.

Answer to Q6: Molar absorptivity (ε) is a measure of how strongly a substance absorbs light. *d–d* transitions have low ε values, whereas charge transfer transitions have high ε values.

Answer to Q7: Atomic term symbols describe the electronic state of atoms or ions and are written as $^{2S+1}L_J$, where: *S* is the total spin, *L* is the total orbital angular momentum and *J* is the total angular momentum.

Answer to Q8: Orgel diagrams are qualitative and show the splitting of electronic terms, while Tanabe–Sugano diagrams are quantitative and provide detailed information about electronic transitions and energy levels.

Answer to Q9: *d–d* transitions involve movement of electrons between split d orbitals of the same metal ion and are usually weak, whereas charge transfer transitions involve transfer of electrons between metal and ligand orbitals and are much more intense.

Answer to Q10: The nephelauxetic effect refers to the expansion of the electron cloud of the metal ion toward the ligands, which reduces electron–electron repulsion in the complex.

O 6.14 FURTHER READING

- Lee, J. D. *Concise Inorganic Chemistry*, 5th ed.; Wiley-Blackwell: Oxford, 1996.
- Shriver, D. F.; Atkins, P. W. *Inorganic Chemistry*, 5th ed.; Oxford University Press: Oxford, 2010.
- Huheey, J. E.; Keiter, E. A.; Keiter, R. L. *Inorganic Chemistry: Principles of Structure and Reactivity*, 4th ed.; Pearson.
- Kumar, A. *Coordination Chemistry*.

M 6.15 MODEL QUESTIONS

Q1. What is meant by electronic transition? What are *d*–*d* transitions? Why are *d*–*d* transitions usually weak?
Q2. What is spin selection and Laporte selection rule?
Q3. What is meant by term symbol? Write the general form of an atomic term symbol. What is the meaning of multiplicity in a term symbol?
Q4. Why are charge transfer bands more intense than *d*–*d* bands?
Q5. Explain the origin of colour in transition metal complexes.
Q6. Write a short note on electronic term symbols.
Q7. Explain the spin selection rule with suitable examples.
Q8. Describe the Laporte selection rule and its significance in electronic spectroscopy.
Q9. Why are *d*–*d* transitions weak in octahedral complexes but stronger in tetrahedral complexes?
Q10. Explain Metal-to-Ligand Charge Transfer (MLCT) transitions with examples.
Q11. Explain in detail the absorption of light and Beer–Lambert law and discuss their significance in electronic spectroscopy.
Q12. Describe the Tanabe–Sugano diagrams and explain their importance in transition metal spectroscopy.
Q13. Explain the different types of charge transfer transitions with suitable examples.
Q14. Discuss the nephelauxetic effect and nephelauxetic ratio, and explain their significance in metal–ligand bonding.
Q15. Explain how Racah parameters and crystal field splitting parameters are determined from electronic spectra.
Q16. Describe how electronic spectroscopy can be used to determine the geometry of coordination compounds.
Q17. A transition metal complex shows an absorption band at 20,000 cm^{-1}. Calculate the value of 10*D*q and *D*q.
Q18. The Racah parameter B for a free metal ion is 900 cm^{-1}, while for its complex it is 720 cm^{-1}. Calculate the nephelauxetic ratio (β).
Q19. The absorbance of a solution is 0.8 in a 1 cm cuvette. If the molar absorptivity is 4000 $Lmol^{-1}cm^{-1}$, calculate the concentration of the solution using the Beer–Lambert law.
Q20. The absorbance of a solution increases from 0.2 to 0.6 when the concentration is tripled. Verify whether the Beer–Lambert law is obeyed.
Q21. A complex has absorption bands at 17,000 cm^{-1} and 24,000 cm^{-1}. Using these values, determine the Racah parameter *B* (conceptual question based on Tanabe–Sugano analysis).
Q22. Explain why tetrahedral complexes show more intense colours than octahedral complexes.
Q23. Discuss how selection rules influence the intensity of spectral bands.

UNIT 7: MAGNETIC PROPERTIES OF TRANSITION METAL COMPLEXES

UNIT STRUCTURE

7.1 Learning Objectives

7.2 Introduction

7.3 Types of Magnetic Bodies

7.4 Antiferromagnetic Coupling

7.5 Magnetic Properties Based on Crystal Field Theory (Spin Only Magnetic Moments)

7.6 Orbital Contribution to Magnetic Moment

7.7 Effect of Temperature on Magnetic Behaviour

7.8 Let Us Sum Up

7.9 Answers to Check Your Progress

7.10 Further Reading

7.11 Model Questions

7.1 LEARNING OBJECTIVES

After studying this unit, you should be able to:

- distinguish between diamagnetic, paramagnetic, ferromagnetic and antiferromagnetic substances
- understand the concept of antiferromagnetic coupling in polynuclear complexes
- apply Crystal Field Theory to interpret magnetic properties of transition metal complexes
- calculate spin-only magnetic moments and relate them to the number of unpaired electrons
- explain orbital contribution to magnetic moment and the concept of quenching of orbital angular momentum
- describe the effect of temperature on magnetic behaviour using Curie and Curie–Weiss laws
- understand the principles and applications of Gouy and Faraday methods of magnetic susceptibility measurement
- correlate magnetic properties with electronic spectra of transition metal complexes

7.2 INTRODUCTION

In the previous unit, you studied electronic spectra of transition metal complexes, where we saw how the interaction of d-orbitals with ligands leads to absorption of light in the visible and near-visible regions. Closely connected to these electronic arrangements is another extremely important property of transition metal complexes,

namely their magnetic behaviour. In fact, the same electrons that are responsible for colour in coordination compounds are also responsible for their magnetic properties.

Magnetic properties provide deep insight into the electronic configuration, oxidation state, number of unpaired electrons, geometry and nature of metal–ligand bonding in complexes. Experimental magnetic moment values are routinely used to distinguish between high-spin and low-spin complexes, to confirm octahedral or tetrahedral geometry, and to understand metal–metal interactions in polynuclear systems.

In this unit, we will learn the basic types of magnetic behaviour such as diamagnetism, paramagnetism, ferromagnetism and antiferromagnetism. We will then discuss antiferromagnetic coupling, which is particularly important in polynuclear complexes. This will be followed by a detailed discussion of magnetic properties from the point of view of Crystal Field Theory (CFT), including spin-only magnetic moments, orbital contribution, quenching of orbital angular momentum, and finally the effect of temperature on magnetic behaviour.

At the undergraduate level, you have already studied basic magnetic concepts such as magnetic moment and magnetic susceptibility. In this unit, these quantities will not be re-derived; instead, they will be used as tools to interpret the electronic structure and magnetic behaviour of transition metal complexes.

7.3 TYPES OF MAGNETIC BODIES

A simple and commonly used way of classifying materials on the basis of their magnetic behaviour is to observe how they respond when placed in an external magnetic field. Once this response is known, we can then examine the nature of interactions or causes responsible for such behaviour.
In some materials, the magnetic moments present at the atomic or ionic level behave independently and do not influence one another. In other materials, however, strong interactions between neighbouring magnetic moments are present. These interactions can give rise to more complex magnetic behaviour, which often depends on the structure and arrangement of atoms or ions in the material.
On this basis, magnetic materials are broadly classified into four main categories.

Diamagnetic Materials

When a substance is exposed to an external magnetic field, the motion of its electrons is slightly modified, leading to the generation of an induced magnetic moment. This induced moment is oriented opposite to the direction of the applied field. Such behaviour is known as the diamagnetic effect and originates from the presence of paired electrons in the system.
Since paired electrons are present in all atoms and molecules, diamagnetism is, in principle, a universal property of matter. However, when a substance contains only paired electrons, this effect becomes dominant. Under these conditions, the substance is classified as diamagnetic and shows a weak repulsion when placed in a magnetic field.

Paramagnetic Materials

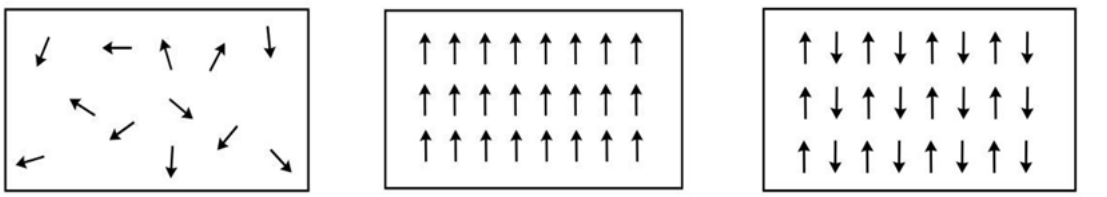
When a substance containing one or more unpaired electrons is placed in an external magnetic field, each unpaired electron contributes a magnetic moment. In the absence of the field, these moments are randomly oriented and the substance shows no net magnetisation. On application of a magnetic field, partial alignment of these magnetic moments occurs, producing a net magnetic moment in the same direction as the applied field.
Compounds that exhibit this behaviour are classified as paramagnetic and are weakly attracted by an external magnetic field. The extent of this attraction decreases with increase in temperature due to thermal agitation, and paramagnetic susceptibility therefore shows a strong temperature dependence.

Ferromagnetic Materials

Ferromagnetic behaviour arises in substances that contain unpaired electrons and, in addition, exhibit a strong interaction between neighbouring magnetic moments. This interaction causes the individual moments to align parallel to one another, even in the absence of an external magnetic field, leading to spontaneous magnetisation.
Such substances are termed ferromagnetic compounds and are strongly attracted by an external magnetic field. Ferromagnetic materials display very large positive magnetic susceptibility and show characteristic properties such as hysteresis and remanence. Their magnetic behaviour depends on both the strength of the applied field and the temperature of the system.

Antiferromagnetic Materials

Antiferromagnetic compounds also contain unpaired electrons; however, the magnetic moments of adjacent metal centres interact in such a way that they align antiparallel to each other. As a result, the individual magnetic moments largely cancel one another.
Compounds showing this type of alignment are classified as antiferromagnetic. They exhibit only a small positive magnetic susceptibility and are therefore weakly attracted by an external magnetic field. The magnetic behaviour of antiferromagnetic compounds is mainly temperature dependent and shows characteristic changes near a critical temperature known as the **Néel temperature** (The temperature at which an antiferromagnetic material loses its ordered antiparallel spin arrangement and begins to behave as a paramagnetic material).



(a)Paramagnetic Material (b) Ferromagnetic Material (c) Antiferromagnetic Material

Fig. 7.1: Schematic representation of arrangement of magnetic dipole moment in (a) Paramagnetic, (b) Ferromagnetic; and (c) Antiferromagnetic materials.

7.4 ANTIFERROMAGNETIC COUPLING

In coordination chemistry, antiferromagnetic behaviour is frequently observed in polynuclear transition metal complexes. In such systems, the magnetic interaction does not arise from isolated metal ions, but from coupling between neighbouring magnetic centres. This interaction, which leads to antiparallel alignment of magnetic moments, is referred to as antiferromagnetic coupling.

Antiferromagnetic coupling occurs when two adjacent metal ions, each possessing unpaired electrons, interact through a bridging ligand such as oxide (O^{2-}), hydroxide (OH^-), halide or carboxylate groups. The interaction is generally mediated through orbital overlap involving the metal ions and the bridging atom, a process often described as superexchange interaction. One example of antiferromagnetism is MnO; where an oxide ion (O^{2-}) serves as bridging ligand (See Fig 7.2). Another example includes *μ*-oxo bridged iron(III) dimers, where strong antiferromagnetic coupling leads to a much lower magnetic moment than expected for two isolated Fe^{3+} ions.

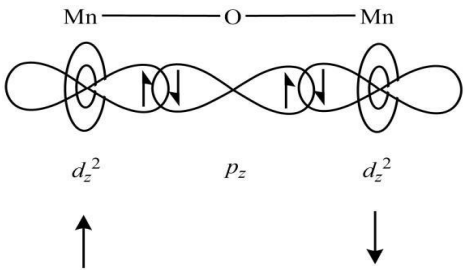


Fig. 7.2. Antiferromagnetic coupling in MnO.

As a result of antiferromagnetic coupling, the magnetic moments of the metal centres align in opposite directions, leading to partial or complete cancellation of the overall magnetic moment. Consequently, polynuclear complexes exhibiting strong antiferromagnetic coupling often show lower magnetic moments than expected on the basis of spin-only values.

The extent of antiferromagnetic coupling depends on several factors, including:

- the nature of the metal ion
- the number of unpaired electrons
- the type of bridging ligand
- the metal–ligand–metal bond angle and distance

Temperature plays an important role in antiferromagnetic coupling. At low temperatures, antiparallel alignment is favoured, resulting in reduced magnetic susceptibility. With increasing temperature, thermal agitation weakens the coupling, and the complex may gradually exhibit paramagnetic behaviour above a certain temperature (Néel Temperature).

Thus, the presence of antiferromagnetic coupling must be considered while interpreting magnetic susceptibility data of polynuclear transition metal complexes.

7.5 MAGNETIC PROPERTIES BASED ON CRYSTAL FIELD THEORY

The discussion so far has shown that magnetic behaviour not only depends on the presence of unpaired electrons but also on interactions between neighbouring metal centres, as seen in antiferromagnetic coupling. However, in a large number of coordination compounds, particularly mononuclear complexes, magnetic behaviour is governed primarily by the electronic configuration of the metal ion and the manner in which its d-orbitals are affected by the surrounding ligands.

Crystal Field Theory (CFT) provides a useful framework for understanding the magnetic behaviour of transition metal complexes by relating it to the electronic arrangement of d-orbitals in the presence of ligands. As discussed in the previous unit on electronic spectra, the approach of ligands towards a metal ion causes splitting of the five degenerate d-orbitals into sets of different energies. The manner in which electrons occupy these split orbitals determines the number of unpaired electrons, and hence the magnetic properties of the complex.

From your earlier studies, you are aware that the paramagnetic moment of a substance arises from contributions due to both the spin and orbital motion of unpaired electrons. The various modes of coupling between these components are spin-spin, spin-orbital and orbital-orbital couplings. Taking all these contributions into account, the paramagnetic moment is given by

$$\mu = g\sqrt{J(J+1)}$$

where *g* is the Landé g-factor, which depends on the values of *L* (orbital angular momentum quantum number), *S* (spin angular momentum quantum number) and *J (*total angular momentum quantum number):

$$g = 1 + \frac{J(J+1) + S(S+1) - L(L+1)}{2\,J(J+1)}$$

For complexes, where spin and orbital contributions are more significant in comparison to negligible spin-orbital coupling, the value of paramagnetic moment becomes:

$$\mu = \sqrt{4S(S+1) + L(L+1)}$$

However, in many coordination compounds of the **first transition series**, this condition is observed as the contribution from orbital angular momentum is largely absent. The experimentally observed magnetic moments are therefore found to be close to the **spin-only values**. Under this approximation, L = 0 and the equation now reduces to

$$\mu = \sqrt{4S(S+1)}$$

which is known as spin only magnetic moment. By replacing *S* with *n*/2 (*n* is number of unpaired electrons), this equation can be further simplified as

$$\mu = \sqrt{n(n+2)}$$

This spin only behaviour can be explained by the phenomenon of **orbital quenching**. In the presence of a ligand field, the degeneracy of the d-orbitals is removed, and the orbital motion of electrons becomes restricted. As a result, the orbital contribution to magnetic moment is effectively suppressed. Orbital quenching is particularly effective in first-row transition metal complexes because of relatively large crystal field splitting and weak spin–orbit coupling. Consequently, the magnetic moment arises predominantly from electron spin, and the **spin-only formula provides a good approximation** for most first-row transition metal complexes. **Table 7.1** shows the calculated and experimental magnetic moments of first-row transition metal complexes, which are consistent with the spin only magnetic moment values.

In contrast, complexes of second- and third-row transition metals often show appreciable orbital contribution due to stronger spin–orbit coupling, leading to deviations from spin-only values. However, in certain octahedral d^4–d^7 systems, particularly iron(II) complexes, a temperature-dependent interconversion between high-spin and low-spin configurations may occur. This phenomenon, known as *spin crossover*, results from a delicate balance between crystal field splitting energy (Δ_0) and pairing energy. As temperature changes, the population of high-spin and low-spin states shifts, leading to measurable changes in magnetic moment. Spin crossover behaviour is of considerable importance in molecular magnetism and materials chemistry.

7.6 ORBITAL CONTRIBUTION TO MAGNETIC MOMENT

In the earlier discussion, the magnetic behaviour of transition metal complexes was interpreted primarily in terms of spin-only magnetic moments, particularly for first-row transition metal complexes. This approximation is valid in many cases due to effective suppression of orbital angular momentum. However, in a general treatment of magnetic properties, it is important to examine the role of orbital contribution and the conditions under which it becomes significant.

The total magnetic moment of a paramagnetic ion arises from two sources: the spin angular momentum of unpaired electrons and their orbital angular momentum. In free metal ions, both these contributions may be present, and the observed magnetic moment reflects their combined effect. In coordination compounds, however, the presence of a ligand field profoundly influences the extent to which orbital motion contributes to the magnetic moment.

In first-row transition metal complexes, the crystal field splitting is relatively large compared to the spin–orbit coupling. This weak spin–orbit interaction leads to the suppression of the orbital contribution and the observed magnetic moment is determined almost entirely by electron spin.

In contrast, second- and third-row transition metal complexes often show appreciable orbital contribution to the magnetic moment. In these complexes, spin–orbit coupling is significantly stronger, and orbital quenching is less effective. As a result, the observed magnetic moments frequently deviate from spin-only values. Such deviations provide

valuable information about the electronic structure, ligand field strength and symmetry of the complex.

Orbital contribution may also become significant in complexes with low symmetry ligand fields, where complete removal of orbital degeneracy does not occur, and in systems containing weak-field ligands. In such cases, partial retention of orbital angular momentum leads to enhanced magnetic moments and deviations from simple magnetic models.

Thus, while the spin-only magnetic moment provides a useful first approximation for interpreting the magnetic behaviour of many transition metal complexes, a complete understanding requires consideration of orbital contribution, particularly for heavier transition metals and low-symmetry systems.

Key Points

- The total magnetic moment of a transition metal complex arises from both spin and orbital contributions.
- In most first-row transition metal complexes, orbital contribution is quenched due to strong crystal field splitting and weak spin–orbit coupling.
- Second- and third-row transition metal complexes often show significant orbital contribution because of stronger spin–orbit coupling.
- Deviations from spin-only magnetic moments provide valuable information about electronic structure, ligand field strength and symmetry of the complex.

Table 7.1: Magnetic properties of some first- row transition metal complexes:

Central metal ion	No. of d electrons	Low Spin Complexes			High Spin Complexes		
		No. of Unpaired Electrons	μ (expt) BM	μ (calc) BM	No. of Unpaired Electrons	μ (expt) BM	μ (calc) BM
Ti^{3+}	1	0	-	-	1	1.73	1.73
V^{4+}	1	0	-	-	1	1.68-1.78	1.73
V^{3+}	2	0	-	-	2	2.75-2.85	2.83
V^{2+}	3	0	-	-	3	3.80-3.90	3.88
Cr^{3+}	3	0	-	-	3	3.70-3.90	3.88
Mn^{4+}	3	0	-	-	3	3.8-4.0	3.88
Cr^{2+}	4	2	3.20-3.30	2.83	4	4.75-4.90	4.90
Mn^{3+}	4	2	3.18	2.83	4	4.90-5.00	4.90
Mn^{2+}	5	1	1.80-2.10	1.73	5	5.65-6.10	5.92
Fe^{3+}	5	1	2.0-2.5	1.73	5	5.70-6.0	5.92
Fe^{2+}	6	0	-	-	4	5.10-5.70	4.90
Co^{3+}	6	0	-	-	4	-	4.90
Co^{2+}	7	1	1.8	1.73	3	4.30-5.20	3.88
Ni^{3+}	7	1	1.8-2.0	1.73	3	-	3.88
Ni^{2+}	8	0	-	-	2	2.80-3.50	2.83
Cu^{2+}	9	0	-	-	1	1.70-2.20	1.73

7.7 TEMPERATURE DEPENDENCE OF MAGNETIC BEHAVIOUR

Magnetic properties of transition metal complexes depend not only on electronic configuration and orbital contributions but also show a pronounced dependence on temperature. The effect of temperature on magnetism arises due to thermal agitation, which affects the orientation and interaction of magnetic moments present in a substance. An understanding of this dependence is essential for the correct interpretation of experimental magnetic data.

In paramagnetic substances, the magnetic moments associated with unpaired electrons are randomly oriented in the absence of an external magnetic field. When a magnetic field is applied, partial alignment of these moments occurs, resulting in a net magnetisation. As the temperature increases, thermal motion opposes this alignment, leading to a decrease in magnetic susceptibility. Consequently, the magnetic susceptibility of paramagnetic complexes decreases with increase in temperature.

This behaviour is described by Curie's law, which states that the magnetic susceptibility (χ) of a paramagnetic substance is inversely proportional to the absolute temperature (T):

$$\chi = \frac{C}{T}$$

where C is the Curie constant. Curie's law is obeyed well by magnetically dilute paramagnetic substances (the paramagnetic centres are well separated by diamagnetic atoms) over a wide temperature range.

In systems which are not magnetically dilute, weak interactions between neighbouring magnetic moments are present and this phenomenon is referred to as magnetic exchange. The temperature dependence of susceptibility for these materials is better described by the **Curie–Weiss law** as:

$$\chi = \frac{C}{T - \theta}$$

where θ is a constant in the units of temperature. The sign and magnitude of θ provide valuable information about the nature of magnetic interactions within the material. A positive value of θ indicates ferromagnetic interactions, while a negative value suggests antiferromagnetic interactions between metal centres.

In antiferromagnetic materials, magnetic susceptibility shows a characteristic temperature dependence. At higher temperatures, these materials often exhibit

paramagnetic behaviour. As the temperature is lowered, antiferromagnetic ordering becomes significant, and the susceptibility passes through a maximum at a characteristic temperature known as the Néel temperature (T_n). Below the Néel temperature, antiparallel alignment of magnetic moments dominates, resulting in a decrease in susceptibility.

Ferromagnetic materials also display strong temperature dependence of magnetic properties. Below a certain temperature known as the Curie temperature (T_c), spontaneous alignment of magnetic moments occurs, leading to ferromagnetism. Above the Curie temperature, thermal agitation overcomes the ordering of magnetic moments, and the material behaves as a paramagnet.

Plot of inverse susceptibility ($1/\chi$) with temperature for three different magnetic behaviours is shown in **Fig. 7.3**.

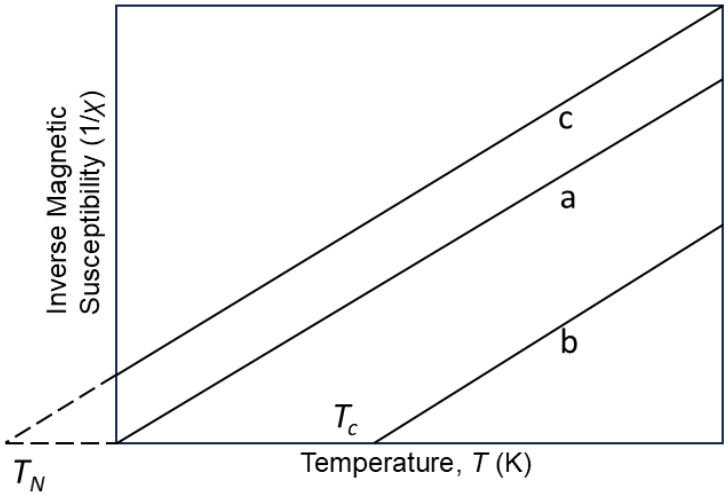


Fig. 7.3. Plot of inverse susceptibility ($1/\chi$) with temperature for three different magnetic behaviours: (a) Curie Law; (b) Curie-Weiss law for ferromagnetic substances; (c) Curie-Weiss law for antiferromagnetic substances.

Thus, the study of temperature dependence of magnetic behaviour serves as a powerful tool for distinguishing between different types of magnetic materials, identifying magnetic interactions, and understanding the electronic structure of transition metal complexes.

w CHECK YOUR PROGRESS

Q1. Answer true or false

a) Diamagnetism arises due to the presence of unpaired electrons in a substance.

b) Paramagnetic substances are weakly attracted by an external magnetic field.

c) Ferromagnetic materials can exhibit magnetisation even in the absence of an external magnetic field.

d) In antiferromagnetic substances, neighbouring magnetic moments align parallel to each other.

e) Antiferromagnetic compounds generally show large positive magnetic susceptibility.

f) Antiferromagnetic coupling in polynuclear complexes often occurs through bridging ligands.

g) The Néel temperature is the temperature below which antiferromagnetic substances behave as paramagnets.

Q2. Calculate the spin-only magnetic moment of both high-spin and low spin d^5 system.

Q3. A complex shows a magnetic moment of 3.87 BM. How many unpaired electrons are present?

Q4. State true or false

a) The experimental magnetic moment of a first-row transition metal complex closely matches the calculated spin-only value.
b) Second- and third-row transition metal complexes often deviate from spin-only values due to orbital contribution.
c) A d^5 high-spin complex always shows zero magnetic moment.

Q5. What is meant by orbital quenching?

Q6. Why do second- and third-row transition metal complexes often deviate from spin-only magnetic moments?

Q7. Under what conditions does orbital contribution become significant in coordination compounds?

Q8. Why does magnetic susceptibility of a paramagnetic substance decrease with increasing temperature?

Q9. How does magnetic susceptibility behave below the Néel temperature in antiferromagnetic materials?

Q10. What is the physical significance of the Curie constant?

7.8 LET US SUM UP

- Magnetic properties of transition metal complexes are closely related to their electronic structure.
- d-electrons are responsible for both colour and magnetic behaviour.
- Substances show diamagnetic, paramagnetic, ferromagnetic, or antiferromagnetic behaviour.
- Antiferromagnetic coupling in polynuclear complexes reduces magnetic moment.
- Crystal Field Theory explains magnetism through d-orbital splitting and unpaired electrons.
- Most first-row complexes obey spin-only magnetic moments due to orbital quenching.
- Deviation from spin-only values provides insight into spin–orbit coupling and ligand field symmetry.
- Heavier complexes show deviations due to orbital contribution.
- Magnetic behaviour varies with temperature as described by Curie and Curie–Weiss laws.
- Curie and Néel temperatures characterize magnetic transitions.
- Magnetic studies help determine electronic configuration, bonding, and geometry.

O 7.9 FURTHER READING

- Huheey, J. E.; Keiter, E. A.; Keiter, R. L.; Medhi, O. K. *Inorganic Chemistry: Principles of Structure and Reactivity*, 4th ed.; Pearson.
- Lee, J. D. *Concise Inorganic Chemistry*, 5th ed.; Wiley-Blackwell: Oxford, 1996.

K 7.10 ANSWERS TO CHECK YOUR PROGRESS

Answer to Q1: (a) False (b) True (c) True (d) False
(e) False (f) True (g) False

Answer to Q2: 5.92 BM and 1.73 BM

Answer to Q3: 3

Answer to Q4: (a) True (b) True (c) False

Answer to Q5: Orbital quenching refers to the suppression or removal of orbital angular momentum contribution to the magnetic moment due to the effect of the ligand field. In coordination compounds, the crystal field removes orbital degeneracy and restricts the free motion of electrons, thereby reducing or eliminating the orbital contribution to magnetism.

Answer to Q6: Second- and third-row transition metal complexes exhibit stronger spin–orbit coupling compared to first-row complexes. Because of this stronger interaction, orbital angular momentum is not completely quenched. As a result, the observed magnetic moment includes both spin and orbital contributions, leading to deviations from spin-only values.

Answer to Q7: Orbital contribution becomes significant:

- In second- and third-row transition metal complexes,
- When spin–orbit coupling is strong,
- In low-symmetry ligand fields where complete removal of orbital degeneracy does not occur,
- In complexes containing weak-field ligands.

Under such conditions, partial retention of orbital angular momentum leads to enhanced magnetic moments.

Answer to Q8: In paramagnetic substances, unpaired electrons align partially in the presence of an external magnetic field. As temperature increases, thermal agitation opposes this alignment. The increased random motion reduces the net magnetisation, and therefore magnetic susceptibility decreases with increasing temperature, in accordance with Curie's law.

Answer to Q9: Below the Néel temperature (T_n), antiferromagnetic ordering becomes dominant, and magnetic moments align antiparallel to each other. As a result, magnetic susceptibility decreases with further decrease in temperature.

Answer to Q10: The Curie constant is a proportionality constant in Curie's law and is related to the number of magnetic centres and their magnetic moments. It provides information about the magnitude of the effective magnetic moment of the paramagnetic substance.

M 7.11 MODEL QUESTIONS

Q1. A transition metal complex shows a magnetic moment close to 1.73 BM. What can you infer about the number of unpaired electrons and the nature of the complex?

Q2. Why do most first-row transition metal complexes obey spin-only magnetic moment values, whereas second- and third-row complexes show deviations?

Q3. Why does the magnetic susceptibility of paramagnetic complexes decrease with increase in temperature?

Q4. Explain how spin–orbit coupling influences the observed magnetic moment.

UNIT 8: ACID-BASE AND REDOX CHEMISTRY

UNIT STRUCTURE

8.1 Learning Objectives
8.2 Introduction
8.3 Introduction to Hard and Soft Acid-Base Concept
8.4 Applications of HSAB Concept
8.5 Standard Electrode Potential
8.6 pH Dependence of Standard Electrode Potential
8.7 Redox Stability of Metal Ions in Water
8.8 Latimer and Frost Diagram
8.9 Let us Sum Up
8.10 Answers to Check Your Progress
8.11 Further Reading
8.12 Model Questions

8.1 LEARNING OBJECTIVES

After studying this unit, learners will be able to:

- Understand the principles of HSAB theory and redox chemistry and explain how the classification of acids and bases influences the stability and reactivity of inorganic systems.
- Explain the concept of standard electrode potential and its dependence on pH, including the application of the Nernst equation in predicting redox behavior under different conditions.
- Analyze the stability of metal ions in aqueous solutions using concepts such as redox stability of water, hydration energy, disproportionation reactions, and graphical tools like Latimer and Frost diagrams.

8.2 INTRODUCTION

After understanding all the detailed knowledge on transition metal complexes and their chemistry, let's move onto another basic and one of the most important topics in inorganic chemistry, which is acid-base and redox chemistry. When we study the chemistry of transition metals and inorganic compounds, two fundamental concepts help us understand their behaviour: acid–base chemistry and redox chemistry. These two ideas explain why certain reactions occur, why particular complexes form, and why some metal ions are stable while others easily undergo oxidation or reduction.

In this lesson, we will explore these ideas gradually, beginning with the Hard and Soft Acid–Base concept, then moving to electrode potentials and their dependence on pH, and finally understanding how Latimer and Frost diagrams help us predict redox stability of metal ions.

8.3 INTRODUCTION TO HARD AND SOFT ACID-BASE CONCEPT

The Hard and Soft Acid–Base (HSAB) concept was introduced by the chemist Ralph G. Pearson to explain the stability of compounds formed between acids and bases. According to this theory, acids and bases can be classified as hard or soft, depending on their size, charge density, and polarizability. In this context, an acid is an electron pair acceptor and a base is an electron pair donor, following the definition proposed by Gilbert N. Lewis. However, Pearson's idea goes further by describing the nature of the interacting species.

Hard acids are typically small ions with high positive charge and low polarizability. Because their charge is concentrated in a small region, they strongly attract electrons but do not easily distort their electron clouds. Examples include ions such as H^+, Al^{3+}, Mg^{2+}, and Fe^{3+}.Hard bases are small, highly electronegative atoms or groups that are difficult to polarize, **Fig. 8.1**. These bases usually contain donor atoms such as oxygen or fluorine. Examples include OH^-, H_2O, F^-, and CO_3^{2-}. Soft acids, on the other hand, are larger ions with lower charge density and higher polarizability. Their electron clouds are more easily distorted, allowing them to interact more effectively with similarly polarizable bases. Examples include Ag^+, Hg^{2+}, Pd^{2+}, and Pt^{2+}. Soft bases are also large and highly polarizable species, usually containing atoms such as sulfur, phosphorus, or iodine. Examples include I^-, S^{2-}, RS^-, and phosphines.

The fundamental principle of the HSAB theory is that hard acids prefer to bind with hard bases, and soft acids prefer to bind with soft bases. This preference arises because interactions between similar types of species produce the most stable bonding interactions.

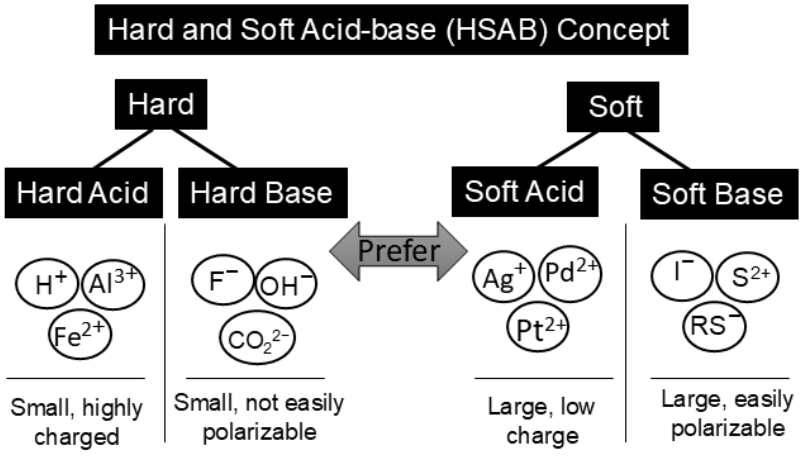


Fig. 8.1. Scheme showing the hard–soft acid–base (HSAB) theory.

8.4 APPLICATIONS OF HSAB CONCEPT

When we study the Hard–Soft Acid–Base (HSAB) principle, the real power of this concept appears in its applications. The theory helps us predict stability of compounds,

direction of reactions, selectivity of ligands in coordination chemistry, and even behaviour of metals in biological and environmental systems. Let us discuss these applications step by step as if we are examining them together in a classroom. The HSAB principle helps explain many chemical phenomena.

Prediction of Stability of Ionic Compounds

One of the most direct applications of the HSAB principle is predicting the relative stability of ionic compounds. According to the principle, hard acids prefer to combine with hard bases, while soft acids prefer to combine with soft bases. This matching produces stronger and more stable interactions.

Hard acids such as Al^{3+}, Mg^{2+}, and Fe^{3+} have high charge density and small ionic radius. These ions interact most strongly with hard bases such as F^-, OH^-, and O^{2-}. The bonding between them is largely ionic because both species are difficult to polarize.

For example, aluminum ion forms a very stable compound with fluoride ion:

$$Al^{3+} + 3F^- \rightarrow AlF_3$$

Here Al^{3+} is a hard acid and F^- is a hard base. Their interaction leads to strong electrostatic attraction and high lattice energy, making the compound very stable.

On the other hand, soft acids such as Ag^+, Hg^{2+}, and Pt^{2+} prefer to combine with soft bases such as I^-, S^{2-}, and phosphines. For example:

$$Ag^+ + I^- \rightarrow AgI$$

Silver ion is a soft acid and iodide ion is a soft base. Their interaction is highly favourable and leads to the formation of a stable precipitate of silver iodide. Thus, the HSAB concept allows chemists to predict which compounds will form preferentially.

Application in Coordination Chemistry

Another very important application of the HSAB principle appears in coordination chemistry, particularly in understanding the stability of metal–ligand complexes. Transition metal ions behave as Lewis acids because they accept electron pairs from ligands. Ligands behave as Lewis bases because they donate electron pairs to the metal center. Hard metal ions such as Fe^{3+}, Cr^{3+}, and Al^{3+} tend to form stronger complexes with ligands that contain oxygen donor atoms, such as water, hydroxide, or carboxylate groups. These ligands are hard bases.

For example, Fe^{3+} strongly binds with oxygen-containing ligands such as oxalate or water. In contrast, soft metal ions such as Pt^{2+}, Pd^{2+}, and Ag^+ prefer ligands containing sulfur or phosphorus donor atoms, which are soft bases. Examples include thiols, sulfides, and phosphine ligands. This principle helps chemists design specific coordination complexes for catalysis, metal separation, and medicinal chemistry.

Application in Predicting Direction of Chemical Reactions

The HSAB concept can also predict which direction a chemical reaction will proceed. Consider the reaction involving exchange of ligands between metal ions. The reaction will proceed in the direction that forms more stable hard–hard or soft–soft interactions.

For instance, if a soft metal ion is bonded to a hard base and a soft base is introduced into the system, the metal ion tends to replace the hard base with the soft base because that interaction is more stable. This concept explains ligand substitution reactions in coordination compounds.

Application in Solubility and Precipitation Reactions

The HSAB principle is extremely useful in understanding precipitation reactions. For example, silver ion forms insoluble precipitates with iodide or sulfide ions because these ions are soft bases and interact strongly with the soft acid Ag^+.

$$Ag^+ + I^- \rightarrow AgI \text{ (insoluble)}$$

Similarly, mercury ion reacts strongly with sulfide ion to form mercury sulfide, which is highly insoluble.

$$Hg^{2+} + S^{2-} \rightarrow HgS$$

These reactions occur because soft–soft interactions produce highly stable compounds with low solubility. This principle is widely used in qualitative inorganic analysis, where selective precipitation helps identify metal ions.

Application in Bioinorganic Chemistry

In biological systems, the HSAB principle helps explain metal ion selectivity in proteins and enzymes. Biomolecules contain donor atoms such as oxygen, nitrogen, and sulfur. The type of donor atom determines which metal ions will bind most strongly. For example, calcium ions (hard acids) bind strongly with oxygen atoms in biological molecules such as carboxylate groups. On the other hand, copper and zinc ions often interact with sulfur-containing amino acids such as cysteine because these metals behave as softer acids. Thus, HSAB theory helps explain metal ion recognition and binding in biological systems.

Application in Catalysis

In catalytic reactions involving transition metals, the HSAB concept helps chemists choose appropriate ligands for catalytic activity. Soft metal centers often work best with soft donor ligands such as phosphines, while harder metal centers prefer oxygen or nitrogen donor ligands. This matching of acid and base types can significantly affect reaction rates, product selectivity, and catalyst stability.

8.5 STANDARD ELECTRODE POTENTIALS

Redox chemistry deals with the transfer of electrons from one species to another. In order to understand and predict redox reactions, chemists use a quantity known as the standard electrode potential.

Standard electrode potential represents the tendency of a chemical species to gain electrons and undergo reduction. These potentials are measured relative to the standard hydrogen electrode, which is assigned a potential of zero volts. To compare how strongly different substances tend to gain electrons, chemists measure a quantity

known as the electrode potential. The standard electrode potential for a half reaction is usually written in the form:

$$\text{Oxidized form} + ne^- \rightarrow \text{Reduced form}$$

If the electrode potential is positive, the species has a strong tendency to accept electrons and act as an oxidizing agent. If the electrode potential is negative, the species prefers to lose electrons and behave as a reducing agent. Thus, standard electrode potentials provide a convenient way to compare the oxidizing and reducing strengths of different chemical species. However, measuring the absolute potential of a single electrode is not possible. Therefore, all electrode potentials are measured relative to a reference electrode. The universally accepted reference electrode is the Standard Hydrogen Electrode, commonly abbreviated as **SHE**.

By convention, the potential of this electrode is taken as zero volts under standard conditions.

Standard conditions include:

Temperature = 298 K (25°C)
Pressure = 1 atm
Concentration of ions = 1 mol L^{-1}

When the potential of an electrode is measured relative to the standard hydrogen electrode under these conditions, the value obtained is called the standard electrode potential, usually written as E°.

Representation of Standard Electrode Potential

A half-cell reaction is usually written in the form of a reduction reaction. For example, the reduction of copper ion is written as

$$Cu^{2+} + 2e^- \rightarrow Cu$$

The standard electrode potential associated with this reaction indicates the tendency of Cu^{2+} ions to gain electrons and be reduced to metallic copper. If the value of E° is positive, the species has a strong tendency to accept electrons and therefore behaves as a strong oxidizing agent. If the value of E° is negative, the species has a lower tendency to gain electrons and may instead lose electrons easily, behaving as a reducing agent.

Measurement of Standard Electrode Potential

To measure the standard electrode potential of a half-cell, it is connected to the standard hydrogen electrode to form a complete electrochemical cell. For example, if we want to measure the electrode potential of the copper electrode, the following cell is constructed:

$$SHE \mid H^+(1M) \mid H_2(g) \parallel Cu^{2+}(1M) \mid Cu$$

The potential difference between these two electrodes is measured using a voltmeter.

If the copper electrode has a higher tendency to accept electrons than hydrogen ions, electrons will flow from the hydrogen electrode to the copper electrode. The measured

potential difference corresponds to the standard reduction potential of the copper half-cell.

Interpretation of Standard Electrode Potential Values

The value of standard electrode potential provides important information about the chemical behaviour of substances. A high positive electrode potential indicates that the species is easily reduced. Such species act as strong oxidizing agents because they readily accept electrons. For example, the reduction potential of fluorine is very high, which means fluorine is a powerful oxidizing agent. On the other hand, metals with large negative electrode potentials lose electrons easily and therefore act as strong reducing agents. For example, alkali metals such as sodium and potassium have very negative electrode potentials and are strong reducing agents. Thus, electrode potentials help us compare the relative strengths of oxidizing and reducing agents.

Electrochemical Series

When the standard electrode potentials of many half-reactions are arranged in order of increasing or decreasing potential, the list obtained is called the electrochemical series, (**Table 8.1)**. This series is extremely useful because it allows us to predict whether a redox reaction will occur spontaneously, which metal can displace another metal from solution, and the relative oxidizing and reducing strength of different substances. For example, if a metal appears higher in the electrochemical series than another metal, it can reduce the ions of the metal below it.

Applications of Standard Electrode Potentials

Standard electrode potentials have many important applications in chemistry. They help predict the direction of redox reactions. A redox reaction will occur spontaneously when the overall cell potential is positive. They are also used to calculate the electromotive force (EMF) of electrochemical cells, which determines the voltage produced by batteries and fuel cells. In corrosion chemistry, electrode potentials help explain why some metals corrode easily while others remain stable. They also play a significant role in understanding biochemical redox processes, electroplating, metallurgy, and energy storage systems.

Relation Between Electrode Potential and Free Energy

Standard electrode potential is closely related to the Gibbs free energy change of a redox reaction. The relationship is expressed by the following thermodynamic equation: where,

$$\Delta G^\circ = -nFE^\circ$$

ΔG° = standard Gibbs free energy change
n = number of electrons transferred
F = Faraday constant
E° = standard electrode potential

From this relationship we can see that when the electrode potential is positive, the free energy change becomes negative. This means the reaction is thermodynamically spontaneous.

Table 8.1: The Standard electrode potentials

Element	*Electrode rection*	*E°(V)*
Li	$Li + e^- \rightarrow Li$	−3.045
K	$K^+ + e^- \rightarrow K$	−2.925
Cs	$Cs^+ + e^- \rightarrow Cs$	−2.923
Ba	$Ba^{2+} + 2e^- \rightarrow Ba$	−2.906
Ca	$Ca^{2+} + 2e^- \rightarrow Ca$	−2.866
Na	$Na^+ + e^- \rightarrow Na$	−2.714
Mg	$Mg^{2+} + 2e^- \rightarrow Mg$	−2.363
Al	$Al^{3+} + 3e^- \rightarrow Al$	−1.662
H_2	$H_2O + 2e^- \rightarrow H_2 + 2OH^-$	−0.829
Zn	$Zn^{2+} + 2e^- \rightarrow Zn$	−0.763
Fe	$Fe^{2+} + 2e^- \rightarrow Fe$	−0.440
Cd	$Cd^2 + 2e^- \rightarrow Cd$	−0.403
Pb	$PbSO_4 + 2e^- \rightarrow Pb + SO_4^{2-}$	−0.310
Co	$Co^{2+} + 2e^- \rightarrow Co$	−0.280
Ni	$Ni^{2+} + 2e^- \rightarrow Ni$	−0.250
Sn	$Sn^{2+} + 2e^- \rightarrow Sn$	−0.136
Pb	$Pb^{2+} + 2e^- \rightarrow Pb$	−0.126
Fe	$Fe^{3+} + 3e^- \rightarrow Fe$	−0.036
H_2	$2H^+ + 2e^- \rightarrow H_2(SHE)$	0
Cu	$Cu^{2+} + e^- \rightarrow Cu^+$	+0.153
S	$S_4O_6^{2-} + 2e^- \rightarrow 2S_2O_3^{2-}$	+0.170
Cu	$Cu^{2+} + 2e^- \rightarrow Cu$	+0.337
I_2	$I_2 + 2e^- \rightarrow 2I^-$	+0.534
Fe	$Fe^{3+} + e^- \rightarrow Fe^{2+}$	+0.77
Ag	$Ag^+ + e^- \rightarrow Ag$	+0.799
Hg	$Hg^{2+} + 2e^- \rightarrow Hg$	+0.854
Br_2	$Br_2 + 2e^- \rightarrow 2Br^-$	+1.066
O_2	$O_2 + 4H^+ + 2e^- \rightarrow 2H_2O$	+1.230
Cr	$Cr_2O_7^{2-} + 14H^+ + 6e^- \rightarrow 2Cr^{3+} + 7H_2O$	+1.330
Cl_2	$Cl_2 + 2e^- \rightarrow 2Cl^-$	+1.359
Au	$Au^{3+} + 3e^- \rightarrow Au$	+1.498
Mn	$MnO_4^- + 8H^+ + 5e^- \rightarrow Mn^2 + 4H_2O$	+1.510
F_2	$F_2 + 2e^- \rightarrow 2F^-$	+2.870

8.6 pH DEPENDENCE OF ELECTRODE POTENTIALS

Now lets understand how electrode potential is related to pH. The electrode potential of a redox couple depends on the concentrations of the reactants and products involved in the half-reaction. When hydrogen ions participate in the reaction, changing the acidity or alkalinity of the solution alters the concentration of H^+ ions. Since pH is defined as the negative logarithm of hydrogen ion concentration, any change in pH directly affects the electrode potential. The relationship between electrode potential and concentration is described by the Nernst equation, which allows us to calculate the potential of a half-cell under non-standard conditions.

Consider a general redox reaction in which hydrogen ions participate:

$$Ox + mH^+ + ne^- \rightarrow Red$$

Applying the Nernst equation, the electrode potential becomes

$$E = E° - \frac{0.0591}{n} log\left(\frac{[Red]}{[Ox][H^+]^m}\right)$$

Since, pH = –log[H^+]

We can rewrite the expression so that the electrode potential depends directly on pH:

$$E = E° - \frac{0.0591}{n} log\left(\frac{[Red]}{[Ox]}\right) \frac{0.0591\ m}{n} pH$$

From this equation we can clearly see that electrode potential decreases linearly as pH increases when hydrogen ions participate in the reduction reaction.

Special Case: Hydrogen Electrode

The Standard Hydrogen Electrode itself shows pH dependence. The half-reaction for this electrode is

$$2H^+ + 2e^- \rightarrow H_2$$

Applying the Nernst equation leads to

$$E = –0.0591 \times pH$$

This means that the potential of the hydrogen electrode decreases by approximately 0.059 V for every unit increase in pH at 25°C.

Graphical Representation of pH Dependence

The relationship between electrode potential and pH can often be represented graphically. If we plot electrode potential on the vertical axis and pH on the horizontal axis, we obtain a straight line for reactions involving hydrogen ions. A conceptual schematic is shown below, (**Fig. 8.2)**. The downward slope indicates that the electrode potential decreases as pH increases. The magnitude of the slope depends on the number of hydrogen ions involved in the reaction relative to the number of electrons transferred.

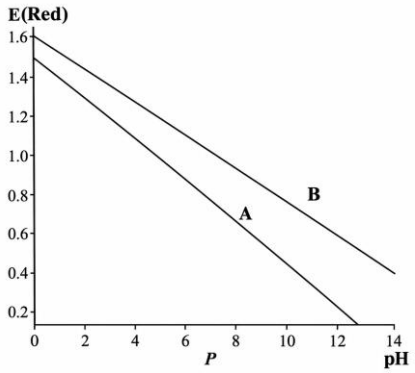


Fig. 8.2. A plot showing change in reduction potential against varying pH for the reduction of two species A and B.

8.7 REDOX STABILITY OF METAL IONS IN WATER

When we study transition-metal ions in aqueous solution, an important question naturally arises: Why are some oxidation states stable in water while others quickly undergo oxidation or reduction? The answer lies in the concept of redox stability of metal ions in water. To understand this properly, we must examine how redox potentials, hydration energies, and the oxidizing or reducing nature of water influence the stability of metal ions. Let us go through the idea carefully.

Fundamental Idea of Redox Stability in Aqueous Solution

When a metal dissolves in water, it generally forms hydrated metal ions, where water molecules coordinate to the metal center. For example,

$$M^{n+} + xH_2O \rightarrow [M(H_2O)_x]^{n+}$$

These hydrated ions may exist in different oxidation states depending on the metal. However, not all oxidation states remain stable in water. Some ions may be reduced, while others may be oxidized, depending on the thermodynamic conditions. The stability of a metal ion in water therefore depends on whether the aqueous environment favours its oxidation or reduction. To understand this, we need to examine the redox behaviour of water itself.

Redox Limits of Water

Water can act both as an oxidizing agent and as a reducing agent. In electrochemical terms, water defines a potential window within which metal ions remain stable. Two important half reactions define this stability range. The first reaction corresponds to the reduction of hydrogen ions to hydrogen gas:

$$2H^+ + 2e^- \rightarrow H_2$$

The second reaction corresponds to the reduction of oxygen to water:

$$O_2 + 4H^+ + 4e^- \rightarrow 2H_2O$$

These reactions establish the redox limits of aqueous solutions. If a metal ion has a reduction potential outside this range, water will either oxidize or reduce the metal species. For example, very strong reducing agents cannot exist in water because they

will reduce water to hydrogen gas. Similarly, extremely strong oxidizing agents will oxidize water to oxygen.

Role of Standard Electrode Potentials

The stability of different oxidation states of metals can be predicted using standard electrode potentials. If the reduction potential of a metal ion is very high, it means the ion strongly prefers to gain electrons and become reduced. On the other hand, if the potential is very negative, the species easily loses electrons and becomes oxidized. By comparing the electrode potential of a metal ion with the redox potentials of water, we can determine whether the metal ion will remain stable in aqueous solution. For instance, alkali metals such as sodium or potassium have very negative reduction potentials. As a result, they react vigorously with water and cannot exist as free metal in aqueous environments.

Effect of Hydration Energy

Another important factor controlling redox stability is hydration energy. When a metal ion dissolves in water, it becomes surrounded by water molecules through ion–dipole interactions. This process releases energy called hydration energy. Highly charged and small metal ions have large hydration energies because their strong electric fields attract water molecules strongly. This stabilization can influence the preferred oxidation state of a metal in water. For example, Fe^{3+} ions are stabilized in aqueous solution due to strong hydration. As a result, iron often exists in the +3 oxidation state in aqueous environments.

Influence of pH on Metal Ion Stability

The stability of metal ions in water also depends strongly on pH. Many metal ions react with water to form hydroxides or oxides depending on the acidity of the solution. At higher pH values, precipitation of hydroxides becomes more favourable. Therefore, the oxidation state and solubility of metal ions depend significantly on the pH of the solution.

Oxidation by Dissolved Oxygen

Another important factor affecting redox stability is atmospheric oxygen dissolved in water. Oxygen acts as a strong oxidizing agent in aqueous environments. Many metal ions in lower oxidation states are easily oxidized by dissolved oxygen. For example, ferrous ions (Fe^{2+}) in aqueous solution are gradually oxidized to ferric ions (Fe^{3+}) by oxygen:

$$4Fe^{2+} + O_2 + 4H^+ \rightarrow 4Fe^{3+} + 2H_2O$$

This process occurs frequently in natural water systems and is responsible for the formation of rust and iron oxide deposits.

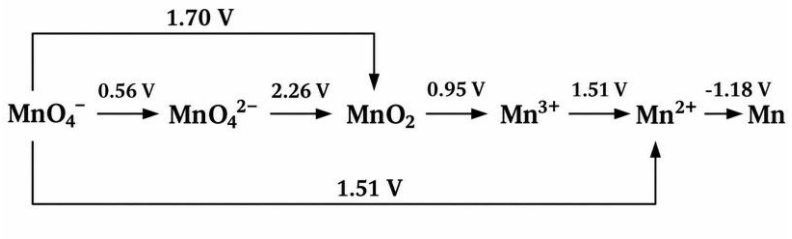
8.8 GRAPHICAL REPRESENTATION OF REDOX STABILITY: LATIMER AND FROST DIAGRAMS

When we study the redox behaviour of elements in different oxidation states, chemists often use graphical tools to organize and interpret the large amount of electrochemical data available. Two very important tools used for this purpose are Latimer diagrams and

Frost diagrams. These diagrams help us understand the relative stability of oxidation states, predict disproportionation reactions, and visualize redox relationships between different forms of an element.

Latimer Diagrams

The Latimer diagram was introduced by Wendell M. Latimer as a compact way to represent the standard reduction potentials between successive oxidation states of an element in a particular medium, usually aqueous solution. In a Latimer diagram, the element is written in various oxidation states arranged from left to right in decreasing oxidation number. Above the arrows connecting these oxidation states, the corresponding standard electrode potentials are written. Each arrow represents a reduction step, and the value above the arrow represents the standard reduction potential (E°) for that step. Thus, a Latimer diagram summarizes a large amount of electrochemical information in a very compact form. Consider an element that exists in several oxidation states in aqueous solution. Its Latimer diagram might appear like this:



This tells us that, MnO_4^- can be reduced to MnO_2 with a potential of 1.70 V. MnO_2 can be reduced to Mn^{3+} with a potential of 0.95 V and Mn^{3+} can be reduced to Mn^{2+} with a potential of 1.51 V. Thus, the diagram quickly shows how easily each oxidation state is reduced.

Sometimes we need to determine the reduction potential between non-adjacent oxidation states. In such cases we cannot simply average the potentials; instead, we must use the relationship between electrode potential and Gibbs free energy.The free energy change of a reaction is related to electrode potential through the equation:

$$\Delta G^\circ = -nFE^\circ$$

Because free energies are additive, we can combine reduction steps to calculate the potential for the overall reaction. This method allows us to determine reduction potentials that are not explicitly shown in the Latimer diagram.

Frost Diagrams

Another very useful graphical representation of redox data is the Frost diagram, developed by Arthur A. Frost. A Frost diagram is essentially a graphical representation of the relative free energies of different oxidation states of an element. In a Frost diagram: (i) the oxidation number of the element is plotted on the horizontal axis. (ii) The vertical axis represents a value proportional to the Gibbs free energy of the species. Thus, each

point on the diagram represents a specific oxidation state of the element. A typical Frost diagram looks like this:

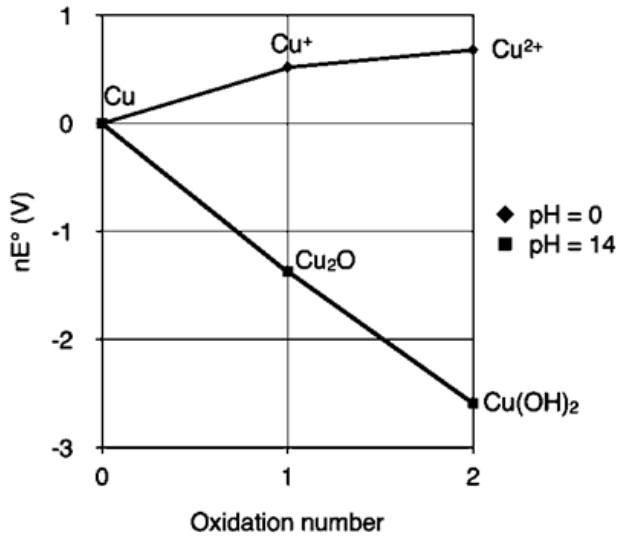


Fig. 8.3. (a) Representative Frost Diagram for Copper under acidic(pH=0) and basic conditions (pH=14)

Each point corresponds to a particular oxidation state. The lower the point on the diagram, the more stable that oxidation state is under the given conditions.

Interpretation of Frost Diagrams

Frost diagrams provide several important pieces of information. **First**, the lowest point on the diagram represents the most stable oxidation state of the element under the specified conditions. **Second**, the slope between two points corresponds to the standard electrode potential for the redox couple connecting those oxidation states. **Third**, the diagram allows us to predict disproportionation reactions. If a point representing a particular oxidation state lies above the straight line connecting two neighbouring oxidation states, the species is unstable and tends to disproportionate. For example, in the **Fig. 8.3**, under acidic conditions Cu^+, lies above the line joining Cu and Cu^{2+}, hence Cu^+ tends to disproportionate to Cu and Cu^{2+}. If the point lies below the line, the species is stable with respect to disproportionation.

Relationship Between Latimer and Frost Diagrams

Latimer diagrams and Frost diagrams are closely related because both are derived from standard electrode potential data. A Latimer diagram provides the numerical values of reduction potentials between successive oxidation states. A Frost diagram converts these values into a graphical representation of relative free energies. Therefore, Latimer diagrams are often used as the starting point to construct Frost diagrams.

Importance in Inorganic Chemistry

Both diagrams are extremely valuable tools in advanced inorganic chemistry because they allow chemists to:

i) understand the relative stability of oxidation states
ii) predict disproportionation and comproportionation reactions
iii) visualize redox relationships between species
iv) interpret electrochemical data quickly

These diagrams are widely used when studying transition metals, redox reactions in aqueous systems, and electrochemical behaviour of elements.

W CHECK YOUR PROGRESS

Q1. What is HSAB theory and who proposed it?
Q2. On what basis are acids and bases classified as hard, soft, or borderline?
Q3. What is meant by standard electrode potential (E°)?
Q4. To which reference electrode are standard electrode potentials compared?
Q5. Why does electrode potential depend on pH?
Q6. State the Nernst equation and explain its significance.
Q7. How does an increase in pH affect hydrogen ion concentration and electrode potential?
Q8. What factors determine the stability of metal ions in aqueous solution?
Q9. What is meant by the redox stability range of water?
What are Latimer diagrams and Frost diagrams, and what information do they provide?

2 8.9 LET US SUM UP

- The HSAB theory was proposed by Ralph G. Pearson to explain stability and reactivity of acids and bases.
- Acids and bases are classified as hard, soft, or borderline depending on their size, charge density, and polarizability.
- The standard electrode potential (E°) measures the tendency of a chemical species to gain electrons (reduction).
- Measured relative to the Standard Hydrogen Electrode (SHE).
- Many redox reactions involve H^+ ions, so electrode potentials depend on pH.
- The relationship between potential and concentration is described by the Nernst equation.
- As pH increases, hydrogen ion concentration decreases, which changes electrode potential. Oxygen reduction potential changes with pH.
- Stability of metal ions in aqueous solution depends on redox potentials and hydration energy.

- Water has a limited redox stability range defined by two reactions: Reduction of H^+ to H_2 and Oxidation of H_2O to O_2. Metal ions with potentials outside this range are unstable in water.
- Hydration energy stabilizes highly charged metal ions in aqueous solution.
- Some metal ions undergo disproportionation reactions.
- Latimer diagram provides a compact representation of standard reduction potentials between oxidation states. Oxidation states are arranged from highest to lowest.
- Frost diagram Graph showing relative stability of oxidation states.
- Acid–base and redox chemistry helps explain reactivity, stability, and electron transfer processes in inorganic systems.

K 8.10 ANSWERS TO CHECK YOUR PROGRESS

Answer to Q1: HSAB theory (Hard and Soft Acids and Bases theory) was proposed by Ralph G. Pearson to explain the stability and reactivity of acids and bases.

Answer to Q2: Acids and bases are classified as hard, soft, or borderline based on their size, charge density, and polarizability.

Answer to Q3: Standard electrode potential (E°) is a measure of the tendency of a chemical species to gain electrons (i.e., undergo reduction).

Answer to Q4: Standard electrode potentials are measured relative to the Standard Hydrogen Electrode (SHE).

Answer to Q5: Electrode potential depends on pH because many redox reactions involve H^+ ions, and their concentration changes with pH.

Answer to Q6: The Nernst equation relates electrode potential to concentration (or activity) of reactants and products, allowing calculation of potential under non-standard conditions.

Answer to Q7: As pH increases, the concentration of H^+ ions decreases, which alters the electrode potential. For example, the oxygen reduction potential changes with pH.

Answer to Q8: The stability of metal ions in aqueous solution depends on redox potentials and hydration energy.

Answer to Q9: The redox stability range of water is defined by: reduction of H^+ to H_2 and oxidation of H_2O to O_2. Metal ions with potentials outside this range are unstable in water.

Answer to Q10: Latimer diagrams provide a compact representation of standard reduction potentials between different oxidation states, while Frost diagrams graphically represent the relative stability of oxidation states.

O 8.11 FURTHER READING

- Lee, J. D. *Concise Inorganic Chemistry*, 5th ed.; Wiley-Blackwell: Oxford, 1996.
- Shriver, D. F.; Atkins, P. W. *Inorganic Chemistry*, 5th ed.; Oxford University Press: Oxford, 2010.
- Huheey, J. E.; Keiter, E. A.; Keiter, R. L. *Inorganic Chemistry: Principles of Structure and Reactivity*, 4th ed.; Pearson.

M 8.12 MODEL QUESTIONS

Q1. Classify acids and bases according to the HSAB concept with suitable examples.
Q2. Explain the importance of polarizability in the HSAB principle.
Q3. Describe the significance of standard electrode potentials in predicting redox reactions.
Q4. Explain why electrode potentials depend on pH.
Q5. Describe the redox limits of water.
Q6. What factors determine the stability of metal ions in aqueous solution?
Q7. Explain the construction of a Latimer diagram.
Q8. Write the steps involved in predicting disproportionation using Latimer diagrams.
Q9. Explain the basic features of a Frost diagram.
Q10. How are Latimer diagrams related to Frost diagrams?
Q11. Why do hard acids prefer to bind with hard bases, while soft acids prefer soft bases?
Q12. Why are high oxidation states of metals often unstable in aqueous solution?
Q13. Why is Cu^{+} unstable in aqueous solution?
Q14. Why are hydration energies important in determining redox stability?
Q15. How does pH influence electrochemical reactions involving protons?

UNIT 9: LANTHANIDES AND ACTINIDES

UNIT STRUCTURE

9.1 Learning Objectives
9.2 Introduction
9.3 Classification of *f*-block Elements:
9.4 Atomic and Ionic Radii - The Lanthanide Contraction
9.5 Actinide Contraction
9.6 Separation of Lanthanides
9.7 Let Us Sum Up
9.8 Answers to Check Your Progress
9.9 Further Reading
9.10 Model Questions

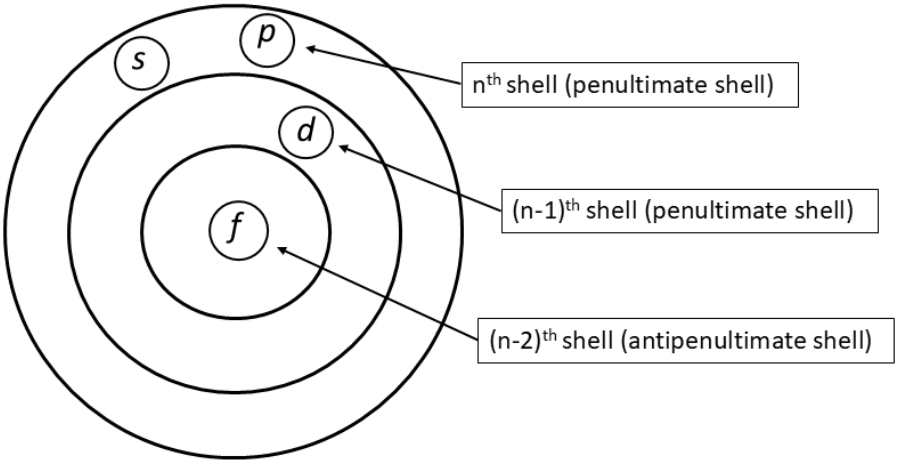
9.1 LEARNING OBJECTIVES

After going through this unit, you will be able to:

- Understand the electronic structure of lanthanides and actinides.
- Explain oxidation states and ionic radii trends.
- Describe lanthanide and actinide contraction.
- Learn the methods of separation of lanthanides.

9.2 INTRODUCTION

The lanthanides and actinides together form the *f*-block elements of the periodic table. In these elements, the additional electron enters the (n-2)*f* energy levels and thus called as *f*-block elements. These elements are also called inner transition elements because the last electron in these elements enters into (n-2) *f*-orbitals *i.e*. inner to the penultimate shell.



9.3 Classification of *f*-block Elements

(1) Lanthanides: The elements in which the last electron enters one of the 4*f*-orbitals are called 4f-elements or first inner transition series. These are also called lanthanides, lanthanones or ***rare earths*** because they appear immediately after the element lanthanum (La) and have strong resemblances to La. The name ***rare earth*** was given to them because they were originally extracted from oxides for which ancient name was ***earth*** and which were considered to be rare. The term ***rare earth*** is avoided now because many of these elements are no longer rare but are abundant. Thus, strictly according to this definition of lanthanides only thirteen elements from Ce_{58} to Yb_{70} should be the members of lanthanide series. However, all the fifteen elements from La_{57} to Lu_{71} are considered as the members of lanthanide series, because all the fifteen elements have similar physical and chemical properties.

Electronic Configuration:

The general electronic configuration of lanthanides is $4f^{0-14}\ 5d^{\ 0 \text{ or } 1}\ 6s^2$.

We know that at Ba_{56} 6s-orbital is completely filled (Ba_{56} - [Xe] $6s^2$) and at La_{57} 5*d*-orbital is singly occupied (La_{57} - [Xe] $5d^1\ 6s^2$). But after La_{57} further filling of 5*d*-orbitals is discontinued. As the nuclear charge increases by one unit from La_{57} to Ce_{58}, the 4*f*-orbitals which were higher in energy fall slightly below the 5*d*-level. 4*f*-orbitals, therefore, begin to fill and are completely filled up to Lu_{71} before the filling of the 5d-orbitals is resumed.

It is seen that the filling of 4*f* orbitals is not regular. Although, it is energetically favourable to move the single 5d electron into 4f level in most of the elements. But in cases of Gd_{64} and Lu_{71}, additional electrons do not enter in the 4*f* levels instead, they enter to 5*d*-level. Because with $5d^1$ configuration, Gd and Lu attain a half-filled and full-filled 4*f* configuration respectively, which are relatively more stable. The lanthanides are characterized by uniform (+III) oxidation state shown by all the elements. They typically form ionic and trivalent compounds. Electronic configuration of lanthanides is shown in **Table 9.1**.

Oxidation States of Lanthanides:

The most common oxidation state of lanthanides is +3. This results from the removal of two 6*s* electrons and one 4*f* or 5*d* electron. The stability of the +3 state is due to the similar energies of these orbitals.

However, some lanthanides exhibit +2 or +4 oxidation states:

Eu^{2+}: stable due to half-filled $4f^7$ configuration.

Yb^{2+}: stable due to filled $4f^{14}$ configuration.

Ce^{4+}: stable because it has an empty 4*f* shell.

Table 9.1. Electronic Configuration of neutral gaseous Lanthanide elements with their corresponding M^{3+} ions

Element	**Symbol**	**Atomic Number**	**Electronic Configuration**	**Electronic Configuration of M^{3+}**
Lanthanum	La	57	[Xe] $4f^0\ 5d^1\ 6s^2$	$4f^0$
Cerium	**Ce**	**58**	**[Xe] $4f^1\ 5d^1\ 6s^2$**	**$4f^1$**
Praseodymium	Pr	59	[Xe] $4f^3\ 6s^2$	$4f^2$
Neodymium	Nd	60	[Xe] $4f^4\ 6s^2$	$4f^3$
Promethium	Pm	61	[Xe] $4f^5\ 6s^2$	$4f^4$
Samarium	Sm	62	[Xe] $4f^6\ 6s^2$	$4f^5$
Europium	Eu	63	[Xe] $4f^7\ 6s^2$	$4f^6$
Gadolinium	**Gd**	**64**	**[Xe] $4f^7\ 5d^1\ 6s^2$**	**$4f^7$**
Terbium	Tb	65	[Xe] $4f^9\ 6s^2$	$4f^8$
Dysprosium	Dy	66	[Xe] $4f^{10}\ 6s^2$	$4f^9$
Holmium	Ho	67	[Xe] $4f^{11}\ 6s^2$	$4f^{10}$
Erbium	Er	68	[Xe] $4f^{12}\ 6s^2$	$4f^{11}$
Thulium	Tm	69	[Xe] $4f^{13}\ 6s^2$	$4f^{12}$
Ytterbium	Yb	70	[Xe] $4f^{14}\ 6s^2$	$4f^{13}$
Lutetium	**Lu**	**71**	**[Xe] $4f^{14}\ 5d^1\ 6s^2$**	**$4f^{14}$**

*[Xe] indicates the complete configuration of the gaseous Xe atom i.e. [Kr]$4d^{10}\ 5s^2 5p^6$.

(2) **Actinides**: The elements in which the last electron enters one of the 5*f*-orbitals of $(n-2)^{th}$ shell are called 5*f*- elements or second inner transition series. These are also called actinides or actionons because they appear immediately after actinium (Ac). Like lanthanides, only thirteen elements from thorium, Th_{90} to No_{102} should be the members of actinides series. However, all fifteen elements from Ac_{89} to Lr_{103} are considered as the members of actinide series, owing to their similar physical and chemical properties.

Electronic Configuration:

The actinide series consists of a series of elements followed by actinium in the seventh period of periodic table i.e. at the final row of the periodic table followed by filling of the 6p orbital. The electronic distribution of these elements starts from the filling of 6*d* and 7*s* orbital, which remains same in each element. But differentiation occurs in 5*f* sub shell, in which electron enters from 1-14 from Pa to Lr. The electronic structure of actinides does not follow the simple pattern found in the lanthanides.

The general electronic configuration of actinides in the ground state may be written as:

[Rn] $5f^{1-14}\ 6d^{0-1}\ 7s^2$

After Lanthanum (La), the 4*f* orbitals become lower in energy than the 5*d* orbitals, so electrons start filling the 4*f* orbitals regularly in the lanthanide series. There are a few exceptions, such as Gd and Lu, owing to their stable half/full filled shell.

Table 9.2. Electronic Configuration of Neutral Gaseous Actinide Elements

Element	Symbol	Atomic Number	Electronic Configuration
Actinium	Ac	89	[Rn] $5f^0\ 6d^1\ 7s^2$
Thorium	Th	90	[Rn] $5f^0\ 6d^2\ 7s^2$
Protactinium	Pa	91	[Rn] $5f^2\ 6d^1\ 7s^2$
Uranium	U	92	[Rn] $5f^3\ 6d^1\ 7s^2$
Neptunium	Np	93	[Rn] $5f^4\ 6d^1\ 7s^2$
Plutonium	Pu	94	[Rn] $5f^6\ 6d^0\ 7s^2$
Americium	Am	95	[Rn] $5f^7\ 6d^0\ 7s^2$
Curium	Cm	96	[Rn] $5f^7\ 6d^1\ 7s^2$
Berkelium	Bk	97	[Rn] $5f^9\ 6d^0\ 7s^2$
Californium	Cf	98	[Rn] $5f^{10}\ 6d^0\ 7s^2$
Einsteinium	Es	99	[Rn] $5f^{11}\ 6d^0\ 7s^2$
Fermium	Fm	100	[Rn] $5f^{12}\ 6d^0\ 7s^2$
Mendelevium	Md	101	[Rn] $5f^{13}\ 6d^0\ 7s^2$
Nobelium	No	102	[Rn] $5f^{14}\ 6d^0\ 7s^2$
Lawrencium	Lr	103	[Rn] $5f^{14}\ 6d^1\ 7s^2$

*[Rn] indicates complete configuration of gaseous Rn atom i.e. [Xe]$4f^{14}5d^{10}\ 6s^2 6p^6$

In the actinide series, it was expected that after Actinium (Ac) the 5*f* orbitals would become lower in energy than the 6*d* orbitals. However, in the first few actinides (Th, Pa, U and Np), the energy difference between 5*f* and 6*d* orbitals is very small. Therefore, electrons may occupy 5*f*, 6*d*, or both orbitals. Later in the series, from Pu onwards, the 5*f* orbitals become significantly lower in energy, so electrons fill the 5*f* orbitals regularly, making the later actinide elements more similar to each other.

Oxidation States of Actinides:

Actinides exhibit a wide range of oxidation states, generally from +3 to +7, which is significantly greater than that observed in lanthanides. This variability arises because the 5*f*, 6*d*, and 7*s* orbitals in actinides are close in energy and can participate in bonding. In the early actinides, higher oxidation states are more stable; for example, thorium commonly shows +4, protactinium +5, and uranium exhibits +3, +4, +5, and +6 oxidation states, with the uranyl ion (UO_2^{2+}) representing the stable +6 state. As the series progresses, the stability of the +3 oxidation state increases, similar to the behavior observed in lanthanides. The presence of multiple oxidation states leads to diverse chemical behavior and the formation of a variety of actinide compounds.

9.4 Atomic and Ionic Radii - The Lanthanide Contraction

In the periodic table, covalent and ionic radii generally increase when moving down a group because additional electron shells are added. However, across a period from left to right, the radii decrease due to the increase in nuclear charge. The additional electrons do not completely shield this increased nuclear charge, so the electrons are

pulled closer to the nucleus. The shielding ability of orbitals decreases in the order *s* > *p* > *d* > *f*.

In the lanthanide series, the decrease in atomic and ionic radii from one element to the next is very small, but the overall reduction across the series (from Ce to Lu) is about 0.2 Å. This gradual decrease in size of lanthanide atoms and ions with increasing atomic number is known as ***lanthanide contraction***. As a result, lanthanum has the largest atomic radius, while lutetium has the smallest among the lanthanides.

Cause of Lanthanide Contraction:

In any period of the periodic table, as we go across a period, the number of protons and electrons increase from one element to other (from left to right→). Increase in number of electrons will try to increase the atomic size due to the inter-electronic repulsion while the increasing number of protons will try to decrease the atomic size by attracting the electrons closer to the nucleus. Due to the higher magnitude of the attractive force, outcome would be a gradual decrease in the atomic radius in the same direction, left to right). In the lanthanide series, electrons are added to the *4f* orbitals, which have poor shielding ability. The *4f* electrons do not effectively shield the increasing nuclear charge from the outer 5d and 6s electrons. Consequently, the effective nuclear charge (Z_{eff}) experienced by the outer electrons increases progressively, pulling them closer to the nucleus and reducing the atomic/ionic radius on moving from La to Lu. This accumulation of successive shrinkage is called lanthanide contraction.

Table 9.3: Ionic radii showing lanthanide contraction

Element	Ionic Radius (Ln^{3+}) in pm	Element	Ionic Radius (Ln^{3+}) in pm
Lanthanum	103.2	Terbium	92.3
Cerium	101.0	Dysprosium	91.2
Praseodymium	99.0	Holmium	90.1
Neodymium	98.3	Erbium	89.0
Promethium	95.8	Thulium	88.0
Samarium	94.7	Ytterbium	86.8
Europium	93.8	Lutetium	86.1
Gadolinium	103.2		

Consequences of Lanthanide Contraction:

1. ***Atomic size***: The lanthanide contraction causes the radii of 5d transition elements to be nearly identical to their *4d* counterparts (e.g., Zr – Hf, Nb-Ta, Mo-W …., *i.e*. 2nd and 3rd row transition elements have almost identical radii). This results in very similar chemical properties.
2. ***Difficulty in separation***: The gradual and small change in ionic radii makes the separation of individual lanthanides extremely challenging, requiring sophisticated techniques like ion-exchange chromatography.

3. ***Effect of Basic Strength***: As ionic radius decreases across the series, the basicity of hydroxides decreases from $La(OH)_3$ to $Lu(OH)_3$. Smaller cations have higher charge density, leading to greater covalent character and reduced basicity.
4. ***Variation in complex stability***: The stability of complexes with a given ligand increases from La to Lu due to increasing charge density.
5. ***Electronegativity***: It increases from the elements La to Lu.
6. ***Ionization Energy***: The stronger attraction between electrons and nuclear charge in 5d elements results in higher ionization energies compared to 3*d* and 4*d* elements. Most 5d elements have a filled *s*-shell, except Pt and Au. From Hf to Re the ionization energy remains nearly constant, after which it increases with increasing shared d-electrons, reaching a maximum for Au and Ir.

9.5 Actinide Contraction

There is a steady and consistent decrease of the ionic radii of actinides with increasing atomic number. The phenomenon is analogous to lanthanide contraction and therefore, is referred to as actinide contraction. The decrease in size is attributed to the imperfect shielding of one 5*f* electron by another in the same shell. In the series, the nuclear charge and valence electrons both increases by one unit at each step, due to diffused shape of 5*f* orbitals the electrons do not shield the nuclear charge efficiently. The valence electrons are strongly pulled towards the nucleus and the sizes decreases. In case of actinide series, 5*f* electrons are slightly more effective in shielding than 4*f* electrons, the contraction is somewhat irregular. The contraction leads to greater covalent character in actinide compounds.

9.6 SEPARATION OF LANTHANIDES

Lanthanide separation is challenging due to their similar chemical properties from nearly identical +3 ionic radii and electronic configurations, but subtle differences from lanthanide contraction enable targeted methods. These techniques exploit variations in hydration, complexation, solubility, and extraction efficiency.

Why separation is difficult

Lanthanides (La to Lu) exhibit +3 as the stable oxidation state, with poor shielding by 4f electrons causing steady ionic radius decrease (lanthanide contraction: Ce^{3+} 103 pm to Lu^{3+} 85 pm). This results in close similarities in solubility, basicity (decreasing $La(OH)_3$ > $Lu(OH)_3$), and complex formation, requiring high-selectivity methods like ion exchange or solvent extraction.

Several methods are used:

- **Ion-exchange method**: uses cation-exchange resins and complexing agents like EDTA for separation.
- **Solvent extraction**: uses organic solvents such as tributyl phosphate (TBP) to selectively extract lanthanide ions.
- **Fractional crystallization**: based on slight solubility differences.

1. Ion Exchange Chromatography:

This is the most important, the most rapid and most effective general method for the separation and purification of the lanthanides. A solution of lanthanide ions from mineral digests (e.g., monazite) is run down a column of synthetic ion-exchange resin such as Dowex-50. This is a sulphonated polystyrene and contains the functional groups SO_3H. The Ln3+ ions are absorbed onto the resin and replace the hydrogen atom on $-SO_3H$.

$$Ln^{3+}(aq) + 3H\text{-resin} \rightarrow Ln(resin)_3 + 3H^+(aq)$$

The individual salts are hydrated to varying degrees. Lutetium, being smallest, is most heavily hydrated, while lanthanum, being largest, is least hydrated. This means that the hydrated radius of lanthanum is smallest, while that of lutetium is the largest. The hydrate mixture is passed down a chromatographic column containing a synthetic ion exchange resin.

This means that the hydrated radius of lanthanum is smallest, while that of lutetium is the largest. The hydrate mixture is passed down a chromatographic column containing a synthetic ion exchange resin. The binding of lanthanide cations to the anionic sites of the exchange resin involves electrostatic attractions. Hence smaller the hydrated radius of the ion, more strongly it is bound. The lanthanum hydrated ion, being the smallest, attach to the resin immediately and get absorbed at the top of the column. The lutetium hydrated ion, being the largest, becomes absorbed at the bottom of the column.

The H^+ ions produced are washed through the column. Then the metal ions are eluted, that is are selectively washed off the column. The eluting agent is a complexing agent, for example a buffered solution of citric acid/ammonium citrate, or a dilute solution of $(NH_4)_3$(H.EDTA) at pH 8.

Note: Heavier lanthanide ions (Ln^{3+}) have a smaller anhydrous ionic size but a larger hydrated radius, such as Lu^{3+}. Because of this, they bind weakly to the resin and elute first when complexing eluants like ammonium citrate or *α*-hydroxyisobutyrate are used at a controlled pH. Lighter lanthanide ions, such as La^{3+}, bind more strongly to the resin and therefore elute later. As a result, the elution order proceeds from Lu^{3+} to La^{3+}.

2. Solvent Extraction:

Lanthanides partition between aqueous (*e.g.*, HNO_3) and organic phases (*e.g.*, tributyl phosphate (TBP) in kerosene). The heavier Ln^{3+} ions are more soluble in tri-n-butylphosphate than the lighter Ln^{3+} ions. Their solubilities in water and ionic solvents, however, are reversed. The heavier Ln^{3+} have higher extraction efficiency due to increased charge density from contraction. The ratios of the partition co-efficient of $La(NO_3)_3$, and $Gd(NO_3)_3$, between a solution of the metal ions in strong HNO_3 and tri-n-butylphosphate is 1: 1.06. This difference is quite small, but by using a continuous counter-current apparatus a very large number of partitions can be performed automatically. Example: Ce^{4+} (oxidized selectively) extracts into TBP/HNO_3, separating from Ln^{3+}; 95% pure Gd obtained at kg scale.

3. Valency Adjustment:

Valency adjustment is used to separate certain lanthanide ions by changing their oxidation state. For example, Ce^{3+} can be oxidized to Ce^{4+} using persulfate and then precipitated as insoluble cerium iodate. Similarly, Eu^{3+} can be reduced to Eu^{2+} by electrolytic reduction, and it precipitates as insoluble $EuSO_4$, similar to Group 2 sulfates.
Yb^{3+} and Sm^{3+} can also be reduced to the +2 oxidation state and separated easily from other lanthanides. After separation, these ions can be reconverted back to their normal +3 state.

Classical Methods

- Fractional Crystallization: Exploit solubility trends (*e.g.,* Lu salts least soluble, crystallize first; non-aqueous solvents like ether for $Nd(NO_3)_3$/$Pr(NO_3)_3$).
- Fractional Precipitation: Use agents like NaOH ($La(OH)_3$ first), oxalates, or iodates.
- Thermal Decomposition: $(NH_4)Ln(SO_4)_2$ decomposes differently (lighter Ln slower).

Method	Basis of Separation	Advantages	Limitations	Best For
Ion Exchange	Hydrated radius differences	High purity (>99%), analytical scale	Slow for bulk, resin cost	Individual Ln isolation
Solvent Extraction	Partition coefficients, charge density	Industrial scale, continuous	Organic waste, selectivity tuning	Heavy Ln enrichment
Valency Change	Redox solubility (e.g., $Eu^{2+}SO_4$)	Simple, selective for Ce/Eu	Limited elements, instability	Pre-separation outliers
Crystallization	Solubility gradients	Low cost	Tedious, impure	Small-scale purification

W CHECK YOUR PROGRESS

Q1. Define lanthanide contraction.
Q2. Why do lanthanides predominantly show the +3 oxidation state?
Q3. Why is the separation of lanthanides difficult?
Q4. What are the main causes of the wide range of oxidation states in actinides?
Q5. Mention two important consequences of lanthanide contraction.

2 9.7 LET US SUM UP

- The lanthanides and actinides together form the *f*-block elements of the periodic table and are characterized by the progressive filling of *f*-orbitals.

- Lanthanides (4*f* series) extend from Ce to Lu (Z = 58–71), while actinides (5*f* series) extend from Th to Lr (Z = 90–103).
- The general electronic configuration of f-block elements can be written as: $(n-2)f^{1-14}(n-1)d^{0-1}ns^2$.
- In lanthanides, the 4*f* orbitals are inner orbitals and are well shielded by the outer 5*s* and 5*p* electrons, resulting in limited participation in chemical bonding.
- The 5*f* orbitals of actinides are more spatially extended than 4*f* orbitals and therefore participate more readily in bonding, leading to greater chemical variability.
- The most common oxidation state of lanthanides is +3, which results from the removal of two n*s* electrons and one (n−1)*d* or (n−2)*f* electron.
- Some lanthanides also show +2 or +4 oxidation states due to the stability of half-filled or fully filled f-subshells (e.g., Eu^{2+}, Yb^{2+}, Ce^{4+}).
- Actinides exhibit a wider range of oxidation states, typically from +3 to +7, because the 5f, 6d, and 7s orbitals have comparable energies.
- A gradual decrease in ionic and atomic radii across the lanthanide series is known as lanthanide contraction, caused by the poor shielding ability of 4*f* electrons.
- Actinide contraction is a similar decrease in size across the actinide series due to ineffective shielding by 5*f* electrons.
- Lanthanide contraction leads to several important consequences, such as:
  i. Similar atomic radii of 4*d* and 5*d* transition metals (*e.g.,* Zr ≈ Hf)
  ii. Gradual increase in density and hardness
  iii. Difficulty in separating lanthanide elements.
- The separation of lanthanides is difficult due to their similar chemical properties and ionic radii. Common separation techniques include: fractional crystallization, ion-exchange chromatography, solvent extraction etc.

K 9.8 ANSWERS TO CHECK YOUR PROGRESS

Answer to Q1: Lanthanide contraction refers to the gradual decrease in atomic and ionic radii across the lanthanide series from lanthanum to lutetium. This occurs because 4f electrons shield the nuclear charge poorly, resulting in an increased effective nuclear attraction that pulls electrons closer to the nucleus.

Answer to Q2: Lanthanides mainly exhibit the +3oxidation state because the removal of two 6s electrons and one 5d or 4f electron results in a relatively stable electronic configuration.

Answer to Q3: Lanthanides have very similar ionic radii and chemical properties, and they mostly exist in the +3 oxidation state. Because of these similarities, their compounds exhibit nearly identical chemical behavior, making separation difficult.

Answer to Q4: Actinides exhibit multiple oxidation states because the 5f, 6d, and 7s orbitals are close in energy, allowing different numbers of electrons to participate in bonding.

Answer to Q5: Two important consequences of lanthanide contraction are:

1. Similarity in size between elements of the second and third transition series, such as zirconium (Zr) and hafnium (Hf).
2. Difficulty in separation of lanthanide elements due to their very similar ionic radii and chemical properties.

O 9.9 FURTHER READING

- Huheey, J. E.; Keiter, E. A.; Keiter, R. L.; Medhi, O. K. *Inorganic Chemistry: Principles of Structure and Reactivity*, 4th ed.; Pearson.
- Shriver, D. F.; Atkins, P. W.; Overton, T.; Rourke, J.; Weller, M.; Armstrong, F. *Inorganic Chemistry*, 5th ed.; Oxford University Press: Oxford, 2010.
- Miessler, G. L.; Fischer, P. J.; Tarr, D. A. *Inorganic Chemistry*, 5th ed.; Pearson: Boston, 2014.
- Lee, J. D. *Concise Inorganic Chemistry*, 5th ed.; Wiley-Blackwell: Oxford, 1996.
- Housecroft, C. E.; Sharpe, A. G. *Inorganic Chemistry*, 4th ed.; Pearson Education: Harlow, 2012.

M 9.10 MODEL QUESTIONS

Q1. Why are lanthanides collectively referred to as rare earth elements?

Q2. Explain why 4*f* orbitals in lanthanides do not participate significantly in chemical bonding?

Q3. Why do actinides show greater tendency to form covalent compounds than lanthanides?

Q4. Discuss the reason for the gradual decrease in ionic radii across the lanthanide series.

Q5. What is the significance of half-filled and completely filled *f*-subshells in determining oxidation states of lanthanides?

UNIT 10: PROPERTIES AND APPLICATION OF LANTHANIDES AND ACTINIDES

UNIT STRUCTURE

10.1 Learning Objectives
10.2 Overview of Lanthanides and Actinides
10.3 Magnetic properties
10.4 Spectral properties
10.5 Stability of lanthanide complexes
10.6 Stability of actinide complexes
10.7 Lanthanide shift reagents (LSRs)
10.8 MRI contrast agents
10.9 Selected applications of lanthanide and actinide properties
10.10 Check Your Progress
10.11 Let Us Sum Up
10.12 Answers to Check Your Progress
10.13 Further Reading
10.14 Model Questions

10.1 LEARNING OBJECTIVES

After going through this unit, you will be able to:

- Understand the basic characteristics of lanthanides and actinides and their *f*-block electronic configurations.
- Explain the magnetic behaviour of lanthanide and actinide ions arising from unpaired *f*-electrons.
- Describe the spectral properties of f-block elements, including 4*f*–4*f* and 5*f*–5*f* electronic transitions.
- Understand the stability and coordination chemistry of lanthanide and actinide complexes.
- Explain the principle and applications of lanthanide shift reagents in NMR spectroscopy.
- Understand the role of lanthanide complexes as MRI contrast agents.
- Recognize important applications of lanthanide and actinide chemistry in science and technology.

10.2 OVERVIEW OF LANTHANIDES AND ACTINIDES

Lanthanides (Ce–Lu) and actinides (Th–Lr) are the ***f*-block** elements, characterized by progressive filling of 4*f* and 5*f* orbitals respectively. Most lanthanides occur commonly in the +3 oxidation state, whereas actinides show a wider range of oxidation states (+3 to +7) and many are radioactive. The partially filled *f* orbitals give rise to characteristic magnetic and spectral behaviour and to specific coordination chemistry that underpins important applications, including NMR shift reagents and MRI contrast agents.

10.3 MAGNETIC PROPERTIES

General features

- Lanthanide and actinide ions with unpaired *f* electrons are paramagnetic; ions with f^0 or f^{14} configurations (e.g. La^{3+}, Lu^{3+}, Ce^{4+}, Yb^{2+}) are diamagnetic.
- Magnetism arises from both spin and orbital angular momentum of '*f* electrons, because the inner 4f/5f orbitals experience relatively weak ligand fields and therefore retain substantial orbital contribution.
- For many lanthanide ions, the experimentally observed magnetic moments deviate from the simple spin only formula and must be described by the Russell–Saunders (LS) coupling scheme and the Landé '*g*' factor.

Lanthanide magnetic behaviour

- The 4*f* electrons are shielded by outer 5s and 5p shells, so crystal field effects are modest and the ground state is best described by $^{2S+1}L_J$ terms with significant orbital contributions.
- The magnetic moments of Ln^{3+} ions often follow the so called "lanthanide magnetism curve", with maxima near Gd^{3+} (seven unpaired electrons, f^7) and decreasing toward both ends where f^0 or f^{14} configurations occur.
- Strong single-ion anisotropy in certain complexes (e.g. oblate vs prolate electron density) is exploited in molecular magnet design and single-molecule magnets based on Dy^{3+}, Tb^{3+}, and related ions.

Magnetic moment:

The magnetic behaviour of lanthanides is determined primarily by unpaired electrons in the 4*f* orbitals.

- La^{3+} ($4f^0$) and Lu^{3+} ($4f^{14}$) have no unpaired electrons and are diamagnetic.
- Most other lanthanide ions contain unpaired electrons and therefore exhibit paramagnetism.

Unlike transition metals, the orbital contribution to magnetism is not quenched in lanthanides because the 4*f* orbitals are shielded from the surrounding ligands. Therefore, both spin and orbital angular momentum contribute to the magnetic moment.

- Magnetic moment for lanthanides can be calculated using the formula

$$\mu = g\sqrt{J(J+1)}$$

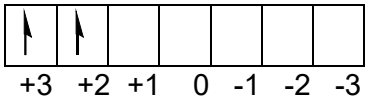
Where g is the Landé splitting factor, given by:

$$g = \frac{3}{2} + \frac{S(S+1) - L(L+1)}{2J(J+1)}$$

J=L+S; more than half filled
=L-S; less than half filled

Example:

For $Pr^{3+} = 4f^2$,



S = ½ + ½ =1

L = 3+2 = 5

J= L-S = 5-1 = 4

Here,

$$g = \frac{3}{2} + \frac{S(S+1) - L(L+1)}{2J(J+1)}$$

$$g = \frac{3}{2} + \frac{1(1+1) - 5(5+1)}{2 * 4(4+1)}$$

$$g = \frac{3}{2} + \frac{28}{40}$$

$$g = 0.8$$

Therefore,

$$\mu = g\sqrt{J(J+1)}$$

$$\mu = 0.8\sqrt{4(4+1)}$$

$$\mu = 3.58\ BM$$

The calculated value is very close to experimental values 3.47 B.M.

The magnetic moments calculated by using the above formula for lanthanides have good agreement with observed values. These calculations are based on the assumption that only the ground electronic state is occupied, i.e. in case of Pr^{3+}, $^3H_4$ (L=5, 2S+1=3, J=4). However, that is not always true.

For most lanthanides the energy difference between the ground electronic state and the first excited state (λ) is about 1000 cm^{-1}. However, the λ value for Eu^{3+} and Sm^{3+} is about 300 cm^{-1} which is very small. This means that the difference in energy between the ground state and the next state is small. Due to the small energy gap the energy of thermal motion of electron is sufficient to promote some electron and partially populated the higher energy state. Thus, there is difference between calculated value and observed value.

If we see the magnetic moment of Eu^{3+} at low temperature, then magnetic moment is close to zero as expected. However, at higher temperature, it deviates considerably to 3.4-3.6 BM.

Ions	**Calculated value (B.M.)**	**Observed value (B.M.)**
Sm^{3+}	0.84	1.5-1.6
Eu^{3+}	0	3.4-3.6

Table 10.1: Calculated and experimental value of magnetic moment, μ_{eff} (in BM) of Ln^{3+} ions:

Ion	Configuration	n	Term	L	J	g	μ_{cal} (BM)	μ_{exp} (BM)
La^{3+}	$4f^0$	0	$^1S_0$	0	0	–	0	0
Ce^{3+}	$4f^1$	1	$^2F_{5/2}$	3	5/2	6/7	2.54	2.3-2.5
Pr^{3+}	$4f^2$	2	$^3H_4$	5	4	4/5	3.58	3.4-3.6
Nd^{3+}	$4f^3$	3	$^4I_{9/2}$	6	9/2	8/11	3.62	3.5-3.6
Pm^{3+}	$4f^4$	4	$^5I_4$	6	4	3/5	2.70	-
Sm^{3+}	$4f^5$	5	$^6H_{5/2}$	5	5/2	2/7	0.84	1.5-1.6
Eu^{3+}	$4f^6$	6	$^7F_0$	3	0	–	0	3.4-3.6
Gd^{3+}	$4f^7$	7	$^8S_{7/2}$	0	7/2	2	7.94	7.8-8.0
Tb^{3+}	$4f^8$	6	$^7F_6$	3	6	3/2	9.70	9.4-9.6
Dy^{3+}	$4f^9$	5	$^6H_{15/2}$	5	15/2	4/3	10.6	10.4-10.5
Ho^{3+}	$4f^{10}$	4	$^5I_8$	6	8	5/4	10.6	10.3-10.5
Er^{3+}	$4f^{11}$	3	$^4I_{15/2}$	6	15/2	6/5	9.6	9.4-9.6
Tm^{3+}	$4f^{12}$	2	$^3H_6$	5	6	7/6	7.6	7.1-7.4
Yb^{3+}	$4f^{13}$	1	$^2F_{7/2}$	3	7/2	8/7	4.5	4.4-4.9
Lu^{3+}	$4f^{14}$	0	$^1S_0$	0	0	–	0	0

Actinide magnetic behaviour

- 5*f* orbitals of actinides are more extended and less shielded than 4*f* orbitals, leading to stronger interaction with ligands and significant covalency in many complexes.
- Magnetic behaviour of actinide ions is influenced by intermediate coupling (between LS and JJ limits) and often cannot be treated by simple spin-only or pure LS coupling models.

Some actinide complexes (*e.g.* U(IV), Np(IV), Pu(III/IV)) show complex temperature-dependent magnetic behaviour and can display both localized and more itinerant *f*-electron character depending on the ligand environment.

10.4 SPECTRAL PROPERTIES

Lanthanide spectral properties

- Lanthanide 4*f*–4*f* transitions are Laporte forbidden and also spin forbidden in many cases, leading to very low molar absorptivities and sharp, weak absorption bands.
- Because 4*f* orbitals are shielded by the 5*s* and 5*p* shells, the energies of 4*f*–4*f* transitions are only slightly affected by ligands; as a result, emission and absorption bands are narrow and almost independent of the chemical environment (so-called “line-like” spectra).

- These sharp transitions give rise to characteristic colours for certain Ln^{3+} ions in the solid state and solution (e.g. green Tb^{3+} emission, red Eu^{3+} emission), widely used in phosphors, lasers and luminescent probes.
- Charge-transfer and 4*f*–5*d* transitions, especially in Ce^{3+} and Eu^{2+}, are allowed and much more intense, and their energies are more sensitive to ligand fields, which is exploited in phosphor design.

Colour of Lanthanides:

The absorption spectra of lanthanide ions are important for both qualitative identification and quantitative estimation of these elements. Because lanthanide ions produce very sharp and characteristic spectral lines, their detection through spectroscopic techniques is relatively straightforward.

Lanthanide elements are sometimes used as biological tracers in medical and biochemical studies. Their spectral peaks are narrow and easily distinguishable, allowing researchers to monitor their presence in complex biological systems.
Most trivalent lanthanide ions exhibit colour due to electronic transitions within the 4*f* orbitals and the colour depends on the number of electrons present in the 4*f* orbitals (See **Table 10.1**).
Certain ions such as Ce^{3+} and Yb^{3+} are colourless because they do not absorb radiation in the visible region. Instead, they show strong absorption in the ultraviolet region resulting from $4f \rightarrow 5d$ electronic transitions.

These transitions are relatively intense for two main reasons:

1. The selection rule $\Delta l = 1$ allows $f \rightarrow d$ transitions, making them spectroscopically (Laporte) allowed.
2. The energy required to promote an electron from 4*f* to 5*d* is relatively accessible in some lanthanide ions.

In contrast, $\boldsymbol{f \rightarrow f}$ transitions are Laporte forbidden. As a result, these transitions generally produce weak absorption bands and the colours of lanthanide ions tend to be pale. Another important contribution to colour is charge transfer transitions, where an electron moves between the ligand and the metal ion. These transitions are more likely when:

- the metal ion is in a high oxidation state, or
- the ligand acts as a strong reducing agent.

Charge transfer transitions often produce intense colours. For example:

- Ce^{4+} solutions appear orange-red due to ligand → metal charge transfer.
- Sm^{2+} solutions exhibit a deep red colour due to metal → ligand charge transfer.

Actinide spectral properties

- 5*f*–5*f* transitions in actinides are also formally forbidden but are more strongly affected by ligand fields than 4*f*–4*f* transitions because 5f orbitals extend further from the nucleus.
- Stronger covalency and ligand-field mixing in actinide complexes lead to broader bands and greater sensitivity of spectra to coordination geometry and oxidation state.

- Intense charge-transfer transitions (ligand-to-metal and metal-to-ligand) are common in high-valent actinyl ions such as UO_2^{2+}, NpO_2^{2+} and PuO_2^{2+}, contributing to their characteristic colours and enabling spectrophotometric analysis in solution.

Table 10.2: Colour of trivalent lanthanide ions

Ion	Electronic Configuration	Colour
La^{3+}	$4f^0$	Colourless
Ce^{3+}	$4f^1$	Colourless
Pr^{3+}	$4f^2$	Green
Nd^{3+}	$4f^3$	Lilac
Pm^{3+}	$4f^4$	Pink
Sm^{3+}	$4f^5$	Yellow
Eu^{3+}	$4f^6$	Pale pink
Gd^{3+}	$4f^7$	Colourless
Tb^{3+}	$4f^8$	Pale pink
Dy^{3+}	$4f^9$	Yellow
Ho^{3+}	$4f^{10}$	Pale yellow
Er^{3+}	$4f^{11}$	Rose pink
Tm^{3+}	$4f^{12}$	Pale green
Yb^{3+}	$4f^{13}$	Colourless
Lu^{3+}	$4f^{14}$	Colourless

10.5 STABILITY OF LANTHANIDE COMPLEXES

Oxidation state and general trends

- The dominant oxidation state of lanthanides in solution is +3, and most coordination chemistry is based on Ln^{3+} ions.
- Ionic radii decrease from La^{3+} to Lu^{3+} (lanthanide contraction), so complex stability often increases across the series because smaller, more highly charged cations bind ligands more strongly.
- Exceptions exist where electronic factors stabilise +2 or +4 oxidation states (*e.g.* Eu^{2+}, Yb^{2+}, Sm^{2+}; Ce^{4+}, Tb^{4+}) under appropriate conditions.

Hard acid–hard base interactions

- Ln^{3+} ions are hard Lewis acids, favouring binding to hard donor atoms such as O and N (carboxylates, phosphonates, β-diketones, polyaminopolycarboxylates like EDTA and DTPA).
- Complexes with multidentate chelating ligands show high thermodynamic stability and kinetic inertness, especially for late lanthanides where ionic radii are smaller.

- Stability constants for Ln^{3+} with polyaminopolycarboxylate ligands typically increase along the series and follow trends related to ionic radius and charge density.

Coordination number and geometry

- Because Ln^{3+} ions are relatively large and primarily ionic, they often adopt high coordination numbers (8–10, sometimes 12) with flexible coordination geometries (capped square antiprismatic, tricapped trigonal prismatic, etc.).
- As the radius decreases from La^{3+} to Lu^{3+}, the average coordination number tends to decrease slightly (for example from 9–10 down to 8–9 in similar ligand sets).

10.6 STABILITY OF ACTINIDE COMPLEXES

Oxidation states and redox stability

- Actinides show a wider range of oxidation states; common oxidation states include +3, +4, +5, and +6, with higher states more prevalent in early actinides (U, Np, Pu).
- The relative stability of oxidation states trends such that higher oxidation states are more stable for lighter actinides and +3 becomes increasingly favoured for heavier actinides, analogous to the lanthanide behaviour.
- Redox equilibria between An(III), An(IV), and actinyl species (e.g. UO_2^{2+}, NpO_2^{2+}) are strongly influenced by ligand type, pH, and complex formation, which is central to nuclear fuel reprocessing and waste management.

Coordination and covalency

- 5*f* orbitals can participate more in bonding than 4*f* orbitals, so actinide–ligand bonding shows greater covalency, especially with soft or borderline donor atoms like N, S and certain organophosphorus ligands.
- Complexation with multidentate ligands such as phosphonates, aminopolycarboxylates, and organophosphorus extractants significantly enhances stability and is used in solvent extraction processes (e.g. PUREX, TALSPEAK variants).

Actinyl cations AnO_2^{n+} (n = 1–2) typically form linear O=An=O units that further coordinate equatorial ligands; their complex stability is crucial for controlling speciation and mobility in environmental systems.

10.7 LANTHANIDE SHIFT REAGENTS (LSRs)

Concept and composition

- Lanthanide shift reagents are paramagnetic lanthanide complexes used in NMR spectroscopy to induce predictable shifts of resonance signals in nearby nuclei in a substrate molecule.
- Classical LSRs are chelates of Ln^{3+} with *β*-diketones or related ligands (e.g. $Eu(fod)_3$, where fod is thenoyltrifluoroacetone), often containing fluorinated ligands to enhance solubility in organic solvents and to minimize their own proton signals.

- The paramagnetic centre (usually Eu^{3+}, Pr^{3+}, or Dy^{3+}) generates a large pseudo-contact shift and sometimes contact contributions that spread out overlapping NMR signals.

Mechanism of shifting

- When a substrate coordinates to the Ln^{3+} centre, nuclei at different positions experience different local magnetic fields, causing their NMR resonances to shift upfield or downfield by varying amounts.
- The magnitude of the shift depends on the distance from the lanthanide ion and the geometry of the complex, often approximated by inverse-cube distance dependence for pseudo-contact contributions.
- By analyzing the pattern of induced shifts, chemists can assign overlapping signals, distinguish diastereotopic protons, and deduce stereochemistry in complex organic molecules.

Practical examples and uses

- $Eu(fod)_3$, (tris[6,6,7,7,8,8,8-heptafluoro-2,2-dimethyl-3,5-octanedionate]) is widely used to resolve overlapping proton NMR signals in alcohols, amines, and other Lewis basic substrates by forming labile adducts.
- Pr^{3+} and Dy^{3+} based reagents are chosen when different ranges or directions of shift are required or when specific nuclei (such as ^{13}C or ^{19}F) are of interest.
- LSRs are especially useful for conformational analysis, chiral recognition, and structural studies where traditional NMR resolution is insufficient.

10.8 MRI CONTRAST AGENTS

Why gadolinium?

- Most clinical MRI contrast agents are chelates of Gd^{3+}, a lanthanide ion with seven unpaired electrons ($4f^7$), giving a very high magnetic moment and strong influence on proton relaxation times.
- Gd^{3+} is chosen because its half-filled *f* shell gives high spin, and the ion is relatively stable in the +3 state under physiological conditions when tightly chelated.
- Free Gd^{3+} is toxic, so it is always administered as highly stable chelate complexes with polyaminopolycarboxylate ligands (e.g. Gd-DTPA, Gd-DOTA).

Mechanism of MRI contrast enhancement

- Gd^{3+} complexes act primarily as $T1$ (longitudinal) relaxation agents, shortening the $T1$ relaxation time of nearby water protons and thereby increasing signal intensity on $T1$-weighted images.
- The unpaired electrons of Gd^{3+} create fluctuating local magnetic fields that efficiently interact with nuclear spins of water protons through dipolar mechanisms.
- Inner-sphere water molecules directly coordinated to Gd^{3+} and outer-sphere water molecules in the second coordination sphere both contribute to relaxation

enhancement; the number and exchange rate of inner-sphere water molecules are key design parameters.

Structure and stability of MRI agents

- Common Gd^{3+} chelates include linear agents (e.g. Gd-DTPA) and macrocyclic agents (e.g. Gd-DOTA); macrocyclic ligands generally provide higher kinetic inertness and thermodynamic stability.
- High complex stability is essential to prevent release of free Gd^{3+} in vivo, which has been associated with conditions such as nephrogenic systemic fibrosis in patients with renal impairment when weaker agents are used.
- Modern contrast agent design focuses on macrocyclic frameworks, higher relaxivity, and targeted agents that bind specific biomolecular sites or accumulate in particular tissues.

Emerging lanthanide MRI and multimodal agents

- Beyond Gd^{3+}, other lanthanides such as Dy^{3+}, Ho^{3+} and Tm^{3+} are investigated for *T*2 or ultra-high-field applications and for dual-modal imaging (MRI plus optical or CT).
- Luminescent lanthanide complexes (e.g. Eu^{3+}, Tb^{3+}) are being explored as combined MRI/optical probes by integrating paramagnetic and emissive centres in one molecular or nanoparticle system.

10.9 SELECTED APPLICATIONS OF LANTHANIDE AND ACTINIDE PROPERTIES

- Lanthanide oxides and phosphors (e.g. Eu^{3+}, Tb^{3+}, Ce^{3+} doped materials) are used in lighting, displays, lasers and security inks, taking advantage of sharp *f*–*f* or allowed 4*f*–5*d* transitions.
- Strong anisotropy and high magnetic moments of certain Ln^{3+} ions are exploited in permanent magnets, magnetic refrigerants, and single-molecule magnets.
- Actinide spectral and redox properties underpin nuclear fuel cycle monitoring, spectrophotometric speciation in processing streams, and environmental tracking of radionuclides.
- Complexation chemistry of both lanthanides and actinides is central to separation technologies such as solvent extraction, ion-exchange, and advanced ligand-designed partitioning of nuclear waste.

W CHECK YOUR PROGRESS

Q1. What are lanthanides and actinides?
Q2. Why do lanthanide ions show strong magnetic properties?
Q3. What are the spectral properties of lanthanide ions?
Q4. What are lanthanide shift reagents and how are they used?
Q5. Why are gadolinium complexes used as MRI contrast agents?

2 10.10 LET US SUM UP

- Lanthanides (Ce–Lu) and actinides (Th–Lr) are *f*-block elements characterized by the progressive filling of 4*f* and 5*f* orbitals. Lanthanides mainly exhibit the +3 oxidation state, while actinides show multiple oxidation states and many are radioactive.
- Magnetic properties of these elements arise from unpaired *f*-electrons. Lanthanides show magnetism due to both spin and orbital contributions, whereas actinides display more complex magnetic behaviour because their 5*f* orbitals interact more strongly with ligands.
- Spectral properties of lanthanides are dominated by sharp 4*f*–4*f* transitions, which are weak but characteristic and produce specific colours such as red Eu^{3+} and green Tb^{3+} emissions. Actinide spectra are broader and more sensitive to the ligand environment.
- Lanthanide complexes are generally stable in the +3 state, prefer hard donor ligands (O and N), and often show high coordination numbers (8–10) due to their large ionic radii and lanthanide contraction. Actinide complexes exhibit greater covalency and variable oxidation states.
- The unique magnetic and coordination properties of lanthanides lead to important applications such as lanthanide shift reagents in NMR spectroscopy and gadolinium-based MRI contrast agents, as well as uses in phosphors, magnets, and nuclear chemistry.

K 10.11 ANSWERS TO CHECK YOUR PROGRESS

Answer to Q1: Lanthanides and actinides are elements that belong to the *f*-block of the periodic table. Lanthanides range from cerium to lutetium and involve filling of the 4*f* orbitals, while actinides range from thorium to lawrencium with progressive filling of 5*f* orbitals. Most lanthanides commonly exist in the +3 oxidation state, whereas actinides show a wider variety of oxidation states from +3 to +7. Actinides are generally radioactive and chemically more reactive than lanthanides. The presence of partially filled f-orbitals leads to unique magnetic, spectral, and coordination properties in these elements.

Answer to Q2: Lanthanide ions often contain unpaired f-electrons, which make them paramagnetic. Their magnetism arises from both spin and orbital angular momentum, unlike many transition metals where orbital contributions are largely quenched. The 4*f* orbitals are well shielded by the outer 5s and 5p orbitals, so ligand fields have only a small effect on them. Because of this shielding, the magnetic moments follow theoretical predictions based on Russell–Saunders coupling and the Landé *g*-factor. The magnetic moment usually reaches a maximum near Gd^{3+}, which has seven unpaired electrons.

Answer to Q3: These 4*f*–4*f* transitions are Laporte forbidden, so the absorption bands are weak and narrow. Because the 4*f* electrons are shielded from ligand fields, their transition energies are only slightly influenced by the surrounding chemical environment. As a result, the spectral lines are almost identical in different compounds of the same ion. These sharp emissions are responsible for the

characteristic colours of ions such as Eu^{3+} (red) and Tb^{3+} (green) used in phosphors and luminescent materials.

Answer to Q4: They typically consist of lanthanide ions such as Eu^{3+}, Pr^{3+}, or Dy^{3+} coordinated with β-diketone ligands. When a substrate molecule coordinates to the lanthanide center, the local magnetic field around different nuclei changes. This causes different nuclei in the molecule to shift upfield or downfield in the NMR spectrum. As a result, overlapping signals become separated, allowing chemists to determine molecular structure and stereochemistry.

Answer to Q5: Gadolinium ions are widely used in MRI because Gd^{3+} contains seven unpaired electrons, giving it a very high magnetic moment. These unpaired electrons interact with nearby water protons and shorten the T1 relaxation time, increasing the brightness of MRI images. However, free Gd^{3+} ions are toxic, so they are administered as stable chelate complexes such as Gd-DTPA or Gd-DOTA. These ligands tightly bind the metal ion and prevent its release in the body. The resulting complexes enhance the contrast of tissues in medical imaging, making internal structures easier to visualize.

O 10.12 FURTHER READING

- Huheey, J. E.; Keiter, E. A.; Keiter, R. L.; Medhi, O. K. *Inorganic Chemistry: Principles of Structure and Reactivity*, 4th ed.; Pearson.
- Shriver, D. F.; Atkins, P. W.; Overton, T.; Rourke, J.; Weller, M.; Armstrong, F. *Inorganic Chemistry*, 5th ed.; Oxford University Press: Oxford, 2010.
- Miessler, G. L.; Fischer, P. J.; Tarr, D. A. *Inorganic Chemistry*, 5th ed.; Pearson: Boston, 2014.
- Lee, J. D. *Concise Inorganic Chemistry*, 5th ed.; Wiley-Blackwell: Oxford, 1996.
- Housecroft, C. E.; Sharpe, A. G. *Inorganic Chemistry*, 4th ed.; Pearson Education: Harlow, 2012.

M 10.13 MODEL QUESTIONS

Q1. Explain the reasons for the lanthanide contraction and its effect on complex stability.
Q2. Describe the magnetic behaviour of actinide ions and explain why their magnetic properties are more complex than those of lanthanides.
Q3. Discuss the differences between 4*f*–4*f* transitions and 5*f*–5*f* transitions in lanthanide and actinide ions.
Q4. Explain the coordination number and geometry commonly observed in lanthanide complexes.
Q5. Describe the role of actinyl ions (AnO_2^{n+}) in actinide chemistry and nuclear fuel processing.

UNIT 11: STABILITY AND REACTIVITY OF COORDINATION COMPOUNDS

UNIT STRUCTURE

11.1 Learning Objectives
11.2 Introduction
11.3 Thermodynamic and Kinetic Stability
11.4 Lability and Inertness
11.5 Stability Constant- Formation Constant of Complexes
11.6 Chelate Effect
11.7 Factors Affecting Stability
11.8 Correlation of Stability Constant with Thermodynamic Factors $-\Delta G$, ΔH and ΔS
11.9 Determination of Stability Constant
  11.9.1 Job's Methods.
  11.9.2 Bjerrum's Method
11.10 Let Us Sum Up
11.11 Answers to Check Your Progress
11.12 Further Reading
11.13 Model Questions

11.1 LEARNING OBJECTIVES

After studying this unit, you should be able to:

- Distinguish between **labile** and **inert** coordination complexes
- Explain thermodynamic and kinetic stability
- Define and interpret stability (formation) constants
- Understand the chelate effect and its origin
- Correlate stability constants with ΔG, ΔH and ΔS
- Describe experimental methods for determining stability constants

11.2 INTRODUCTION

In earlier units, you have learned about bonding, structure, and electronic properties of coordination compounds. In this unit, we move a step further and ask two very important questions:

- How stable is a coordination compound once it is formed?
- How fast or slow does it undergo chemical change?

These questions are very important while understanding coordination chemistry, because many applications—from biological systems to industrial catalysis—depend not only on whether a complex forms, but also on how stable it is and how reactive it is. The idea of stability in coordination chemistry was first systematically explored after the establishment of coordination theory by Alfred Werner.

However, stability is not a single concept. When chemists say that a complex is "stable", they may mean:

- It forms in large amount at equilibrium
- It does not break down easily
- It reacts very slowly with other ligands

In this unit, we will carefully separate these ideas and study them from the thermodynamic and kinetic viewpoints.

11.3 THERMODYNAMIC AND KINETIC STABILITY

The stability of a coordination compound refers to its ability to maintain its existence without decomposition or transformation over a period of time under given conditions. In simple terms, a stable complex is one that can be formed and stored for a reasonable length of time without breaking down.

However, it is important to understand that stability is not an absolute term. A complex that appears stable under one set of conditions (such as room temperature or in the absence of light) may become unstable under another set of conditions (such as heating or exposure to light or reactive chemicals). Therefore, stability is always considered a relative concept.

In coordination chemistry, stability is mainly discussed from two different but complementary viewpoints:

1. Thermodynamic stability
2. Kinetic stability

Both must be considered to fully understand the behaviour of coordination compounds.

1. Thermodynamic Stability: Thermodynamic stability refers to the extent to which a complex is formed and remains intact at equilibrium under a given set of conditions. In other words, it tells us whether the formation of a complex is energetically favourable.

A thermodynamically stable complex is one that:

• Exists predominantly in the complexed form at equilibrium

• Does not readily transform into another species because such transformation would require an increase in free energy

Thermodynamic stability is closely related to the strength of the metal–ligand bonds and is quantitatively expressed by the stability (formation) constant. It is important to note that: Thermodynamic stability does not provide any information about how fast or slow a reaction occurs. A complex may be thermodynamically stable but still react rapidly, or it may be thermodynamically unstable but react very slowly.

Based on thermodynamic behaviour of complexes in solution, Biltz classified coordination compounds into:

• **Stable complexes**: The complexes which possess sufficient stability to retain their identity in solution.

• **Unstable complexes**: These are reversibly dissociated in solution into their components.

2. Kinetic Stability: While thermodynamic stability tells us whether a complex is stable at equilibrium or not, kinetic stability tells us how fast or slow a complex reacts. Thus, kinetic stability is directly related to the rate of chemical reactions, particularly ligand substitution reactions. Kinetic inertness is associated with high activation energy barriers, which slow down ligand substitution even when the reaction is thermodynamically favourable.

Kinetic stability deals with:

- Rate of ligand replacement
- Reaction mechanisms
- Formation of intermediate species

Based on kinetic behaviour, Henry Taube (1950) classified coordination compounds into two classes *viz*. labile and inert complexes.

Important Relationship Between Thermodynamic and Kinetic Stability:

It is essential to clearly distinguish between these two concepts:

- If a complex is thermodynamically stable, it will not transform into another species under normal conditions because such a transformation is energetically unfavourable. However, under forcing conditions, transformation may still occur.
- If a complex is thermodynamically unstable, it can easily be transformed into another species because such a change is energetically favourable.

However, kinetic studies are required to determine how fast such transformations occur. Even if a reaction is thermodynamically allowed, it may proceed very slowly if the activation energy is high.

11.4 LABILITY AND INERTNESS

Lability and inertness are kinetic concepts related to the rate of ligand substitution reactions. A labile complex is one in which one or more ligands in the coordination sphere are rapidly replaced by other ligands while an inert complex is one in which ligand substitution occurs very slowly, or only under forcing conditions such as heating or strong reagents. These terms do not indicate how stable a complex is at equilibrium; they only describe how fast it reacts.

To clear the concept how labile and inert complexes are different from thermodynamically stable and unstable complexes, let us consider three extremely thermodynamically stable cyano complexes: $[Ni(CN)_4]^{2-}$, $[Mn(CN)_6]^{3-}$, and $[Cr(CN)_6]^{3-}$. Although thermodynamically stable, kinetically they behave quite differently. ^{14}C labelled cyanide is introduced to measure the rate of exchange of cyanide ligand and it was found that, despite its thermodynamic stability, the complex $[Ni(CN)_4]^{2-}$exchanges the cyanide ligand very rapidly i.e. the complex is kinetically labile.

$$[Ni(CN)_4]^{2-} + 4\,^{14}CN^- \rightarrow [Ni(^{14}CN)_4]^{2-} + 4CN^- \qquad t_{1/2} \approx 30s$$

The hexacyanomanganese ($[Mn(CN)_6]^{3-}$) complex is found to be moderately labile ($t_{1/2}$ ≈ 1 hr) while the complex $[Cr(CN)_6]^{3-}$can be treated as an inert one with $t_{1/2}$ ≈ 24 days:

$$[Mn(CN)_6]^{3-} + 6^{14}CN^- \rightarrow [Mn(^{14}CN)_6]^{3-} + 6CN^- \qquad t_{1/2} \approx 1\ hr$$

$$[Cr(CN)_6]^{3-} + 6^{14}CN^- \rightarrow [Cr(^{14}CN)_6]^{3-} + 6CN^- \qquad t_{1/2} \approx 24 days$$

The terms labile and inert are relative to each other and their usage may vary depending on the system and conditions considered. In general, complexes that undergo ligand substitution completely within approximately one minute at 25 °C are considered labile, whereas those that require a significantly longer time are regarded as inert.

The complex $[Ni(CN)_4]^{2-}$is a very good example of kinetically labile as well as thermodynamically stable complex. In the opposite way, example of kinetically inert but thermodynamically unstable complex includes hexaamminecobalt(III) in acidic solution. Even under thermodynamically favourable conditions, the degradation of the complex requires several days. This inert behaviour arises from the absence of a suitable low-energy reaction pathway for the acidolysis process.

11.5 STABILITY CONSTANT (FORMATION CONSTANT OF THE COMPLEXES)

When a coordination complex is formed in solution, the metal ion usually does not bind all ligands at once. Instead, ligands attach to the metal one after another. Let us consider a general complex of the type ML_n, where:

- M is the central metal ion,
- L is a monodentate ligand, and
- n is the maximum number of ligand molecules that can coordinate to the metal ion.

Now, let's see how the complex forms. Think of the metal ion as gradually welcoming ligands into its coordination sphere. Each ligand joins in a separate step, and each step has its own equilibrium.

The first ligand attaches as:

$$M + L \rightleftharpoons ML$$

The equilibrium constant for this step is called the first stepwise formation constant, K_1 and

$$K_1 = \frac{[ML]}{[M][L]}$$

Next, a second ligand joins:

$$ML + L \rightleftharpoons ML_2$$

This step is characterized by another constant, K_2 and

$$K_2 = \frac{[ML_2]}{[ML][L]}$$

This process continues until the maximum coordination number is reached:

$$ML_{n-1} + L \rightleftharpoons ML_n$$

The corresponding constant for this step is K_n.

The constants $K_1, K_2, \ldots, K_n$ are known as **stepwise** (or successive) **formation constants**. Each one tells us how favourable it is for the next ligand to attach.

Sometimes, instead of looking at each step separately, we can represent the **overall formation** of the complex as**:**

$$M + nL \rightleftharpoons ML_n$$

The equilibrium constant for this overall reaction is called the **overall or cumulative formation constant**, denoted by β_n and

$$\beta_n = \frac{[ML_n]}{[M][L]^n}$$

Generally, the overall formation constant (β_n) is the product of individual stepwise formation constants ($K_1, K_2, \ldots, K_n$) for the addition of n ligands, expressed as

$$\beta_n = K_1 \times K_2 \times K_3 \times \ldots \times K_n$$

In other words, the overall stability of the complex depends on the combined effect of all stepwise processes.

Except in a few special cases, it is generally observed that the magnitudes of the stepwise formation constants decrease progressively from K_1 to K_n.

Let us take the example of **Cd^{2+}–NH_3 system**, where NH_3 is a neutral ligand. The values of stepwise constants decrease steadily as more ammonia molecules bind to the metal ion. Although each step becomes less favourable, the complex still forms successfully because the overall stability constant is reasonably large.

$$Cd^{2+} + NH_3 \rightarrow [Cd(NH_3)]^{2+} \qquad K_1 = 10^{2.65}$$

$$[Cd(NH_3)]^{2+} + NH_3 \rightarrow [Cd(NH_3)_2]^{2+} \qquad K_2 = 10^{2.10}$$

$$[Cd(NH_3)_2]^{2+} + NH_3 \rightarrow [Cd(NH_3)_3]^{2+} \qquad K_3 = 10^{1.44}$$

$$[Cd(NH_3)_3]^{2+} + NH_3 \rightarrow [Cd(NH_3)_4]^{2+} \qquad K_4 = 10^{0.93}$$

Now, the overall formation constant,

$$\beta_4 = K_1 \times K_2 \times K_3 \times K_4$$
$$= 10^{2.65} \times 10^{2.10} \times 10^{1.44} \times 10^{0.93}$$
$$= 10^{7.12}$$

In the **Cd^{2+}–CN^- system**, where the ligand is a charged one, the stepwise constants are much larger than those for ammonia. This tells us that cyanide binds much more strongly to Cd^{2+} than ammonia does. As a result, the overall stability constant is extremely high, indicating a very stable complex.

$$Cd^{2+} + CN^- \rightarrow [Cd(CN)]^+ \qquad K_1 = 10^{5.48}$$

$$[Cd(CN)]^+ + CN^- \rightarrow [Cd(CN)_2]^- \qquad K_2 = 10^{5.12}$$

$$[Cd(CN)_2]^- + CN^- \rightarrow [Cd(CN)_3]^- \qquad K_3 = 10^{4.64}$$

$$[Cd(CN)_3]^- + CN^- \longrightarrow [Cd(CN)_4]^{2-} \qquad K_4 = 10^{3.55}$$

Here, $\beta_4 = K_1 \times K_2 \times K_3 \times K_4$

$= 10^{5.48} \times 10^{5.12} \times 10^{4.64} \times 10^{3.55}$

$= 10^{18.8}$

The gradual decrease in the values of K_1, K_2, … ,K_n as more ligands are added can be understood in a simple way. As ligands progressively occupy the coordination sphere of the metal ion, fewer water (aqua) molecules remain available to be replaced by incoming ligands. At the same time, as the coordination sphere becomes more saturated, the metal ion's tendency to attract additional electron pairs decreases. Consequently, each successive ligand binds less strongly than the previous one. It is important to remember that although each stepwise formation constant decreases, the overall formation constant may still be very large. This means that even if later steps are less favourable, the final complex can still be highly stable.

In Simple Words

- Complex formation happens step by step
- Each step has its own stability constant
- Stepwise constants usually decrease
- Overall stability depends on the combined effect of all steps

11.6 CHELATE EFFECT

As discussed earlier in the section on polydentate ligands (see unit 3.3.4), chelation involves the formation of cyclic metal complexes through multidentate coordination. While the structural aspects of chelates have already been introduced, the present section aims to examine the remarkable stability of such complexes. This unusual enhancement in stability, commonly referred to as the **chelate effect**, arises primarily from thermodynamic considerations, particularly entropy changes during complex formation.

The principal driving force behind the chelate effect is the increase in entropy during complex formation. The free energy change of a reaction is given by:

$$\Delta G^\circ = \Delta H^\circ - T\Delta S^\circ$$

or $$\Delta G^\circ = -RT \ln K$$

where:

ΔG° = Standard free energy change
ΔH° = Enthalpy change
ΔS° = Entropy change
K = Stability constant

Since the enthalpy change (ΔH°) for chelated and non-chelated complexes is nearly the same (due to similar donor atoms), the difference in stability mainly arises from the entropy term (ΔS°).

During chelation, replacement of coordinated solvent molecules by a multidentate ligand results in an increase in the number of free species in solution, thereby increasing randomness. A more positive $\Delta S°$ makes $\Delta G°$ more negative, which leads to a higher stability constant (K). Let us take the example of following complex formation reactions:

$$Cd^{2+} + 4NH_3 \rightleftharpoons [Cd(NH_3)_4]^{2+}$$

$$Cd^{2+} + 4MeNH_2 \rightleftharpoons [Cd(MeNH_2)_4]^{2+}$$

$$Cd^{2+} + 2en \rightleftharpoons [Cd(en)_2]^{2+}$$

The values of thermodynamic parameters and stability constants for those reactions are shown below:

Ligand	**ΔG (in $kJmol^{-1}$)**	**ΔH(in $kJmol^{-1}$)**	**ΔS(in $Jmol^{-1}K^{-1}$)**	**logβ**
NH_3	-42.5	-53.2	-35.5	7.44
$MeNH_2$	-37.2	-57.3	-67.3	6.52
en	-60.7	-56.5	+13.8	10.62

The data clearly show that:

- The chelated complex $[Cd(en)_2]^{2+}$ is far more stable than the analogous complexes with monodentate ligands.
- The enhanced stability is primarily due to a positive entropy change.
- Therefore, the chelate effect is predominantly an entropy-driven phenomenon, rather than an enthalpy-driven one.

This thermodynamic evidence strongly supports the fundamental concept of chelation in coordination chemistry.

Note

The chelate effect is:

- A thermodynamic stability phenomenon
- Predominantly entropy-driven
- Strongly influenced by denticity and ring size
- Modulated by metal ion properties and ligand characteristics

11.7 FACTORS AFFECTING STABILITY

The stability of coordination compounds depends on a number of factors associated with both the metal ion and the ligand, as well as the geometry of the complex and the nature of the solvent. These factors influence the strength of metal–ligand interactions and determine the extent to which a complex can exist without undergoing dissociation. Understanding these factors is essential for interpreting the formation and behaviour of coordination compounds in chemical and biological systems.

The factors on which the stability of metal complexes depend are-

1. Nature of the central metal ion

2. Nature of the ligand
3. Macrocyclic effect
4. Resonance effect
5. Crystal Field Stabilization Energy (CFSE)

1. Nature of the central metal ion:

a) Charge on the metal cation: In general, metal ions in higher oxidation states tend to form more stable complexes than those in lower oxidation states, particularly with neutral ligands such as NH_3 and H_2O. This is because an increase in positive charge enhances the electrostatic attraction between the metal ion and the donor atoms of the ligand.

However, important exceptions are observed with certain ligands such as CO, PMe_3, o-phenanthroline, 2,2′-bipyridyl, and CN^-. These ligands often form more stable complexes with metals in lower oxidation states. This behaviour arises from their ability to participate in *π*-back bonding or strong *π*-interactions, which are more effective when the metal ion has greater electron density, as in lower oxidation states.

***b) Size of the metal cation*:** In general, small metal cations carrying a higher positive charge tend to form more stable coordination complexes. This is because such ions possess a high charge-to-size ratio, which leads to stronger metal–ligand interactions and hence more stable coordinate bonds.

This trend is illustrated by the following series, where stability decreases with increasing ionic size or decreasing charge:

$Li^+ > Na^+ > K^+ > Rb^+ > Cs^+$
$Th^{4+} > Y^{3+} > Ca^{2+} > Na^+$
$La^{3+} > Sr^{2+} > K^+$
$Fe^{3+} > Fe^{2+}$

These examples clearly show that, for metal ions of similar nature, an increase in positive charge or a decrease in ionic radius enhances the stability of the corresponding complexes.

2. Nature of the ligand:

a) Basic Character and Electronic Nature of Ligands: The stability of a coordination complex is significantly influenced by the **basicity of the ligand**, that is, its tendency to donate an electron pair to the metal centre. A ligand with greater basic character possesses higher electron density at the donor atom and can therefore form stronger *σ* (sigma) coordinate bonds with the metal ion. As a consequence, an increase in ligand basicity generally leads to enhanced complex stability.

For first-row (3*d*-series) transition metal ions, the stability order observed with simple monodentate ligands is: $NH_3 > H_2O > F^-$

This trend reflects differences in donor strength and electron-donating ability. Ammonia, being a better *σ*-donor than water and fluoride, forms more stable complexes under comparable conditions.

***b) Covalent Character of the Metal–Ligand Bond*:** Beyond simple electrostatic considerations, the **degree of covalent character** in the metal–ligand bond also plays a crucial role in determining stability. Greater orbital overlap between the metal and ligand orbitals enhances covalency, which in turn strengthens the bonding interaction. This effect is clearly illustrated in the stability order of silver(I) dihalide complexes:

$$AgI_2^- > AgBr_2^- > AgCl_2^- > AgF_2^-$$

The stability increases from fluoride to iodide because iodide is larger and more polarizable, promoting stronger covalent interaction with the relatively soft Ag^+ ion. Thus, covalency becomes an important stabilizing factor.

***c) Role of π-Interactions**:* Ligands capable of *π*-interactions further enhance complex stability. Ligands such as CO, CN^-, alkenes, and phenanthroline possess vacant *π** orbitals (*π*-acceptor ligands) or filled *π*-orbitals (*π*-donor ligands) that can engage in synergic bonding with the metal. In particular, *π*-back donation from metal d-orbitals into ligand *π** orbitals strengthen the overall metal–ligand interaction and lowers the energy of the complex. Therefore, ligands capable of *σ*-donation combined with *π*-bonding interactions generally form exceptionally stable complexes, especially with metals in lower oxidation states.

3. Macrocyclic effect:

It has been observed that metal complexes formed with macrocyclic ligands of appropriate size exhibit significantly greater stability than those formed with comparable open-chain multidentate (chelating) ligands. This enhanced stability, known as the macrocyclic effect, arises mainly from the reduced entropy loss during complex formation and the optimal fit between the metal ion and the rigid ligand framework. Typical examples of macrocyclic ligands include crown ethers, porphyrins such as heme, and related cyclic polyethers.

4. Resonance effect:

Resonance plays an important role in enhancing the stability of coordination complexes. Ligands that exhibit resonance can delocalize electron density over a larger framework, which stabilizes both the free ligand and the resulting metal complex. A well-known example is the acetylacetonate anion. This ligand exists in resonance-stabilized forms, and upon coordination with a metal ion, it forms particularly stable complexes. During complex formation, metal–ligand *π* interactions increase the extent of electron delocalization compared to that in the free enolate ion. This enhanced delocalization lowers the overall energy of the system and thereby contributes to the increased stability of the complex.

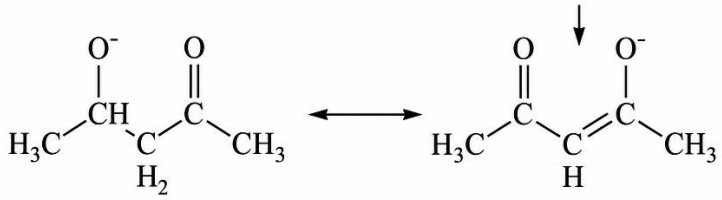


Fig 11.1: Resonance structures of acetylacetonate ligand

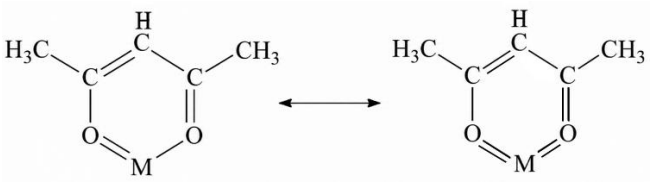


Fig 11.2: Acetylacetonate-metal complex.

5. Crystal Field Stabilization Energy (CFSE):

Crystal Field Stabilization Energy (CFSE) is one of the most significant electronic factors governing the stability of coordination complexes. When a metal ion approaches a set of ligands, the electrostatic field created by the ligands splits the degenerate d-orbitals of the metal ion. If the distribution of d-electrons in the resulting crystal field leads to a net lowering of energy, the complex gains additional stabilization—this is referred to as CFSE. A higher magnitude of CFSE implies greater thermodynamic stability of the complex. In many cases, it also contributes to kinetic inertness, meaning that such complexes undergo ligand substitution reactions very slowly.

Notable examples include low-spin $5d^6$ complexes of Pt^{4+} and Ir^{3+}, as well as square planar $5d^8$ complexes of Pt^{2+}. These systems possess substantial CFSE, which makes them both thermodynamically stable and kinetically inert. As a result, they exhibit exceptionally slow ligand exchange reactions.

11.8 CORRELATION OF STABILITY CONSTANT WITH THERMODYNAMIC FACTORS

The stability of a coordination complex is quantitatively expressed by its stability constant (Stepwise constant, K or overall formation constant, β). From a thermodynamic viewpoint, the value of the stability constant is directly related to the changes in Gibbs free energy ($\Delta G°$), enthalpy ($\Delta H°$), and entropy ($\Delta S°$) associated with complex formation.

The relationship between the stability constant and Gibbs free energy change is given by the equation:

$$\Delta G° = - RT \ln K$$

This equation shows that a larger value of the stability constant, K corresponds to a more negative $\Delta G°$, indicating that the formation of the complex is thermodynamically more favourable.

Further, the free energy change is related to enthalpy and entropy changes by the fundamental thermodynamic relation:

$$\Delta G° = \Delta H° - T\Delta S°$$

From this expression, it becomes clear that the magnitude of the stability constant depends on both enthalpy change and entropy change during complex formation.

A **negative $\Delta H°$** (exothermic metal–ligand bond formation) contributes to **increased stability** by lowering $\Delta G°$. Also, a **positive $\Delta S°$** (increase in disorder, often due to release of solvent molecules or the chelate effect) also makes $\Delta G°$ more negative and thus **enhances stability**.

In many coordination complexes, particularly chelate and macrocyclic complexes, the increased stability is largely entropy-driven, even when ΔH° values are comparable. Conversely, complexes with strong covalent metal–ligand interactions may show high stability primarily due to favourable enthalpy changes.

Thus, the stability constant of a coordination compound reflects the combined influence of enthalpic factors (bond strength, CFSE, covalency) and entropic factors (chelation, solvation, molecular rearrangement). A proper understanding of this correlation provides deeper insight into why certain complexes are exceptionally stable while others are not.

11.9 DETERMINATION OF STABILITY CONSTANT

The determination of stability constants of metal complexes can be carried out using several experimental techniques, most notably spectroscopic and potentiometric methods. Evaluation of stability constants is of considerable importance, as it provides valuable insight into the strength of metal–ligand interactions and the role of ligands in stabilizing metal ions in solution. Such information is essential for understanding complex behaviour in diverse areas including biological systems, environmental chemistry, metallurgy, food chemistry, and various industrial processes.
Some of the commonly employed methods for the determination of stability constants are discussed below.

11.9.1 Job's Method

Job's Method of Continuous Variations (MCV) is a widely used technique for investigating complex formation and, under suitable conditions, for estimating stability constants. Primarily, this method is employed to determine the stoichiometric composition of a metal–ligand complex in solution. It may be regarded as a modified spectroscopic approach, since the measurements are generally based on changes in absorbance or another measurable physicochemical property.
The method is particularly applicable to systems in which only a single predominant complex is formed in solution. By systematically varying the mole fraction of metal and ligand while keeping the total concentration constant, the composition of the complex can be determined from the maximum observed in the measured property.

The fundamental principle of Job's method is that **maximum complex formation occurs when the reacting species are present in their exact stoichiometric ratio**.
In this method, a series of solutions is prepared in which:

- The **total molar concentration** of metal ion and ligand remains constant.
- The **mole fractions** of the metal and ligand are varied systematically.

A measurable physicochemical property, usually **absorbance**, which is directly proportional to the concentration of the complex, is recorded for each solution.
When absorbance is plotted against the mole fraction of one component, the resulting curve shows a maximum. The position of this maximum corresponds to the stoichiometric ratio of the complex formed.
Let,

C_M=concentration of metal ion

C_L=concentration of ligand

Since the total concentration is kept constant,

$$C_M + C_L = C(\text{constant})$$

Dividing throughout by C:

$$\frac{C_M}{C} + \frac{C_L}{C} = 1$$

The mole fraction of the ligand is defined as:

$$mf = \frac{C_L}{C}$$

Therefore,

$$\frac{C_M}{C} = 1 - mf$$

If the complex formed has the general formula ML_n, then:

$$n = \frac{C_L}{C_M}$$

Substituting in terms of mole fraction:

$$n = \frac{mf}{1 - mf}$$

Thus, by determining the mole fraction at the point of maximum absorbance, the stoichiometric coefficient n can be calculated and the composition of the complex ML_n is established.

***Experimental procedure*:**

- A series of solutions is prepared with varying mole fractions of metal and ligand while maintaining constant total concentration and total volume.
- Absorbance is measured at a wavelength where the complex absorbs strongly, but the free metal ion and ligand show negligible absorption.
- A plot of absorbance versus mole fraction is constructed to determine the point of maximum complex formation.

***Limitations**:*

- The method is applicable only when one complex species predominates under the experimental conditions.
- It is not suitable for systems involving multiple equilibria or stepwise complex formation.
- Accurate results require a significant measurable change in absorbance upon complex formation.
- The total concentration and experimental conditions must remain strictly constant.

Applications:

Job's method is extensively used for:

- Determining stoichiometry of coordination complexes

- Studying metal–ligand interactions in solution
- Investigating organometallic complexes
- Preliminary evaluation of complex formation before detailed thermodynamic analysis

11.9.2 Bjerrum's Method

Bjerrum's method is a classical **potentiometric technique** used for the determination of **stepwise and overall stability constants** of metal–ligand complexes in solution. The method is based on the measurement of hydrogen ion concentration during the interaction of a metal ion with a ligand capable of protonation. It is particularly useful for studying complexes of ligands such as ammonia, amines, and carboxylic acids.

The principle of Bjerrum's method is based on the fact that complex formation between a metal ion and a ligand affects the protonation equilibrium of the ligand. When a metal ion binds to a ligand, it competes with protons for the donor atoms, leading to changes in hydrogen ion concentration. By monitoring the pH variation during titration of: a) only ligand and b) ligand in the presence of metal ion, the extent of complex formation can be determined.
The method introduces the concept of average number of ligands bound per metal ion, denoted by $\bar{n}$.
The average number of ligands coordinated per metal ion is defined as:

$$\bar{n} = \frac{Total\ bound\ ligand}{Total\ metal\ ion}$$

For a system forming complexes ML, ML_2, ML_3,…the formation function is expressed as:

$$\bar{n} = \frac{K_1[L] + 2K_1K_2[L]^2 + 3K_1K_2K_3[L]^3 + \cdots}{1 + K_1[L] + K_1K_2[L]^2 + K_1K_2K_3[L]^3 + \cdots}$$

where K_1, K_2, K_3 are the stepwise stability constants.

In Bjerrum's method, two potentiometric titrations are carried out:

1. **Ligand–acid system,** and
2. **Metal–ligand–acid system**

The pH values obtained from both titrations are used to calculate:

- Free ligand concentration
- Bound ligand concentration
- Average coordination number $\bar{n}$

A plot of $\bar{n}$ versus log[L] is constructed, known as the **Bjerrum formation curve**. From the formation curve:

- The value of K_1 corresponds to $\bar{n}$=0.5
- The value of K_2 corresponds to $\bar{n}$=1.5
- Higher stepwise constants are obtained similarly

Overall stability constants are calculated using:

$$\beta_n = K_1 \times K_2 \times K_3 \times \cdots \times K_n$$

The main advantages of Bjerrum's method are that it can be used in the determination of both stepwise and overall stability constants and is applicable to weak and moderately strong complexes. This method is highly useful for solution equilibria studies.

However, this method is applicable mainly to ligands capable of protonation and less suitable for very strong complexes.

Thus, Bjerrum's method provides a reliable potentiometric approach for evaluating metal–ligand stability constants of coordination compounds and is widely used in bioinorganic chemistry and environmental metal–ligand equilibrium studies. Its theoretical foundation and quantitative treatment make it an important tool in understanding solution equilibria of coordination compounds.

W CHECK YOUR PROGRESS

Q1. What is meant by thermodynamic stability?

Q2. What is meant by kinetic inertness?

Q3. Name one example of a thermodynamically stable but kinetically labile complex.

Q4. Fill in the blanks:

(a) Thermodynamic stability of a coordination complex is related to the value of the _____ constant.

(b) A complex that undergoes ligand substitution very slowly is said to be _____.

(c) The overall formation constant β_n is equal to the product of _____ formation constants.

Q5. State true or false:

(a) Thermodynamic stability provides information about the rate of ligand substitution.

(b) Labile and inert are kinetic terms, not thermodynamic terms.

(c) A kinetically inert complex always has low thermodynamic stability.

(d)Stability of a complex is an absolute property independent of conditions.

Q6. Why are chelated complexes generally more stable than analogous monodentate complexes?

Q7. Write the mathematical relationship between $\Delta G°$ and $\log\beta$.

Q8. What is the importance of charge and size of the metal ion in determining the complex stability?

Q9. The overall stability constant (β) for the formation of a coordination complex at 298 K is given as: $\log\beta = 8.5$. Calculate the standard Gibbs free energy change ($\Delta G°$) for the complex formation. (Take R=8.314 $J mol^{-1} K^{-1}$)

Q10. State True or False:

(a) Complexes of highly charged and small metal ions are usually more stable.
(b) A negative value of $\Delta S°$ always favours complex formation.
(c) Macrocyclic ligands generally form more stable complexes than open-chain multidentate ligands.
(d) Job's method can determine both stoichiometry and stepwise stability constants accurately.
(e) CFSE contributes to thermodynamic stability of transition metal complexes.

2 11.10 LET US SUM UP

- This unit deals with the stability of coordination compounds from thermodynamic and kinetic perspectives. A clear distinction is made between thermodynamic stability, which depends on the extent of complex formation at equilibrium, and kinetic stability, which relates to the rate of ligand substitution reactions. The concepts of labile and inert complexes are discussed to highlight this difference.
- The formation of complexes is explained using stepwise and overall stability constants, and the factors influencing stability—such as metal ion properties, ligand characteristics, chelate and macrocyclic effects, resonance stabilization, and crystal field stabilization energy—are examined. The relationship between stability constants and thermodynamic parameters ($\Delta G°$, $\Delta H°$, and $\Delta S°$) is also established.
- Finally, experimental methods such as Job's method and Bjerrum's potentiometric method are introduced for determining the stoichiometry and stability constants of coordination complexes.

K 11.11 ANSWERS TO CHECK YOUR PROGRESS

Answer to Q1: Thermodynamic stability refers to the tendency of a coordination complex to exist in equilibrium once it is formed. It depends on the magnitude of its formation (stability) constant. A complex with a large formation constant is said to be thermodynamically stable.

Answer to Q2: Kinetic inertness refers to the resistance of a coordination complex to undergo ligand substitution or other chemical change. A kinetically inert complex reacts very slowly, even if the reaction is thermodynamically favorable.

Answer to Q3: Such an example is **$[Cu(NH_3)_4]^{2+}$**, which is thermodynamically stable (high formation constant) but kinetically labile (undergoes ligand substitution rapidly).

Answer to Q4: (a) formation (stability) (b) inert (c) stepwise

Answer to Q5: (a) False (b) True (c) False (d) False

Answer to Q6: Chelated complexes are generally more stable due to the chelate effect. When a polydentate ligand binds to a metal ion, it forms one or more rings which leads to:

- Entropy increase (more particles are released during chelation compared to monodentate substitution).
- Ring formation, which reduces the probability of ligand dissociation.
- Multiple bonding sites, making simultaneous bond breaking less likely.

As a result, chelated complexes are thermodynamically more stable than analogous complexes containing only monodentate ligands.

Answer to Q7: The relationship between standard Gibbs free energy change (ΔG°) and the overall formation constant (β) is: $\Delta G^\circ = -RT\ln\beta$

Answer to Q8: The charge and size of the metal ion strongly influence complex stability:

- Higher charge on the metal ion increases electrostatic attraction between the metal and ligands, increasing stability.
- Smaller ionic size increases charge density, leading to stronger metal–ligand interactions.
- Metal ions with high charge and small radius generally form more stable complexes.

Thus, stability increases with increasing charge and decreasing ionic radius of the metal ion.

Answer to Q9: $\Delta G^\circ \approx -48.4\ kJmol^{-1}$

Answer to Q10: (a)True (b)False (c)True
(d)False (e) True

O 11.12 FURTHER READING

- Cotton, F. A.; Wilkinson, G.; Murillo, C. A.; Bochmann, M. *Advanced Inorganic Chemistry*; Wiley.
- Puri, B. R.; Sharma, L. R.; Kalia, K. C. *Principles of Inorganic Chemistry*.
- Weller, M.; Overton, T.; Rourke, J.; Armstrong, F. *Inorganic Chemistry*, 7th ed.; Oxford University Press, 2018.

M 11.13 MODEL QUESTIONS

Q1. Explain the concepts of thermodynamic stability and kinetic stability of coordination compounds. Clearly distinguish between labile and inert complexes with suitable examples.

Q2. What are stepwise and overall stability constants? Explain the relationship between them and discuss why successive stability constants usually decrease

Q3. Explain the chelate effect using thermodynamic parameters. Illustrate how entropy plays a dominant role in enhancing the stability of chelated complexes

Q4. Discuss how chelate effect and macrocyclic effect determines the stability of coordination compounds.

Q5. Discuss Job's method and Bjerrum's method, highlighting their principles, applications, and limitations.

UNIT 12: LIGAND SUBSTITUTION REACTIONS IN COORDINATION COMPOUNDS

UNIT STRUCTURE

12.1 Learning Objectives
12.2 Introduction
12.3 Introduction to Ligand Substitution Reactions
12.4 Mechanisms in Substitution Reactions
12.5 Substitution Reactions in Octahedral Complexes
12.6 Substitution Reactions in Square Planar Complexes
12.7 Rate of Water Replacement Reactions
12.8 Let Us Sum Up
12.9 Answers to Check Your Progress
12.10 Further Reading
12.11 Model Questions

12.1 LEARNING OBJECTIVES

After going through this unit, you will be able to:

- learn the concept of ligand substitution reactions.
- differentiate between various substitution mechanisms.
- learn about the mechanism of substitution in octahedral complexes.
- explain ligand substitution behaviour in square planar complexes.
- learn about the rate of water exchange reactions in transition metal complexes.

12.2 INTRODUCTION

We will start with the basics of ligand substitution reactions and understand the concept of labile and inert complexes. We will explore the various mechanisms followed in substitution reactions and gain understanding in its subsequent application.

Next, we will cover the substitution reactions in octahedral and square planar complexes, explore the rate of these reactions, changes in stereochemistry and understand the experimental observations. Then, we will move on to rate of water substitution reactions and factors affecting the rate of these reactions.

12.3 INTRODUCTION TO LIGAND SUBSTITUTION REACTIONS

Substitution reactions in coordination chemistry are a class of reactions in which one ligand, which is attached to a metal ion, is replaced by another ligand. Since one ligand is substituted for a different ligand, these reactions are more specifically known as Ligand Substitution reactions. Ligand Substitution reactions are fundamental reactions that occur in coordination complexes.

In a ligand substitution reaction:

$$M{-}X + Y \longrightarrow M{-}Y + X$$

where, X is the leaving group and Y is the entering group.

An example of ligand substitution reaction is:

$$[Co(H_2O)_6]^{2+}(aq) + Cl^-(aq) \longrightarrow [CoCl(H_2O)_5]^+(aq) + H_2O(l)$$

In the above reaction, $Cl^-$is the leaving group and H_2O is the entering group.

An important attribute of ligand substitution reactions is the rate of these reactions. The rate can be defined to how fast one ligand is exchanged by another ligand in a coordination complex. The rate of ligand substitution reactions varies for different complexes. While some complexes undergo ligand substitution very fast, some other complexes undergo substitution very slowly, under similar conditions. The variation in rates of ligand substitution reactions is due to several underlying factors. Therefore, knowledge about the rates of these reactions is crucial for understanding the behaviour and reactivity of coordination complexes.

On the basis of the rate of ligand substitution reactions, coordination complexes can be broadly classified as labile or inert. Coordination complexes in which rapid exchange of one or more ligands from their coordination sphere takes place can be said to be labile. On the other hand, complexes that survive for significantly longer periods (by convention, at least a minute) are said to be inert. It is worth mentioning that there is no relation between the thermodynamic stability of a complex and its lability towards substitution. An example of a labile complex is $[Ni(H_2O)_6]^{2+}$. This complex survives for a few milliseconds before the H_2O in the coordination sphere is replaced by another H_2O molecule or by a stronger ligand. On the other hand, $[Co(NH_3)_5(H_2O)]^{3+}$can be termed as a non-labile or inert complex. This is because the H_2O molecule in the coordination sphere survives for several minutes as a ligand before it is replaced by a stronger ligand.

So, is it possible to predict whether a complex is labile or inert? As discussed above, this difference in the reaction rates can be attributed to various factors associated with the coordination complex. These factors include the identity of the central metal ion, the nature of the ligands bound to the central metal ion and the structure of the complex. Some general trends that follow are:

i. For transition metals, octahedral d^3, low spin d^4-d^6, and square planar d^8 complexes tend to be inert.
ii. Lability decreases down the group in the periodic table. For example, in group 10, the lability diminishes from Ni to Pd to Pt. This can be attributed to the increasing covalency in complexes, due to the soft nature of the metal ions, going from top to bottom in a group.
iii. Complexes of the d^{10} ions (Zn^{2+}, Cd^{2+}, and Hg^{2+}) are generally quite labile.
iv. Complexes of *d*-block M^{3+} ions are significantly less labile than d-block M^{2+} ions.

Another important factor that influences the rate of ligand substitution reactions is the nature of the ligands. Typically, coordination complexes are labile when the ligand is a good leaving group. A ligand is generally a good leaving group if it is stable in the

uncoordinated form. For example, chloro is a better leaving group as compared to an alkyl group as the chloride ions are relatively more stable than an alkylide anion in the uncoordinated (free) form. In addition to the entering and leaving groups, there are another set of ligands that do not directly participate in substitution but can influence the reaction rates. Such ligands are known as spectator ligands. For example, it is seen that for square-planar complexes, the ligand trans to the leaving group, X has a significant effect on the rate of substitution of X by the incoming group, Y.

12.4 MECHANISMS IN SUBSTITUTION REACTIONS

One important aspect of understanding any reaction is the determination of its reaction mechanism. Knowledge about the mechanism of a reaction can provide significant information about the sequence of elementary steps that take place during the transformation of reactants into products.

In inorganic substitution reactions, three major types of reaction mechanism have been generally recognised:

i. **Dissociative (D) mechanism**: In this type of ligand substitution mechanism, a coordination complex ML_5X first loses a ligand, X to form an intermediate of lower coordination number, ML_5. The incoming ligand, Y then reacts with this intermediate to form the complex ML_5Y. It is worth mentioning that ML_n (the metal atom and any spectator ligands), which is a true intermediate, can be detected or even isolated, in some cases.
An illustration of ligand substitution by dissociative mechanism for an octahedral ML_5X complex is shown below:

$$ML_5X \rightarrow ML_5 + X$$
$$ML_5 + Y \rightarrow ML_5Y$$

An example of a ligand substitution proceeding in a dissociative manner is the substitution of hexacarbonyltungsten, $W(CO)_6$ by phosphine, PPh_3. $W(CO)_6$ first loses a CO ligand followed by coordination of the incoming ligand, PPh_3.

$$W(CO)_6 \rightarrow W(CO)_5 + CO$$
$$W(CO)_5 + PPh_3 \rightarrow W(CO)_5(PPh_3)$$

ii. **Associative (A) mechanism**: In associative substitution reactions, the entering ligand Y attacks the ML_5X complex to form an intermediate ML_5XY. Coordinatively unsaturated complexes or complexes containing ligand(s) that can change its hapticity with the central metal ions generally proceed via the associative mechanism.
A mechanistic illustration for ligand substitution on an octahedral ML_5X complex proceeding in an associative manner is shown below:

$$ML_5X + Y \rightarrow ML_5XY$$
$$ML_5XY \rightarrow ML_5Y + X$$

The exchange of ^{14}CN with the unlabelled ligands in the square-planar complex $[Ni(CN)_4]^{2-}$ is an example of a ligand substitution reaction proceeding via associative mechanism. In this example, a five-coordinate intermediate is formed first by addition of the entering ligand, ^{14}CN followed by loss of one CN^- ligand to give the final product.

$$[Ni(CN)_4]^{2-} + {}^{14}CN^- \rightarrow [Ni(CN)_4(^{14}CN)]^{3-}$$

$$[Ni(CN)_4(^{14}CN)]^{3-} \rightarrow [Ni(CN)_3(^{14}CN)]^{2-} + CN^-$$

It is significant to note that many ligand substitution reactions of square-planar Au(III), Pt(II), Pd(II), Ni(II), and Ir(I) d^8 complexes proceed via the associative mechanism.

It is important to note that the intermediate formed in an associative mechanism is of a higher coordination number than the original complex. This is in contrast to dissociative mechanism where the intermediate has a reduced coordination number as compared to the original complex. However, intermediates formed in both these mechanisms are true in nature *i.e.* they can be detected or even isolated, is some cases. Another common feature of these two mechanisms is that they both proceed via a two-step pathway: the first step involves the formation of the intermediate followed by the dissociation of the intermediate into the final product.

iii. **Interchange (I) mechanism**: The interchange mechanism, common for many six-coordinate complexes, proceeds via a single step where the exchange of outgoing and incoming groups takes place simultaneously. This mechanism does not involve the existence of a true intermediate but occurs by the formation of a transition state.

$$ML_5X + Y \rightarrow X\cdots ML_5\cdots Y \rightarrow ML_5Y + X$$

Depending on the rate of the reaction, the interchange mechanism is further classified into two types:

a. Dissociative interchange (I_d), in which bond cleavage dominates over bond formation. The reaction rate displays very little dependence on the entering group.
b. Associative interchange (I_a), in which bond formation dominates over bond cleavage. The reaction rate shows significant dependence on the entering group.

It is generally challenging to differentiate between A and I_a, *D* and I_d, and I_a and I_d mechanisms.

The typical forms of reaction profile diagrams for these three major types of reaction mechanism is shown in **Fig. 12.1**.

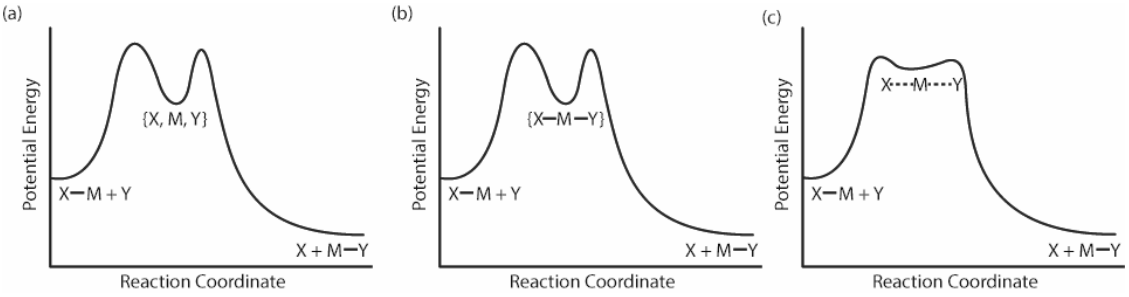


Fig. 12.1. An illustrative representation of a reaction profile diagram having a (a) dissociative, (b) associative and (c) interchange mechanism.

12.5 SUBSTITUTION REACTIONS IN OCTAHEDRAL COMPLEXES

Almost all ligand substitution reactions in octahedral complexes proceed via the interchange mechanism. The only determining factor for the reaction mechanism is whether the rate-determining step is associative (I_a) or dissociative (I_d). The rate-determining step, therefore, depends on either the formation of the new Y···M bond or the cleavage of the original M···X bond. Complexes of Cr(III) (d^3) and low-spin Co(III) (d^6) are kinetically inert with slow enough reaction rates to enable extensive studies.

Experimentally verified rate constants together with equilibrium studies confirm the I_d mechanism for such substitution reactions consistent with the Eigen-Wilkins mechanism. In the Eigen-Wilkins mechanism, the substrate, ML_6 and the incoming ligand, Y first form a weakly bound encounter complex, $\{ML_6,Y\}$ in a pre-equilibrium step.

$$ML_6 + Y \rightleftharpoons \{ML_6,Y\} \qquad K_E = \frac{[\{ML_6,Y\}]}{[ML_6]\,[Y]}$$

where, K_E is the equilibrium constant and can be determined theoretically.

This is followed by the loss of the outgoing ligand, L. This step is also the rate-determining step in the reaction.

$$\{ML_6,Y\} \rightleftharpoons ML_5Y + L \qquad \text{rate} = k_r[\{ML_6,Y\}]$$

The overall rate law is given as:

$$\text{rate} = \frac{k_r K_E [M]_T [Y]}{1 + K_E[Y]} \qquad \text{where, } [M]_T = [\{ML_6,Y\}] + [ML_6] \qquad \textbf{12.1}$$

At low concentrations of the incoming ligand, Y, $K_E[Y]<<1$. The rate equation 12.1 now transforms as:

$$\text{rate} = k\,K_E\,[M]_T\,[Y] = k_{obs}[M]_T\,[Y]$$

where, k_{obs} is the experimentally measured rate constant.

For the reaction,

$$[Ni(H_2O)_6]^{2+} + Y \rightarrow [Ni(H_2O)_5(Y)]^{2+} + H_2O$$

The variation in the value of *k* for various incoming ligands is shown in **Table 12.1**. As observed, the change in value of *k* is minimal which indicates that the reaction pathway is largely independent of the identity of the entering group. This strongly suggests that the reaction proceeds through an I_d mechanism.

Table 12.1: Variation of rate constants for different entering ligands in the above reaction.

Entering Ligand (Y)	NH_3	py	CH_3COO^-	F^-	SCN^-
k X 10^{-4} (s^{-1})	3	3	3	0.8	0.6

On the other hand, at a high concentration of the entering ligand, Y, the rate equation 1 approximates to:

$$\text{rate} = k[M]_T$$

Ligand substitution in Co(III) complexes is observed to proceed mostly through the I_d mechanism. This is inferred from the limited dependence of ligand substitution rates on the nature of the incoming ligand. Experimental observations indicate an I_d for the following reaction:

$$[Co(NH_3)_5X]^{2+} + H_2O \rightarrow [Co(NH_3)_5(H_2O)]^{3+} + X^-$$

This is because the reaction rate depends strongly on the nature of the outgoing group. For the above reaction, the rate of the reaction increases with X^- in the order shown below:

$$OH^- < N_3^- \approx NCS^- < CH_3COO^- < Cl^- < Br^- < I^- < NO_3^-$$

This trend is consistent with the strength of the M-X bond. The stronger the M-X bond, the more difficult it is to dissociate from the complex and, consequently, slower the rate of ligand substitution. This observation implies a mechanism in which the rate-determining step involves bond breaking, signifying a dissociative pathway.

For the reverse reaction as well, *i.e*. anation of $[Co(NH_3)_5(H_2O)]^{3+}$, the ligand substitution rate is largely independent of the nature of the entering groups.

$$[Co(NH_3)_5(H_2O)]^{3+} + X^{n-} \rightarrow [Co(NH_3)_5X]^{m+} + H_2O$$

(Anation reactions are a class of ligand substitution reactions in coordination complexes in which an uncharged ligand (*e.g*. H_2O), coordinated to the central metal ion, is replaced by an incoming anionic ligand *e.g*. Cl^-).
Another important aspect in the ligand substitution of octahedral complexes is the study of stereochemistry of substitution.
Consider the hydrolysis reactions of *cis*- and *trans*- $[CoX(en)_2Y]^+$ as shown below:

$$[CoX(en)_2Y]^+ + H_2O \rightarrow [Co(H_2O)(en)_2Y]^{2+} + X^-$$

If the reaction is to proceed via a dissociative mechanism, it must begin with the departure of the outgoing ligand, X^-. This should be followed by the subsequent addition of the incoming ligand, H_2O. The stereochemistry of the product, $[Co(H_2O)(en)_2Y]^{2+}$ must, therefore, be independent of the nature of the leaving group and instead be a result of the structure of the intermediate. As shown in the **Fig. 12.2**, two different intermediate structures are possible, a square pyramidal intermediate and

a trigonal bipyramidal intermediate. A square pyramidal intermediate strictly proceeds through retention of stereochemistry as the entering group attacks the position vacated by the outgoing group. Whereas, in a trigonal bipyramidal intermediate, the incoming group can coordinate at any one of the three available sites in the equatorial plane. This will result in an approximately 2:1 mixture of *cis*- and *trans*-isomers.

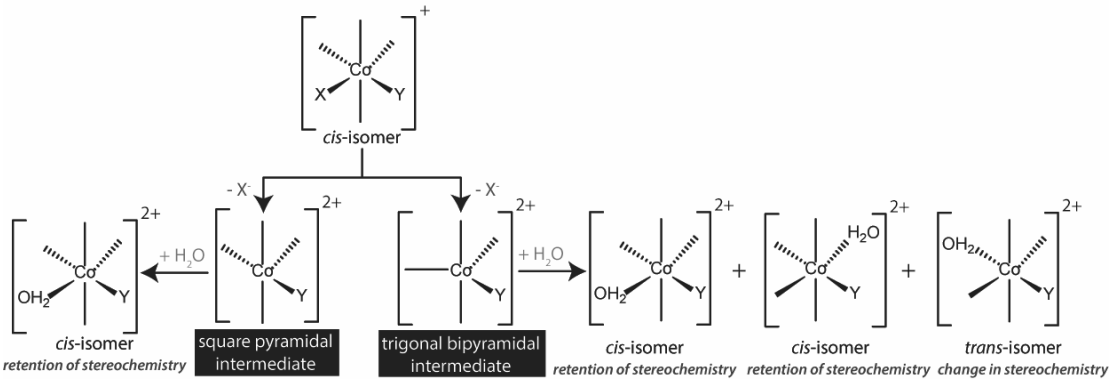


Fig. 12.2: Ligand Substitution reaction pathways in an octahedral Co(III) complex.

Table 12.2 shows the experimentally observed isomer distribution for the reactions of water with $[CoX(en)_2Y]^+$. For a pair of reactions, Y^- is kept unchanged while varying only the outgoing group, X^- (Cl^- or Br^-), to accurately understand the stereochemistry of the product. It is observed that any specific *cis*- and *trans*-$[CoX(en)_2Y]^+$ pair does not yield a common *cis-/trans*-$[Co(H_2O)(en)_2Y]^{2+}$ isomer distribution. This observation can be attributed, partially, to the relatively small difference between these two five-coordinate intermediate types, square pyramidal and trigonal bipyramidal. The attack of H_2O molecule is, therefore, believed to be faster than the interconversion of the five-coordinate intermediate.

Table 12.2: Isomer distribution patterns for the reactions of *cis*- and *trans*-$[CoX(en)_2Y]^+$with water at 298 K.

***cis*-$[CoX(en)_2Y]^+ + H_2O \longrightarrow [Co(H_2O)(en)_2Y]^{2+} + X^-$**			***trans*-$[CoX(en)_2Y]^+ + H_2O \longrightarrow [Co(H_2O)(en)_2Y]^{2+} + X^-$**		
Y^-	**X^-**	**% of *cis*-isomer**	**Y^-**	**X^-**	**% of *trans*-isomer**
$[OH]^-$	Cl^-	84	$[OH]^-$	Cl^-	30
$[OH]^-$	Br^-	85	$[OH]^-$	Br^-	29
Cl^-	Cl^-	75	Cl^-	Cl^-	74
Br^-	Br^-	73.5	Br^-	Br^-	84.5
$[N_3]^-$	Cl^-	86	$[N_3]^-$	Cl^-	91
$[N_3]^-$	Br^-	85	$[N_3]^-$	Br^-	91
$[NO_2]^-$	Cl^-	100	$[NO_2]^-$	Cl^-	100
$[NO_2]^-$	Br^-	100	$[NO_2]^-$	Br^-	100
$[NCS]^-$	Cl^-	100	$[NCS]^-$	Cl^-	58.5
$[NCS]^-$	Br^-	100	$[NCS]^-$	Br^-	57

12.6 SUBSTITUTION REACTIONS IN SQUARE PLANAR COMPLEXES

Square planar complexes are typically formed for metal ions having d^8 configuration, particularly in complexes having large crystal fields. Square planar complexes are generally formed for complexes containing Rh(I), Ir(I), Pt(II), Pd(II), Au(III) as metal centres. Ligand exchange mechanism has been widely studied owing to the convenient reaction timescales. The four-coordinate square planar complexes present a sterically uncrowded environment in comparison to the six-coordinate octahedral systems. As a result, the ligand substitution reaction is largely believed to proceed via an associative mechanism (A or I_a).

$$ML_4 + Y \rightarrow [ML_4Y]^{\ddagger} \rightarrow ML_3Y + L$$

Square planar complexes generally have rate law of the form:

$$\text{rate} = k_1[ML_4] + k_2[ML_4][Y]$$

where, $[ML_4]$ is the concentration of the square planar complex and, [Y] is the incoming ligand.

The associative pathway is believed to proceed through a five-coordinate transition state or intermediate, $ML_4Y^{\ddagger}$. An important example of ligand substitution in square planar complexes is the hydrolysis of *cis*-$[Pt(NH_3)_2Cl_2]$, a compound of significant biological interest considering its utility in inhibiting the growth of malignant tumours. The reaction is as shown below:



A study of the activation parameters of a series of square planar complexes with different incoming ligands also indicate an associative pathway. As seen in **Table12.3**, negative values for entropies of activation, $\Delta S^{\ddagger}$ and volumes of activation, $\Delta V^{\ddagger}$ strongly advocate an associative mechanism.

Table 12.3: Various activation parameters for substitution reactions in a series of square planar complexes.

Reactants	$\Delta H^{\ddagger}$ (kJ mol^{-1})	$\Delta S^{\ddagger}$ (J K^{-1} mol^{-1})	$\Delta V^{\ddagger}$ (cm^3 mol^{-1})
$[Pt(dien)Cl]^+ + H_2O$	+84	-63	-10
$[Pt(dien)Cl]^+ + [N_3]^-$	+65	-71	-8.5
trans-$[PtCl_2(PEt_3)_2]$ + py	+14	-25	-14
trans-$[PtCl(NO_2)(py)_2]$ + py	+12	-24	-9

Another important indication for the associative mechanism in square planar complexes is observed in the replacement of Cl^- by H_2O in a series of Pt(II) complexes, *viz*. $[PtCl_4]^2$, $[PtCl_3(NH_3)]^-$, $[PtCl_2(NH_3)_2]$ and $[PtCl(NH_3)_3]^+$. Similar rate constants are

observed for all of these reactions which suggest that there is no dependence of the rate of the reaction on the charge of the complex. This observation also hints towards an associative pathway while subtly negating the existence of a dissociative mechanism.

$$PtL_3X + Y \rightarrow PtL_3Y + X$$

The rate law for this reaction can be written as:

$$\text{rate} = \frac{-d[PtL_3X]}{dt}$$

$$= k_1[PtL_3X] + k_2[PtL_3X][Y]$$

Considering the fact that Y will be present in large excess, the reaction can be considered as a pseudo-first order reaction. The consequent rate law will then transform as:

$$\text{rate} = \frac{-d[PtL_3X]}{dt} = k_{obs}[PtL_3X]$$

$$k_{obs} = k_1 + k_2[Y]$$

The k_2 term is consistent with an associative pathway which involves the attack of Y on PtL_3X. The k_2 term dominates when Y is a good nucleophile. On the other hand, when k_1 term dominates, the reaction is considered to be primarily proceeding via a dissociative pathway. Another indicator of an associative mechanism is the diminution of both k_1 and k_2 terms which can happen when steric bulk of Y or L increases.

In most of the substitution reactions for square planar Pt(II) complexes, the stereochemistry is retained. This means that the incoming group occupies the coordination position vacated by the departing group. The associative pathway (A or I_a) involves a rearrangement between the two possible five-coordinate geometries (square pyramidal or trigonal bipyramidal) unless it is sterically hindered or the lifetime is too short. The incoming ligand initially enters from above or below the square plane. The entering group then coordinates to the central metal atom and forms a trigonal bipyramidal complex in an associative pathway. In the final step, the departing group leaves this complex with retention of stereochemistry in the final product. This is shown in **Fig. 12.3**.

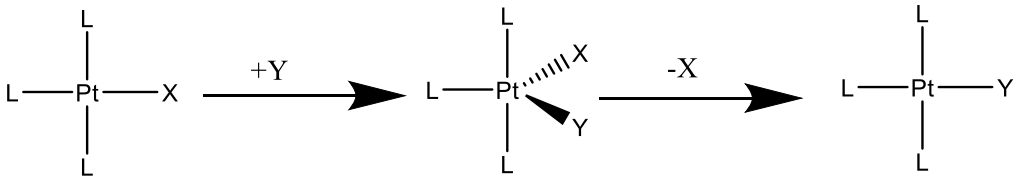


Fig. 12.3: Cartoon representation of the coordination of an incoming group, Y, to a square planar Pt(II) complex leading to a trigonal bipyramidal species followed by loss of outgoing group, X.

It is observed that the nature of the ligand *trans* to the leaving group plays an important role in determination of the kinetics of the reaction. The trans effect is prominently affected by the trans influence. The trans influence arises because the ligands trans to each other uses the same metal orbitals for bond formation. A good σ-donor or π-

acceptor can significantly weaken the bond trans to it in a complex. The experimentally observed reaction rates of substitution are influenced by the trans influence, a ground state phenomenon as well as the *trans* effect, a kinetic phenomenon.

Another significant aspect in study of the rates of substitution reactions is the nucleophilicity parameter, *n*. The nucleophilicity parameter elucidates the relationship between the nucleophilicity of the incoming group and the substitution rate in a square planar complex.

$$trans\text{-}[PtCl_2(py)_2] + Y \xrightarrow{k_2} trans\text{-}[PtClY(py)_2]^+ + Cl^-$$

Observation of the rate of substitution in the Pt(II) complex by the incoming group, Y suggests that the rate constant k_2 increases with Y as:

$$H_2O < NH_3 \approx Cl^- < py < Br^- < I^- < CN^- < PR_3$$

The nucleophilicity parameter, *n* can be written as:

$$n = \log k_2/k_2'$$
$$\text{or, } n = \log k_2 - \log k_2'$$

The values of *n* illustrate the effect of nucleophilicity of the incoming group on the rate of substitution reaction. This is shown in **Table 12.4**.

Table 12.4: Observed values of nucleophilicity parameter, *n* for a series of incoming ligands, Y, for the above reaction, relative to the *n* values for MeOH = 0 and at 298 K.

Ligand	Cl^-	NH_3	py	Br^-	I^-	CN^-	PPh_3
Nucleophilicity parameter (*n*)	3.04	3.07	3.19	4.18	5.46	7.14	8.93

12.7 RATE OF WATER REPLACEMENT REACTIONS

The rate of coordinated water exchange for d-block elements (M^{2+} and M^{3+}) vary over a much larger range as compared to the group 1, 2 and 13 elements. Several factors contribute to this wide range such as the ligand field effects and the d^n-electronic configurations. To understand the rate of water exchange, replacement of coordinated water molecule with isotopically labelled water has studied extensively for a series of $M(H_2O)_6]^{n+}$ octahedral coordination complexes. The rate of reactions as shown below can be experimentally determined using ^{17}O NMR spectroscopy.

$$M(H_2O)_6]^{n+} + H_2(^{17}O) \rightarrow [M(H_2O)_5\{(^{17}O)H_2\}]^{n+} + H_2O$$

where, M is an *s*-, *p*- or *d*-block metal.

The table below lists the observed activation volumes with some first-row transition metal elements.

Table 12.5: Comparison of the values of volumes of activation, $\Delta V^{\ddagger}$ for water exchange reactions in the above reaction form.

Metal ion	High spin d^n configuration	$\Delta V^{\ddagger}$ (cm^3/mol)
V^{2+}	d^3	-4.1
Mn^{2+}	d^5	-5.4
Fe^{2+}	d^6	+3.7
Co^{2+}	d^7	+6.1
Ni^{2+}	d^8	+7.2
Ti^{3+}	d^1	-12.1
V^{3+}	d^2	-8.9
Cr^{3+}	d^3	-9.6
Fe^{3+}	d^5	-5.4

A shift from associative to dissociative mechanism is concluded from the increase of volume of activation, $\Delta V^{\ddagger}$ from negative to positive values on moving from d^3 to d^8 configurations. An associative pathway is expected for M^{3+} ions as observed from the $\Delta V^{\ddagger}$ values in the above table. For second and third transition metal ions, an associative mechanism is observed from whatever data is experimentally determined. This may be attributed to the possibility of larger metal ions to accommodate the incoming ligand.

For the first row high-spin M^{2+} hexa aqua transition metal ions, the rate of water exchange can be arranged in the following order:

$$V^{2+} < Ni^{2+} < Co^{2+} < Fe^{2+} < Mn^{2+} < Zn^{2+} < Cr^{2+} < Cu^{2+}$$

and, for M^{3+} first row high-spin hexa aqua *d*-block ions, the order can be written as:

$$Cr^{3+} << Fe^{3+} < V^{3+} < Ti^{3+}$$

Considering the same charge and similar sizes of the complexes above and proceeding via the same reaction pathway, we can safely assume that the collision frequencies and entropy of activation, $\Delta S^{\ddagger}$ are reasonably constant. The variation in rate of the water exchange reaction, if any, will arise from the variation of enthalpy of activation, $\Delta H^{\ddagger}$. The variation in $\Delta H^{\ddagger}$ can result from the loss or gain of CFSE in the complex. A decrease in CFSE is indicative of increasing energy of activation and hence decreasing rate of the water exchange reaction. A seemingly high lability is seen for Cr^{2+} (*aq*) (high-spin d^4) and Cu^{2+} (*aq*) (d^9) complexes. This increased lability can be ascribed to weakly coordinated axial ligands due to the possibility of Jahn-Teller distortion.

Table 12.6: Change in CFSE values on geometry change of a high-spin octahedral complex into a square pyramidal transition state and a trigonal bipyramidal transition state, keeping other factors constant.

Metal ion (High Spin)	d^n	ΔCFSE /Δ_{oct}		Metal ion (High Spin)	d^n	ΔCFSE /Δ_{oct}	
		Square Pyramidal	Pentagonal bipyramidal			Square Pyramidal	Pentagonal bipyramidal
Sc^{2+}	d^1	+0.06	+0.13	Fe^{2+}	d^6	+0.06	+0.13
Ti^{2+}	d^2	+0.11	+0.26	Co^{2+}	d^7	+0.11	+0.26
V^{2+}	d^3	-0.20	-0.43	Ni^{2+}	d^8	-0.20	-0.43
Cr^{2+}	d^4	+0.31	-0.11	Cu^{2+}	d^9	+0.31	-0.11
Mn^{2+}	d^5	0	0	Zn^{2+}	d^{10}	0	0

W CHECK YOUR PROGRESS

Q1. What are ligand substitution reactions in coordination chemistry?
Q2. Define labile and inert complexes?
Q3. What are three major types of reaction mechanisms in ligand substitution reactions?
Q4. What is the most commonly followed mechanism in substitution reactions of octahedral complexes?
Q5. What are anation reactions?
Q6. Name the two possible intermediate structures for ligand substitution in octahedral complexes.
Q7. What is the fate of the stereochemistry in ligand substitution reactions for square planar complexes?
Q8. What is the significance of the nucleophilicity parameter?
Q9. How is the rate of water exchange reactions studied?
Q10. Fill in the blanks:

i. Ligand substitution in Co(III) octahedral complexes is observed to proceed mostly through the _____ mechanism.
ii. Negative values for entropies of activation, $\Delta S^{\ddagger}$ and volumes of activation, $\Delta V^{\ddagger}$ strongly support _____ mechanism.
iii. In water exchange reactions, a shift from associative to dissociative mechanism is concluded from the _____ of volume of activation, $\Delta V^{\ddagger}$ from negative to positive values on moving from d^3 to d^8 configurations.

2 12.7 LET US SUM UP

- Ligand substitution reactions in coordination complexes involve replacement of an outgoing group by an incoming group.
- Complexes may be classified as labile or inert depending on the rate of the reaction.
- The rate of substitution reaction depends on the identity and oxidation state of the central metal ion, its d-electron configuration, nature of the ligands, nature of the outgoing group and geometry of the complex.

- There are three major mechanisms followed in ligand substitution reactions: dissociative, associative and interchange.
- Ligand substitution in octahedral complexes generally proceed via the interchange mechanisms. Substitution reaction in octahedral Co(III) complexes follow the I_d, where the rate depends primarily on the leaving group ability.
- d^8 square planar d^8 generally follow an associative mechanism in ligand substitution reactions, passing through a five-coordinate intermediate with retention of stereochemistry.
- Other factors such as trans effect, nucleophilicity of the incoming group and crystal field stabilisation energy (CFSE) effects significantly influence activation parameters and rate of water exchange in octahedral metal aqua complexes.

K 12.8 ANSWERS TO CHECK YOUR PROGRESS

Answer to Q1: Substitution reactions in coordination chemistry are defined as reactions in which one ligand, originally attached to a metal ion, is replaced by another ligand. Since one ligand is substituted for new ligand, these reactions are more specifically known as ligand substitution reactions.

Answer to Q2: Depending on the rate of ligand substitution reactions, coordination complexes are categorised as labile or inert. Labile complexes are complexes in which one or more ligands are replaced rapidly from the coordination. On the other hand, inert complexes are complexes that remain unchanged for comparatively longer periods of time (conventionally, at least one minute).

Answer to Q3: The three major types of reaction mechanisms in ligand substitution reactions are: i. Dissociative, ii. Associative and, iii. Interchange mechanisms

Answer to Q4: Interchange mechanism is the most commonly followed mechanism in substitution reactions of octahedral complexes.

Answer to Q5: Ligand substitution reactions in which a neutral ligand, such as water, coordinated to a central metal ion, is replaced by an entering anionic ligand, such as Cl^- are known as anation reactions.

Answer to Q6: The two different intermediate structures for ligand substitution in octahedral complexes are square pyramidal and trigonal bipyramidal.

Answer to Q7: For square planar complexes, stereochemistry is generally retained in ligand substitution reactions.

Answer to Q8: The nucleophilicity parameter explains the relationship between the nucleophilicity of the incoming group and the rate of substitution reaction in a square planar complex.

Answer to Q9: To study the rate of water exchange, a coordinated water molecule is replaced with isotopically labelled water for a series of $M(H_2O)_6]^{n+}$ octahedral complexes.

Answer to Q10: i) interchange dissociative (I_d) ii) associative iii) increase

O 12.9 FURTHER READING

- Huheey, J. E.; Keiter, E. A.; Keiter, R. L. *Inorganic Chemistry: Principles of Structure and Reactivity*, 4th ed.; Pearson.
- Miessler, G. L.; Tarr, D. A. *Inorganic Chemistry*, 4th ed.; Pearson.
- Shriver, D. F.; Atkins, P. W. *Inorganic Chemistry*, 5th ed.; Oxford University Press: Oxford, 2010.
- Housecroft, C. E.; Sharpe, A. G. *Inorganic Chemistry*, 5th ed.; Pearson, 2018.
- Kettle, S. F. A. *Physical Inorganic Chemistry: A Coordination Chemistry Approach*; Springer, 1996.

M 12.10 MODEL QUESTIONS

Q1. Why is rate of a reaction important in ligand substitution reactions?

Q2. What are some factors due to which rate of a reaction varies for different coordination complexes?

Q3. How is a dissociative mechanism different from an associative mechanism?

Q4. Explain the ligand substitution in octahedral complexes using the Eigen-Wilkins mechanism.

Q5. Describe ligand substitution in octahedral Co(III) complexes using proper structures.

Q6. Why do most substitution reactions in square planar Pt(II) complexes show retention of stereochemistry?

Q7. Give an example of ligand substitution reaction in square planar complexes.

Q8. Using activation parameters, explain why square planar complexes with different incoming ligands follow an associative pathway?

Q9. Explain the trend of rate of water exchange reactions for first row high-spin M^{2+}hexaaqua transition metal ions.

Q10. How does CFSE values affect the rate of water substitution reactions for different ligand substitution reactions?

UNIT 13: SOLVOLYSIS, HYDROLYSIS AND TRANS EFFECT

UNIT STRUCTURE

13.1 Learning Objectives
13.2 Introduction
13.3 Acid Hydrolysis
13.4 Base Hydrolysis
13.5 Trans Effect and its importance
13.6 Theories of Trans Effect
13.7 Let Us Sum Up
13.8 Answers to Check Your Progress
13.9 Further Reading
13.10 Model Questions

13.1 LEARNING OBJECTIVES

After going through this unit, you will be able to:

- learn the concept of acid hydrolysis in substitution reactions, understanding its influence on the rate of the reaction.
- learn about base hydrolysis, its reactions, and understand the mechanism.
- familiarize yourself with the trans effect in square planar complexes and its significance.
- understand the theoretical aspects of trans effect and explain its influence on substitution reactions.

13.2 INTRODUCTION

We will start with the basics of acid and base catalysed hydrolysis reactions, typical examples and their mechanistic pathways.

Next, we will cover the basics of trans effect, including some important examples, the explanation of the ligand trans effect series. Then, we will move on to the theoretical description of the trans effect and study its importance in various reactions.

13.3 ACID HYDROLYSIS

The presence of an acid in aqueous solutions play a major role in certain substitution reactions. This is primarily dependent on the identity of the coordinated outgoing group bearing lone pairs of electrons. The lone pairs on the leaving group can facilitate its interaction with H^+ ions resulting in the weakening of the bond between the outgoing group and the central metal atom.

Consider the following reaction:

$$[Cr(H_2O)_5F]^{2+} + H^+ \rightarrow [Cr(H_2O)_5{-}F\cdots H]^{3+}$$

$$[Cr(H_2O)_5{-}F{\cdots}H]^{3+} + H_2O \rightarrow [Cr(H_2O)_6F]^{3+} + HF$$

The lone pairs of the leaving group, F^- interaction with the H^+ ions in solution resulting in the formation of HF, a weak acid. In acidic solution, the rate for the overall reaction is 1.4×10^{-8} s^{-1} as compared to 6.2×10^{-10} s^{-1} in neutral solution. However, replacement of the leaving group with ammonia does not accelerate the rate of the reaction. This acceleration of reaction rate in acidic medium can, therefore, be attributed to the interaction of lone pairs of the bound leaving group with the acid present in solution.

13.4 BASE HYDROLYSIS

Substitution reactions of octahedral complexes with ligands bearing acidic hydrogens are sufficiently accelerated in the presence of OH^- ions.

Consider the following reaction:

$$[CoCl(NH_3)_5]^{2+} + OH^- \rightarrow [Co(OH)(NH_3)_5]^{2+} + Cl^-$$

The rate equation for this reaction is:

$$\text{rate} = k[CoCl(NH_3)_5^{2+}][OH^-]$$

The appearance of OH^- signifies the importance of hydroxide ions in the rate determining step of the reaction. However, this second order reaction is not due to a simple attack of OH^- on the central metal ion. Rather, the OH^- ions react by withdrawing a proton from the coordinated NH_3 ligand. Therefore, the OH^- ions behave as a Bronsted base and not as an incoming group. This conjugate base mechanism (S_N1CB) is as shown below:

$$[CoCl(NH_3)_5]^{2+} + OH^- \rightarrow [CoCl(NH_2)(NH_3)_4]^+ + H_2O$$

$$[CoCl(NH_2)(NH_3)_4]^+ \rightarrow [Co(NH_2)(NH_3)_4]^{2+} + Cl^- \qquad \text{(slow step)}$$

$$[Co(NH_2)(NH_3)_4]^{2+} + H_2O \rightarrow [Co(OH)(NH_3)_5]^{2+} \qquad \text{(fast step)}$$

The reaction begins by deprotonation of NH_3 ligand resulting in the formation of its NH_2^-, the conjugate base of NH_3 as a ligand. Due to a lower charge of the deprotonated complex, the tendency of the complex to lose a Cl^- is greater compared to protonated form, leading to speeding up of the reaction. In accordance with the conjugate base mechanism, the deprotonation of NH_3transforms the ligand from a σdonor (NH_3) to a strong σ and π donor (NH_2^-). This transformation readily stabilizes the five-coordinate transition state formed during the reaction in addition to promoting the loss of Cl^- ion. The structure of the five-coordinate transition state is shown below:

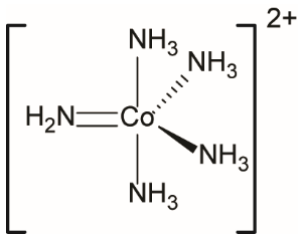


Fig. 13.1. Structure of the five-coordinate transition state formed during the base hydrolysis of $[CoCl(NH_3)_5]^{2+}$.

The conjugate-base mechanism can be suggested based on two specific observations:

i. involvement of competing nucleophiles, such as azides, do not render any change in the base catalysed hydrolysis reaction. This is indicative of the fact that OH^- behaves as a base and not as a nucleophile.

ii. replacement of H (in NH_3) for D in alkaline D_2O occurs much faster than the rate of the base hydrolysis reaction.

It is also seen that complexes such as $[Co(py)_4Cl_2]^+$ and $[Co(CN)_5Cl]^{3-}$ do not display the typical base accelerated hydrolysis reactions. The hydrolysis in these cases is relatively slow and does not depend on the presence of the OH^- ion. The slow reaction rate can be attributed to the absence of ionisable hydrogens in the above complexes, a key requirement of S_N1CB mechanistic pathway. This observation further reiterates the conclusion that the base hydrolysis reaction proceeds via a conjugate base mechanism.

13.5 TRANS EFFECT AND ITS IMPORTANCE

As shown in the reaction below (**Fig. 13.2**), two different isomers of the square planar complex diamminedichloroplatinum(II) are possible. In the first step, since all the four groups in **A** are identical, only a single compound, **B** is formed. However, in the next step, two potential products can be formed. It is interesting to note that the only isomer that forms exclusively is the one in which replacement of a ligand trans to a chloride ion takes place, *i.e.* **D**. The isomer **C** is not formed during the reaction. This formation of an exclusive isomer can be attributed to the labilization of ligands located trans to specific ligands. It can, therefore, be reasonably concluded that the nature of ligands trans to the leaving group, also known as spectator ligands, significantly affect the reaction rate in square planar complexes. This effect is known as the trans effect.

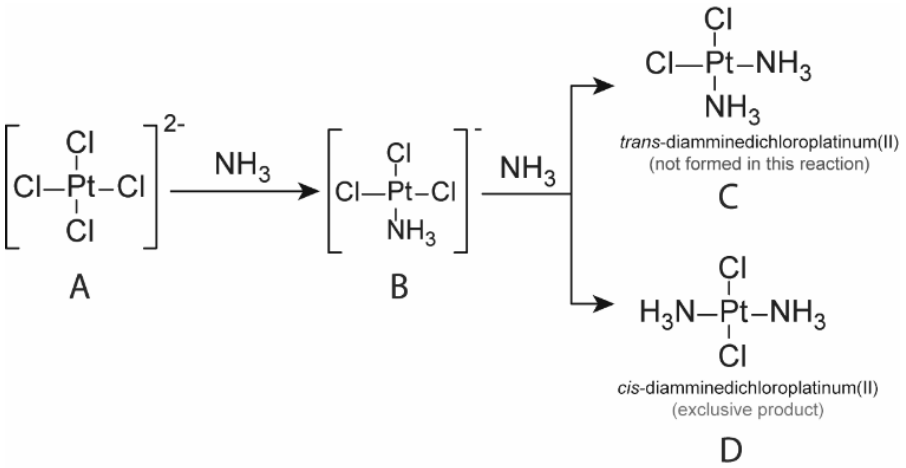


Fig. 13.2. Reaction of tetrachloroplatinate(II) ion with ammonia leading to possibility of formation of two isomers of diamminechloroplatinum(II).

It must also be noted that this effect must be kinetically controlled as the most stable thermodynamic isomer is not always formed.

Consider the reactions in **Fig. 13.3.** As previously discussed, the reaction (a) forms the cis isomer exclusively instead of the trans isomer. This is due to the stronger trans

effect of chloride as compared to ammonia. This is evident from the fact that the second replacement occurs trans to chloride and not ammonia. In reactions (b) and (c), there two possible first replacements with chloride, one trans to pyridine (b) and another trans to ammonia (c). However, the final step depends entirely on the trans directing ability of the chloride ion, generating identical products in both the cases.
A large number of compounds were synthesized by Chernyaev and the trans effect of various ligands was established as:

$$CN^- \sim CO \sim C_2H_4 < PH_3 \sim SH_2 > NO_2^- > I^- > Br^- > Cl^- > NH_3 \sim py > OH^- > H_2O$$

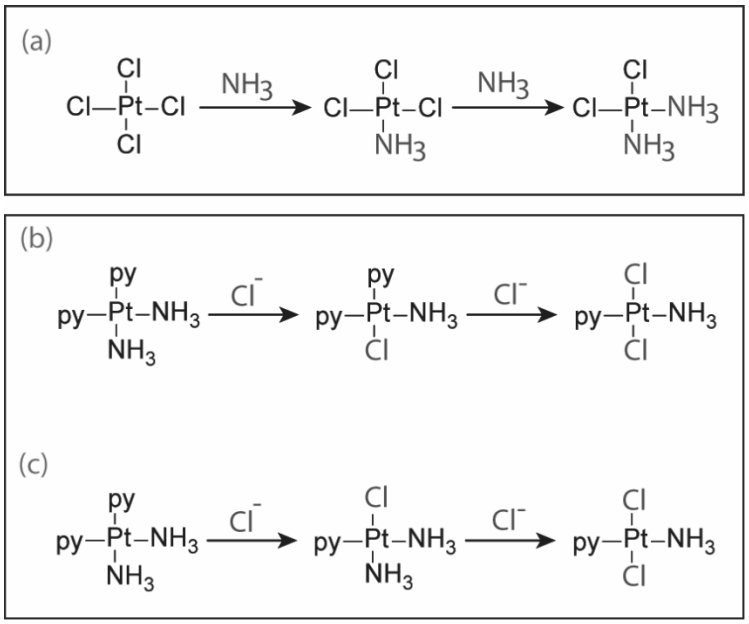


Fig. 13.3. Trans effect in two series of reactions involving Pt(II) complexes (charges have been omitted for clarity).

13.6 THEORIES OF TRANS EFFECT

Trans effect is believed to be a combination of two separate influences: the trans influence and the transition state effect. The trans influence is a ground state phenomenon and signifies how strongly the spectator ligand (T) weakens the metal-ligand bond *trans* to itself in the coordination complex. The trans influence takes into account the extent of σ-donation ability of the ligand (T) to the central metal ion. A strong donor ligand will significantly weaken the bond trans to itself resulting in its relatively weaker bonding interaction with the central metal ion. This is because both the ligand and the group trans to it use the same metal orbitals for bond formation. A strong σ-donor is more likely to form a stronger bond with the central ion allowing limited donation scope from the ligand trans to it, thereby leading to a weaker bond trans to itself. As seen in **Fig. 13.4**, the Pt p_x and $d_{x^2-y^2}$ orbitals are used in the formation of both Pt-X and Pt-T bonds. A substantial part of these orbitals is used for the formation of a strong Pt-T σ bond, leaving relatively less for the Pt-X bond.

A stronger Pt-X bond is formed when the trans effect is minimum leading to a lower energy ground state and higher energy of activation (**Fig. 13.5(a)**). On the other hand,

a lesser overlap results in a weaker Pt-X bond and a high energy ground state. This leads to lower activation energy requirement for breaking of the Pt-X bond (**Fig. 13.5(b)**). The assessment of the trans influence is determined quantitatively by measurement of bond lengths, metal-to-ligand NMR coupling constants and stretching frequencies.

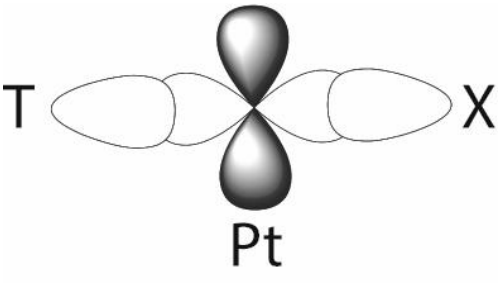


Fig. 13.4. Cartoon representation σ-bonding effect during the formation of Pt-T and Pt-X bonds.

An additional factor involved in trans effect deals with the π-acceptor ability of the ligand. Any spectator ligand that is able to accept the excess electron density built up on the metal due to coordination with the ligand will stabilize the transition state. As a result, the activation energy of the transition state is consequently lowered even though the ground state of the reactant is not affected significantly (**Fig. 13.5(c)**).

It can thus be concluded that a combination both the σ-donating and π-accepting ability of the ligand leads to the overall trans effect in a complex.

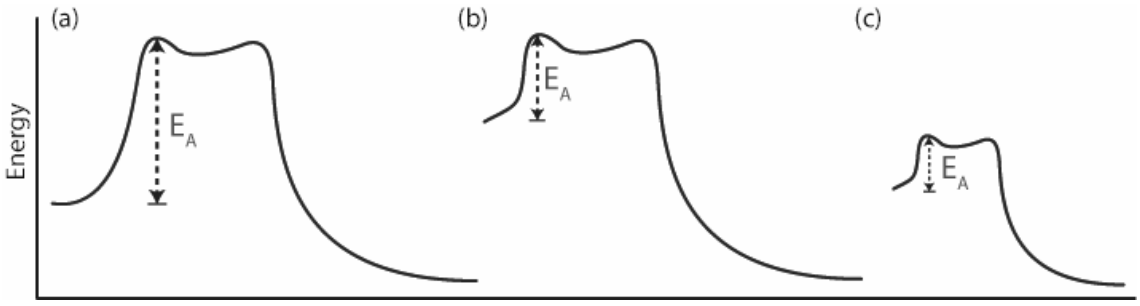


Fig. 13.5. Graphical representation of the activation energy and the trans effect (graph not to scale). (a) poor trans effect with a low ground state and high activation energy, (b) trans influence dominates leading to strong σ-bonding effect and a high energy ground state, (c) π-acceptor effect resulting in a lower energy transition state.

Depending on the type of spectator ligand (trans to the leaving group), an expanded arrangement of ligands in the form of a series can be written as follows:

$$\sigma\text{-donor: } OH^- < NH_3 < Cl^- < Br^- < CN^-, CH_3^- < I^- < SCN^- < PR_3, H^-$$

$$\pi\text{-acceptor: } Br^- < I^- < NCS^- < NO_2^- < CN^- < CO, C_2H_4$$

It is worth noting that a minimal *cis*-effect also does exist, but the *trans*-effect is generally more important.

W CHECK YOUR PROGRESS

Q1. What is the primary requirement in acid catalysed hydrolysis reactions in coordination complexes?
Q2. How do acids speed up hydrolysis reactions?
Q3. What is the primary requirement in base catalysed hydrolysis reactions in coordination complexes?
Q4. Do hydroxide ions behave as a base or a nucleophile in base catalysed hydrolysis reactions?
Q5. What is trans effect?
Q6. Which isomer is produced in the substitution reaction of diamminedichloroplatinum(II) ion with ammonia?
Q7. What are two important theories of *trans* effect?
Q8. How is the quantitative assessment of trans influence done?
Q9. What are the overall properties of a ligand that lead to a strong trans effect in a complex?
Q10. Fill in the blanks:
i. A _____ coordinate transition state is formed during the base catalysed hydrolysis reactions in coordination complexes.
ii. The ligand present trans to the leaving group in a complex is known as a _____ ligand.
iii. The trans influence is a _____ state phenomenon.

2 13.7 LET US SUM UP

- Presence of lone pairs on ligands can allow interaction with H^+ from an acid, leading to weakening of the metal-ligand bond and accelerating ligand substitution reactions in coordination complexes.
- Substitution reactions in complexes having ligands containing acidic hydrogens are accelerated by the presence of OH^- ions, leading to higher hydrolysis reaction rates.
- A conjugate-base mechanism (S_N1_{CB}) is followed in the base hydrolysis reaction where the conjugate base of the coordinated ligand is formed after deprotonation with OH^- ions followed by departure of the outgoing group.
- The trans effect plays an important role is certain square planar complexes by playing a dominant role in controlling the direction and reaction rates in ligand substitution reactions.
- The trans effect is a combination of two different factors: a ground state trans influence (σ-donation effect) and a transition-state stabilization effect (π-acceptor spectator ligands).

K 13.8 ANSWERS TO CHECK YOUR PROGRESS

Answer to Q1: The presence of lone pairs on the ligand is the primary requirement of acid catalysed hydrolysis in coordination complexes.

Answer to Q2: Acids speed up hydrolysis reaction by protonation of the ligand resulting in weakening of the metal-ligand bond ultimately leading to hydrolysis.

Answer to Q3: The presence of acidic hydrogens on the ligand is the primary requirement of base catalysed hydrolysis in coordination complexes.

Answer to Q4: Hydroxide ions behave as a base in base catalysed hydrolysis reactions.

Answer to Q5: The nature of ligands trans to the leaving group in square planar complexes significantly affect the rate of the substitution reaction. This effect is known as the trans effect.

Answer to Q6: *cis*-diamminedichloroplatinum(II) is the exclusive isomer produced in the substitution reaction of diamminedichloroplatinum(II) ion with ammonia

Answer to Q7: Two important theories of trans effect are the trans influence and transition state effect.

Answer to Q8: The quantitative assessment of the trans influence is done by measurement of bond lengths, metal-to-ligand NMR coupling constants and stretching frequencies.

Answer to Q9: A combination of both the σ-donating and π-accepting tendency of the ligand contributes to a strong trans effect in a complex.

Answer to Q10: i) five ii) spectator iii) ground

O 13.9 FURTHER READING

- Huheey, J. E.; Keiter, E. A.; Keiter, R. L. *Inorganic Chemistry: Principles of Structure and Reactivity*, 4th ed.; Pearson.
- Miessler, G. L.; Tarr, D. A. *Inorganic Chemistry*, 4th ed.; Pearson.
- Shriver, D. F.; Atkins, P. W. *Inorganic Chemistry*, 5th ed.; Oxford University Press: Oxford, 2010.
- Housecroft, C. E.; Sharpe, A. G. *Inorganic Chemistry*, 5th ed.; Pearson, 2018.

M 13.10 MODEL QUESTIONS

Q1. Explain the acid hydrolysis of $[Cr(H_2O)F]^{2+}$ giving relevant reactions?

Q2. Elucidate the conjugate base mechanism for the base hydrolysis of $[CoCl(NH_3)_5]^{2+}$?

Q3. Draw the structure of the five-coordinate transition state formed during the base hydrolysis of $[CoCl(NH_3)_5]^{2+}$?

Q4. Why do complexes such as $[Co(py)_4Cl_2]^{+}$ and $[Co(CN)_5Cl]^{3-}$ do not show the typical base accelerated hydrolysis reactions?

Q5. What are the two specific observations to suggest that base hydrolysis reactions proceed via the conjugate base mechanism?

Q6. Explain trans effect with a suitable example.

Q7. Illustrate with the help of a diagram, the orbital overlap during the σ-bonding effect.

Q8. How does the π-acceptor ability of the ligand contribute to the overall *trans*-effect?

Q9. Provide a graphical representation of the relationship between the trans effect and the corresponding activation energy

Q10. Analogous to trans effect, does a *cis* effect also exist?

UNIT 14: ELECTRON TRANSFER REACTIONS

UNIT STRUCTURE

14.1 Learning Objectives
14.2 Introduction
14.3 Types of Electron Transfer Reactions
  14.3.1 Outer Sphere Electron Transfer Reactions
  14.3.2 Inner Sphere Electron Transfer Reactions
14.4 Mechanism of Outer Sphere Electron Transfer Reactions
14.5 Marcus Theory
14.6 Mechanism of Inner Sphere Electron Transfer Reactions
14.7 Let Us Sum Up
14.8 Answers to Check Your Progress
14.9 Further Reading
14.10 Model Questions

14.1 LEARNING OBJECTIVES

After going through this unit, you should be able to:

- understand the concept of electron transfer reactions in coordination compounds,
- distinguish between outer sphere and inner sphere electron transfer mechanisms,
- explain the mechanistic steps involved in both types of reactions,
- discuss factors affecting the rates of electron transfer reactions,
- appreciate the role of bridging ligands, electronic structure and thermodynamics in electron transfer processes.

14.2 INTRODUCTION

Redox reactions are commonly introduced as processes involving changes in oxidation states. However, in coordination chemistry, it is equally important to understand the *pathway* through which these oxidation–reduction changes occur. Merely knowing the initial and final oxidation states does not explain how electrons actually move between metal centres in solution.

In many coordination compounds, electron transfer can occur either directly between two metal complexes or through the participation of ligands bound to the metal ions. The manner in which electron transfer takes place has a profound influence on reaction rates, mechanisms, and product formation. As a result, electron transfer reactions form a central theme in the study of inorganic reaction mechanisms.

Based on whether or not the coordination environment of the metal ions changes during the reaction, electron transfer processes are broadly classified into **outer sphere** and **inner sphere** reactions. In outer sphere reactions, electron transfer occurs without any alteration in the coordination spheres of the reacting species, whereas in inner sphere reactions, electron transfer takes place through a ligand that temporarily links the oxidant and the reductant.

In this unit, we will examine these two mechanisms in detail, focusing on their fundamental principles, mechanistic steps, and the factors that control their rates. This discussion will provide a deeper understanding of how structure, bonding, and reactivity are interconnected in coordination chemistry.

14.3 TYPES OF ELECTRON TRANSFER REACTIONS

Electron transfer reactions can be classified as:

1. Outer sphere electron transfer reactions, and
2. Inner sphere electron transfer reactions

1. Outer Sphere Electron Transfer Reactions

An outer sphere electron transfer reaction is characterised by electron transfer between two coordination complexes without any alteration in their inner coordination environments. The ligands surrounding each metal ion remain bound throughout the reaction, and no bridging interaction is established between the two species.

Such reactions are most commonly observed when both complexes are substitutionally inert, preventing ligand exchange. Electron transfer therefore occurs through space or through solvent-mediated interaction, while the structural framework of each complex remains unchanged. Example of outer sphere reaction is the electron transfer between $[Fe(CN)_6]^{4-}$ and $[IrCl_6]^{2-}$, where the coordination environments remain unchanged and electron is transferred from Fe(II) toIr(IV):

$$[Fe(CN)_6]^{4-} + [IrCl_6]^{2-} \longrightarrow [Fe(CN)_6]^{3-} + [IrCl_6]^{3-} \qquad 14.1$$

2. Inner Sphere Electron Transfer Reactions

In an inner sphere electron transfer reaction, the two metal centres become linked through a bridging ligand prior to electron transfer. This temporary association modifies the coordination environment of at least one of the reacting species.

For this mechanism to operate, one reactant must contain a ligand capable of functioning as a bridge, and the other must be sufficiently labile to allow formation of the bridged

intermediate. Electron transfer then occurs through this linkage and may be accompanied by ligand transfer. An example of inner sphere electron transfer reaction is shown in Eq 14.2. It shows the reaction between $[Co^{III}(NH_3)_5NCS]^{2+}$ and $[Cr^{II}(H_2O)6]^{2+}$ under acidic conditions. The reaction passes through an intermediate bridged complex, where the ligand NCS acts as a bridge between the oxidant (CoIII) and the reductant (CrII) species. Finally, the inner spheres of both the Co and Cr get altered.

$$[Co(NH_3)_5NCS]^{2+} + [Cr(H_2O)_6]^{2+} \longrightarrow [_5(H_3N)Co \cdots NCS \cdots Cr(OH_2)_5]^{4+}$$

$$\downarrow$$

$$[Co(H_2O)_6]^{2+} + [Cr(H_2O)_5SCN]^{2+} + 5NH_4^+ \qquad 14.2$$

General Considerations in Electron Transfer Reactions

Before analysing the detailed pathways of inner sphere and outer sphere electron transfer reactions, it is important to understand certain basic principles that govern all electron transfer processes in coordination chemistry. These principles provide a common framework for interpreting both the mechanism and the rate of such reactions.

First, electron transfer always occurs at the molecular orbital level. The electron is donated from the highest occupied molecular orbital **(HOMO)** of the reducing species and accepted into the lowest unoccupied molecular orbital **(LUMO)** of the oxidising species. Therefore, electron transfer should be viewed as an interaction between orbitals rather than simply between metal ions.

Secondly, prior to electron transfer, the reacting species must undergo **chemical activation**. This involves bringing the oxidant and reductant into a favourable orientation and electronic state. Efficient electron transfer requires compatibility between the donor and acceptor orbitals. When both orbitals are of similar type, electron transfer occurs with minimal structural adjustment.

14.4 MECHANISM OF OUTER SPHERE ELECTRON TRANSFER REACTIONS

An outer sphere electron transfer reaction is one in which electron transfer occurs without any change in the inner coordination spheres of either the oxidant or the reductant. No ligand is shared or transferred between the two metal centres. Such reactions are commonly observed between substitutionally inert complexes, where ligand exchange is difficult.

The outer sphere mechanism may be explained by considering a simple collision model. The mechanism mainly involves the following steps:

1. **Formation of a precursor complex:** The oxidant (O) and the reductant (R) come close to each other, usually within a solvent cage, without any bond formation to form a precursor complex.

$$O + R \longrightarrow [O\text{-------}R]$$

2. **Activation of the precursor complex and electron transfer:** Activation of the precursor complex occurs by reorganization of the solvent molecules and also by changing the metal–ligand bond distances. After these structural adjustments, allowing the electron to transfer from the reductant to the oxidant occurs.

$$[O\text{-------}R] \longrightarrow [O\text{-------}R]^*$$
$$[O\text{-------}R] \longrightarrow [O^{-}\text{-----}R^{+}]$$

3. **Formation of products:** The successor complex dissociates to give the final oxidized and reduced species as follows:

$$[O^{-}\text{-----}R^{+}] \longrightarrow O^{-} + R^{+}$$

It has been observed that the formation of the precursor complex and the dissociation of the successor complex are both rapid steps, whereas the electron transfer itself is relatively slow and determines the overall reaction rate.

The overall activation energy of outer-sphere electron transfer reactions can be given as:

$$\Delta G^{\ddagger} = \Delta G_t^{\ddagger} + \Delta G_o^{\ddagger} + \Delta G_i^{\ddagger}$$

where,

i) $\Delta G_t^{\ddagger}$represents the energy required to bring the reacting species close to each other against electrostatic (Coulombic) repulsion.

ii) $\Delta G_o^{\ddagger}$corresponds to the energy needed for solvent reorganisation. Strong solvent–complex interactions, such as hydrogen bonding, increase this energy and slow down the reaction, whereas weakly interacting solvents facilitate faster electron transfer.

iii) $\Delta G_i^{\ddagger}$is the energy associated with internal structural reorganisation, mainly changes in metal–ligand bond lengths, required to bring the interacting orbitals to comparable energies. According to the Franck–Condon principle, electronic transitions occur much faster than nuclear motion; therefore, bond lengths must adjust before effective electron transfer can take place. Since metal–ligand distances depend strongly on the oxidation state, such reorganisation is essential for electron transfer.

The reorganisation of surrounding solvent molecules and metal–ligand bond distances before the electron can transfer in outer sphere electron transfer reaction requires energy and is called the reorganisation energy (λ).

The total reorganisation energy is expressed as:

$$\lambda=\lambda_{inner}+\lambda_{outer}$$

where:

λ_{inner} represents changes in metal–ligand bond distances

λ_{outer} represents solvent reorientation

Potential energy diagrams provide a useful way of understanding how molecular motion influences electron transfer reactions. The collective motion of the reactant molecules and the surrounding solvent nuclei before electron transfer can be approximated by a harmonic potential energy surface. In this approximation, the system behaves like a set of coupled oscillators, and the potential energy varies parabolically with changes in nuclear configuration (**Fig 14.1a, R**). The potential energy of the products and the associated solvent nuclei after electron transfer can likewise be approximated by a similar form (**Fig 14.1a, P**). It is clear from the figure that the reactants and products have same energy for homonuclear electron transfer reactions. At the point where the two potential energy surfaces intersect (represented as I in the **fig 14.1**), the energies of the electron in the donor and acceptor states become equal, thereby satisfying the condition necessary for electron transfer. However, coupling of vibrational and electronic motion must take place at I, for efficient electron transfer. This coupling interaction is directly linked to the energy ΔEas shown in the figure. When bond distortion is small, the coupling interaction becomes strong which implies favorable electron transfer. Very weak coupling interaction is associated with large bond distortion which favors slow electron transfer reaction. For heteronuclear reactions also, these considerations are equally applicable and are depicted in **Fig 14.1b**.

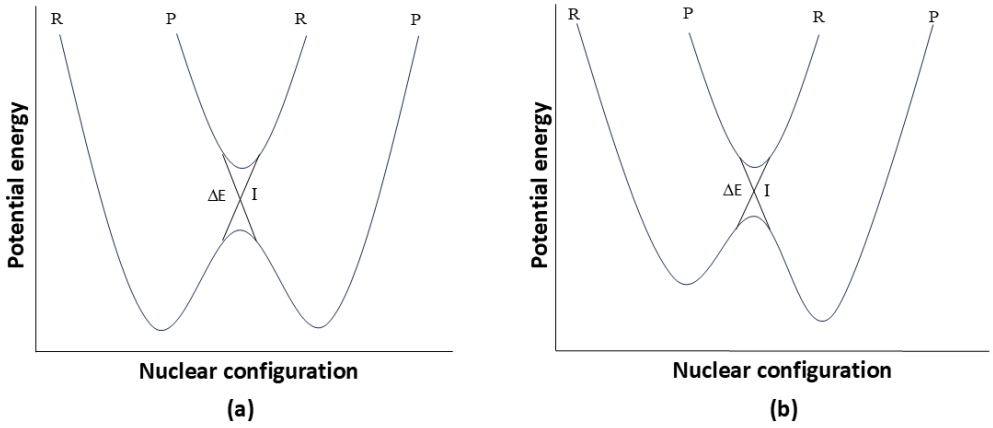


Fig 14.1: Potential energy diagram of (a) homonuclear electron transfer reaction and (b) heteronuclear electron transfer reaction.

The rate of outer sphere electron transfer is influenced by several important factors:

1. **Orbital Symmetry:** Efficient outer sphere electron transfer requires interaction

between orbitals of compatible symmetry. In octahedral complexes, an $e_g \rightarrow e_g$ ($\sigma^* \rightarrow \sigma^*$) transition involves significant changes in metal–ligand bond lengths because σ* orbitals are directed toward the ligands. This leads to large structural reorganisation and poor effective overlap, resulting in slow electron transfer. In contrast, a $t_{2g} \rightarrow t_{2g}$ ($\pi/\pi^* \rightarrow \pi/\pi^*$) transition requires comparatively smaller changes in bond lengths. Since these orbitals are oriented between ligand axes, steric interference is minimal and overlap is more favourable. Consequently, such transitions generally proceed at faster rates, depending also on the ligand environment.

2. **Extent of Orbital Overlap:** The efficiency of electron transfer increases with better orbital overlap between donor and acceptor orbitals. Outer sphere reactions are often faster for second- and third-row transition metal ions (4*d* and 5*d* series) than for first-row (3*d*) metals. This is attributed to the more diffuse nature of 4*d* and 5*d* orbitals, which allows improved overlap. Additionally, stronger crystal fields in heavier transition metals lead to smaller bond length distortions during electron transfer. Ligands possessing extended *π*-systems further enhance electron delocalisation and promote faster transfer.
3. **Electronic Configuration and Spin State:** If electron transfer involves a change in electronic configuration, such as a transition between high-spin and low-spin states, additional electronic rearrangement is required. This increases the activation energy barrier and slows the reaction. Significant changes in electron distribution also cause greater variation in metal–ligand bond lengths, increasing internal reorganisation energy and reducing the rate of electron transfer.

14.5 MARCUS THEORY

Rudolph A. Marcus developed a theoretical expression from first principles to estimate the rate constant of an outer-sphere electron transfer reaction. For this pioneering work on the theoretical understanding of electron transfer processes in chemical systems, Marcus was awarded the Nobel Prize in Chemistry in 1992. His framework, now known as **Marcus theory**, provides a unified kinetic and thermodynamic description of one-electron outer-sphere electron transfer reactions.

His treatment shows that the rate of a cross reaction (electron transfer takes place between the complexes of different metal ions) can be predicted from the self-exchange reaction (electron transfer between two same metal ions in different oxidation states) rate constants of the two participating redox couples and the equilibrium constant of the overall reaction.

The relationship is commonly written as:

$$k_{12}=(k_{11}\, k_{22}\, K_{12}\, f_{12})^{1/2} \qquad 14.3$$

Here,

- $k_{11}$and k_{22} are the self-exchange rate constants of the two redox couples,
- K_{12} is the equilibrium constant for the cross reaction, and
- *f* is a correction factor that accounts for differences in free energy between the reactants and is usually close to unity.

The factor *f* depends on thermodynamic parameters and adjusts the expression for deviations arising from unequal driving forces in the two half-reactions.

Now let us consider the cross reaction:

$$[Fe(CN)_6]^{4-}+[Mo^*(CN)_8]^{3-}\longrightarrow[Fe(CN)_6]^{3-}+[Mo^*(CN)_8]^{4-} \qquad 14.4$$

For this reaction, we will calculate the rate constant $k_{12}$from the following self-exchange processes:

$$[Fe(CN)_6]^{4-}+[Fe^*(CN)_6]^{3-}\longrightarrow[Fe(CN)_6]^{3-}+[Fe^*(CN)_6]^{4-} \qquad 14.5$$

$$[Mo(CN)_8]^{3-}+[Mo^*(CN)_8]^{4-}\longrightarrow[Mo(CN)_8]^{4-}+[Mo^*(CN)_8]^{3-} \qquad 14.6$$

k_{11}, $k_{22}$are the rate constants for the self-exchange processes involving the hexacyanoferrate complexes (Eq. 14.5) and octacyanomolybdenum complexes (Eq. 14.6) respectively.

K_{12} is the equilibrium constant for the overall cross reaction (Eq. 14.4)

$$[Fe(CN)_6]^{4-}+[Mo^*(CN)_8]^{3-}\rightleftharpoons[Fe(CN)_6]^{3-}+[Mo^*(CN)_8]^{4-} \qquad 14.7$$

Experimentally, the values of k_{11}, k_{22} and K_{12} from equations14.5, 14.6, and 14.7 are found to be:

$k_{11} = 7.4 \times 10^2\ M^{-1}s^{-1}$

$k_{22} = 3 \times 10^4\ M^{-1}s^{-1}$

$K_{12} = 1.0 \times 10^2$

Also, $\log f_{12} = (\log K_{12})^2 / 4 \log(k_{11}k_{22}/Z^2)$

where the term *Z* is the collision frequency of the two uncharged particles in solution and is taken as $10^{11}M^{-1}s^{-1}$. The value of *f* in this case is 0.85. Putting all these values in Eq 14.3, the value of rate constant for the overall reaction, **k_{12} is found to be $4 \times 10^4\ M^{-1}s^{-1}$**. This value is in good agreement with the experimental value of **$3 \times 10^4\ M^{-1}s^{-1}$**.

The Marcus equation establishes a direct link between thermodynamics and kinetics by relating the rate constant k_{12} to the equilibrium constant K_{12}. As the thermodynamic favourability of the reaction increases, reflected by a larger value of K_{12}, the rate of

electron transfer also increases. Consequently, outer sphere electron transfer reactions that are thermodynamically more favourable generally occur at faster rates than those that are less favourable. Thus, Marcus theory demonstrates that the rate of electron transfer is controlled not only by the thermodynamic driving force of the reaction, but also by the energy required for nuclear reorganisation of both the reactants and the surrounding solvent. Even a thermodynamically favorable reaction may proceed slowly if the reorganisation energy is large.

Moreover, according to Marcus theory, the free activation energy ($\Delta G^{\ddagger}$) for an outer sphere electron transfer reaction is related to the reorganisation energy (λ) and the standard free energy change ($\Delta G°$) of the reaction by the expression:

$$\Delta G^{\ddagger} = \frac{(\lambda + \Delta G°)^2}{4\lambda}$$

This equation shows that the activation barrier depends not only on the thermodynamic driving force ($\Delta G°$), but also on the energy required for structural reorganisation of the system. When the reorganisation energy is large, the activation barrier increases, even if the reaction is thermodynamically favourable.

14.6 MECHANISM OF INNER SPHERE ELECTRON TRANSFER REACTIONS

Inner sphere electron transfer reactions are inherently more complicated than outer sphere reactions because, in addition to electron transfer, they involve the breaking and formation of metal–ligand bonds. Here, electron transfer occurs through a ligand that temporarily bridges the oxidant and reductant. As a result, the inner coordination spheres of one or both metal centres change.

The class example of this type of mechanism is the reduction of Co(III) in $[Co(NH_3)_5Cl]^{2+}$ by Cr(II) in $[Cr(H_2O)_6]^{2+}$. This was provided by Henry Taube, using isotopic tracer studies, for which he was awarded the Nobel Prize in 1983. This reaction was deliberately selected because

a) both Co(III) and Cr(III) form inert complexes and
b) the corresponding Co(II) and Cr(II) complexes are labile.

Under these conditions, the chloride ligand remains strongly bound to the inert Co(III) ion centre and is able to displace a water molecule from the labile Cr(II) complex. This results in the formation of a **chloride-bridged intermediate**, which facilitates electron transfer via an inner sphere mechanism:

$$[Co(NH_3)_5Cl]^{2+} + [Cr(H_2O)_6]^{2+} \longrightarrow [(H_3N)_5Co - Cl - Cr(OH_2)_5]^{4+} + H_2O$$

Electron transfer then occurs within the dinuclear bridged complex, leading to the formation of reduced Co(II) and oxidised Cr(III). The Cr(III) species forms an inert chloro aqua complex, whereas Co(II) is substitutionally labile. Consequently, the bridged intermediate dissociates, with the chloride ligand remaining coordinated to the chromium centre.

$$[(H_3N)_5Co \text{ —— } Cl \text{ —— } Cr(OH_2)_5]^{4+} \longrightarrow [(H_3N)_5Co]^{2+} + [ClCr(OH_2)_5]^{2+}$$

The five-coordinate Co(II) species rapidly coordinate a water molecule to complete its octahedral coordination sphere and subsequently undergoes fast hydrolysis to form $[Co(H_2O)_6]^{2+}$. Formally, the inner sphere reaction may be viewed as the transfer of a chloride ligand from the cobalt centre to the chromium centre. During this process, cobalt is reduced (its oxidation state decreases), while chromium is oxidised (its oxidation state increases). Apart from the self-consistency of the inert and labile species of the above model and the experimental observation of a chlorochromium product, additional support for this mechanism was obtained through isotopic labelling studies. When the reaction was carried out in the presence of free radioactive chloride ions in solution, only a negligible amount of the labelled chloride appeared in the final product. This observation clearly indicates that the chloride ligand is transferred directly through the bridged intermediate, instead of indirectly through free chloride.

The main factors affecting the inner sphere electron transfer are:

1. **Bridging Complex**: It has been observed that instead of the electron transfer step, the formation of the bridging complex can also be the rate-determining step, sometimes. This will primarily be dependent on how labile or inert the complexes are. Furthermore, it is also possible that the scission of the bridging complex is actually playing as the rate-limiting step.

2. **Electronic Configuration**: The interaction between eg orbitals and the bridging ligand is greater than their t2g counterparts which can be attributed to the orientation of the lobes along the bonding axis. Hence, an acceleration in rates is observed as we go from outer to inner sphere mechanism due to the facilitation of electron transfer via bridging ligands and orbital symmetries.

3. **Nature of the bridging ligand**: The rate of inner-sphere electron transfer mechanism is highly sensitive to the nature of the bridging ligand. The rate of the reaction generally increases with the increase in the nucleophilic character of the bridging ligand. Furthermore, the substitution on the bridging ligand can also affect the rate significantly. The importance of the nature of the bridging ligand in inner sphere reaction can be better understood from the **Table 14.1**.

4. **Rate of ligand exchange**: Since ligand substitution is an essential step in the mechanism, the rate of an inner sphere electron transfer reaction cannot exceed the

rate of ligand exchange in the absence of a redox process. Consequently, if an electron transfer reaction is observed to occur faster than ligand exchange, it must proceed via an outer sphere mechanism.

Table14.1: Rate constants for the reactions of $[Co(NH_3)_5X]^{n+}$ with Cr^{2+}

X	Rate (*k* in $M^{-1}s^{-1}$)
NH_3	8.9×10^{-5}
H_2O	0.5
F^-	2.5×10^5
Cl^-	6×10^5
Br^-	1.4×10^6
I^-	3×10^6

W CHECK YOUR PROGRESS

Q1. Fill in the Blanks:

a) In inner sphere reactions, the electron transfer occurs through a _____ ligand.
b) In outer sphere electron transfer reactions, the electron is transferred without any change in the _____ sphere of the complexes.
c) Isotopic labelling studies show that ligand transfer in inner sphere reactions occurs via a _____ intermediate.
d) Marcus theory provides a unified _____ and _____ description of electron transfer reactions.
e) Inert complexes generally favour_____ sphere electron transfer mechanisms.

Q2. State true or false

a) In an outer sphere electron transfer reaction, the coordination spheres of both reactants remain unchanged.
b) Inner sphere electron transfer reactions require the formation of a bridged intermediate.
c) According to Marcus theory, an increase in equilibrium constant always leads to a decrease in reaction rate.
d) Isotopic labelling experiments provide strong evidence for inner sphere mechanisms.
e) Marcus theory applies only to inner sphere electron transfer reactions.

Q3. Why is a bridging ligand necessary for inner sphere reactions?

Q4. Name two ligands that commonly act as bridging ligands.

Q5. Which type of electron transfer reaction is generally faster and why?

Q6. The self-exchange rate constants for two redox couples are k_{11} = 1.0 × 10⁴ $M^{-1}s^{-1}$ and k_{22} = 4.0 × 10⁴ $M^{-1}s^{-1}$. The equilibrium constant for the cross reaction is K_{12} = 100. Assuming f = 1, calculate the rate constant k_{12} for the cross reaction using the Marcus equation.

Q7. For a self-exchange reaction, the reorganisation energy λ = 80 kJ mol^{-1} and $\Delta G°$ = −20 kJ mol^{-1}. Calculate the free energy of activation $\Delta G^{‡}$ using Marcus theory.

Use: $\Delta G^{‡} = (\lambda + \Delta G°)^2 / 4\lambda$

2 14.7LET US SUM UP

- Electron transfer reactions in coordination compounds occur mainly through **outer sphere** or **inner sphere** mechanisms.
- In **outer sphere reactions**, electron transfer takes place without any change in the coordination spheres of the reactants. These reactions are favoured by inert complexes and depend strongly on orbital symmetry, overlap, and reorganisation energy.
- **Marcus theory** provides a unified framework linking thermodynamics and kinetics through reorganisation energy and predicts reaction rates using self-exchange rate constants and equilibrium constants.
- **Inner sphere reactions** involve the formation of a bridged intermediate, requiring ligand substitution and bond formation. Hence, their rates are limited by ligand exchange kinetics.
- Experimental evidence such as **isotopic labelling** strongly supports the inner sphere mechanism by confirming direct ligand transfer through a bridge.
- The rate and mechanism of both the electron transfer reactions depend on orbital symmetry, ligand lability, thermodynamics, and the nature of bridging ligands. Understanding these mechanisms provides deep insight into redox behaviour in coordination chemistry.
- A simple **comparison between outer sphere and inner sphere electron transfer reactions** are shown below:

Feature	**Outer Sphere**	**Inner Sphere**
Change in coordination sphere	No	Yes
Bridging ligand	Not required	Required
Ligand transfer	Absent	May occur
Typical reactants	Inert complexes	At least one labile complex

Feature	Outer Sphere	Inner Sphere
Mechanistic complexity	Simpler	More complex

K 14.8 ANSWERS TO CHECK YOUR PROGRESS

Answer to Q1: a) bridging b) coordination c) bridged

d) kinetic, thermodynamic e) outer

Answer to Q2: a) True b) Truec) False d) Truee) False

Answer to Q3: A bridging ligand connects the oxidant and reductant, allowing electron transfer through a shared pathway.

Answer to Q4: Cl^- and NCS^-.

Answer to Q5: Inner sphere reactions may be faster when bridge formation and ligand exchange are rapid.

Answer to Q6: k_{12} $= \sqrt{(1.0\times10^4 \times 4.0\times10^4 \times 100 \times 1)}$

$= \sqrt{(4\times10^{10})}$

$= 2.0 \times 10^5\ M^{-1}s^{-1}$

Answer to Q7: $\Delta G^{\ddagger}$ $= (80 + (-20))^2 / (4 \times 80)$

$= (60)^2 / 320$

$= 3600/320$

$= 11.25\ kJ\ mol^{-1}$

O 14.9 FURTHER READING

- Huheey, J. E.; Keiter, E. A.; Keiter, R. L. *Inorganic Chemistry: Principles of Structure and Reactivity*, 4th ed.; Pearson.
- Miessler, G. L.; Tarr, D. A. *Inorganic Chemistry*, 4th ed.; Pearson.
- Balzani, V., ed. *Electron Transfer in Chemistry*. Wiley-VCH, 2001.
- Cotton, F. A.; Wilkinson, G. *Advanced Inorganic Chemistry*; Wiley.
- Weller, M.; Overton, T.; Rourke, J.; Armstrong, F. *Inorganic Chemistry*, 7th ed.; Oxford University Press, 2018.

M 14.10 MODEL QUESTIONS

Q1. Distinguish between outer sphere and inner sphere electron transfer reactions with suitable examples.

Q2. Describe the mechanism of an inner sphere electron transfer reaction, highlighting experimental evidence in support of the mechanism.

Q3. Explain Marcus theory of electron transfer reactions.

Q4. Given k_{11} = 7.4 × 10^2 $M^{-1}s^{-1}$, k_{22} = 3.0 × 10^4 $M^{-1}s^{-1}$ and K_{12} = 1.0 × 10^2, with f = 0.85, calculate k_{12}. Compare your answer with an experimental value of 3 × 10^4 $M^{-1}s^{-1}$ and comment.

Q5. What are factors that affects inner sphere electron transfer? Explain.

Q6. What are factors that affects outer sphere electron transfer? Explain.